Regulation of O-GlcNAc Transferase in breast cancer and its role in regulating lipid metabolism

By Valerie Sodi

December 2016

A Dissertation Presented to the Faculty of Drexel University College of Medicine in partial fulfillment of the Requirements for the Degree of Doctor of Philosophy in Molecular & Cellular Biology and Genetics

_____	_____
Jane Clifford (Chair)	Mauricio Reginato
Department Chair, Full Professor	Full Professor
Department of Biochemistry	Department of Biochemistry
DUCOM	DUCOM
_____	_____
Todd Strochlic	Gregg Johannes
Assistant Professor	Assistant Professor
Department of Biochemistry	Department of Biochemistry
DUCOM	DUCOM

_____

Kathryn Wellen

Assistant Professor

Department of Cancer Biology

University of Pennsylvania

I dedicate this thesis to my family, without whom, I would not be here.

ACKNOWLEDGEMENTS:

I would like to acknowledge my mentor Dr. Mauricio Reginato for his guidance over the last half-decade. He has been a great example of a hard-worker and had consistently pushed myself and my lab members to take every opportunity to produce high quality in depth work and to share our work with others. He has been very patient and understanding and for that I am appreciative. I would like to thank my committee members, Dr. Jane Clifford for extraordinary support in both science and personal life at times when it is most needed, Dr. Todd Strochlic for being a great source of advice and friendship, Dr. Gregg Johannes for his support and time within the program and with technical skills, and Dr. Kathryn Wellen for her unending willingness to help with science in both suggestions and lab collaborations. I would also like to thank; Dr. Michael Bouchard and Dr. Eishi Noguchi for running our program, Dr. Karen Berkowitz, Dr. Christian Sell and Dr. Claudio Torres for their friendship and help, and Kate Maum, Lucia Boyer and Jenny Sherwood for their administrative expertise. I would like to acknowledge the friendship and support as well as lab help from Dr. Christina Ferrer and Dr. Sergey Karakashev who molded my graduate career, as well as Dr. Diane Keane who served as a great example and model. I am thankful for the friendship of Sakina Khaku, Zachary Bacigalupa, Neha Akella, Peter Michener and Dimpi Muckhopadhyay in the Reginato lab. Sakina Khaku, Christina Ferrer, Zachary Bacigalupa, Wiktoria Gocal, and Nicholas Xerri all contributed to the work presented in this thesis. Collaborators that contributed to this work are; Dr. David Vocadlo, Dr. Tiffany Seagroves, Luciana Schwab, Raisa Krutilina, Dr. Kathryn Wellen and Joyce Lee. Outside of the Reginato lab, Dr. Sinan Ferit Tuzer, Dr. Timothy Nacarelli, and Ashley Azar also provided technical help and friendship. I would like to thank Lina Maciunas, Melissa Manners, Tanu Singh, Kristen Maslar, Suyash Bhatnagar, Raelle Jackson, Sumedha Bagga, Jenna Marinock, Tong Lu, Andrea Lomotan, Siddhartha Rawat, Kelly Donovan, Elizabeth Upton, Oleg Alekseev, Yi Guo, Sam Flashner, Patrick Williams, Emily McMillan, Gieira Jones, Arpita Mondal, Marina Tuyishime and Kelly Whalen for their friendship and for sharing great memories. I cannot thank my family enough for their endless support through difficult times. My parents who never let me give up and motivate me to work harder, care for me tirelessly and are truly the kindest people I know, my sister Tara and my brother-in-law Steve who are not just family but my best friends who always know how to make me smile, Chris who never fails to show his support and love, shares the best of times and helps me through the worst of times, and Gunner who loves unconditionally.

TABLE OF CONTENTS

LIST OF ABBREVIATIONS:

HBP- Hexosamine Biosynthetic Pathway

GFAT- glutamine:fructose-6-phosphate amidotransferase

OGT- O-GlcNAc Transferase

UTP- uridine triphosphate

ES cells- embryonic stem cells

OGA- meningioma expressed antigen 5

SNP- single nucleotide polymorphism

ER- endoplasmic recticulum

EPS- early prenatal stress

H2B- histone 2B

ARNT/BMAL1- Aryl hydrocarbon receptor nuclear translocator/ ARNT-like 1

CLOCK- clock circadian regulator

PER1/2- period circadian clock 1/2

CRY1/2- cryptochrome circadian clock 1/2

Elk1- ETS Transcription factor

E2F- retinoblastoma-associated factor 1

PTM- post-translational modification

AD- Alzheimer's disease

PI3K/AKT- Phosphatidylinositol-4,5 Bisphosphate 3 kinase catalytic subunit A/ protein kinase B

PPP- pentose phosphate pathway

HIF1- hypoxia inducible factor 1

BRCA- breast and ovarian cancer susceptibility protein 1

P53- TP53- Tumor protein 53

Nf-KB- Nuclear factor Kappa B subunit 1

DCIS- ductal carcinoma in situ

PTEN- phosphatase and tensin homolog

RB- retinoblastoma associated protein

17-AAG- 17-Demethoxy-17-allyaminogeldanmycin
KRAS- Kirsten rat sarcoma viral oncogene homolog

GATA3- GATA binding protein 3

ER- estrogen receptor

PR- progesterone receptor
ERK- mitogen-activated protein kinase 1

mTOR- mechanistic target of rapamycin

MEK- mitogen-activated protein kinase kinase 1

FDG-PET- fludexoyglucose positron emission tomography

CoA- Co-enzyme A

NADPH- nicotinamide adenine dinucleotide phosphate

TSC1/2- tuberous sclerosis 1/2

MAX- myc associated factor x

AMP- adenosine monophosphate

ATP- adenosine triphosphate

TCA- tricarboxylic acid

HSP90- heat shock protein 90

MEF- mouse embryonic fibroblasts

PGC1-peroxisome proliferator activated receptor gamma coactivator 1 alpha

PPAR- peroxisome proliferator activated receptor

SCD1- stearoyl-CoA desaturase 1

shRNA- short hairpin RNA

CRISPR- Clustered regularly interspaced short palindromic repeats

WT- wild type

ROS- reactive oxygen species

UPR- unfolded protein response

SCAP- SREBP-cleavage activating protein

BCAA- branched-chain amino acids

ChREBP- Carbohydrate responsive element binding protein

FACS- fluorescence-activated cell sorting

GC-MS- gas chromatography mass spectrometry

LC-MS- liquid chromatography mass spectrometry

OAA- oxaloacetate

G6P- glucose-6-phsophate

F6P- fructose-6-phosphate

PEP- Phosphoenolpyruvic acid

R5P- Ribose-5-Phosphate

αKG- alpha-Ketoglutarate

PCR- polymerase chain reaction

DNA- deoxyribonucleic acid

mRNA- messenger ribonucleic acid

BIM- Bcl2-like 11

FBXW7- F-box and WD repeat domain containing 7

GSK3B- glycogen synthase kinase 3 beta

ECM- extracellular matrix

EGFR- epidermal growth factor receptor

JAK- Janus kinase

GFP- green fluorescent protein

STAT-Signal transducer and activator of transcription

LXR- Liver X receptor

DMEM- Dulbecco's Modified Eagle medium

FBS- fetal bovine serum

HIF- hypoxia inducible factor

SREBP-1 – Sterol regulatory element binding protein 1

TET- Ten-eleven translocation enzymes

TPR- tetratricopeptide repeats

PPO- phosphoinositide binding domain

INT- p-Iodonitrotetrazolium

ACC- Acetyl-CoA Carboxylase

FAS- fatty acid synthase

ACLY- ATP citrate lyase

PDHB- Pyruvate Dehydrogenase (polyamide) beta

ENO1- enolase 1

DEGS1- Sphingolipid delta 4 desaturase

4EBP1- Eukaryotic translation initiation factor 4E binding protein 1

S6K1- ribosomal protein S6 kinase 1

FAME- fatty acid methyl ester analysis

PRL- prolactin

IHC- immunohisotchemistry

FFA- free fatty acid

LDHA- lactate dehydrogenase A

PKM2- pyruvate kinase M2

CR- caloric restriction

HER2/ErbB2- Human epidermal growth factor receptor 2

HR- hormone receptor

TN- triple negative

IRS1/2- insulin receptor substrate ½

SP1- specificity protein 1

ABSTRACT:

Cancer cells exhibit altered metabolism characterized by increased glucose and glutamine uptake. Altered utilization of these substrates directly contributes to O-linked-β-N-acetylglucosamine (O-GlcNAc) modifications on intracellular proteins. Multiple cancers contain elevated total O-GlcNAcylation, in part, by increasing O-GlcNAc transferase (OGT) levels, the enzyme that catalyzes this modification. Although cancer cells require OGT for oncogenesis, it is not clear how tumor cells regulate OGT expression and O-GlcNAcylation. Here, we show that the PI3K/mTOR/MYC pathway is required for elevation of OGT and O-GlcNAcylation in breast cancer cells as treatment with PI3K and mTOR inhibitors reduced OGT protein expression and decreased levels of overall O-GlcNAcylation. Downstream of mTOR, the oncogenic transcription factor c-MYC is required and sufficient for increased OGT protein expression in an RNA-independent manner and c-MYC regulation of OGT in cancer cells requires the expression of c-MYC target HSP90A. Mammary tumor epithelial cells derived from MMTV-c-myc transgenic mice contain elevated OGT and global O-GlcNAcylation and OGT inhibition in these tumor cells induces apoptosis. In an attempt to further address consequences of elevated O-GlcNAcylation in breast cancer, we performed comprehensive metabolomics. Metabolomics analysis revealed that reducing OGT levels in breast cancer cells altered a number of metabolic pathways including amino acids and nucleotides, however, the largest change was seen in fatty acid metabolites. We show that O-GlcNAcylation regulates the transcription factor sterol regulatory element binding protein 1 (SREBP-1) and its transcriptional targets, critical enzymes involved in lipid synthesis. OGT regulates SREBP-1 protein expression and stability/degradation via AMP Activated protein kinase (AMPK). SREBP-1 is critical for OGT-mediated regulation of cell survival and of lipid synthesis, as overexpression of SREBP-1 rescues lipogenic defects

associated with OGT suppression, and tumor growth *in vitro* and *in vivo.* We also find that OGT regulates these factors in lactating mammary glands, highly lipogenic normal tissue. These results unravel a previously unidentified link between O-GlcNAcylation, lipid metabolism and the regulation of SREBP-1 in cancer. These finding suggests OGT may be a novel therapeutic target for the treatment of lipid-dependent cancers.

CHAPTER 1: O-GLCNACYLATION AND OGT

1.1 Introduction to O-GlcNAcylation

Many processes exist within a cell to guarantee homeostasis in response to the availability of required cellular sustenance. A cells response to adequate or inadequate nutrient supply dictates its survival and appropriate epigenetic, genetic, transcriptional, translational and post-translational machinery must work in harmony to coordinate this response correctly. In the past years, there has been much interest in all of the regulatory aspects of this response, especially as they exist in metabolic pathologies where nutrient responsive pathways are dysregulated. With respect to post-translational modifications, much attention has been given to phosphorylation which serves as an important modification not only in the context of nutrient changes but in virtually every alteration inside and outside of the cell. One less well studied modification that is now recognized as an important contributor to many cellular processes, is O-linked β N-acetylglucosaminylation (O-GlcNAcylation). This modification serves as a powerful regulator of cellular biology and behavior, particularly in response to nutrients, as it is directly dependent on flux through glycolysis and therefore glucose levels in the cell. Although the majority of glucose taken up by the cell is metabolized through the glycolytic pathway, 3-5% is diverted into the hexosamine biosynthetic pathway (HBP) [1], where it is converted to glucosamine-6-phosphate (GlucN-6-P) by the rate limiting enzyme glutamine:fructose-6-phosphate amidotransferase (GFAT) [2] (Figure 1). Subsequently, GlucN-6-P is converted to uridine-5-diphosphate-N-acetylglucosamine (UDP-GlcNAc), which then serves as a substrate for N-linked glycosylation of proteins in the ER and Golgi as well as O-linked glycosylation of nuclear and cytoplasmic

proteins [3]. The enzyme O-GlcNAc transferase (OGT) uses UDP-GlcNAc as a substrate to add O-linked sugar moieties onto serine and threonine residue hydroxyl groups of a diverse range of nuclear and cytoplasmic proteins (Figure 2) [4, 5]. The production of UDP-GlcNAc requires the contributions of glutamine from amino acid metabolism, acetyl-CoA from fatty acid metabolism, and UTP from nucleotide metabolism, further demonstrating how in tune this modification is to cellular nutrient status [6]. The process of O-GlcNAc cycling is highly dynamic. The addition and removal of O-GlcNAc is performed solely by the two enzymes OGT and O-GlcNAcase (OGA), respectively, a striking contrast to the over 600 human kinases and phosphatases required for phosphorylation [7]. The addition of this unique O-linked sugar is an important post-translational modification (PTM) with the ability to influence many biological processes by altering protein stability, interaction capabilities, degradation and/or stability and even phosphorylation status [8]. The role of O-GlcNAc extends to diverse cellular processes, as its known targets include a wide range of proteins including transcription factors, signaling proteins and receptors [9]. O-GlcNAcylation plays an important role in normal biology and is deregulated in a wide range of pathologies including cardiovascular and neurodegenerative diseases as well as metabolic syndromes such as diabetes [10] and cancer which will be covered more thoroughly later.

1.1.1 OGT/OGA proteins

O-GlcNAc modifications are added to hydroxyl groups of serine and threonine of target proteins by the glycosyltransferase OGT. This enzyme was identified in the early 1990s [11] and was cloned in 1997. Human full-length OGT protein was determined to contain 13 N-terminal tetratricopeptide repeats (TPRs), a number which varies in other isoforms

and organisms (Figure 3) [11]. In 2004 OGT protein crystal structure was solved revealing superhelical structures formed by the TPRs as well as demonstrating the ability of OGT to form a homodimer [12]. The structure of the C-terminal catalytic domain of OGT was solved years later and showed that this domain was a lobular structure. There remains structurally undetermined portions that have been implicated in interaction with membranes based on the prevalence of basic residues [6]. The C-terminal portion of OGT also contains a phosphoinositide binding domain (PPO) demonstrated to have activity in protein-lipid binding to several lipid species [13]. OGT is not a promiscuous glycosyltransferase, however, the mechanism of recognition of target proteins for modification by OGT remains unknown. TPR domains are known to function in protein-protein interaction and are required for recognition of target proteins, however no strict consensus sequence for modification exists. Truncation of these domains demonstrated a loss in ability to bind target proteins [14]. Although the substrate protein may be bound by the TPR repeats, the structure of OGT imposes restrictions that define some sequence specificity [15]. Recognition still remains mysterious, but these studies of structure have provided valuable information about reaction kinetics demonstrating that OGT first binds UDP-GlcNAc, then binds substrate peptides before a reaction occurs [6].

This enzyme has recently been shown to perform a non-glycosyltransferase protease role by two groups [16, 17]. OGT was found to cleave the transcription factor host-cell factor1 (HCF-1), important in cell-cycle progression. Cleavage of this factor is required to ensure effective and appropriate cytokinesis but despite the importance OGT may play mechanistically in this event, lack of cleavage and *ogt* deletion do not

phenocopy in mammalian cells [6]. OGT is also implicated in scaffolding due to its occupation in several stable protein complexes in cells [6].

1.1.2 The function of OGT and O-GlcNAcylation in biology

In normal biology OGT and O-GlcNAcylation play critical roles in cell differentiation, growth and development as deletion of the *ogt* gene, which is located in the mammalian X chromosome, is lethal in ES cell culture and mouse embryogenesis [18]. The first connection made between OGT mutation and human pathology was just elucidated in an X chromosome exome screen. Two separate mutations (one missense and one SNP) in the TPR domain of OGT, resulting in decreased protein stability or altered protein-protein interactions, were linked to X-linked intellectual disabilities (XLID) [19]. Due to its requirement in development evident by embryonic lethality mentioned above, conditional knockout of *ogt* is the only means to study the role of OGT in different adult tissues. The few studies utilizing conditional deletion of *ogt* have examined the role of O-GlcNAcylation in beta cells, the placenta, and T cells, the latter examining both normal development and malignant transformation. Conditional deletion of *ogt* was shown to perturb ER homeostasis, and crucial signaling in beta cells resulting in beta cell failure and diabetes in mice [20]. ER stress induced in this model is similar to the effects seen upon inhibition of OGT in breast cancer cells which our lab has previously examined [21]. It is not surprising that OGT expression is required for beta cell survival as these cells, much like cancer cells, are incredibly metabolic. Targeted deletion of *ogt* in the placenta mimicked phenotypes found in early prenatal stress (EPS) consisting of changes in gene expression which alter response to both endocrine and inflammatory signaling. Offspring of adults containing *ogt* placental deletion had lower body weight and

increased hypothalamic-pituitary-adrenal stress responsiveness. This study strongly implicates OGT expression as an important indicator of maternal stress and a regulator in programming of offspring metabolic- and neuro-development [22]. Deletion of *ogt* in progenitor T cells showed that OGT expression was required for T cell development *in vivo* [23]. OGT expression was also required for transformation of T cell progenitors into T cell acute lymphoblastic leukemia using a different mouse model in the same study, highlighting the importance of this factor in normal T cell biology as well as cancer development in this particular model [23]. This study serves as the first to address the requirement of *ogt* gene expression in a genetic mouse model of cancer. OGA was originally identified in meningioma as an autoantigen and named MGEA5 however, was later determined to act as a hydrolase removing O-GlcNAc modifications from proteins [24, 25]. It was found that the N-terminus of this protein contains the domain responsible for its O-GlcNAcase activity and a C-terminal domain that resembles a histone acetyltransferase (HAT). While this HAT-like domain has been controversial, recently several papers have supported the idea that OGA has HAT activity [24, 26, 27]. Unlike *ogt* deletion which was embryonic lethal, genetic deletion of *mgea5* (OGA) is perinatal lethal and although heterozygous animals were found to be viable, they exhibited gross changes in both transcription and metabolism [28].

The enzymatic activity of OGT is responsive to levels of UDP-GlcNAc which can vary greatly based on tissue and also change during cellular and tissue conditions such as inflammation and nutrient availability [7]. It has recently been suggested that O-GlcNAcylation may serve as a signal on proteins during translation as a mark of protection from proteasomal degradation [29].

It is apparent that OGT and O-GlcNAcylation require strict regulation in normal physiology, as aberrations are found in a variety of pathologies (Figure 4). It has profound effects on many cellular processes including general mechanisms of gene expression. It is presumed that OGT can regulate transcriptional activation as it was found to directly modify Histone 2B (H2B) S112 which correlated with sites of active transcription distributed over multiple chromosomes [30]. OGT was found to interact with and directly modify several Ten-eleven translocation enzymes (TET) family members (TET1, TET2, and TET3) (Figure 5) [31]. These enzymes act to demethylate 5-methocytosine (5mC) DNA bases. O-GlcNAcylation has also been determined to affect methylation specifically through modification of zeste homolog 2 (EZH2) which allows for the methylation modification H3K27me3. Transcriptionally silenced chromatin is found to contain this trimethylation modification on histone 3 [32]. Transcription is regulated on a circadian basis within cells which is also found to be controlled by O-GlcNAcylation. O-GlcNAcylation functions to stabilize the clock proteins ARNTL/BMAL1 and CLOCK which in turn mediate transcription of genes such as PER1/2 and CRY1/2 which are also important core components to the regulation of the circadian clock (Figure 5) [33]. OGT additionally plays a role in repression of transcription through its interaction with the corepressor mSin3A at promoter sites [34]. All of these mechanisms by which OGT and O-GlcNAcylation act to enhance or decrease gene transcription within cells demonstrate the importance of controlling a balance of levels of both OGT and O-GlcNAcylation to ensure proper cellular function. It is clear from many studies showing altered levels of O-GlcNAcylation in disease state that too little or too much compromises normal function and behavior (Figure 4).

1.1.3 Regulation of OGT

While it is clear that both expression and activities of OGT and OGA are responsible for levels of O-GlcNAcylation on target proteins, the affinities of these proteins for O-GlcNAcylated substrate proteins has led researchers to believe that the stronger determinant and therefore the more crucial governing factor is OGT [35]. Since OGT is altered in many disease states, it is imperative to understand what controls OGT expression. The factors involved in transcriptional activation and repression of OGT are largely unknown, although recently several regulatory factors were identified. OGT mRNA expression was upregulated in response to overexpression of the transcription factor Elk1, but its occupancy on the promoter of OGT or ability to bind this region were not examined in this study [36]. E2F Transcription Factor 1 (E2F) was found to bind the promoters of both OGT and OGA and has a role in repressing OGT expression in an Rb-1 dependent manner [37]. In terms of cancer, specifically breast cancer, several reports have examined mRNA expression. While others have reported a correlative change in OGT and OGA mRNA expression with progression of breast ductal carcinoma indicating an increase in OGT and decrease in OGA expression as grades progress [38], our own comparison between normal tissue and several subtypes of breast cancer showed no change in OGT mRNA expression [21]. Expression of OGT mRNA was not found to correlate to overall or metastasis-free survival in breast cancer patients or to show significant changes between normal patient breast samples and diseased breast of various subtypes based on our analysis [21].

OGT protein can be modified by direct O-GlcNAcylation and tyrosine phosphorylation however there are likely other PTMs not yet identified on this protein

[39]. OGT is turned over via proteasomal degradation requiring ubiquitination on OGT [40]. Beyond these modifications, little is known about the regulation of OGT protein expression. In this thesis we will specifically address regulation of OGT protein in breast cancer.

1.2 O-GlcNAcylation and OGT in disease

1.2.1 OGT and neurodegenerative disease

As mentioned above, because of the paramount role O-GlcNAcylation seems to play in maintaining homeostasis of a variety of important cellular activities and systems, and due to its utilization of and requirement for glucose, it is only natural that O-GlcNAcylation would be investigated in the context of the central nervous system (CNS) and that many proteins would be highly O-GlcNAcylated. When Trinidad et. Al examined O-GlcNAcylation in the murine synaptasome they determined 19% of proteins were O-GlcNAcylated. The idea that disruption of glucose metabolism could contribute to diseases of the brain, specifically Alzheimer's disease (AD), along with the high abundance of O-GlcNAcylated proteins in brain has led many to investigate a role for OGT and O-GlcNAc in this pathology. The neuronal glucose transporter GLUT3 is decreased in AD brains leading to compromised glucose metabolism [41]. It was determined that a microtubule associated protein key to the AD phenotype, tau, which becomes aggregated in diseased circumstances, is itself O-GlcNAcylated [42]. It was also determined that in AD, tau is hyperphosphorylated and O-GlcNAcylated less [43, 44]. It is now hypothesized that the alterations in glucose utilization decrease O-GlcNAcylation on tau and increase its hyperphosphorylation. These conditions are consistent with tau

pathology which correlates with severity of dementia [43]. Another neurodegenerative disease, amyotrophic lateral sclerosis (ALS) may also be linked to changes in O-GlcNAcylation. ALS is characterized by accumulation of neurofilamental proteins NF-L and NF-M (the light and medium chains of neurofilament proteins) which are phosphorylated as well as O-GlcNAcylated [45]. In this context, O-GlcNAcyaltion could play a neuroprotective role similar to that hypothesized in AD [46].

1.2.2 OGT and diabetes

Yet another pathology consisting of altered energy and glucose metabolism is diabetes. Determining the unknown underlying mechanisms responsible for the development of this disease is important because 7.8 % of the United States population is diagnosed with diabetes [47]. Type 2 diabetes is characterized by elevated blood glucose and insulin insensitivity. A normal liver should activate insulin receptor when bound to insulin, recruiting insulin receptor substrate (IRS1 or IRS2). Ultimately this activation results in translocation of the glucose transporter GLUT4 to the membrane through PI3K/AKT [47]. IRS1 is O-GlcNAcylated on at least three sites resulting in altered phosphorylation status of this protein and subsequent attenuation of insulin signaling [48]. OGT also O-GlcNAcylates PI3K and AKT [47]. It is suggested that O-GlcNAc could be a biomarker of prediabetes since elevated blood glucose levels could increase levels of O-GlcNAcylation in red blood cells [49].

1.2.3 OGT and Cancer

Elevated O-GlcNAcylation has been observed in various cancer types, and inhibiting O-GlcNAcylation reduces several cancer phenotypes. The Warburg hypothesis (discussed

more thoroughly in later chapters) states that cancer cells display altered metabolic features in order to support their rapid growth and biosynthetic demands. It is also characterized by increased glycolytic flux, even in the presence of oxygen, in order to synthesize necessary building blocks required by rapidly growing cells [50]. It is currently understood that this shift is supported by oncogenic mutations allowing not only for increased uptake of metabolites such as glucose but also for the continual consumption of such metabolites in synthetic processes [50]. Recently, much attention has been given to understanding the therapeutic potential of targeting metabolic pathways in cancer, as these highly proliferative cells are incredibly dependent upon these pathways for their sustained growth and survival.

This increased glycolytic flux observed in cancer cells feeds not only glycolysis but to other glucose dependent pathways as well, such as the Hexosamine Biosynthetic Pathway (HBP), which as described above, provides the substrate to OGT for O-GlcNAc modification [4, 51]. It is not surprising that a nutrient sensitive modification would be altered in conditions where more glucose and glutamine are available and utilized differently. O-GlcNAcylation provides a driver of tumorigenic phenotypes as many modified proteins have roles in oncogenesis [52]. These proteins include well known and highly influential factors such as; c-Myc, AKT, PI3K, SP1 and p53 [53-56]. When examining the effects of this modification on oncogenic drivers, it is important to remember that O-GlcNAcylation can modulate a proteins function by altering stability, localization, protein-protein interaction, phosphorylation status, and/or DNA binding ability [57]. With regard to biological results, modulation of cellular O-GlcNAc levels has been linked to altered cellular development, mitotic progression, growth and survival

patterns [58]. Hyper-O-GlcNAcylation appears to be a common feature of various cancers as elevation of OGT and this modification have been observed in breast [59], prostate [60], lung, colorectal, liver, and pancreatic malignancies [61]. It also appears that this modification exerts influence over many hallmarks of cancer including angiogenesis, invasion, proliferation, and survival (Table 1).

Our lab was the first to show that both O-GlcNAcylation and OGT levels are increased in breast cancer cells (Table 1) and that reduction of OGT and O-GlcNAcylation in cancer cells results in decreased growth and metastasis *in vivo* [59, 60]. Inhibition of OGT and O-GlcNAcylation was shown to activate the cellular nutrient sensor 5' AMP-activated protein kinase (AMPK) and induce apoptosis in breast cancer cell lines through ER stress pathway activation. However, reducing OGT levels in normal immortalized mammary epithelial cells had no effect on these pathways. Thus, cancer cells are more sensitive to inhibition of O-GlcNAcylation [21].

As mentioned above, critical regulators of oncogenesis, including the c-Myc oncogene [53], the tumor suppressor p53 [63], and viral oncoprotein SV40 large T antigen [64], have been previously shown to be O-GlcNAcylated lending the idea that O-GlcNAcylation may play a key role in the pathogenesis of tumors [65, 66]. A critical role of O-GlcNAcylation on NF-□B [67] function, combined with work in our lab provided the first evidence that total O-GlcNAcylation and OGT was required for tumor growth *in vitro* and *in vivo* [59]. A number of groups have subsequently shown that OGT and O-GlcNAcylation levels are elevated in various different epithelial cancers including breast [68, 69], prostate [60, 70], lung [71], colon [72], liver [73], bladder [74] as well as in chronic lymphatic leukemia (CLL) (Table 1) [75]. A critical role for O-GlcNAcylation in

cancer metabolism emerged as OGT was found to be required for expression of a major glycolytic driver, hypoxia-inducible factor (HIF-1α), along with its transcriptional target glucose transporter 1 (GLUT1) [21, 59, 62]. This mechanism is critical for breast cancer cell survival both *in vitro* and *in vivo* [76]. O-GlcNAcylation has also recently been shown to influence the Pentose Phosphate Pathway (PPP) through regulation of Phosphofructokinase 1 activity [71]. In some cancers, increased total O-GlcNAcylation may be due to increased OGT levels and/or decreased OGA levels as seen in breast [76, 77], liver [73] and colon [78] cancers. Specificity Protein 1 (SP1) transcription factor is elevated in a variety of cancers including glioma, pancreatic, lung, breast, gastric and thyroid cancer and is directly O-GlcNAc modified [79]. This modification stabilizes SP1 protein in the context of diabetes and increases in transcriptional activity in both diabetes, hyperglycemia in retinal cells and lymphoma [80-82]. While it has become evident that OGT and O-GlcNAc play critical roles in cancer metabolism and survival, it remains unclear how OGT is elevated in cancer cells.

1.3 Figures and Figure Legends

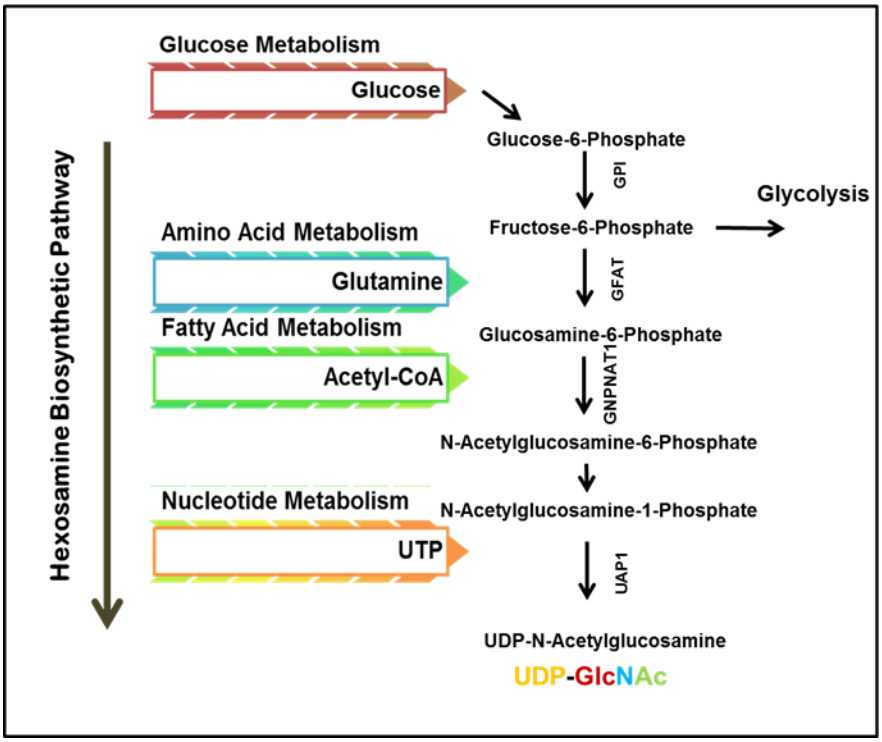

Figure 1: Hexosamine Biosynthetic Pathway The hexosamine biosynthetic pathway diverges from glycolysis at fructose-6-phosphate and combines metabolic intermediates from amino acid, fatty acid and nucleotide metabolism to generate the amino-sugar UDP-GlcNAc. The rate limiting enzyme in this pathway is GFAT.

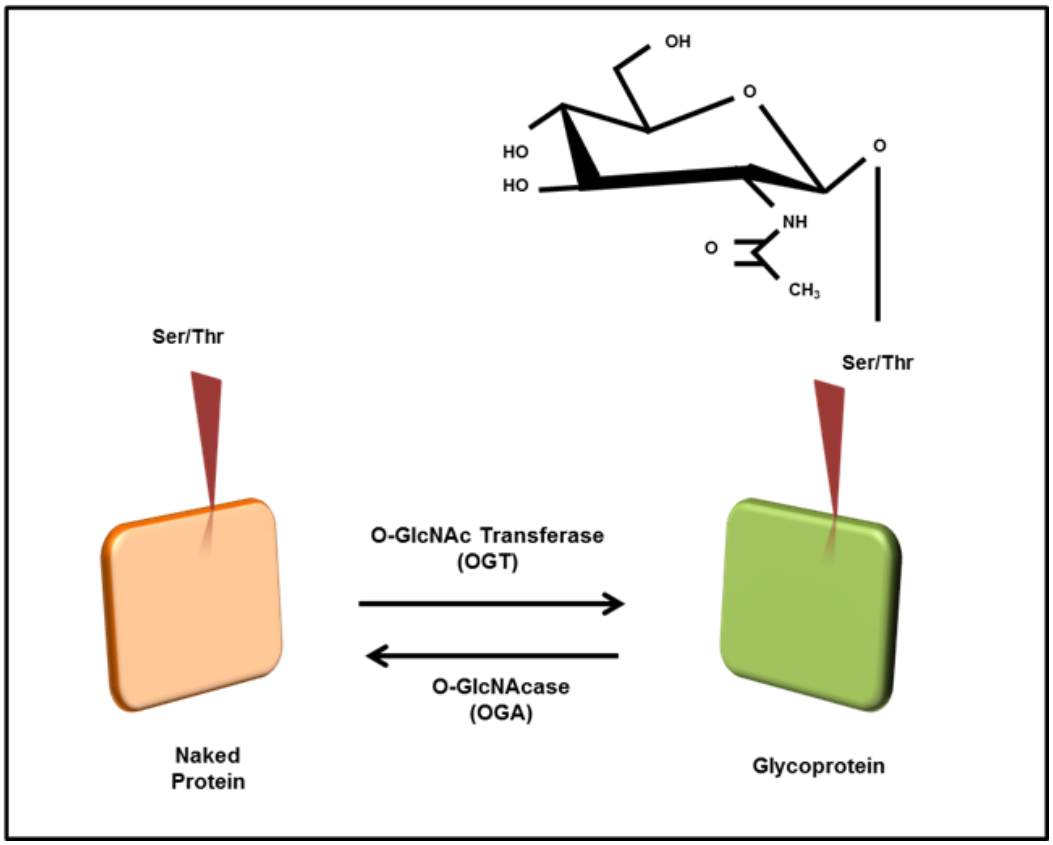

Figure 2: O-GlcNAcylation

Diagram depicting the dynamic and reversible O-GlcNAc modification in which N-Acetylglucosamine is attached to serine and threonine residues of target proteins via O-GlcNAc Transferase (OGT) and removed by O-GlcNAcase (OGA)

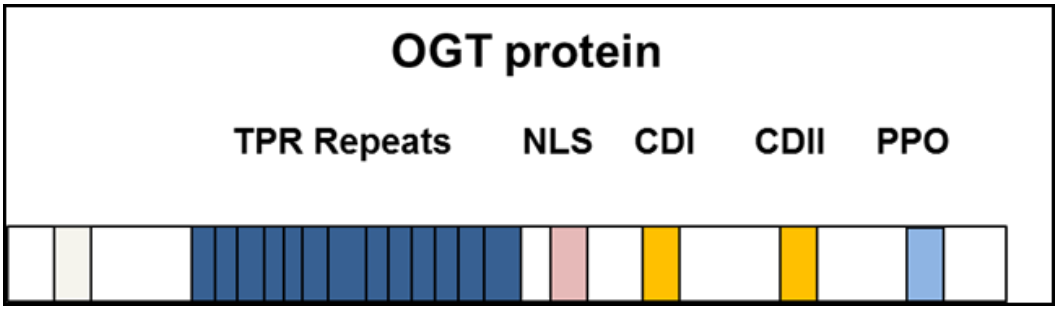

Figure 3: O-GlcNAc Transferase

Full length human OGT contains 13 tetracopeptide repeat domains (TPR) which facilitate interaction with other proteins, and two catalytic domains (CDI and CDII) separated by a nuclear localization domain (NLS). Adjacent to the CDII at the C-terminus, OGT protein has a PPO domain responsible for binding phosphoinositide species.

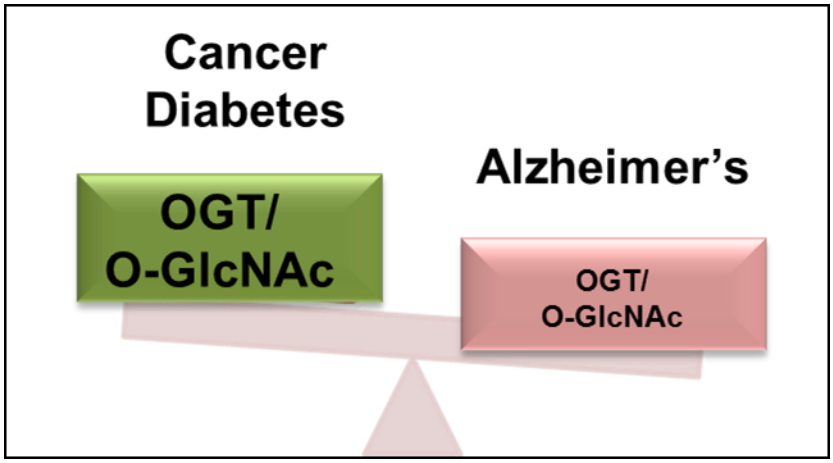

Figure 4: O-GlcNAcylation and OGT levels in disease

OGT/O-GlcNAcylation is elevated in a wide variety of cancers as well as diabetes. This modification is globally decreased in Alzheimer's disease which corresponds to an increase in OGA and a decrease in OGT.

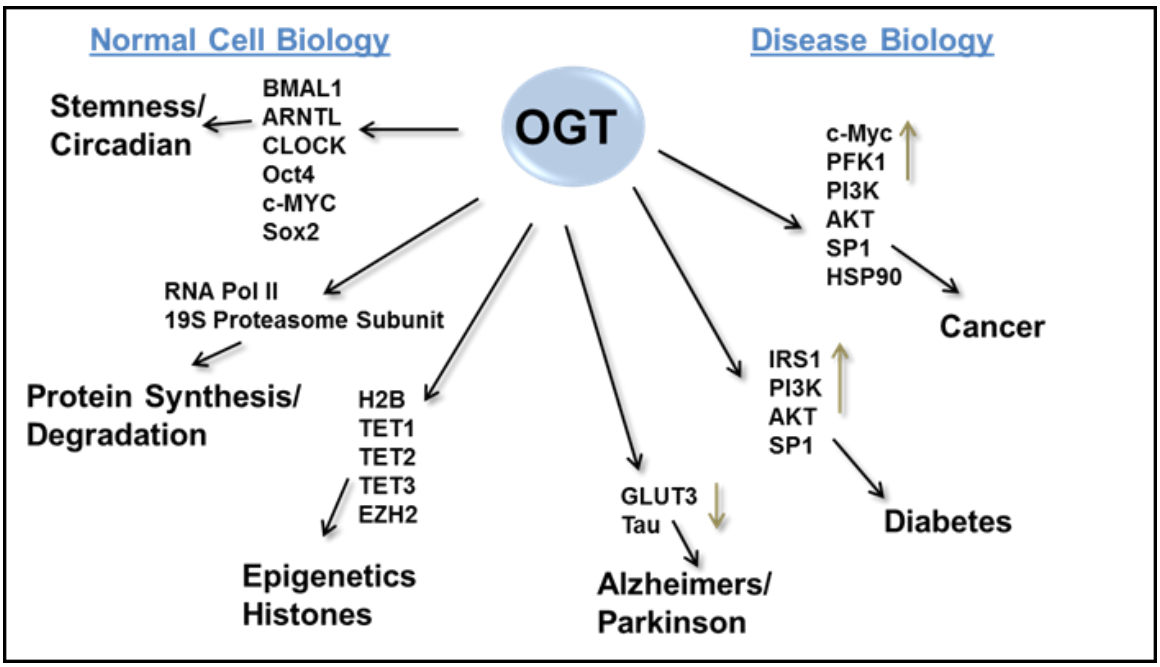

Figure 5: OGT relevance in normal biology and disease

OGT directly O-GlcNAc modifies many known proteins in normal biology acting to regulate stemness, circadian rhythm, protein degradation and synthesis and epigenetics. Many of these proteins are deregulated and have altered levels of O-GlcNAc modification which directly contributes to or correlates with disease states including cancer, diabetes and Alzheimer's disease

Cancer:	Expression:	Refs:
Breast	*Elevated OGT/O-GlcNAc in cancer cells and OGT RNA elevated in invasive breast cancer; OGT increase, OGA decrease associated with grade, lymph node metastasis; OGA levels decrease associated with poor overall survival; O-GlcNAcylation/OGT increased in primary malignant tumors compared to benign tumors*	*Oncogene 2010* *Cancer Research 2010* *Clin Exp Med. 2012* Proteomics 2013
Prostate	*Elevated OGT/O-GlcNAc in cancer cells; OGT increase associated with progression and poor survival; increased OGT associated with high Gleason Score and correlates with Myc expression*	*J. Biol Chem 2012* *Cancer Research 2013*
Lung	*O-GlcNAcylation and OGT levels (IHC) are elevated in lung squamous cell carcinoma tissue compared to adjacent lung tissue; PFK-1 is hyper-O-GlcNAcylated in cancer tissue.*	*BBA 2011* *Science 2012*
Liver	*O-GlcNAcylation elevated (IHC) in* hepatocellular carcinoma compared to healthy liver; O-GlcNAcylation elevated in recurrent HCC patients; Low OGA expression predicts metastatic recurrence in HCC patients.	*Med Oncol 2012*
Colon	O-GlcNAcylation and OGT elevated in colon cancer tissue compared to adjacent colon tissue; SW620 metastatic clone contains increased O-GlcNAcylation and decreased OGA expression compared to primary clone, SW480	*BBA 2011* *J Biol Chem 2012*
Bladder	OGT transcript level was significantly higher in grade II and III in comparison to grade I bladder cancer; significant increase in OGT expression between early bladder cancers and invasive or advanced bladder cancers	Clin Lab 2012
Pancreatic	*Elevated O-GlcNAcylation, OGT and decreased OGA found in human pancreatic cancer cell lines compared to non-tumorigenic pancreatic epithelial cells.*	*J Biol Chem 2013*
Leukemia	*Chronic lymphocytic leukemia patients contain elevated O-GlcANcylation compared to normal circulating B cells*	*Leukemia* 2010

Table 1: OGT/O-GlcNAc and OGA status in different cancer types

OGT (transcript or protein) and/or O-GlcNAc are elevated in all cancers listed. OGA levels were determined to be decreased in or correlate with survival in several cancers examined. Citations provided for work summarized in table.

CHAPTER 2: BREAST CANCER OVERVIEW AND CANCER METABOLISM

2.1 Breast Cancer Overview

2.1.1 Breast Cancer Subtypes

Breast cancer is a heterogeneous disease developing as a consequence of genetic mutation influenced by a variety of factors. Globally, deaths attributed to this disease are estimated at 450,000 annually [83]. Looking more specifically at the United States, it is estimated that 1 in 8 women will develop breast cancer in their lifetime and it is the second most lethal cancer in U.S. females [84]. Despite increased ability of detection and treatment, insight into biological heterogeneity remains incomplete. Stratification and classification by molecular markers has greatly improved treatment guidelines and our understanding of prognosis and risk factors. Extensive characterization of genetic profiles of breast cancer (DNA or mRNA instead of histology) has resulted in classification into 4 main subtypes of breast cancer [83, 85]. These subtypes consist of luminal A, luminal B, HER2-enriched and Basal-like. Molecular markers related to both luminal A and B subtypes are involved in proliferation and cell cycle as well as hormonal/luminal signaling [83]. Luminal breast cancers represent the majority of hormone receptor (HR)+/ HER2- cancers. When comparing luminal A and B, luminal B has higher expression of proliferative markers and less expression of luminal markers like progesterone receptor (PR). HER2-enriched subtype cancers have high expression of the receptor tyrosine kinase ErbB2/HER2, moderate expression of luminal genes and very low expression of basal-like genes. This subtype has the most genomic mutations and a high percentage of P53 mutation (72%) [83]. Basal-like breast cancers have the highest P53 mutations

(80%), high expression of keratins normally found expressed in the basal epithelium and moderate to low expression of HER2 and luminal markers. Basal-disease is also associated with BRCA mutations and aggressive clinical presentation [83]. Historically triple-negative (TN) and basal-like have been used interchangeably and most TN breast cancers (thought of as ER-,PR-,HER2-) qualify as basal-like (86%). When Prat et. Al examined almost 900 TN tumors, 86.1%, 9.1%, 3.2% and 1.6% were identified as basal-like, HER2+, luminal B and luminal A respectively highlighting that characterization is strong however imperfect when pathology and molecular markers are taken into account [83].

2.1.2 Breast Cancer Development

The hallmarks of cancer not only outline the biological changes required to define a malignant cell but also put forth a model by which progressive evolution from a normal cell to a malignant cell occurs. This model dictates that genetic instability (combinations of epigenetic and genetic changes) which is also considered a hallmark of cancer, occur over time generating the genetic diversity that result in behavioral differences allowing for the ability of cells to escape confinements of normal cells and proliferate rapidly. Through alterations in signaling driven by genomic modifications, cancer cells also meet each category/hallmark, including things such as; immune and apoptotic avoidance, sustained proliferation and angiogenesis, altered metabolic regulation and invasion and metastasis [86]. Breast cancer exists as a wildly heterogeneous disease exhibiting both inter- and intra-tumoral diversity. This variety stems from the range of cell types which comprise breast tumors as well as the differences in genetics within cells. Broad groupings based on molecular expression (outlined above) has aided in classifying patient

tumors into subtypes, dictating treatment strategy and predicting tumor progression and outcome. Development of breast cancer, regardless of subtype, is initiated and driven by genetic changes attained as well as influence from tumor microenvironment. Family history is one of the strongest determinants of risk, along with the well-documented risk factor – age [87]. Well known DNA repair genes (namely BRCA1, BRCA2 and TP53) can contain germline mutations accounting for excess risk of cancer development [88]. However, the excess risk added by the occupancy of these high-penetrance mutations is low leading researchers to believe that moderate and low-penetrance heritable mutations may account for other cases [88]. Pathological breast cancer initiation and progression involves ductal hyperproliferation, ductal carcinoma in situ (DCIS), and finally malignant invasive disease [88]. The evolution from accelerated proliferation and escape from growth restraints to metastasis requires that cells degrade the physical barrier of the basement membrane, leave the primary site via vasculature, survive in circulation and then seed and proliferate at metastatic sites (Figure 7) [88]. Cancer development and progression are influenced by the microenvironment which consists of cells both surrounding and integrated into the tumor. These include endothelial cells, cancer-associated fibroblasts, inflammatory immune cells, bone marrow-derived stromal cells and cancer stem cells [86]. It was previously hypothesized that mutation occurred in a preferred order, whereby each new mutational step led to clonal expansion of cells containing that mutation increasing the probability of multiple mutations occurring within the same cell [89]. Stepwise mutational changes resulting in the development of cancer are clear in particular cancer types such as colorectal however do not account for the vast molecular subtypes found in other cancers like breast cancer. Breast cancer may require

much more complex models to explain neoplastic changes and heterogeneity [83, 89]. Both epidemiological and human tumor analysis suggest that breast cancer arises from two distinct mammary cell types resulting in basal-type and non-basal subtypes [83].

Incredible changes in both genetic and epigenetics within cells contribute to the development of breast cancer. Somatic mutations, altered protein and miRNA (microRNA) expression, copy number changes and acetylation and methylation deregulation all contribute to the pathogenesis of cancer and the development of cancer progenitor cells [84]. When examining somatic mutation in coding exons within 100 tumors, Stephens et. Al. found nearly 7,500 somatic point mutations in 21,416 genes that code for protein. While individual tumors mutation numbers were very diverse, many mutations occurred in genes classified as oncogenes or tumor suppressors such as BRCA1, TP53, AKT1, PTEN, RB1, KRAS and PI3KCA. Somatic mutations were found in 10% of all breast cancers in PI3KCA, TP53 and GATA3 in analysis by the Cancer Genome Atlas. Interestingly, within molecular subtype, mutation number as well as type differed. One example of this is TP53 mutations which generally contained missense mutations in luminal A and B subtypes but often contained frameshift and nonsense mutations in basal-like breast cancer [85].

2.1.3 Breast Cancer Treatment

Receptor status/molecular subtype of breast cancer aids in predictive response to particular therapies and is used to dictate therapy. In the case of suspected metastasis, biopsies are performed to confirm the presence of secondary tumors and molecular subtype [90]. Metastatic disease outcome has been improved through treatment with

targeted therapies against HER2 in HER2-enriched breast cancer and endocrine therapies in ER+ and PR+ breast cancers. Metastatic disease that is ER+, PR+ and even HER2+ will eventually develop resistance to endocrine and HER2 targeted therapies requiring cytotoxic chemotherapy [90]. Currently there are not effective targeted therapies available for the treatment of TN breast cancer, which is quite aggressive [91]. Metastatic disease will eventually exhaust available chemotherapeutic options which is why is it incurable [90]. Treatment failure and recurrence or persistence of disease can result from intrinsic resistance to standard therapies that exists in cells prior to treatment or resistance that is developed through acquired mechanisms resulting from treatment [92].

Mechanisms to overcome resistance are being explored in all subtypes of breast cancer. A persistent risk of recurrence exists even in early stage ER+ breast cancer patients which is only modestly reduced by extending treatment periods for endocrine therapy [90, 93]. The dormancy of tumor cells within the system is thought to be responsible for recurrence in patients who experience long periods between initial treatment and development of relapse [90]. Some have determined that metastatic ER+ breast cancers have either mutant ER, or deregulated downstream factors such as PI3K/AKT or mTOR. A strategy for overcoming developed resistance and recurrence could be targeting these other factors [90]. A second strategy to combat resistance to endocrine therapy is to downregulate ER using agents such as fulvestrant in combination with endocrine therapy. Benefits to combinations depended on prior patient treatment as well as dosing and addition of other therapies [90]. Impressive pre-clinical and phase 2 results in combination treatment with cell-cycle kinase inhibitor palbociclib and tamoxifen or letrozole (both hormone therapies) led to approval of these combinations for treatment of

some metastatic ER+ breast cancers [90]. The standard of care in the treatment of HER2+ breast cancer is the use of targeted therapies such as lapatinib, pertuzumab, and trastuzumab emtansine [90]. Many mechanisms of resistance have been found to these targeted agents including several that activate downstream pathways despite blocking HER2 or receptors with which HER2 binds to activate signaling. These downstream pathways consist of PI3K (also responsible for resistance in ER+ breast cancer as mentioned above), ERK signaling pathway, and mTOR [94]. Mutations in HER2 itself or loss of HER expression can also account for resistance to HER2-targeting agents [95, 96]. Targeting these downstream effectors, as mechanisms of resistance involving them are revealed, is currently underway with testing the addition of mTOR inhibitors and MEK inhibitors to HER2 targeted therapies [94, 97]. Targeted agents are needed for the treatment of TN breast cancer as current strategies employed to treat this subtype of breast cancer are limited to more general chemotherapeutic agents. Platinum treatment has emerged as a beneficial treatment agent in some patients as well as the use of poly(adenosine diphosphate-ribose) polymerase (PARP) inhibitors specifically in *BRCA* mutant patients [90]. The expansion of clinical trials to include the use of new agents, as more mechanisms of resistance are unveiled have and will undoubtedly lead to better outcomes in patients through revision of treatment options available. This is precisely why persistence in expanding our knowledge of signaling pathways that regulate cancer cell growth and survival and their interplay with current targets for therapy, along with identification of novel targets in different types of breast cancer are required and important.

2.2 Cancer Cell Metabolism

2.2.1The Warburg Effect

Cancer cells exhibit altered metabolism characterized by increased glucose and glutamine uptake to promote glycolysis in the presence of normal oxygen conditions [50, 98]. This modified metabolic state, known as the Warburg effect, allows cancer cells to acquire a large allotment of nutrients from their environment, a phenomenon that is widely used *in vivo* to monitor tumor growth using 2FDG-PET imaging [50, 98]. Although this use of nutrients is inefficient in terms of the amounts of ATP produced, a sizeable amounts of carbon and nitrogen in the form of lactate and ammonia are secreted from cancer cells into the extracellular environment. These excreted nutrients can then be taken in by neighboring tumor cells for use as fuel. Aerobic glycolysis maintains an adequate amount of carbon backbones for macromolecular synthesis in the form of acetyl-CoA, NADPH and amino acids important in providing the biomass required for cancer cell growth and proliferation in conjunction with maintaining a redox balance by means of production of large amounts of NADPH [98, 99].

2.2.2 Drivers of altered metabolism

It is now understood that this metabolic phenomenon first reported by Otto Warburg [100], is generated largely through oncogenic activation of signal transduction pathways and transcription factors as well as loss of tumor suppressors [101-104]. The phosphatidylinositol-3-kinase (PI3K)/Protein kinase B (or AKT)/mechanistic target of rapamycin (mTOR) is an important pathway (Figure 6) that lies downstream of receptor tyrosine kinase (RTK) activation and is known to be deregulated in a wide majority of cancer types [101, 104, 105]. Ligand binding to RTKs upstream activates PI3K which in turn results in phosphorylation of phosphoinositol lipids at the plasma membrane. This

activation then recruits and triggers AKT. PI3K activity is under regulation by the tumor suppressor phosphatase and tensin homolog (PTEN), however many transformed cells contain inactivating mutations in *PTEN* [104]. The PI3K/AKT pathway directly contributes to altered metabolism of cancer cells by inducing cells to take up excess glucose via regulation of glucose transporters [50, 102] and via activation of the mechanistic target of rapamycin complex 1 (mTOR1) signaling pathway [106]. In response to changes in energy status, regulation of cell growth by AKT is mediated through downstream phosphorylation and inhibition of tuberos sclerosis complex 1/2 (TSC1/2), a factor which acts to inhibit mTORC1. The mTOR pathway senses the energy status of a cell in response to a number of environmental cues and in turn alters cell growth and metabolism. One factor in energy status is amino acid availability which activates mTORC1-dependent translation factors 4E-binding protein 1 (4E-BP1) and p70 S6 kinase 1 (S6K1) to enhance protein synthesis of main transcription factors that control metabolism such as c-MYC, sterol regulatory element binding protein 1 (SREBP-1), and hypoxia inducible factor 1-alpha (HIF-1α) [101]. c-MYC and SREBP-1 relation to OGT/O-GlcNAcylation will be discussed in depth later in this thesis.

The oncogenic transcription factor c-MYC is overexpressed in many cancer types. Despite its prevalence for deregulation it is very infrequently mutated in coding sequence [107]. c-Myc is elevated at the protein level through amplification, chromosomal translocation and post-translational modification including phosphorylation [107]. Binding to DNA and transcriptional activity requires binding to its obligatory partner MAX as it functions as a heterodimer in combination with this protein [107]. c-Myc promotes glutamine uptake and utilization via transcription of several of its targets

(Figure 6) [108]. This yields nitrogen required to synthesize nucleotides and amino acids [98]. In addition, glutamate production dependent on c-MYC, acts to feed the TCA cycle whose intermediates react to increase NADPH production, thus maintaining the redox balance in cancer cells [98, 109]. The oncogene c-MYC is involved in the regulation of cell cycle progression, cell growth, glucose uptake and glycolysis and is commonly amplified in breast cancer [110]. Moreover, MYC overexpression is associated with highly aggressive clinical features correlating with poor patient outcome [111].

As mentioned above SREBP-1 functions as a transcription factor downstream of mTORC1. SREBP-1 acts to induce expression of genes involved in *de novo* fatty acid biosynthesis providing membrane components for the generation of new cells [101]. High SREBP-1 expression is associated with poor prognosis in a number of cancer types, and has been shown to sustain cancer cell growth and survival through lipogenic functions [112, 113].

In the progress of cancer growth, rapid cellular proliferation removes tumors from proper proximity to the blood supply generating low oxygen tension, or hypoxia [114, 115]. When exposed to these conditions, hypoxia inducible factor (HIF-1αβ) functions to promote cell survival through induction of transcriptional targets including glucose transporters and glycolytic genes as well as angiogenic factors to promote restoration of oxygen concentration [115]. HIF-1 transcription factor consists of HIF-1α which is stabilized in the absence of oxygen, and a constitutively expressed binding partner HIF-1β which bind together at hypoxic regulatory elements in promoters of target genes [115]. Prolyl hydroxylation occurs at two proline residues on HIF-1α, when oxygen is ample, allowing for ubiquitination and recognition of HIF-1α by its E3 Ubiquitin ligase von

hippel lindau protein (pVHL) [115]. This precedes HIF-1α ubiquitination and proteasomal degradation, which is perturbed in hypoxic environments. Some renal cancers contain germline loss-of-function mutations in *VHL* [115]. Low oxygen concentration is associated with increased metastasis and decreased survival in breast and ovarian cancer patients and can result from resistance to radiation and chemotherapy [115, 116]. Several mechanisms exist in which HIF-1α protein expression may be increased independent of oxygen concentration [115].

Another important pathway downstream of activated RTKs is the RAS/RAF/MAPK pathway (Figure 8). This functions to regulate both normal cell growth and malignant transformation [104]. Glucose uptake and utilization to feed anaerobic glycolysis and the uptake of lysophospholipids contributing to lipid pools and energy are driven by mutations in oncogenic *Ras* in some cancers [104, 117, 118].

Metabolism and energy homeostasis are controlled at least partly through the liver kinase B1 (LKB1)/AMP-activated protein kinase (AMPK) signaling axis [119, 120]. AMPK acts through sensing and responding to changes in the cellular AMP to ATP ratio as it functions to block growth pathways that consume metabolic precursors and cost energy [119-121]. A major task for AMPK is inhibiting mTORC1 through phosphorylation of the TSC1/2 complex and mTORC1 complex protein RAPTOR which blocks the kinase activity of mTOR [119, 122]. Loss of tumor suppressor *LKB1*, which acts upstream of AMPK, in somatic cells is associated with the progression in a variety of cancers (Figure 8) [119]. This nutrient sensor and mitogenic restraint is a crucial factor in cancer development, progression and survival and is viewed as a potential area where therapeutics may be developed [123].

2.3 Figures and Figure Legends

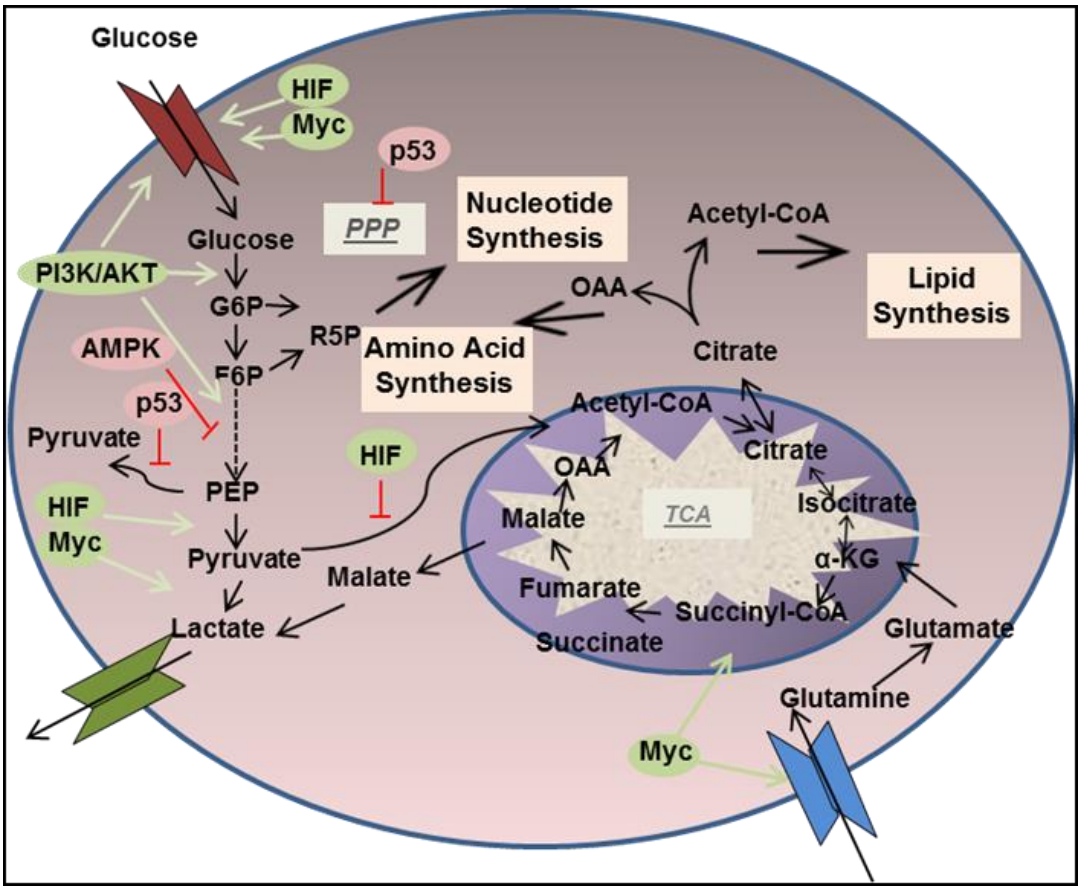

Figure 6: Warburg Effect: Metabolism in Cancer

Diagram of metabolism in cancer cells. The rate of glucose uptake in cancer is achieved through upregulation of glucose transporters through oncogenic signaling. This glucose is utilized through glycolysis (driven by oncogenes and inhibited by tumor suppressors that are often downregulated) to produce more lactate that is secreted from the cell. Glycolytic intermediates are diverted through the pentose phosphate pathway (PPP) to support nucleotide synthesis. Glutamine uptake is also upregulated by oncogenes feeds to the TCA cycle which also utilizes pyruvate. Lipid synthesis is supported by citrate derived acetyl-CoA as amino acid synthesis is supported by citrate derived oxaloacetate (OAA). G6P (Glucose-6-Phosphate), F6P (Fructose-6-Phosphate), PEP (Phosphoenolpyruvic acid), R5P (Ribose-5-Phosphate), αKG (alpha-Ketoglutarate).

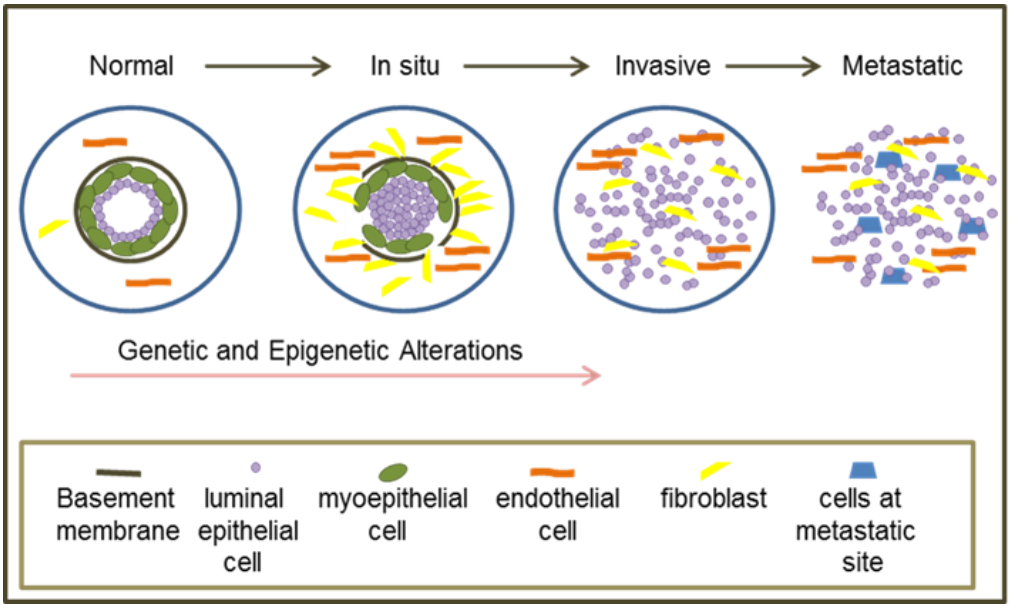

Figure 7: Model of breast cancer progression

Normal breast cells are contained by a basement membrane and organized, polarized layers of luminal epithelial and myoepithelial cells. Through genetic and epigenetic alterations, normal cells become hyperproliferative. Influences from the microenvironment come from different cell types including fibroblasts and endothelial cells. Transitions from an in situ state to invasive status required degradation of the basement membrane and escape from containment as well as survival through the travel to a metastatic site where cancer cells seed and proliferate.

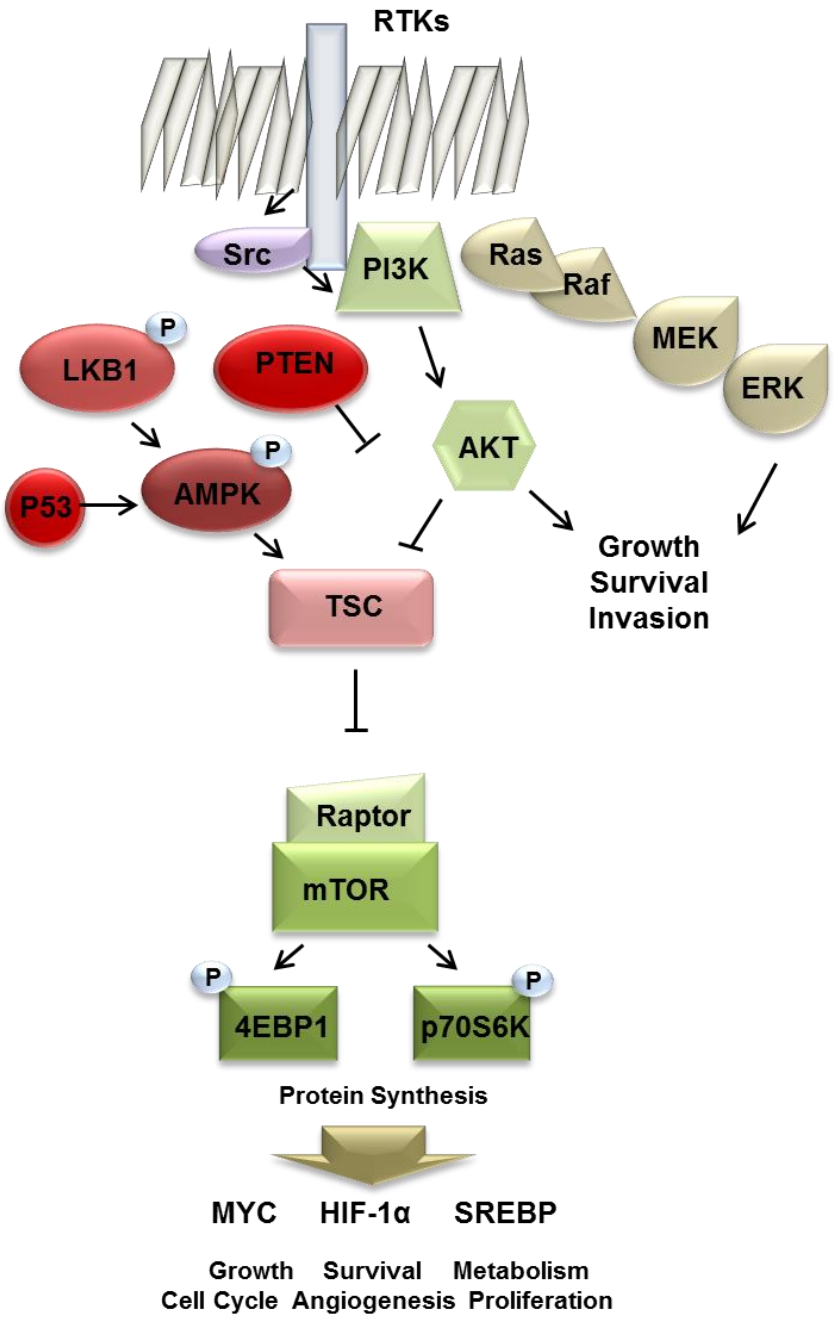

Figure 8: Major Signaling pathways in cancer Receptor Tyrosine Kinases (RTKs) can activate downstream signaling to promote cancer cell growth and survival, angiogenesis, cell cycle and promote the Warburg Effect. Downstream pathways such as the Ras/Raf/MEK/ERK and PI3K/AKT mTOR are required for these processes through upregulation of specific transcription factors. These can be upregulated through amplification and upregulation of oncogenes and loss of tumor suppressors.

CHAPTER 3: PI3K/MTOR/MYC AXIS REGULATES OGT EXPRESSION IN BREAST CANCER

3.1 Introduction:

Here, we show that the master nutrient signaling PI3K/AKT/mTOR pathway is required for elevation of OGT and O-GlcNAcylation in breast cancer cells. We also demonstrate that hyperactivation of AKT or mTOR is sufficient to elevate OGT protein and O-GlcNAcylation levels. Downstream of mTOR activation, we observe that c-MYC is required and sufficient to drive OGT protein elevation and increase O-GlcNAcylation in cancer cells via c-MYC regulation of HSP90A. Importantly, we show that Myc-driven cancer cells elevate OGT and O-GlcNAcylation and require OGT activity for cancer cell survival. Our data is the first to link mTOR/MYC activity to increased OGT/O-GlcNAcylation that contributes to the oncogenic phenotype seen in multiple cancers.

3.2 Results

3.2.1 O-GlcNAcylation and OGT levels require PI3K and mTOR activation in cancer cells

We have previously demonstrated that breast cancer cells contain elevated OGT and O-GlcNAcylation levels compared to normal mammary epithelial cells [59]. In addition, stable overexpression of the active form of the receptor tyrosine kinase ErbB2/HER2 in non-transformed mammary epithelial MCF-10A cells resulted in elevated OGT and O-GlcNAc levels [59]. Since ErbB2 activation stimulates numerous signaling cascades including PI3K/AKT, Ras/MEK/ERK and mTOR [111], we examined which signaling pathway was responsible for increased OGT and O-GlcNAc levels in breast cancer cells

(Figure 9). We aimed, through these studies, to determine how OGT protein was regulated in breast cancer since little was known of its regulation in either cancer or normal cells. We had previously found that mRNA of OGT was not significantly increased in any breast cancer subtypes examined compared to normal samples which leaves a question as to how OGT protein is elevated in breast cancer [21]. We tested a panel of breast cancer cells that represent different subtypes including: estrogen receptor positive (MCF-7 cells), ErbB2/HER2 positive (SKBR-3 cells), and triple negative/basal breast cancers (MDA-MB-231 and SUM-159 cells) [124]. We expected that inhibition of one or several pathways/axes would result in reduced OGT protein expression providing us with insight into what lay upstream of OGT. Cells were treated with vehicle control (DMSO) or pharmacological inhibitors against the PI3K, mTOR and MEK signaling pathways (Figure 9). Treatment of all breast cancer cells with PI3K (LY294002) and mTOR inhibitor (Rapamycin) reduced O-GlcNAc levels compared to control and decreased OGT protein levels (Figure 10-11). Treatment of breast cancer cells with PI3K inhibitor (LY294002) significantly reduced OGT levels in MDA-MB-231, SKBR-3, MCF-7 but not SUM-159 cells. Inhibition of MEK (U0126) had negligible effects on OGT levels and O-GlcNAcylation (Figure 10-11). These data suggest that the PI3K /mTOR pathway is a key regulator of OGT and O-GlcNAc levels in multiple breast cancer cell lines with different genetic origins. To determine if the PI3K/mTOR pathway regulates OGT at the level of RNA, quantitative real-time PCR (qRT-PCR) was performed. Treatment of breast cancer cells MDA-MB-231, MCF-7, SKBR-3 and SUM-159 (Figure 10-11) with inhibitors of PI3K, mTOR or MEK pathways did not significantly reduce OGT RNA levels suggesting that PI3K/mTOR-mediated regulation

of OGT protein levels is RNA-independent. Interestingly, protein levels of OGA were not elevated in breast cancer cells treated with PI3K or mTOR inhibitors (Figure 12) suggesting that the decrease in O-GlcNAcylation caused by inhibitors of PI3K/mTOR pathway is primarily a result of diminished OGT protein levels. Thus, OGT protein and global cellular O-GlcNAcylation levels are maintained in breast cancer cells via PI3K and mTOR activation independent of OGT mRNA regulation.

3.2.2 AKT or mTOR activation is sufficient to elevate OGT protein expression and O-GlcNAcylation

Since cancer cells require PI3K and mTOR activation to maintain OGT and O-GlcNAc levels, we examined whether these pathways were sufficient to increase OGT and O-GlcNAcylation levels. PI3K can activate many pathways including the kinase AKT (Protein Kinase B) [125]. To determine whether AKT activation alone was sufficient to increase OGT and O-GlcNAc levels in epithelial cells, we stably overexpressed an active form of AKT1 (Myr-AKT1) in the normal mammary epithelial cell line MCF-10A. Cells stably expressing Myr-AKT contained increased phosphorylated AKT and activated mTOR pathway as measured by phosphorylation of p70 S6 kinase (S6K) (T389) as well as elevated OGT protein levels and increased overall protein O-GlcNAcylation compared to control cells (Figure 13A). Consistent with the MEK-inhibitor results, MCF-10A cells overexpressing a constitutively active form of MEK2 (MEK2-DD) did not alter OGT and protein O-GlcNAcylation levels (Figure 15A). This result is notable since MCF-10A-MEK2-DD cells have a pronounced phenotype when cultured in a three-dimensional (3D) culture system (Figure 15B) that allows bypass of growth suppression and anoikis resistance [126]. This result

demonstrated that OGT and O-GlcNAcylation levels are not elevated simply as a result of hyperproliferation which is important in concluding that OGT protein is specifically regulated by the PI3K/AKT pathway. We conclude that activation of the AKT pathway, but not MEK/ERK pathway, is sufficient to elevate OGT and O-GlcNAcylation levels in human breast epithelial cells.

To test whether mTOR activation is also sufficient to increase levels of OGT and O-GlcNAcylation, we examined OGT/O-GlcNAc levels in mouse embryo fibroblasts (MEFs) containing deletion of *TSC2*. As mentioned previously, TSC1 and TSC2 are components of a complex that negatively regulates mTORC1 nutrient signaling and interestingly, inactivation of either *TSC1* or *TSC2* results in elevated mTOR activity, is associated with uncontrolled cell growth and division and is linked to benign tumor growth [106]. To determine if mTOR activation was sufficient to increase OGT and O-GlcNAc levels, wild-type and *TSC2* deficient MEFs were analyzed. As expected, basal phosphorylation levels of mTOR targets p70 S6K (T389) and 4EBP1 (T70) were elevated in the *TSC2* null cells compared to wildtype MEFs (Figure 13B) verifying constitutive mTOR activation. Interestingly, *TSC2* null cells showed elevated OGT and O-GlcNAc levels (Figure 13B-C) further implicating the mTOR pathway in the regulation of O-GlcNAc cycling. However, *TSC2* null cells also displayed significantly lower OGA levels (Figure 14B) suggesting that increased O-GlcNAcylation in these cells may be due to both elevation of OGT and reduction of OGA. To determine if OGT and O-GlcNAc levels were directly controlled by deregulated mTOR activity in these cells, *TSC2* null MEFs were treated with Rapamycin. Similar to the cancer cells, inhibition of mTOR in *TSC2* null MEFs resulted in a decrease in OGT and O-GlcNAcylation (Figure 14A).

These results reveal that, in addition to AKT, activation of mTOR is also sufficient to increase OGT protein levels and increase O-GlcNAcylation.

3.2.3 c-MYC regulates O-GlcNAcylation and OGT protein expression in cancer cells.

Many pathways are altered by activation of mTOR [106]. Since OGT is required for metabolic pathways in cancer cells [76], we hypothesized that pathways downstream of mTOR associated with metabolic regulation may be involved in OGT/O-GlcNAc regulation. Since c-MYC is a key metabolic transcription factor downstream from the mTOR pathway [127], we examined whether this transcription factor is involved in OGT and O-GlcNAc regulation in cancer cells. c-MYC is amplified in multiple cancers, plays a significant role in cancer cell proliferation, growth and apoptosis and has been strongly implicated in regulating cancer metabolism [110]. To verify that c-MYC expression is downstream of mTOR in breast cancer cells, we examined c-MYC levels in breast cancer cells after treatment with Rapamycin or LY294002. Inhibition of PI3K and mTOR, but not MEK, significantly reduced c-MYC expression in MDA-MB-231, SKBR-3, MCF-7 and SUM-159 breast cancer cells and correlated with reduced OGT protein levels in these cells (Figure 10A, 11A, 12C). To test whether c-MYC was required for OGT expression in breast cancer cells, we targeted c-MYC with two different lentiviral shRNA constructs and determined that decreasing MYC expression in MDA-MB-231 significantly reduced OGT levels and O-GlcNAcylation compared to cell containing control shRNA (Figure 16A-B). Consistent with our data regarding OGT expression under conditions of inhibition of PI3K and mTOR, there was no significant difference in OGT mRNA in cells expressing c-MYC RNAi as compared to control cells (Figure 18A). Thus, both

PI3K/mTOR and c-MYC regulate OGT protein levels independently of mRNA. To determine if c-MYC expression is sufficient to regulate OGT expression, we overexpressed c-MYC in MCF-10A cells. Cells overexpressing c-MYC displayed increased expression of its transcriptional target cyclin D1 (Figure 17A) and significantly upregulated OGT protein levels and O-GlcNAcylation compared to control cells (Figure 17A-B). The increase in OGT protein levels in MYC-overexpressing MCF-10A cells was also independent of changes in OGT mRNA levels (Figure 18B). Thus, downstream from mTOR, c-MYC is required and sufficient to regulate OGT protein levels and O-GlcNAc cycling in an RNA-independent fashion.

3.2.4 c-MYC regulation of HSP90A is required for OGT expression in cancer cells

Recent studies have shown that the chaperone HSP90A can bind OGT and regulate its proteasomal degradation in endothelial cells [40]. Interestingly, HSP90A is a c-MYC transcriptional target and contributes to c-MYC-induced transformation [128], thus we examined the potential connection between c-MYC, HSP90A and proteasomal degradation of OGT in cancer cells. To test whether reducing c-MYC levels in cancer cells led to reduction of OGT protein via the proteasome, we treated MDA-MB-231 cells containing c-MYC RNAi with the proteasome inhibitor lactacystin. Cells treated with lactacystin reversed MYC-RNAi induced reduction of OGT protein compared to control treated cells (Figure 19A) demonstrating that MYCs control of OGT requires the proteasome. Consistent with the idea that mTOR regulation of Myc can control OGT via proteasomal degradation, we found that the decrease in OGT protein levels observed with Rapamycin treatment was also reversed following lactacystin treatment (Figure 20A). Thus, mTOR and c-MYC regulation of OGT protein levels is proteasomal-dependent.

Consistent with previous findings that c-MYC regulates HSP90A, MDA-MB-231 cells stably expressing c-MYC shRNA contained significant decreases in HSP90A protein levels (Figure21A) and RNA levels (Supplemental Figure 21B) compared to control RNAi cells. Conversely, MCF-10A cells overexpressing c-MYC contained increased levels of HSP90 compared to control cells (Figure 17A). To determine whether OGT interacts with HSP90 in breast cancer cells, we immunoprecipitated either OGT or HSP90 and examined interaction between these two proteins. Immunoprecipitating either OGT (Figure 22A) or HSP90 (Figure 22B) from MDA-MB-231 cell lysates showed that endogenous OGT and HSP90 interact in breast cancer cells. To test whether HSP90A activity in cancer cells is associated with OGT and O-GlcNAc cycling, we treated MDA-MB-231 cells with HSP90 specific inhibitor 17-Demethoxy-17-allyaminogeldanmycin (17-AAG) [129]. Inhibition of HSP90 increases ubiquitination and proteasome-dependent degradation of client proteins [130]. Consistent with the idea that OGT is an HSP90A client protein, MDA-MB-231 cells treated with 17-AAG displayed decreased OGT and O-GlcNAcylation levels compared to control cells (Figure 23A). This decrease in OGT expression was independent of changes in Myc levels and was partially reversed when cells were also treated with lactacystin to block proteasomal degradation (Figure 20A). To test directly whether HSP90A is required for OGT expression in cancer cells, we reduced HSP90A expression in breast cancer cells using two different RNAi constructs. Reducing HSP90A levels in MDA-MB-231 cells resulted in significant decreases in OGT protein levels and reduced O-GlcNAcylation (Figure 24A-B). Conversely, overexpressing HSP90 in HEK-293T cells increased both OGT levels and elevated O-GlcNAcylation (Figure 23B). In addition, MCF-10A-MYC overexpressing cells contain

increased HSP90A expression and increased OGT and O-GlcNAcylation as mentioned above, (Figure 25A-B) suggesting increased association between OGT and HSP90A in a MYC-dependent manner. Reducing HSP90A levels via RNAi in MYC-overexpressing cells resulted in significant inhibition of OGT protein levels and reduced total O-GlcNAcylation (Figure 25A-B). Together these results show that MYC regulation of HSP90A controls OGT protein levels and O-GlcNAcylation in cancer cells.

3.2.5 Myc-driven tumor cells contain elevated OGT and O-GlcNAc levels and require OGT for survival.

Overexpression of c-Myc under the control of mouse mammary tumor virus (MMTV) results in the development of mammary tumors [131]. To determine if c-MYC driven tumors show elevated OGT and O-GlcNAcylation, we compared COMMA-1D cells, isolated from a mid-pregnant Balb/C mouse, to mammary tumor epithelial cells (MTECs) isolated from MMTV-MYC transgenic mice. The MTEC-MYC cells displayed elevated c-MYC levels as well as an increase in both OGT protein and O-GlcNAcylation (data not shown). To examine whether MYC-driven tumors have altered OGT and O-GlcNAcylation in vivo, we compared the levels of OGT and O-GlcNAc from mammary tissues harvested over the course of tumor progression from nulliparous female MMTV-MYC transgenic mice. O-GlcNAcylation was elevated in MYC-driven hyperplasic lesions compared with normal mammary glands of Myc+ females, and was further increased in late stage carcinomas relative to the hyperplasias (Figure 26A). Tumor tissue also displayed significantly upregulated OGT expression compared to normal mammary glands (Figure 26B).

MYC-driven cancers are known to be highly proliferative but also have high levels of apoptosis [110]. We examined whether targeting OGT using a chemical inhibitor could sensitize these cells to apoptosis compared to non-tumorigenic mammary epithelial cells. Treatment of MTEC-MYC cells or MCF-10A cells with OGT inhibitor Ac-5SGlcNAc reduced total levels of O-GlcNAcylation (Figure 27A, 28A). However, Ac-5SGlcNAc treatment increased caspase-3 cleavage (Figure 27A) and significantly reduced cell viability as measured by crystal violet staining (Figure 28B, 29A) solely in the MTEC-MYC cells as apoptotic markers and cell viability was not altered in MCF-10A cells upon treatment. Since we have recently shown that reducing OGT in cancer cells leads to ER stress and apoptosis in a CHOP-dependent manner [76] we examined whether inhibiting OGT in MYC-driven cancer cells also activated ER stress. Indeed, treating MTEC-MYC cells with OGT inhibitor Ac-5SGlcNAc induced phosphorylation of eIF2□, increased expression of CHOP, and increased Bcl-2 BH3-only pro-apoptotic protein Bim (Figure 27A). Importantly, treating MCF-10A cells with this inhibitor did not activate ER stress or induce expression of these markers (Figure 27A). This selective cell death of MYC-driven cancer cells was also observed in 3D culture as MTEC-MYC cells treated with the OGT inhibitor contained elevated cleaved caspase-3 staining compared to MCF-10A cells (Figure 29B). Thus, Myc-driven breast cancer cells increase OGT and O-GlcNAcylation and inhibition of O-GlcNAcylation in these cells induces ER stress and apoptosis.

3.3 Figures and Figure Legends

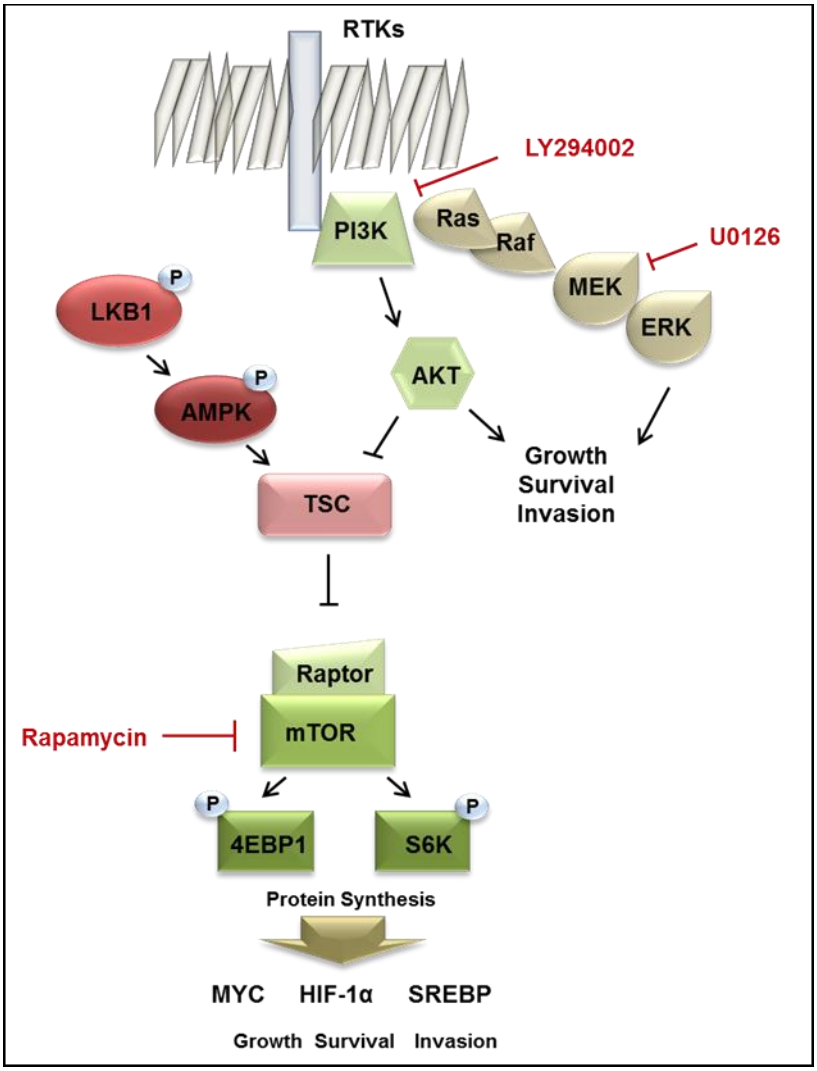

Figure 9: RTK/PI3K/mTOR pathway altered in majority of cancers Receptor Tyrosine Kinases (RTKs) can activate downstream signaling to promote cancer cell growth and survival. Downstream pathways such as the Ras/Raf/MEK/ERK and PI3K/AKT mTOR are important in many cancers and are upregulated through oncogenes and loss of tumor suppressors. In the subsequent studies shown here, inhibitors are used to decipher signaling. Inhibitors LY204992 (PI3K targeting), U0126 (MEK targeting, and Rapamycin (mTOR targeting) are used in these studies.

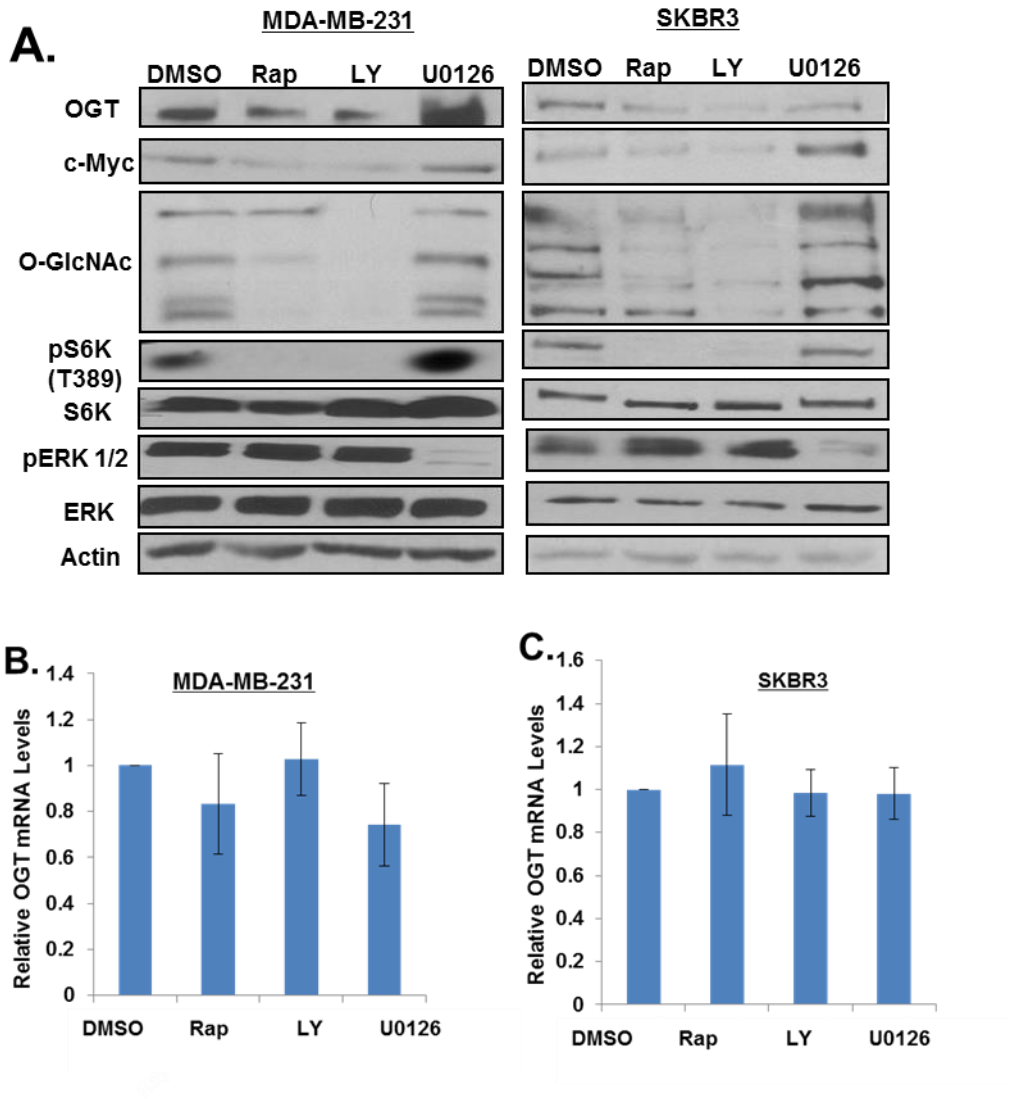

Figure 10: mTOR and PI3K are required for OGT protein expression

(A) Western blot analysis of MDA-MB-231 and SKBR3 cells treated with inhibitors Rapamycin (Rap), LY294002 (LY) , U0126 or vehicle control (DMSO) were analyzed using the indicated antibodies. (B-C) RNA was isolated from cells treated with the same conditions as (A) and analyzed via qRT-PCR for mRNA expression. Changes in mRNA not significant.

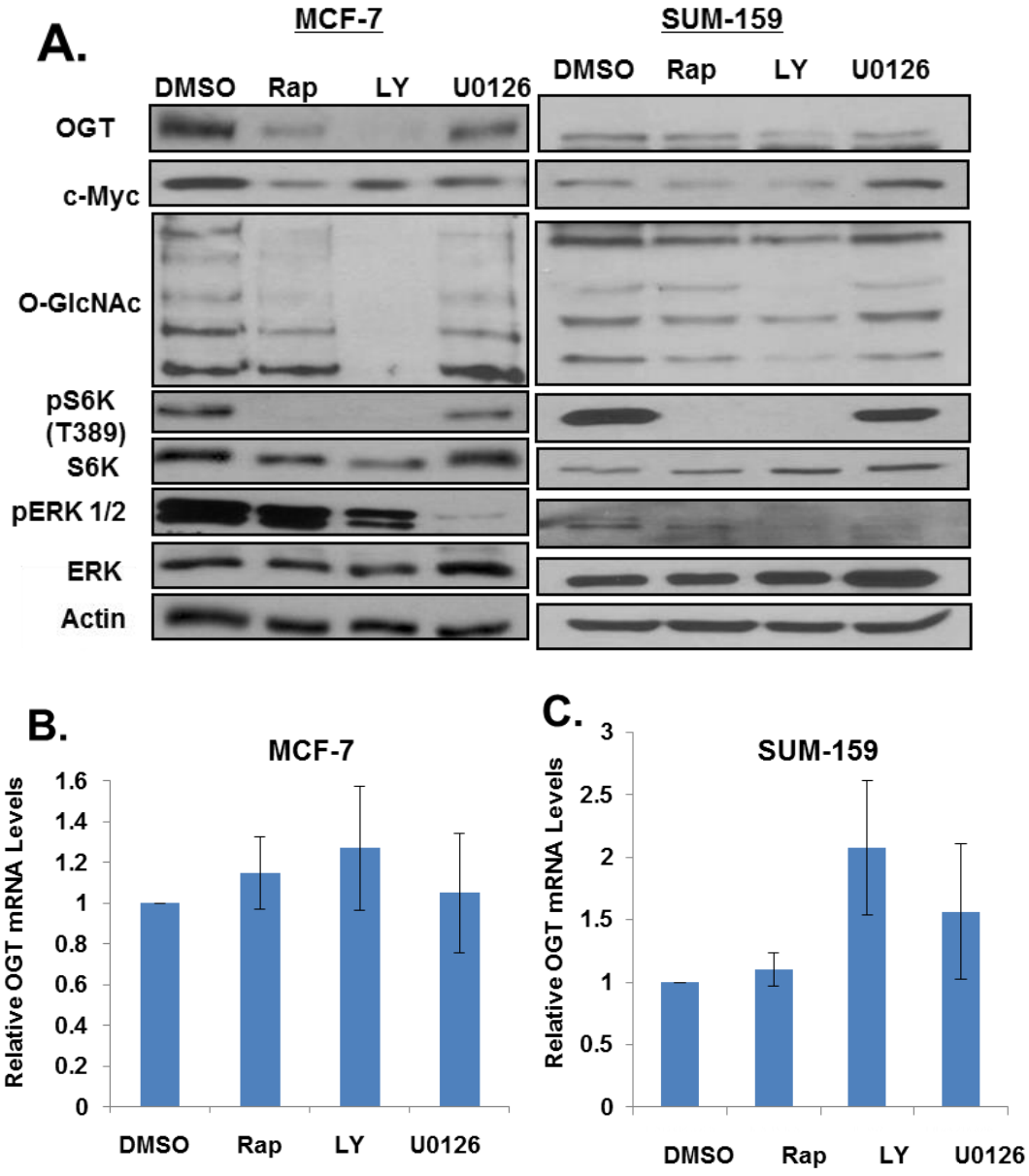

Figure 11: mTOR and PI3K are required for OGT protein expression

(A) Western blot analysis of MCF-7 and SUM-159 cells treated with inhibitors Rapamycin (Rap), LY294002 (LY) , U0126 or vehicle control (DMSO) were analyzed using the indicated antibodies. (B-C) RNA was isolated from cells treated with the same conditions as (A) and analyzed via qRT-PCR for mRNA expression. Changes in mRNA not significant.

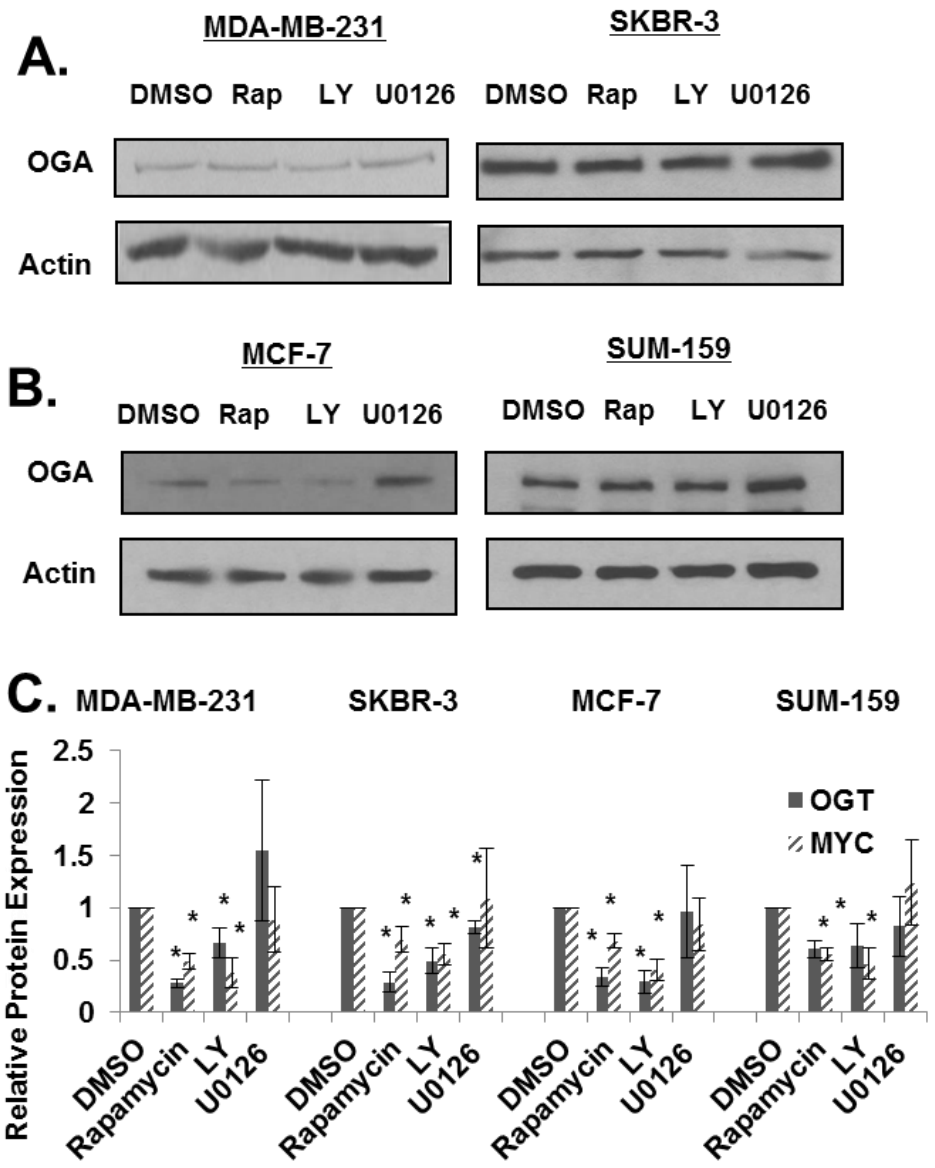

Figure 12: Changes in O-GlcNAcylation are independent of OGA expression and correlate with MYC expression in breast cancer cells treated with inhibitors to mTOR and PI3K (A-B) Western blot analysis of MDA-MB-231, SKBR3, MCF-7 and SUM-159 cells treated with inhibitors Rapamycin (Rap), LY294002 (LY) , U0126 or vehicle control (DMSO) were analyzed using the indicated antibodies. (C) Quantification of western blot analysis in represented in Figures 5 & 6. Mean +/- SE *$p<0.05$.

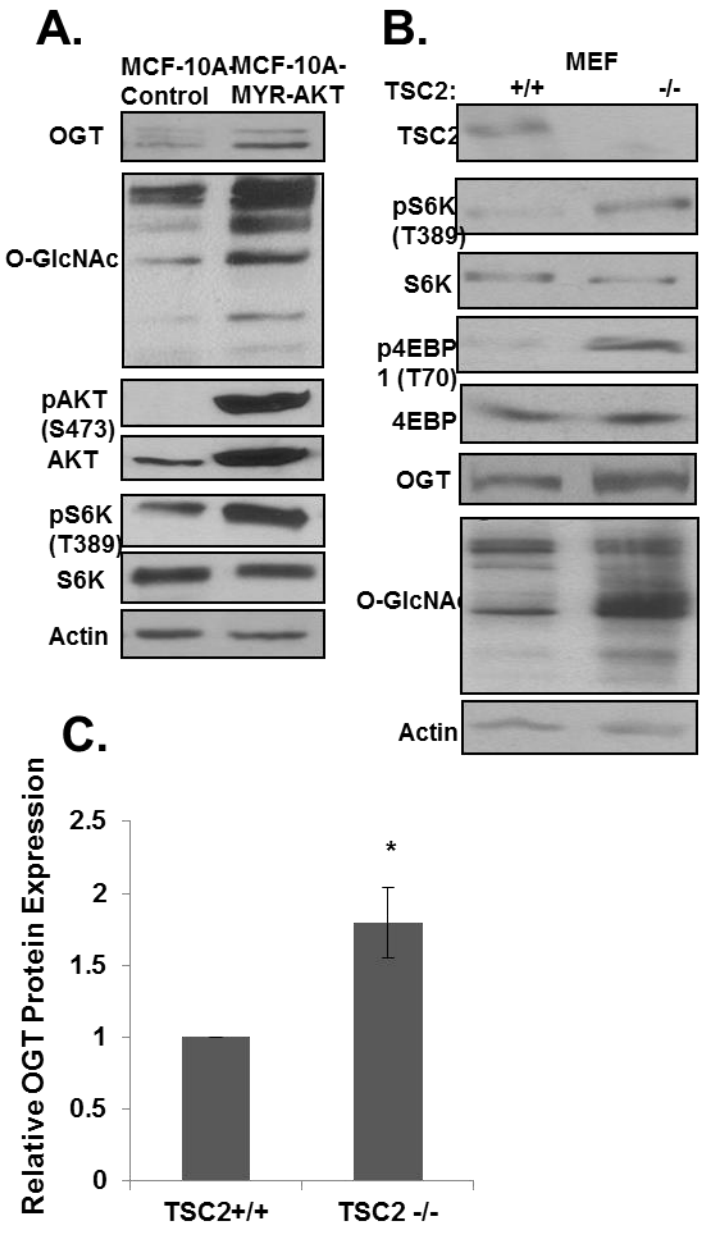

Figure 13: PI3K/Akt and mTOR are sufficient to elevate OGT expression,.(A-B) Western blot analysis of MCF10A cells containing control or Myr-Akt overexpression and WT and TSC2-/- MEFs were analyzed using the indicated antibodies. (C) Quantification of western blot analysis represented (B). Mean +/- SE *p<0.05.

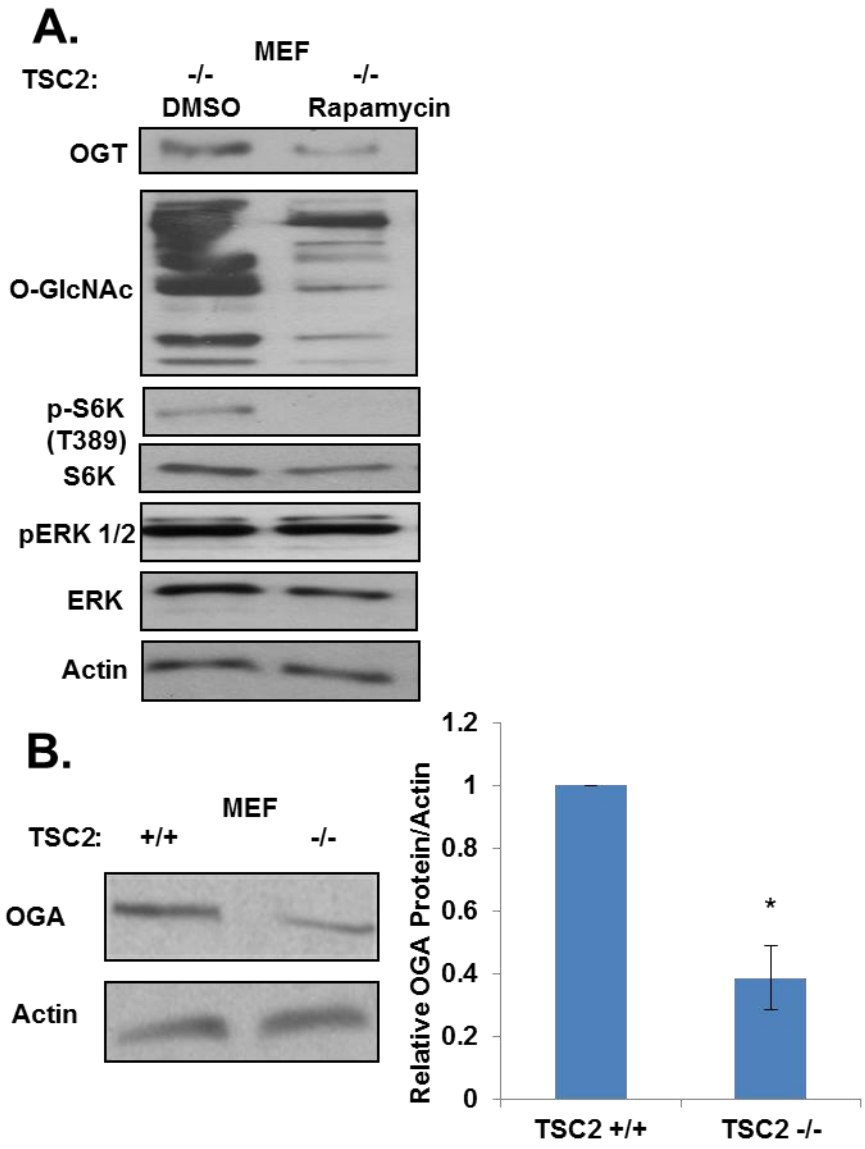

Figure 14: mTOR signaling is required for OGT protein expression independent of changes in OGA (A) Western blot analysis of TSC2 -/- MEFs treated with vehicle control (DMSO) or Rapamycin analyzed using the indicated antibodies. (B) Western blot analysis of WT and TSC2-/- MEFs analyzed with the indicated antibodies. Quantification of western blot analysis. Mean +/- SE *$p<0.05$.

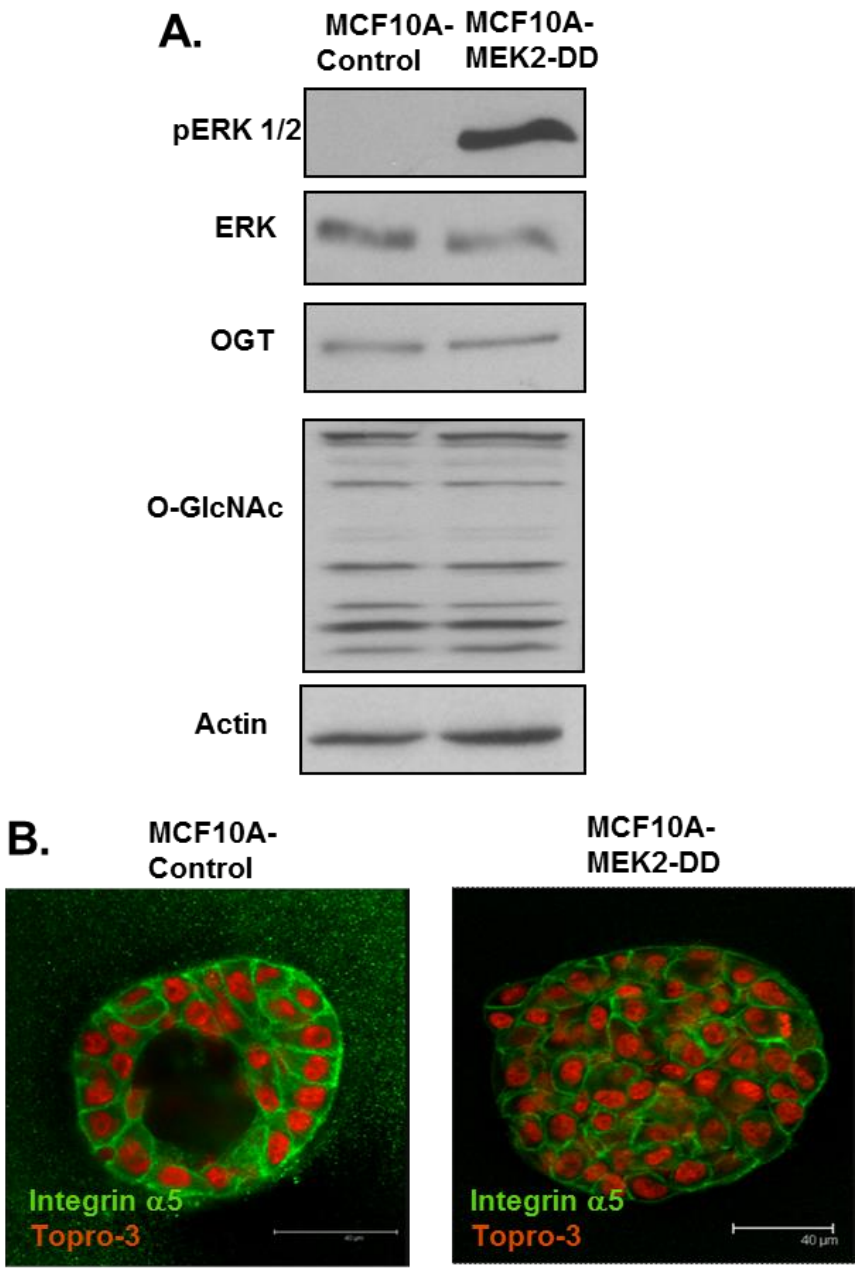

Figure 15: MEK/ERK pathway is not sufficient to regulate OGT and O-GlcNAcylation levels. (A) Protein was collected from MCF-10A cells stably expressing Control (pBabe) or an active form of MEK2 (pBabe-MEK-2-DD), and analyzed using western blot analysis with indicated antibodies. (B) MCF-10A-Control or MCF-10A-MEK2-DD cells were placed in 3D culture. At day 10, cells were fixed and stained with the indicated antibody and Topro-3 (nuclear stain), then imaged using confocal microcopy.

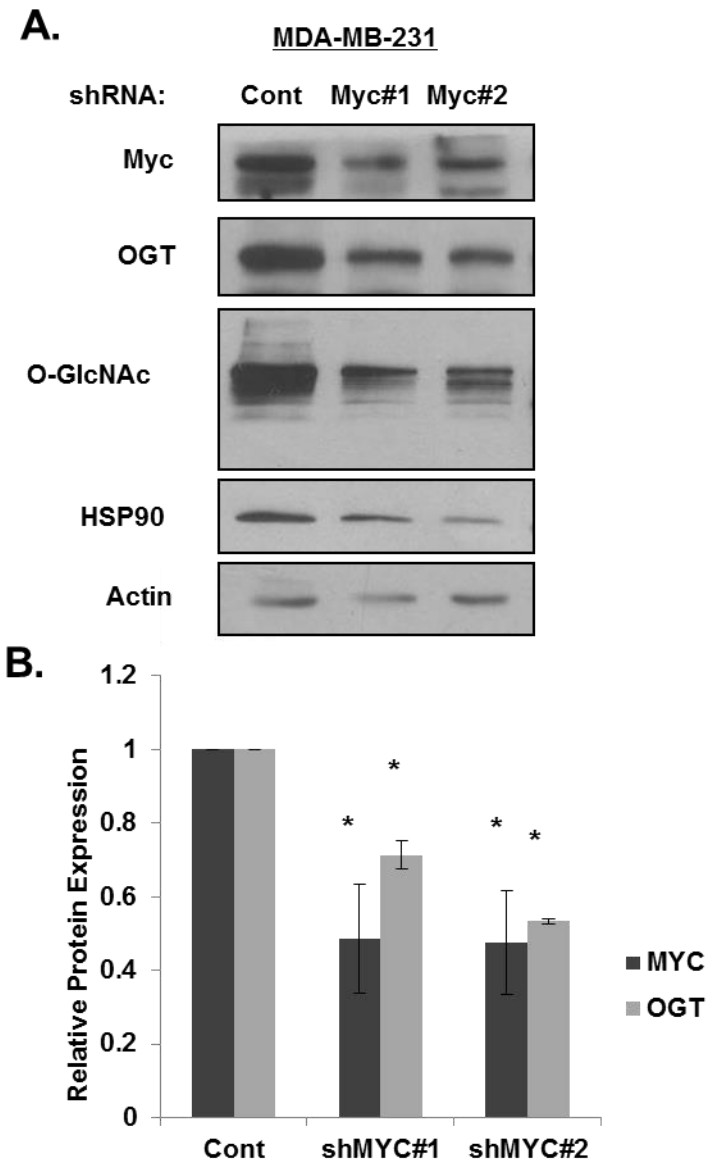

Figure 16: MYC is required for OGT protein expression (A) MDA-MB-231 cells containing control, shMYC-1, or shMYC-2 plasmids were analyzed by western blot with the indicated antibodies. (B) Quantification of western blot analysis. Mean +/- SE *$p<0.05$. Statistical analysis performed for separate proteins examined comparing shMYC#1 and shMYC#2 samples to control.

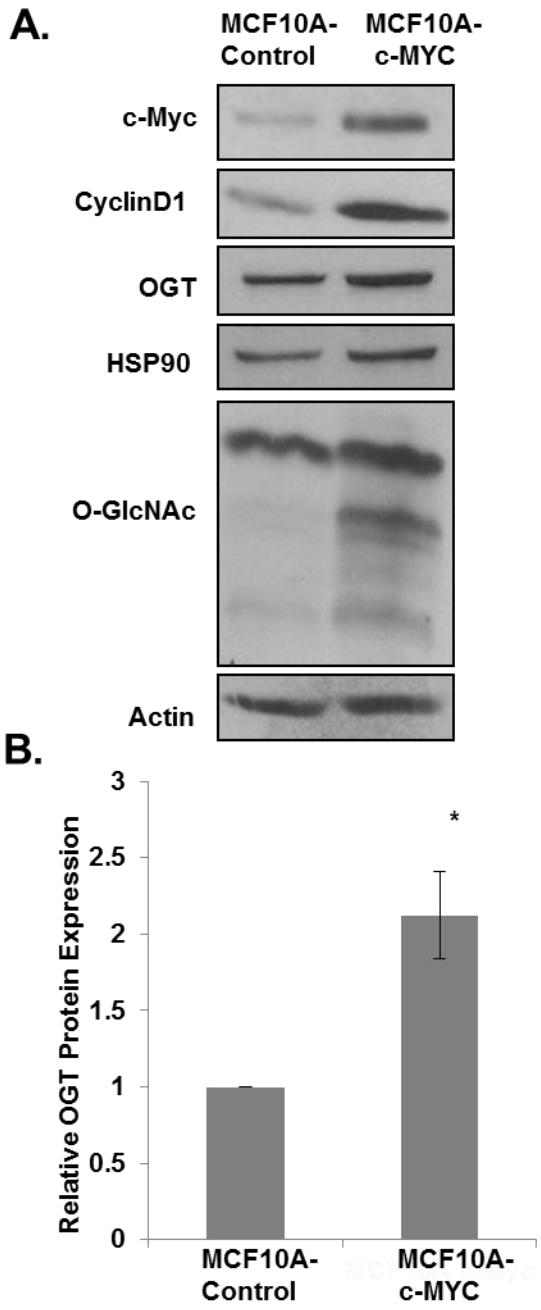

Figure 17: MYC is sufficient for OGT protein expression (A) MCF10A- control and MCF10A-cMYC cells were analyzed by western blot with the indicated antibodies. (B) Quantification of western blot analysis. Mean +/- SE *p<0.05.

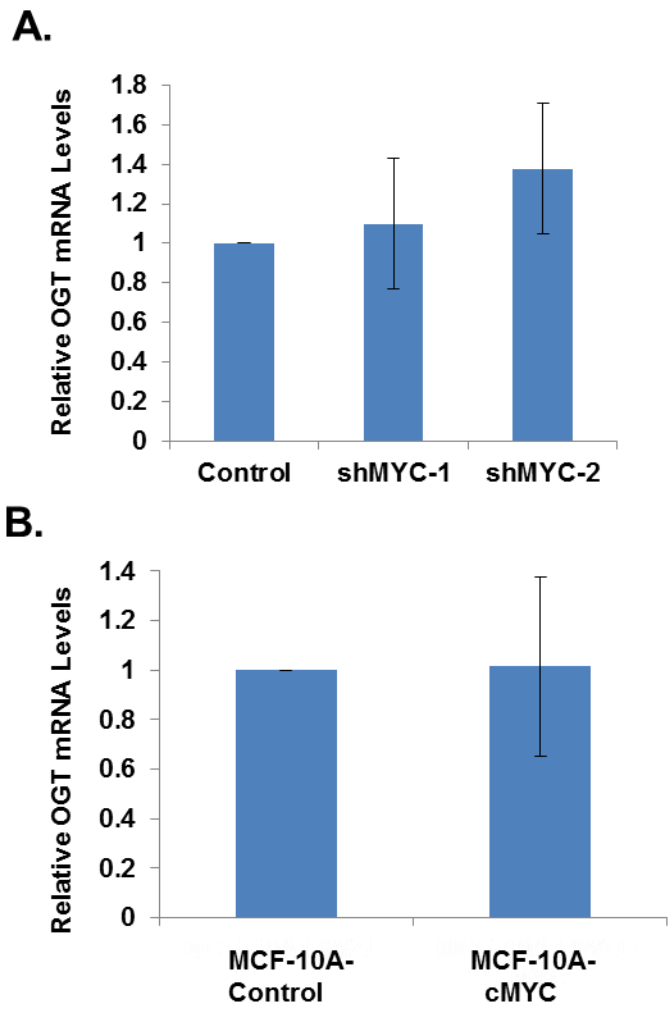

Figure 18: MYC is required and sufficient for OGT protein expression independent of OGT mRNA (A) mRNA was isolated from MDA-MB-231 cells containing control, shMYC-1, or shMYC-2 plasmids and analyzed by qRT-PCR. (B) mRNA was isolated from MCF10A-control and MCF10A-cMYC cells and analyzed by qRT-PCR. OGT mRNA was normalized to PPIA expression in each sample then to control. Mean +/- SE *$p<0.05$, changes were not significant.

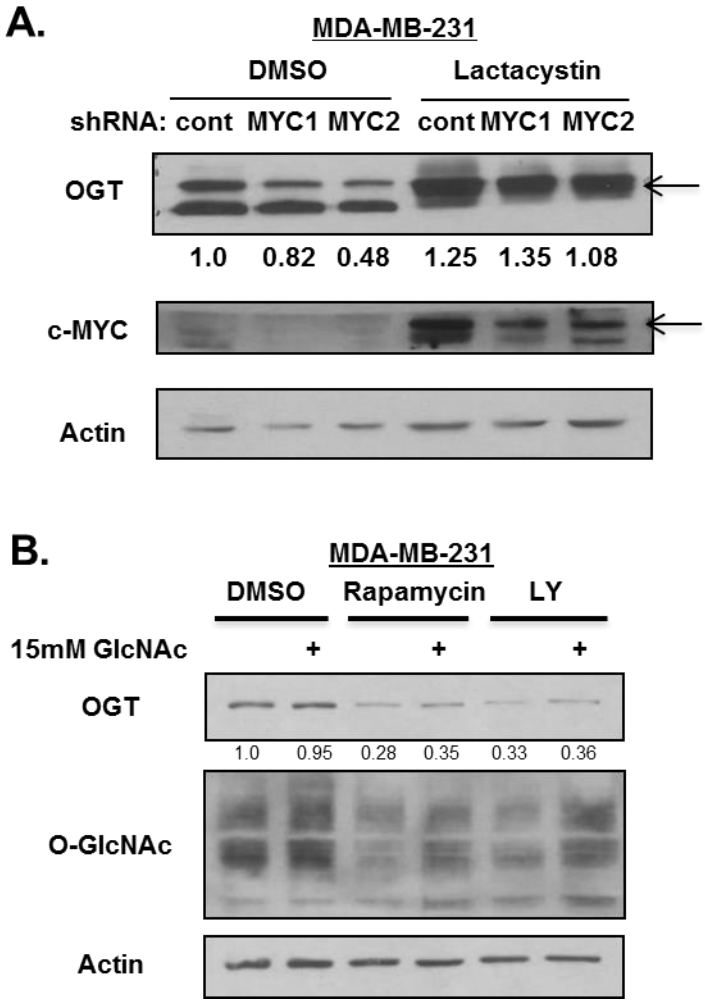

Figure 19: MYC regulates OGT via proteasomal degradation and OGT expression is not dramatically altered by substrate availability (A) Western blot analysis of MDA-MB-231 cells containing control, shMYC-1 or shMYC-2 plasmids, treated with vehicle control (DMSO) or proteasomal inhibitor lactacystin. Quantification was determined using ImageJ. (B) Western blot of MDA-MB-231 cells treated with vehicle control (DMSO), Rapamycin or LY294002 +/- 15mM GlcNAc was analyzed with the indicated antibodies. OGT protein expression was quantified using ImageJ software and displayed below.

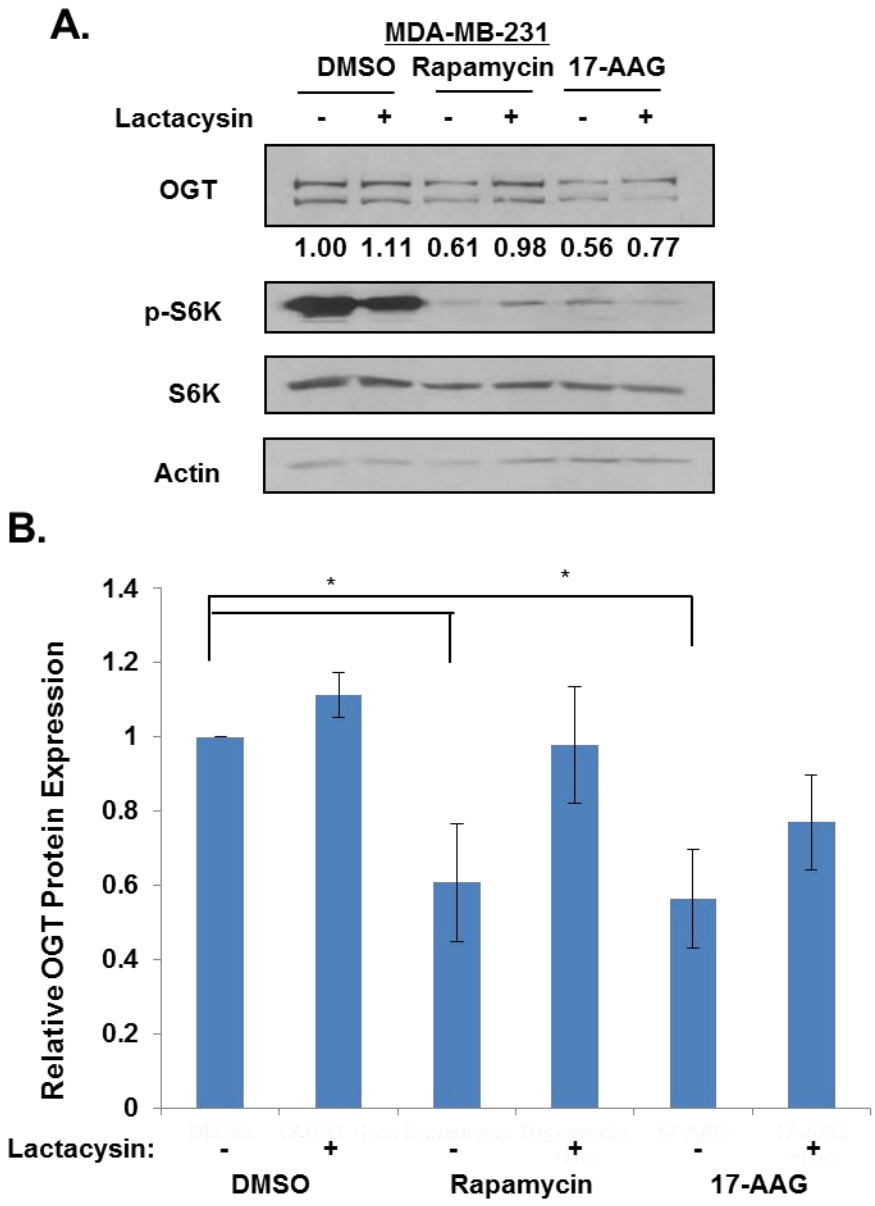

Figure 20: mTOR and HSP90 regulation of OGT is at least partly dependent on the proteasome (A) MDA-MB-231 cells treated with vehicle control (DMSO), Rapamycin, or 17-AAG and +/- Lactacystin were analyzed with the indicated antibodies. Quantification of OGT protein expression was performed using ImageJ and is displayed below and in (B. Mean +/- SE *p<0.05.

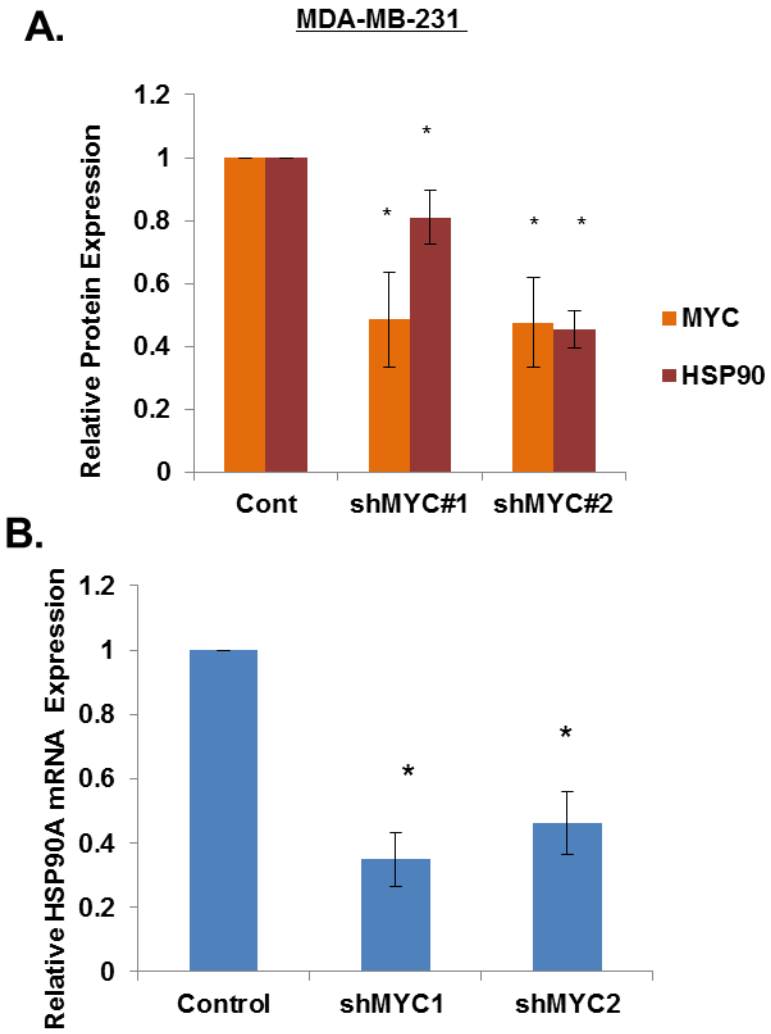

Figure 21: MYC inhibition decreases HSP90 protein and mRNA in MDA-MB-231 cells (A) MDA-MB-231 cells containing control, shMYC-1, or shMYC-2 were analyzed via western blot and protein expression was quantified and normalized to control. (B) mRNA was isolated from MDA-MB-231 cells containing control, shMYC-1 or shMYC-2 cells and analyzed by qRT-PCR. HSP90 mRNA was normalized to PPIA expression in each sample then to control. Mean +/- SE *$p<0.05$. Statistical analysis performed for separate proteins examined comparing shMYC#1 and shMYC#2 samples to control.

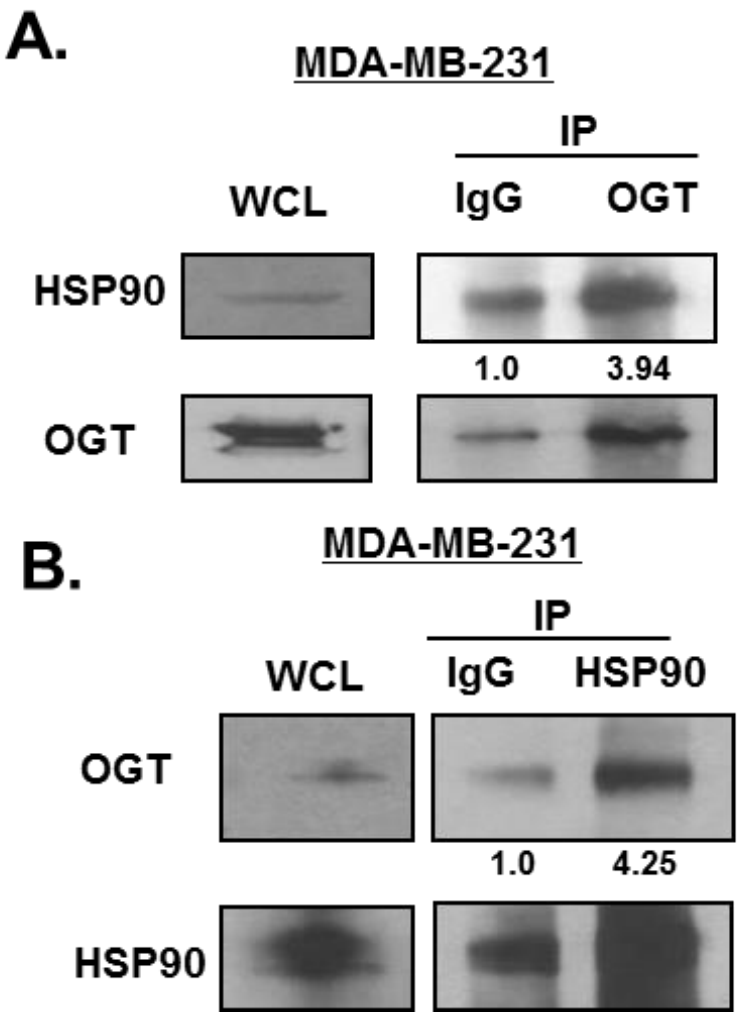

Figure 22: OGT and HSP90 interact in MDA-MB-231 cells (A-B) Immunoprecipitation of control IgG, OGT or HSP90 from MDA-MB-231 cells analyzed by western blot with the indicated antibodies Quantification displayed below. Mean changes were significant $p<0.05$. Immunoprecipitations normalized to expression in IgG control lanes.

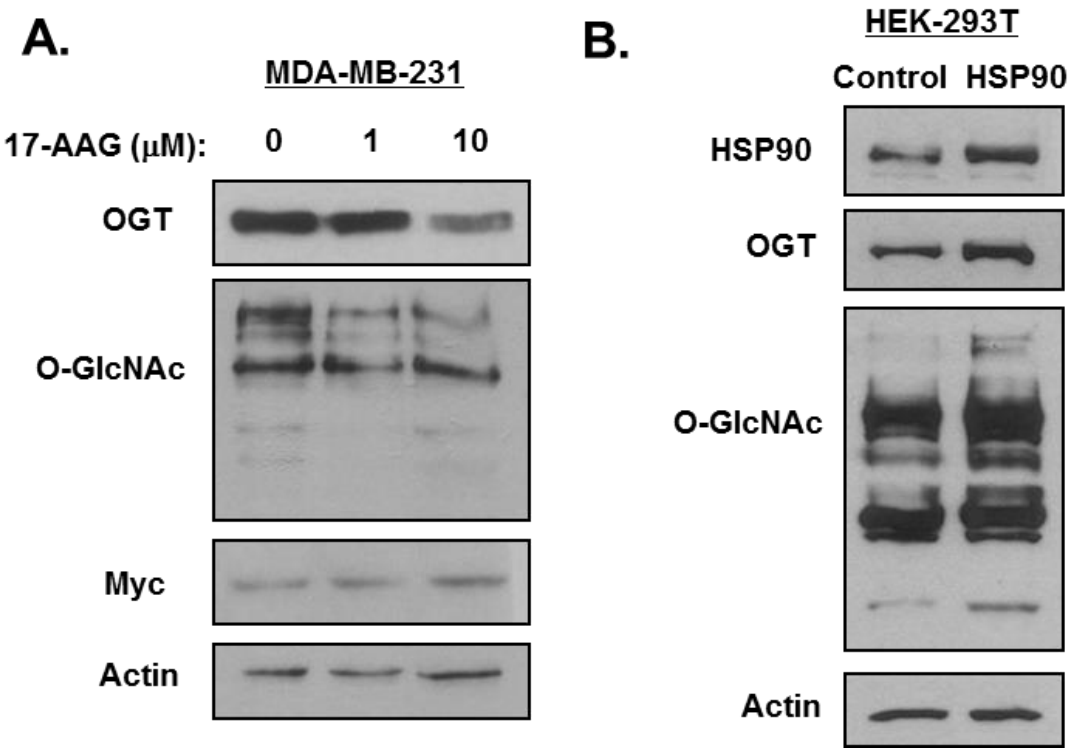

Figure 23: HSP90 is required and sufficient for OGT expression (A) MDA-MB-231 cells were treated with increasing doses of 17-AAG and analyzed by western blot using the indicated antibodies. (B) Western blot of HEK-293T cells transfected with control or HSP90 plasmids were analyzed with the indicated antibodies.

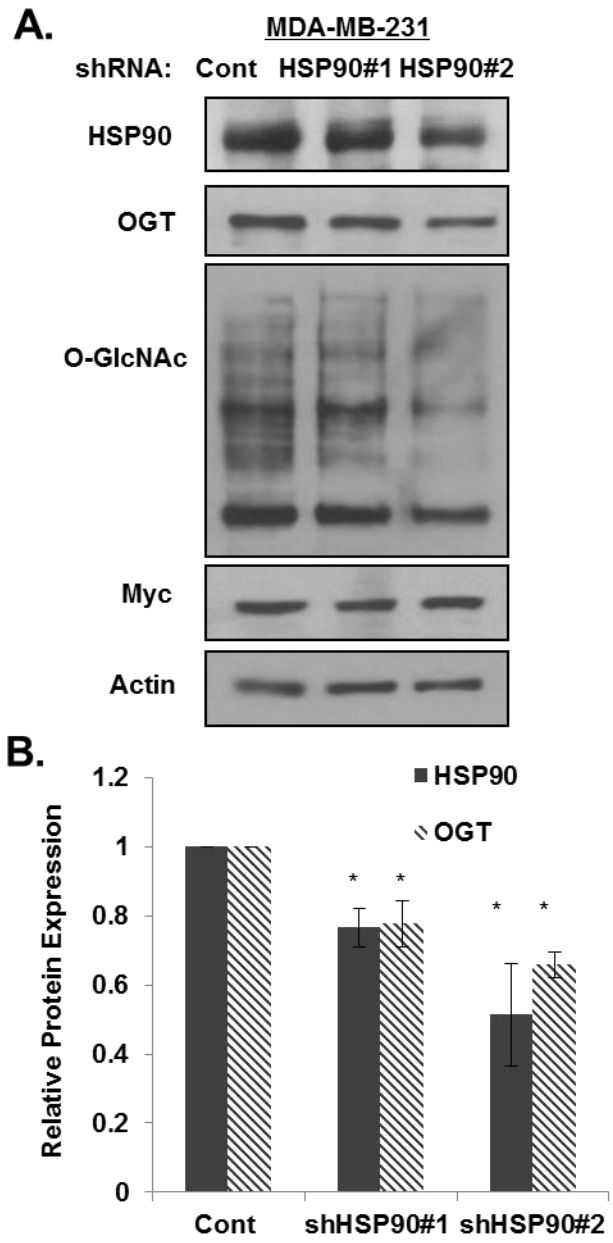

Figure 24: HSP90 is required for OGT expression (A) MDA-MB-231 cells containing control, shHSP90 -1 or shHSP90-2 plasmids were analyzed by western blot using the indicated antibodies. (B) Quantification of protein expression from conditions in (A). Mean +/- SE *p<0.05. Statistical analysis performed for separate proteins examined comparing shHSP90#1 and shHSP90#2 samples to control.

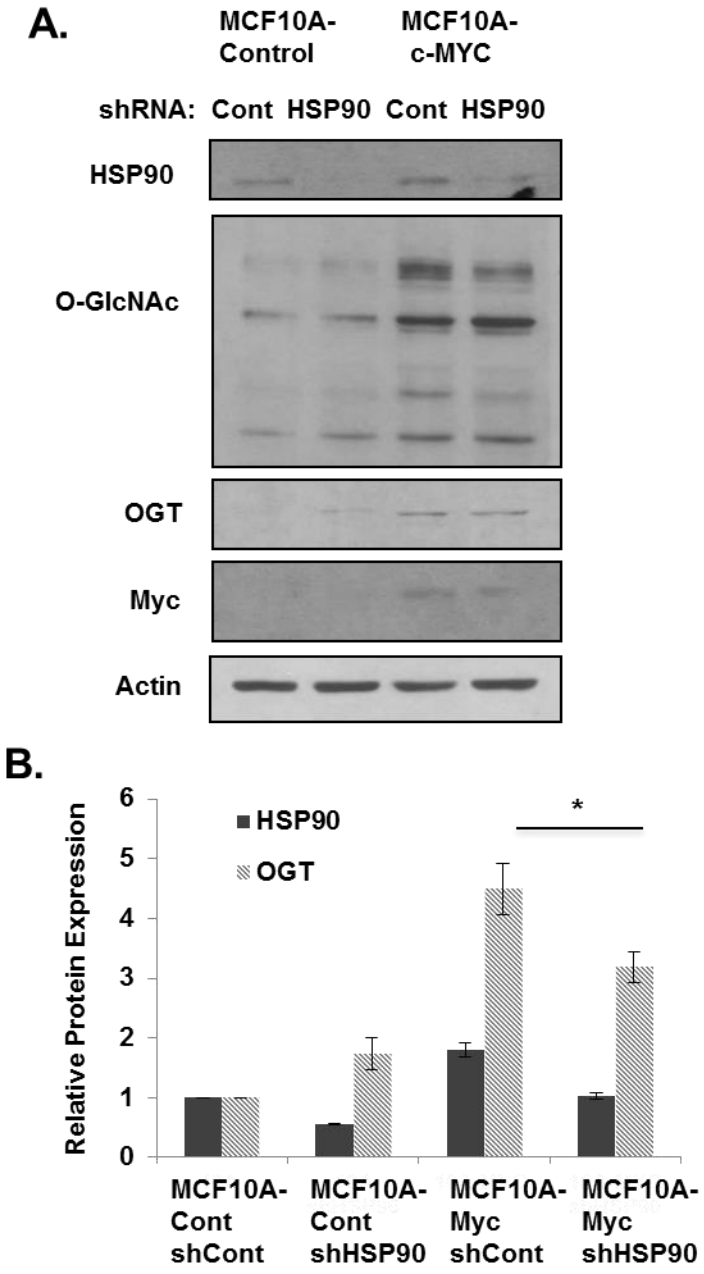

Figure 25: HSP90 regulates OGT expression only in the presence of MYC.(A) MCF10A-control and MCF10A-cMYC cells containing control, or shHSP90 -1 plasmids were analyzed by western blot with the indicated antibodies. (B) Quantification of protein expression from conditions in (A). Mean +/- SE *p<0.05.

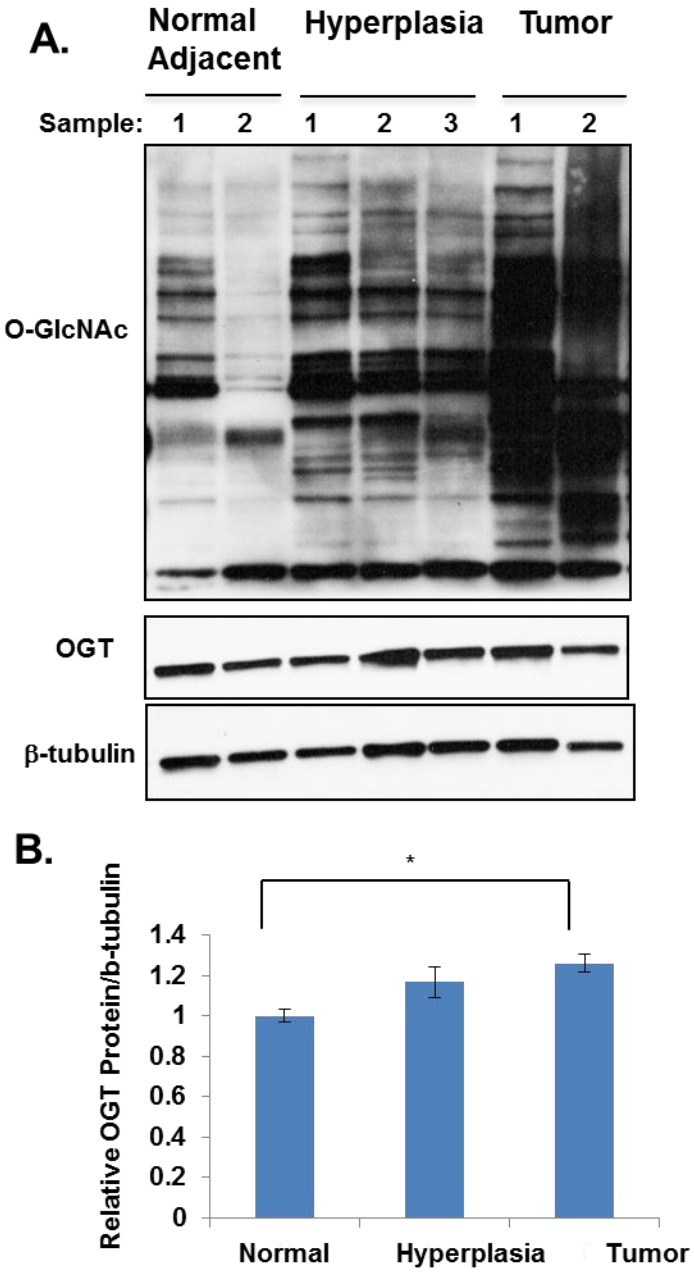

Figure 26: OGT expression and O-GlcNAcylation are elevated in MMTV-MYC tumor compared to normal adjacent tissue (A) Western blot analysis of protein extracted from tissue collected from MMTV-MYC normal adjacent mammary, hyperplastic and tumor tissue analyzed with the indicated antibodies. B) Quantification of OGT protein expression from conditions in (A). Mean +/- SE *p<0.05. *Western blot provided by T. Seagroves, R. Krutilina, L. Schwab*.

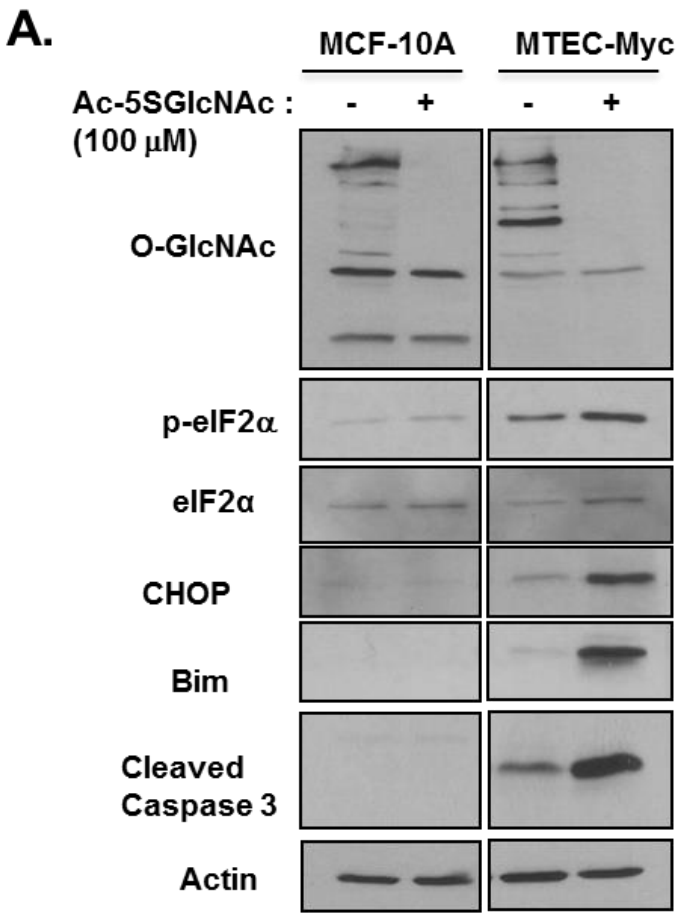

Figure 27: OGT inhibition induces cell death and ER stress in MTEC-MYC cells but not normal mammary epithelia cells (A) Western blot analysis of MCF10A and MTEC-MYC cells (derived from MMTV-MYC tumor) were treated with vehicle control (DMSO) or 100uM Ac-5sGlcNAc and analyzed with the indicated antibodies.

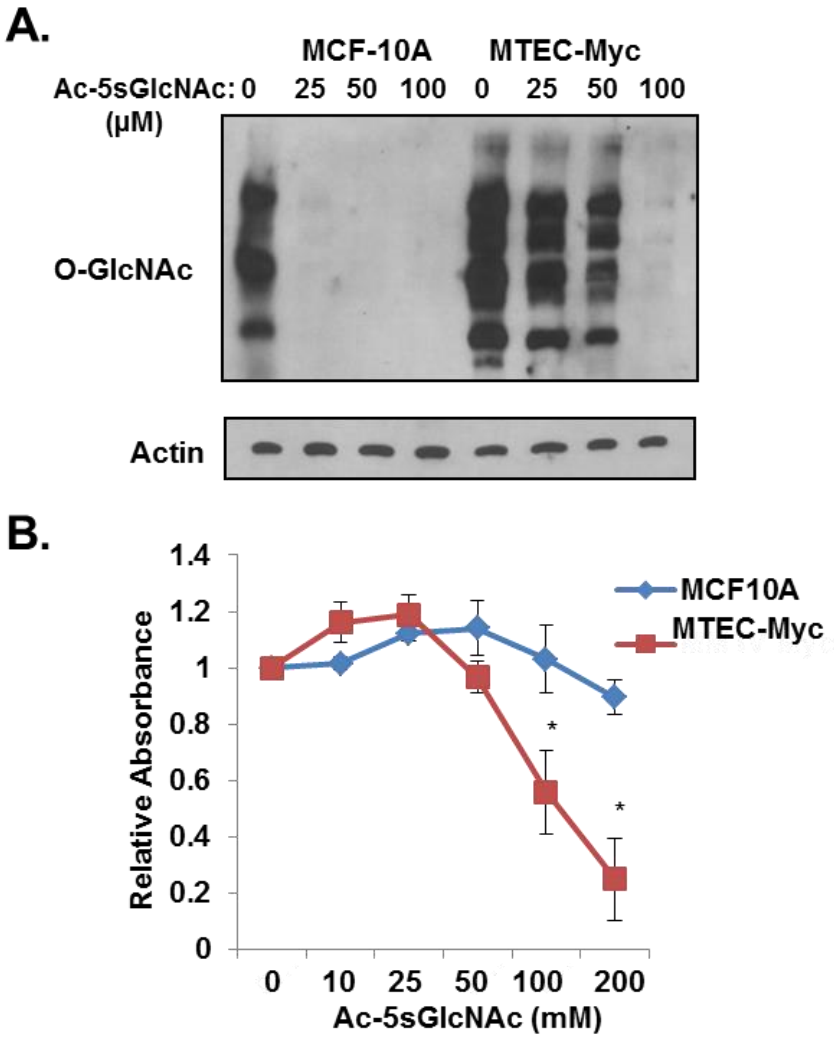

Figure 28: OGT inhibition induces cell death and ER stress in MTEC-MYC cells but not normal mammary epithelia cells (A) Western blot analysis of MCF10A and MTEC-MYC cells (derived from MMTV-MYC tumor) were treated with vehicle control (DMSO) or increasing doses of Ac-5sGlcNAc and analyzed with the indicated antibodies. (B) Viability as determined by absorbance after crystal violet staining of MCF10A and MTEC-MYC cells treated with control or increasing doses of Ac-5sGlcNAc. Mean +/- SE *$p<0.05$.

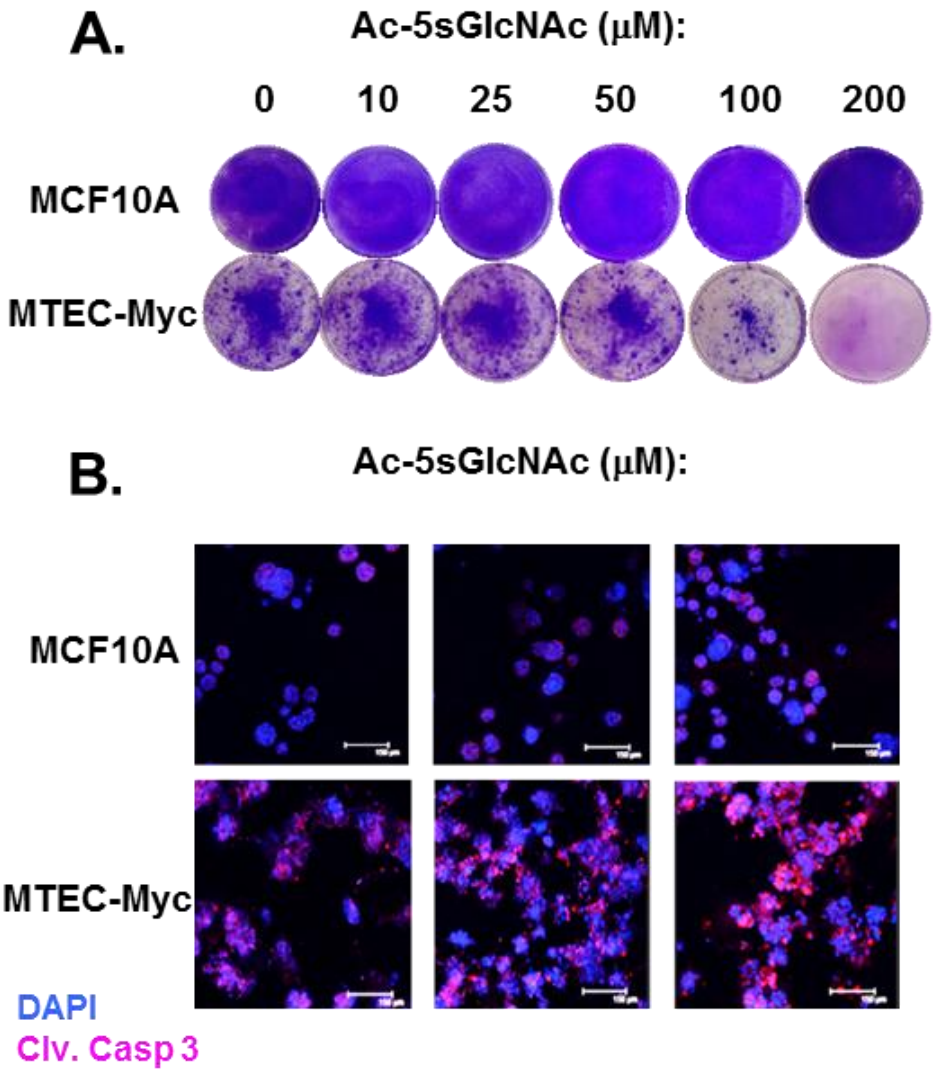

Figure 29: OGT inhibition induces cell death and ER stress in MTEC-MYC cells but not normal mammary epithelia cells (A) Crystal violet staining of MCF10A and MTEC-MYC cells treated with control or increasing doses of Ac-5sGlcNAc. (B) Representative images of immunofluorescent stained 3D cultured MCF10A and MTEC-Myc cells treated with vehicle control (DMSO) or increasing doses of Ac-5sGlcNAc for 48 hours.

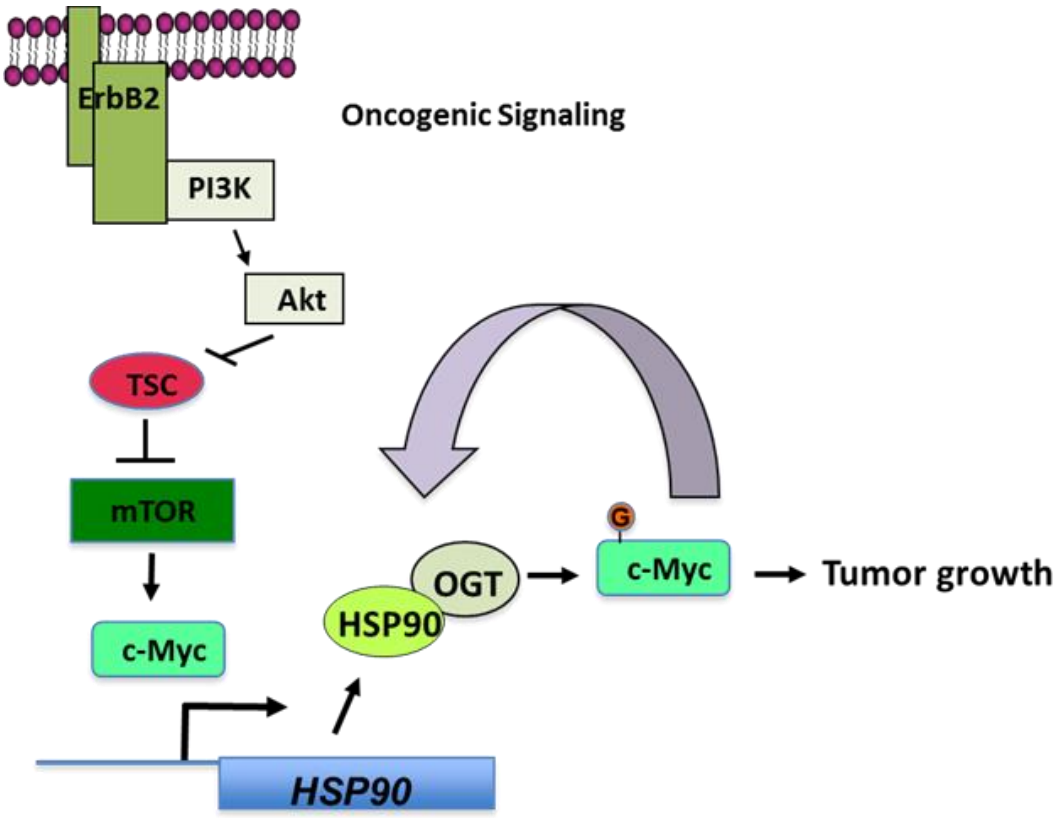

Figure 30: Model of OGT regulation in breast cancer cells via PI3K/mTOR/MYC/HSP90 Signaling through RTKs activating PI3K/AKT/mTOR is required and sufficient for OGT upregulation through c-MYC and HSP90 stabilizing OGT protein. c-MYC itself is O-GlcNAcylated which promotes c-MYC expression and generates a feed forward loop promoting tumor growth.

3.4 Discussion

Elevation of O-GlcNAcylation has been implicated in a wide range of cancers. However, the pathways responsible for the regulation of OGT and the O-GlcNAc modification in cancer cells remained unclear. Here, we show for the first time that the PI3K/mTOR pathway via regulation of the oncogenic transcription factor c-MYC is responsible for increased OGT and O-GlcNAcylation levels observed in breast cancer cells. We demonstrate that,the AKT/mTOR, but not MEK/ERK, pathways were sufficient to elevate OGT and O-GlcNAcylation. We found that elevation of OGT and O-GlcNAcylation in cancer cells is regulated by the oncogenic transcription factor c-MYC. c-MYC is both required and sufficient to elevate OGT protein levels and global O-GlcNAcylation in breast cancer cells. Importantly, we found that c-MYC driven tumor cells also displayed elevated OGT and O-GlcNAcylation *in vivo*. Our data is consistent with previous work showing that c-MYC can regulate total O-GlcNAcylation as Rat1A $myc^{+/+}$ fibroblasts contained increased O-GlcNAcylation compared to Rat1A $myc^{-/-}$ cells [132]. However, this change in O-GlcNAcylation in Rat1A cells was not associated with changes in OGT expression as found in our study. It is likely that c-MYC also contributes to the supply of essential substrates required for hexosamine biosynthesis as c-MYC can increase glucose and glutamine flux in these cells [132] as well as in cancer cells [108].

Interestingly, c-MYC regulates OGT at the post-transcriptional level as we did not detect changes in OGT mRNA expression in cells with altered c-MYC or PI3K/mTOR pathways. This may help explain why OGT RNA levels are not found to be elevated in breast cancer microarray analysis [76]. Although c-MYC is commonly known for its role as a transcription factor, it has been shown to stabilize protein levels of the enzyme

glutaminase without affecting RNA expression levels [133]. c-MYC also directly increases transcription of the heat shock protein HSP90A [128] which plays an important role in protein folding, degradation and maturation. HSP90A is also known to stabilize a subset of kinases, steroid receptors, and transcription factors, which are overexpressed in cancers [134]. It was recently demonstrated that HSP90A directly interacts with OGT, and inhibition of HSP90 reduces the half-life of the OGT protein, leading to decreased global O-GlcNAcylation in endothelial cells [40]. Consistent with this data, we showed that MYC–induced regulation of OGT, in part, requires HSP90A expression in cancer cells. Therefore, we propose a model (Figure 30) in which MYC regulation of OGT occurs via its transcriptional activation of HSP90A which facilitates maintenance of OGT protein through stabilization or prevention of degradation by the proteasome.

Previous studies have found that c-MYC can be O-GlcNAcylated [53, 135] in normal cells, and more recently in prostate cancer cells [70]. Reducing O-GlcNAcylation in PC-3 prostate cancer cells leads to reduced c-MYC protein O-GlcNAcylation, decreased c-MYC stability and was associated with decreased growth and survival of prostate cancer cells [70]. HSP90A has also been shown to be O-GlcNAcylated [136]. These data, together with our results, suggest that c-MYC, HSP90A and OGT/O-GlcNAcylation may be part of a feed-forward-regulatory loop present in cancer cells (Figure 30). Amplification of c-MYC in cancer cells can transcriptionally induce HSP90A expression leading to increased OGT levels and total O-GlcNAcylation (Figure 30) that feeds back to O-GlcNAcylate c-MYC, increasing its stability and thus enabling cancer cell growth. Consistent, with this idea, we show that MYC overexpression leads to elevated HSP90A

protein levels that are required for increased OGT and O-GlcNAcylation levels. Importantly, we show that OGT is required for MYC-mediated cancer cell survival.

Targeting c-MYC as a cancer therapeutic has proved to be incredibly challenging. Direct targeting has yielded few positive results however attempts persist. The most encouraging results were recently generated through targeting the MAX binding domain on c-MYC [107]. A small molecule screen identified one particular compound, 10058-F4, that inhibits c-MYC transcriptional activity and elicits cancer cell apoptosis *in vitro* [137]. Despite promise from *in vitro* studies, this compound fell short of expectation in animal models and requires further improvement [138]. Other promising strategies for targeting MYC lie in indirectly blocking transcriptional activity by disrupting the bromodomain and extra-terminal (BET) coactivator protein BRD4 [107]. Our results suggest that OGT may also serve as a potential therapeutic target in MYC-amplified breast cancers, and potentially other cancers with amplification of this oncogene, such as prostate, neuroblastoma and multiple myeloma. Since increased O-GlcNAcylation can also positively regulate c-MYC and other oncogenic transcription factors including FoxM1 [59, 60] as well as HIF-1α [76], reducing O-GlcNAcylation in cancer cells via OGT inhibition may be an important therapeutic option for a number of cancers. We also feel that investigation of the use of OGT inhibitors should be performed in combination with therapeutic agents targeting HSP90, more than a dozen of which have at least entered clinical trials [139].

CHAPTER 4: O-GLCNACYLATION AND OGT REGULATE LIPID METABOLISM IN BREAST CANCER

4.1 Introduction

4.1.1 Warburg Effect: Fatty Acid Metabolism

Most work describing the mechanism of lipid synthesis and regulation of lipid homeostasis has been conducted in the highly lipogenic tissue of the liver [140]. Increasing evidence indicates that cancer cells display specific alterations in pathways that drive lipogenesis to support membrane synthesis and generate signaling molecules required for rapid cell growth [86]. Most normal adult tissues obtain lipids from the bloodstream in the form of dietary free fatty acids, however, cancer cells reactive *de novo* lipogenesis, a process normally turned off after development [141]. Production of lipids functions to build new membranes, serve as signaling molecules and contribute to post-translational modifications (Figure 31B) [86]. This consists of activation and expression of enzymes involved in generating lipids, that are normally expressed at low levels in most adult tissues, such as Fatty acid synthase (FAS), Acetyl-CoA carboxylase (ACC), and ATP-citrate lyase (ACLY) as well as a transcription factor responsible for these enzymes, Sterol regulatory element binding protein (SREBP-1) [142]. The SREBP-1c and SREBP-2 transcription factors are known to regulate many proteins involved in lipid and cholesterol synthesis, respectively, while the SREBP-1a isoform is an activator of all SREBP-responsive genes [140]. SREBP family transcription factors are synthesized as inactive precursors which reside in the endoplasmic reticulum (ER) membrane and nuclear envelope (Figure 32B) [140]. Upon decreases in sterol or lipid levels, [143] these

proteins are bound by SREBP-cleavage activating protein (SCAP) and proteolytically cleaved generating an N-terminal region containing the basic helix-loop-helix–leucine zipper (bHLH-Zip) for DNA binding [140]. Mature SREBPs can then enter the nucleus and associate with Sterol Regulatory Element (SRE) regions of target gene promoters. Aberrant activation of these genes has been found in various cancer types including breast, ovarian, and prostate [144]. It is evident the up-regulation of many of these enzymes is accomplished through oncogenic signaling pathways such as Akt/mTORC1 or altered growth factor receptor signaling [142, 144].

4.1.2 Lipogenic enzymes and cancer

Previous studies have shown the necessity for lipogenic enzymes and lipids in cancer cell survival. Transcription factor SREBP-1 has been identified as an important contributor to cancer phenotypes and survival through its activation of lipid synthetic enzymes such as FAS, ACLY, ACC, and SCD1 (stearoyl-CoA desaturases), many of which are rate limiting enzymes in lipid synthesis pathways (Figure 32A) [142, 145]. SREBP-1 overexpression has been found in colorectal, prostate, breast, endometrial and hepatocellular carcinoma [146] and knockdown of SREBP-1 in endometrial cancer cells resulted in significant cell death *in vitro* and slowed tumor growth *in vivo*, as well as induced cell death in glioblastoma cells in culture [62]. ACLY, a key lipogenic enzyme and transcriptional target of SREBP-1, has displayed increased activity and expression in various cancers [141, 144, 147-149] and suppression of this enzyme results in the induction of cancer cell growth arrest or death, thereby supporting it as a possible therapeutic target [150-152]. ACLY has also been shown to be required for cellular transformation *in vitro* and *in vivo* [150] demonstrating its significance in maintaining

cancer phenotypes. The use of acetyl-CoA in acetylation can directly affect cell metabolism, as glucose dependent acetylation of histones, which regulates expression of glycolytic enzymes, requires ACLY in adipocytes [153]. Another transcriptional target of SREBP-1, FAS, has been examined as a therapeutic target in cancer as inhibition of this enzyme results in apoptosis *in vitro* and *in vivo* in breast cancer models [154].

AMPK is an important metabolic sensor that is implicated in cancer growth and survival [155]. This kinase has been well characterized in tissues such as liver and skeletal muscle for its role in halting anabolic processes in response to AMP/ATP ratio changes. AMPK activation occurs in response to a variety of cellular stressors including low glucose and depletion of ATP levels [155]. Downstream of AMPK, mTOR and other drivers of cellular growth are directly phosphorylated to inhibit their synthetic actions within cells to ration energy and substrates [156]. Expression of a dominant negative AMPK results in acceleration of prostate cancer cells and restoration of AMPK activity in LKB1 deficient lung cancer cells through reconstitution of wild-type LKB1 results in inhibition of cancer cell growth [155]. Together, these demonstrate the importance of AMPK in cancer and its value as a potential tool in the treatment of cancer. AMPK directly regulates lipid metabolism in hepatic, muscle and adipose tissue through phosphorylation of SREBP-1 and ACC, and indirect regulation of PGC1α and PPARs resulting in changes in lipid synthesis and lipolysis [157, 158]. Due to its centralized position within highly cancer related networks, its direct relationship with mTOR signaling, and its role in regulating processes essential to cancer survival, it has become an area of interest in cancer research and a treatment focus [159]. Its tumor suppressive role is well documented in a variety of cancers through its regulation of mTOR,

ACC/FAS and inflammation; however a direct connection to SREBP-1 in cancer has not yet been established.

Several studies have provided evidence that inducing metabolic stress in cancer cells, such as that resulting from glucose deprivation or treatment with 2-deoxy-D-glucose, leads to the accumulation of unfolded proteins, endoplasmic reticulum (ER) stress and death [160, 161]. Nutrient deprivation activation of apoptotic mediators (such as the Bcl-2-family BH3-only proteins Noxa, Puma and Bim) in response to nutrient stress has been linked to the induction of the unfolded protein response (UPR) in the endoplasmic reticulum [162]. The UPR is characteristically exploited by cancer cells as a necessary mechanism for supporting survival as it reduces the burden on the ER caused by persistent elevated levels of unfolded proteins [163]. Cancer cells are highly dependent on the metabolic pathways driving the Warburg effect as well as pathways such as the UPR which allow for survival of these cells under highly stressful circumstances. Therefore it stands to reason that targeting pathways that regulate cancer cell metabolism and their coping strategies could be a way to induce cell death. Indeed, we are not the first to postulate that exploiting this reliance could be used as a therapeutic. It has been shown previously that inhibition of a variety of enzymes important to metabolic pathways, such as glycolysis, decrease cancer phenotypes, alone or in combination [164, 165]. Previous studies determined that inhibiting proteins important to lipogenesis, SREBP-1 and ACLY, in cancer cells induced ER stress resulting in cell death [62, 166].

The complex regulation of SREBP-1 allows a window of opportunity, lacking for most transcription factors, in which SREBP-1 can be inhibited. Kamisuki has shown that the inhibitor fatostatin binds SREBP-cleavage activating protein (SCAP) resulting in

decreased mature SREBP-1 (as well as SREBP-2) and the transcriptional targets of these factors [167, 168]. This drug has shown efficacy in reducing prostate cancer cell growth as well as tumor size in an *in vivo* model [167] as well as reduced 3D morphology of several breast cancer cell lines [169].

4.1.3 OGTs connection to lipids in other systems

Links between OGT and lipids exist in normal and diseased biology. As noted previously, OGT contains a phosphoinositide binding domain (PPO) demonstrated to have activity in protein-lipid binding to several lipid species [13]. In response to insulin stimulation, the PIP3 binding domain in OGT has been shown to recruit OGT to the cell membrane [13]. In the liver, OGT was shown to directly interact with and O-GlcNAc modify ChREBP (Carbohydrate responsive element binding protein) stabilizing this transcription factor to promote activation of lipogenic genes [170].

Here, we demonstrate a connection between nutrient sensor O-GlcNAcylation and lipid synthesis in cancer. Our results show that OGT and O-GlcNAcylation are required for lipid synthesis in breast cancer cells through the regulation of SREBP-1 in an AMPK-dependent manner. OGTs regulation of cancer growth and survival requires SREBP-1 expression and its control of lipids, as restoring SREBP-1 expression in the context of OGT inhibition prevented cancer cell death *in vitro* and restored tumor growth *in vivo*. Thus, O-GlcNAcylation serves to link cancer cell nutritional status to lipid metabolism and cell survival via regulation of SREBP-1.

4.2 Results

4.2.1 O-GlcNAcylation regulates lipid metabolism in breast cancer cells

To understand the impact of O-GlcNAcylation on cancer metabolism, global metabolomics analysis using liquid and gas chromatography-mass spectrometry (LC-MS/GC-MS) was utilized to investigate the effect of OGT reduction on metabolites in triple-negative human breast cancer cells MDA-MB-231. The metabolic analysis of MDA-MB-231 cells containing OGT RNAi for 48 hours (Figure 33A) demonstrated statistically significant ($p<0.05$) changes in 124 out of 301 metabolites examined when compared to control RNAi cells (Figure 34B). The effects of reducing OGT levels in cancer cells on carbohydrate metabolism have been reported elsewhere [21]. Levels of the branched-chain amino acids (BCAA) isoleucine and leucine were significantly reduced with OGT knockdown, while valine demonstrated a non-significant reduction (Figure 38A). These decreases may reflect increased catabolism as levels of several BCAA catabolites were significantly elevated in cells where OGT was suppressed, as compared to control cells. These included 4-methyl-2-oxopentanoate, 3-methyl-2-oxovalerate, isovalerylcarnitine, 2-methylbutyrylcarnitine, and isobutyrylcarnitine (Figure 38A). We also found decreases in histidine, lysine, phenylalanine and tyrosine metabolites when OGT was suppressed (Figure 38A). Nicotinate and nicotinamide metabolites as well as nucleotide sugars and pentose and purine metabolites also significantly decreased in MDA-MB-231-shOGT cells compared to MDA-MB-231-control (Figure 39A).

The largest change in metabolites, upon reduction of OGT levels in cancer cells, was in lipids. Of the lipid metabolites measured, 43% significantly decreased following OGT inhibition, compared to decreases in 27% of the measured amino acids, decreases in 21% of the carbohydrate metabolites and 14% of nucleotides (Figure 34B). Levels of free fatty

acids, including the polyunsaturated fatty acid linoleate (that cannot be generated by mammalian cells), decreased significantly in shOGT-treated cells compared to control cells (Figure 35A-36A). The idea of decreased uptake of essential fatty acids was supported by significant decreases in a variety of other essential fatty acids with OGT inhibition as well as decreased intake of a fluorescent C16 lipid mimetic in shOGT cells compared to control (Figure 40B-C). Similar to free fatty acids, several lysolipids and a number of long chain fatty acids were less abundant in shOGT cells, as compared to control cells at 48 hours (Figure 36A, 37A). In response to OGT inhibition, decreased free fatty acid pools may result in reduced phospholipid synthesis and/or increased fatty acid mobilization from phospholipids resulting in the observed decrease in lysolipids. Carnitine metabolites increased with OGT suppression indicating that beta-oxidation may be increased (Figure 40A). Due to the immense body of literature relating to the requirement of lipid synthesis for cancer growth and survival we aimed to confirm metabolomics profiling results relating to *de novo* lipogenesis (Figure 35A). To achieve this we measured free fatty acids in MDA-MB-231 cells and found a ~50% decrease in free fatty acid levels in OGT knockdown cells compared to control cells (Figure 41A-B). We found a similar reduction of free fatty acid levels in the breast cancer cell lines MCF-7 (Figure 45B), BT474 (ER+/ErbB2+) (Figure 48B), and SUM-159 (Figure 47B) stably expressing OGT RNAi compared to control cells. In addition, cancer cells MDA-MB-231 (Figure 41C) and MCF-7 (Figure 45C) also contained lower levels of intracellular lipid droplets as measured by nile red staining (fluoresces in large hydrophobic cores of lipid droplets and has minimal interaction with cellular membranes) when OGT was suppressed [171]. Conversely, overexpression of OGT in MCF-7 cells (Figure 42A)

significantly increased free fatty acid levels (Figure 42B) and nile red staining (Figure 49A). Treatment of MDA-MB-231 cells with the OGT pharmacological inhibitor Ac-5sGlcNAc also resulted in a significant decrease in free fatty acids (Figure 43A) and lipid droplets (Figure 43B). To determine if lipids contribute to OGT-mediated phenotypes of cell growth, we treated MDA-MB-231 cells stably expressing OGT RNAi with exogenous lipids (palmitate/oleic acid). Treatment with exogenous lipids partly rescued growth defects resulting from OGT suppression (Figure 44A) and reduced levels of apoptotic marker cleaved PARP (Figure 44B). These data suggest a decrease in rates of fatty acid synthesis as a result of reduced O-GlcNAcylation contributes to growth defects in breast cancer cells. Thus, O-GlcNAcylation regulates levels of lipid metabolites and free fatty acids in breast cancer cells.

4.2.2 O-GlcNAcylation regulates master lipid regulator SREBP-1 and lipid enzymes in breast cancer cells

SREBP-1 is a critical regulator of lipid metabolism and in cancer cells is responsible for sustaining necessary production of lipids [141]. To examine whether O-GlcNAcylation may regulate lipid metabolism via SREBP-1, we first asked whether expression of SREBP-1, OGT and global O-GlcNAcylation change as mammary tumors progress in a spontaneous breast cancer model *in vivo*. To achieve this, we examined tissue throughout progression of breast tumor formation in the MMTV-PyMT transgenic breast cancer mouse model. Mammary hyperplasia can be detected in this model as early as 4 weeks and a large percentage of mice developed carcinoma at ~14 weeks [172] (Figure 45A). Protein expression of OGT and O-GlcNAcylation levels increased notably from week 8 to 12 during progression in this tumor model. Correlating with this increase, we found

nuclear SREBP-1 protein (N) levels and its transcriptional target ACLY increase during this time frame (Figure 45B). Consistent with increased SREBP-1 expression in the MMTV-PyMT derived mammary tissue, nile red staining was increased in MMTV-PyMT derived mammary gland at week 8 compared to a wildtype mouse mammary gland of the same background (Figure 45C).

To directly examine whether O-GlcNAcylation regulates SREBP-1 and lipogenic enzymes in breast cancer cells, we targeted OGT both genetically and pharmacologically. Inhibition of OGT via RNAi in breast cancer cells MDA-MB-231 (Figure 46A-B), MCF7 (Figure 48A, 52A), and SUM159 (Figure 50A, 51A, 52B) results in decreased protein expression of both the ER transmembrane precursor (P) and the cleaved nuclear transcription factor form of SREBP-1 (N). Consistent with a decrease in SREBP-1 expression, OGT inhibition resulted in decreased protein expression of SREBP-1 transcriptional targets ACLY and FAS in MDA-MB-231 (Figure 46A), MCF-7 (Figure 48A) and SUM-159 (Figure 50A) breast cancer cell lines. MDA-MB-231 cells stably expressing OGT RNAi also contain decreased levels of mRNA of SREBP-1 transcriptional targets *FASN, ACLY, ELOVL7* (ELOVL Fatty Acid Elongase 7), *ACC and LPL* (Lipoprotein Lipase) compared to controls (Figure 47A). Pharmacological inhibition of OGT using Ac-5sGlcNAc resulted in reduced total O-GlcNAcylation and similar decreases in SREBP-1 and FAS in MBA-MB-231 cells (Figure 47B). Conversely, overexpression of OGT in MCF-7 cells increased SREBP-1 protein levels as well as levels of ACLY and FAS (Figure 47C, 49B) consistent with increased nile red (Figure 49A) and free fatty acid levels (Figure 42B).

Project Achilles contains organized data about requirement for viability in hundreds of different cells lines after genetic deletion using shRNA or CRISPR targeting a large quantity of genes. These "gene requirement" or "essentiality scores" define the requirement of expression of a particular gene for survival of cancer cells. When searching these genome scale pooled shRNA screening data for breast cancer cell lines requirement of OGT and comparing to lipid related genes with similar essentiality scores we found correlation to FASN, ACLY, ACC, Sphingolipid delta 4 desaturase (DEGS1), and Pyruvate Dehydrogenase (polyamide) beta (PDHB) using Pearson correlation and Spearman rank correlation. We also found correlation to the glycolytic enzyme ENO1 as well as HIF1α which we have previously found to be regulated by OGT thereby increasing our confidence in our findings that cancer cells have a similar requirement for expression of OGT and the lipogenic genes listed above (Figure 53) [21].

4.2.3 O-GlcNAcylation regulates SREBP-1 expression in a proteasomal and AMPK-dependent manner

We next examined the mechanism by which OGT and O-GlcNAcylation regulates SREBP-1 in cancer cells. SREBP-1 protein can be regulated by proteasomal degradation [173] thus we examined whether O-GlcNAc regulation is proteasome-dependent. Treatment of breast cancer cells with proteasomal inhibitor MG132 blocked the OGT suppression-induced decrease in nuclear SREBP-1, and to a lesser extent precursor SREBP-1 compared to control (Figure 54B) and reversed decreases in SREBP-1 transcriptional target ACLY (Figure 54B). While SREBP-1 mRNA was decreased upon OGT inhibition this could be a consequence of SREBP-1 protein levels as it transcriptionally controls itself. We chose to mechanistically pursue regulation of

SREBP-1 protein by OGT. SREBP-1 does not appear to be directly O-GlcNAcylated as immunoprecipitation of exogenous SREBP-1 contained no detectable O-GlcNAcylation when compared to a known target (data not shown). This does not rule out the possibility that SREBP-1 is O-GlcNAc modified but suggests that O-GlcNAcylation may regulate SREBP-1 protein stability indirectly.

We have previously demonstrated that reduction of OGT via RNAi, in breast cancer cells, results in metabolic stress and leads to activation of the AMPK pathway [21]. AMPK is activated under low nutrient conditions to inhibit mTOR and downstream pathways thereby reducing mitogenic signaling. Reducing O-GlcNAcylation leads to an increase in phosphorylated AMPK (T172), an indicator of activated AMPK, as well as a decrease in mTOR signaling [76]. AMPK is known to phosphorylate SREBP-1 on Ser372 and inhibit its cleavage and maturation in hepatocytes [158]. Thus, we examined whether OGT may regulate SREBP-1 in an AMPK-dependent manner. Using a phospho-antibody that recognizes SREBP-1 phosphorylation on Ser372, we observe an increase in SREBP-1 phosphorylation when OGT is suppressed in MDA-MB-231 cells, correlating with activation of AMPK as measured by phosphorylation at T172 (Figure 55A). We tested the requirement of AMPK in OGT-mediated changes in SREBP-1 in MDA-MB-231 cells by treating cells with the AMPK inhibitor Compound C. MDA-MB-231 cells treated with Compound C contained decreased AMPK phosphorylation and activation as measured by phosphorylation of its substrate Raptor (Ser792) compared to control cells. The reduced SREBP-1 protein levels observed upon suppression of OGT were partly reversed by treatment with Compound C (Figure 57A right, 54A). Similar results were obtained in MDA-MB-157 cells (Figure 57A left) suggesting that OGT regulation of

SREBP-1 is AMPK-dependent in multiple breast cancer cells. We then assessed whether regulation of SREBP-1 by OGT required AMPK using WT and AMPK-/- mouse embryonic fibroblasts (MEFs). In WT MEFs, OGT inhibition results in decreased SREBP-1 protein expression and transcriptional targets ACLY and FAS, consistent with our observations in breast cancer cell lines (Figure 56A). However, AMPK null MEFs showed little change in SREBP-1, ACLY and FAS protein expression upon OGT inhibition. Thus, regulation of SREBP-1 by OGT is, at least partially, AMPK dependent (Figure 56-57). Addition of methyl pyruvate after OGT suppression reversed activation of AMPK and SREBP-1 phosphorylation and restored total levels of SREBP-1 to that of control cells (Figure 56B). SREBP-1 is known to be degraded by the proteasome and is bound by the E3 Ubiquitin ligase FBXW7. Others have demonstrated that phosphorylation of SREBP-1 by GSK3β precedes interaction with the tumor suppressor and E3-ubiquitin ligase FBXW7 [173, 174]. We examined expression of FBXW7 (FBW7) in MDA-MB-231 cells and determined that basal protein levels increased when OGT was suppressed via RNAi (Figure 58A). Due to the known requirement of GSK3β in FBW7- dependent degradation of SREBP-1, we treated cells with the GSK3β inhibitor SB216763. Addition of this compound to MDA-MB-231-shOGT cells prevented a decrease in SREBP-1 nuclear protein (Figure 58B) indicating that GSK3β may be necessary for OGT regulation of SREBP-1. Immunoprecipitation revealed that interaction between SREBP-1 and FBW7 increased when OGT was inhibited (Figure 59A-B). This data implies that mechanisms for degrading SREBP-1 are also partly responsible for OGT regulation of SREBP-1 protein.

4.2.4 O-GlcNAcylation-mediated cancer cell survival requires SREBP-1 regulation of lipid and glucose metabolism in cancer cells

To determine if changes in SREBP-1 were required for the lipid defects observed upon OGT inhibition, we overexpressed exogenous SREBP-1 to restore levels in the context of OGT knockdown. While SREBP-1 nuclear protein levels were still affected by OGT suppression in cells where exogenous SREBP-1 was expressed, they were comparable to levels in control cells thereby ensuring that SREBP-1 had been restored to basal levels (Figure 61A-B). Cells stably overexpressing exogenous SREBP-1 significantly restored free fatty acid levels (Figure 60A) and nile red staining (Figure 60B) in OGT knockdown cells to levels similar to control cells. Consistent with a rescue in free fatty acids, overexpression of SREBP-1 rescued protein levels of transcriptional targets ACLY and FAS in OGT knockdown cells compared to controls (Figure 61A). This indicated that decreases in lipid droplets and free fatty acid levels resulting from OGT suppression were due to OGT effects on SREBP-1 protein levels.

We have previously shown that OGT suppression in MDA-MB-231 cells results in inhibition of growth and survival [76]. We next tested whether regulation of SREBP-1 by OGT played a role in cancer cell survival. Growth inhibition resulting from OGT suppression was partially reversed by re-expressing SREBP-1 (Figure 62A). We have also previously reported that OGT inhibition decreased soft agar colony formation [59]. This measure of anchorage-independent growth was restored when SREBP-1 was expressed in OGT knockdown MDA-MB-231 cells, as was growth in 3D culture (Figure 62A, 63A-B). Apoptotic factors such as cleaved caspase 3 and cleaved PARP, which are

induced upon OGT suppression, were no longer activated with SREBP-1 restoration and the loss of anti-apoptotic Bcl2 was prevented in these cells (Figure 62B).

Although exogenous lipids were able to partially prevent decreased cell growth upon OGT knockdown cells (Figure 44A), we noticed that SREBP-1 overexpression rescued growth to an even greater extent (Figure 62A). Since we have previously shown that OGT regulates HIF-1α and its transcriptional target GLUT1, and overexpression of a HIF-1α stable mutant or GLUT1 can also fully rescue OGT knockdown phenotypes, we examined expression of HIF-1α and GLUT1 in SREBP-1 overexpressing cells. In cells overexpressing SREBP-1 we did not detect any changes in HIF-1α however, surprisingly, we found maintenance of GLUT1 in OGT knockdown cells (Figure 64A). Consistent with the idea that SREBP-1 overexpression may be regulating GLUT1 function, we found that glucose uptake inhibition caused by OGT-knockdown was reversed in SREBP-1 overexpressing cells (Figure 64A). Similar reversal was seen in lactate production suggesting that SREBP-1 can also regulate OGT-mediated glycolytic flux (Figure 65A-B). It makes sense that in order for exogenous SREBP-1 protein expression to restore relative free fatty acid levels in the context of OGT knockdown that not only would expression of lipogenic enzymes be required, but also a replenishment of substrates for the synthesis of lipids.

We next examined if signaling through growth pathways such as mTOR were restored by SREBP-1 re-expression. Indeed, SREBP-1 expression prevented decreases in mTOR signaling seen with OGT suppression in control cells, as measured by phosphorylated 4EBP-1 and S6 Ribosomal protein (Figure 64A). Downstream of mTOR, c-Myc protein expression was also rescued by SREBP-1 over-expression which may

explain the restoration of GLUT1 (Figure 64A). Restoration of the mTOR signaling pathway and c-Myc are consistent with a restoration in glycolytic flux, showing that re-establishing SREBP-1 expression in the context of OGT suppression allows for cell growth and metabolic signaling characteristics consistent with control cells. We noted that in agreement with these changes in mTOR signaling we also see a reversal of activation of AMPK as measured by phospho-AMPK (T132) which occurs with decreased OGT (Figure 64A). SREBP-1 re-constitution also prevented the increase in intracellular ROS following OGT inhibition which may be due to SREBP-1 regulation of G6PD (Figure 66A) [175]. Whether this has any bearing on or contribution to survival has yet to be determined. Interestingly, several other signaling pathways were also rescued by SREBP-1 restoration in conditions of OGT suppression including ERK activation (to a much lesser extent than mTOR pathway activation) as well as preventing activation of stress pathway P38 MAPK (Figure 66B). Basal ERK activation was also elevated solely by increasing SREBP-1 expression in MDA-MB-231 cells. There was also a lack of activation of DNA damage/ double strand breaks, as measured by H2Ax phosphorylation, upon OGT suppression when SREBP-1 was present (Figure 66B). ER stress activation previously reported as a consequence of OGT inhibition was not prevented by SREBP-1 overexpression. SREBP-1 overexpressing cells in fact had higher expression of several proteins induced by activation of ER stress than the basal levels displayed in control cells, including phospho-eif2α, and BIM (Figure 67A). Using stable isotope labeling in MDA-MB-231 cells we were unable to show that OGT inhibition decreased the use of glucose in the synthesis of fatty acid palmitate. C^{13}-Glucose containing media was fed to MDA-MB-231 cells expressing control or OGT shRNA for

48 hours. Lipids were then extracted from equal cell numbers from each condition and subjected to fatty acid methyl ester analysis (FAME). The final step (GC-MS) then analyzed palmitate species. These results confirmed that unlabeled palmitate was decreased by OGT suppression. However, in MDA-MB-231 shOGT cells, glucose was still used to generate newly synthesized palmitate, to a greater extent than control cells when comparing some labelled species (Figure 68A). It is possible that glutamine use in lipid synthesis is affected more by OGT manipulation as we have yet to determine if glucose or glutamine contributes more to this synthetic process in these cells. These results demonstrate that SREBP-1 is an important downstream effector of OGT-suppression induced phenotypes in breast cancer. These include; decreased lipogenic factors, induction of apoptosis, decreased glycolytic factors and metabolic changes.

4.2.5 SREBP-1 is critical for OGT-mediated regulation of breast cancer tumorigenesis *in vivo*

To determine if the regulation of SREBP-1 by OGT was important for tumor growth and survival *in vivo*, we employed an orthotopic xenograft animal model. We injected MDA-MB-231- Luciferase cells containing control vectors, stable OGT suppression, or cells containing exogenous SREBP-1 overexpression with and without OGT suppression into the inguinal fat pad of female 6-8 week old Nu/Nu mice. We monitored tumor growth as a readout of bioluminescence intensity and using caliper measurements. At animal endpoint we observed a significant rescue of tumor volume when SREBP-1 was restored compared to tumors where OGT was stably suppressed (Figure 69A-B, 70A). This result establishes that SREBP-1 is an important downstream effector of OGT in the promotion of cancer cell growth *in vivo*.

4.3 Figures and Figure Legends

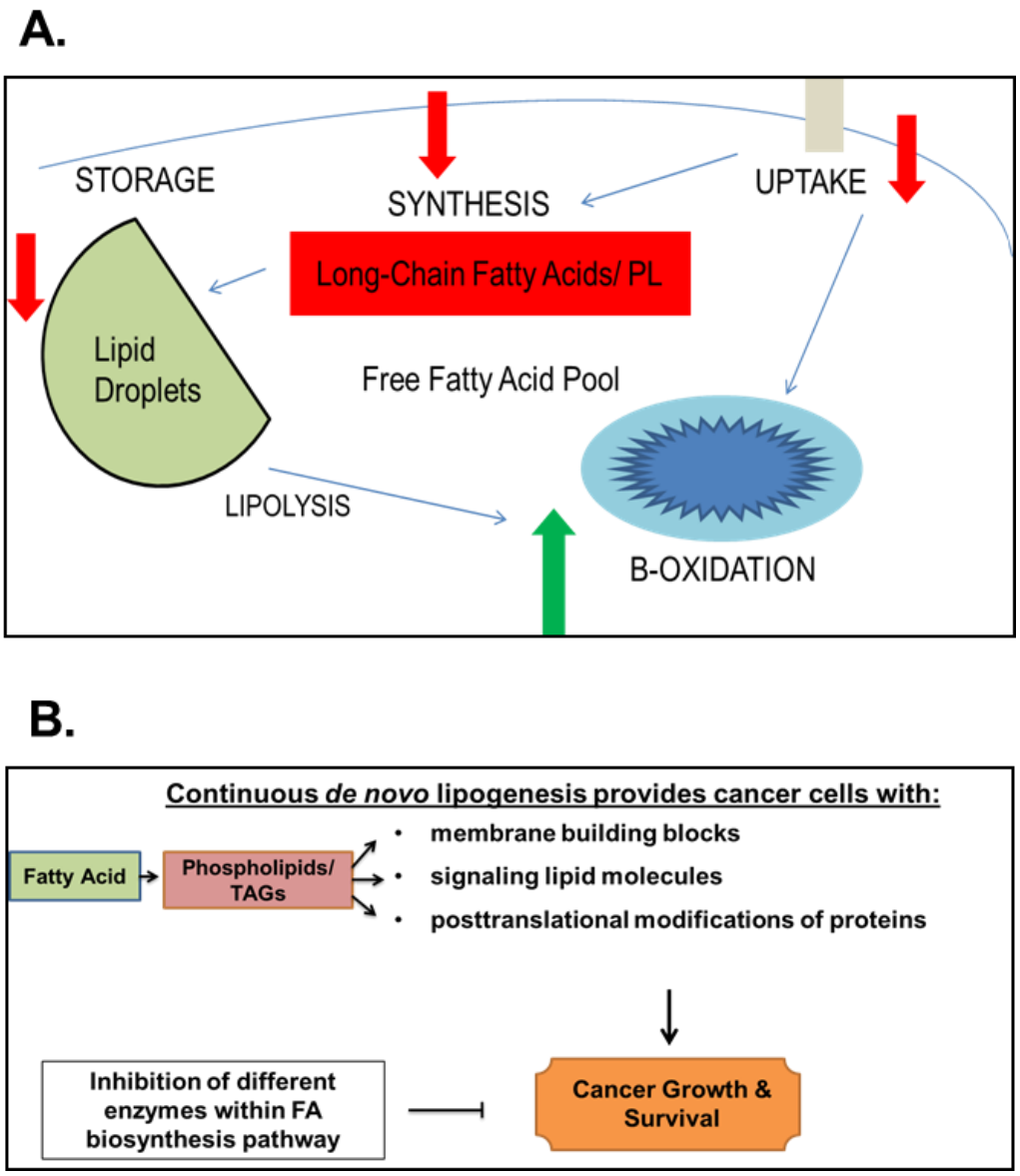

Figure 31: Model of cellular contributions to the free fatty acid pool and importance of fatty acids (A) Arrows indicate decreases (red) and increases (green) in processes that could result in increases in the free fatty acid pool within cells. (B) Diagram demonstrating how fatty acids contribute to cancer cell growth and survival. Inhibition of enzymes in lipogenesis has been determined to decrease cancer cell viability.

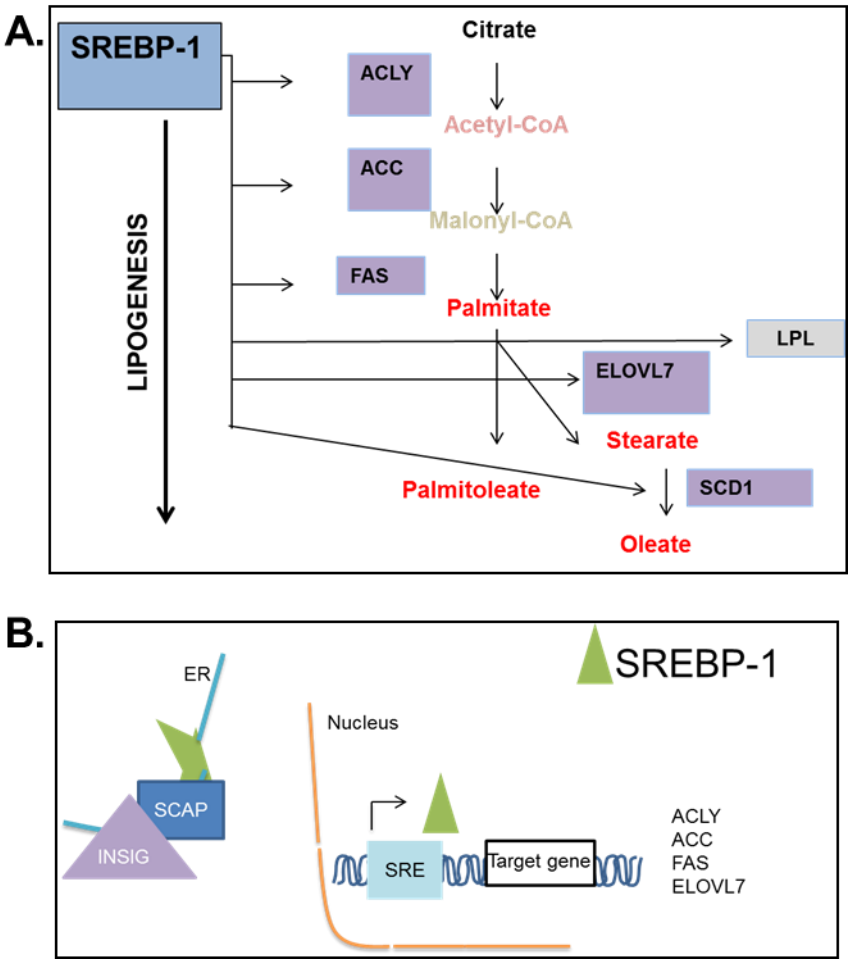

Figure 32: Model of SREBP-1 transcriptional control of lipogenesis and SREBP-1 cellular localization (A) Signaling through RTKs activating PI3K/AKT/mTOR is required and sufficient for OGT upregulation through c-MYC and HSP90 stabilizing OGT protein. c-MYC itself is O-GlcNAcylated which promotes c-MYC expression and generates a feed forward loop promoting tumor growth.

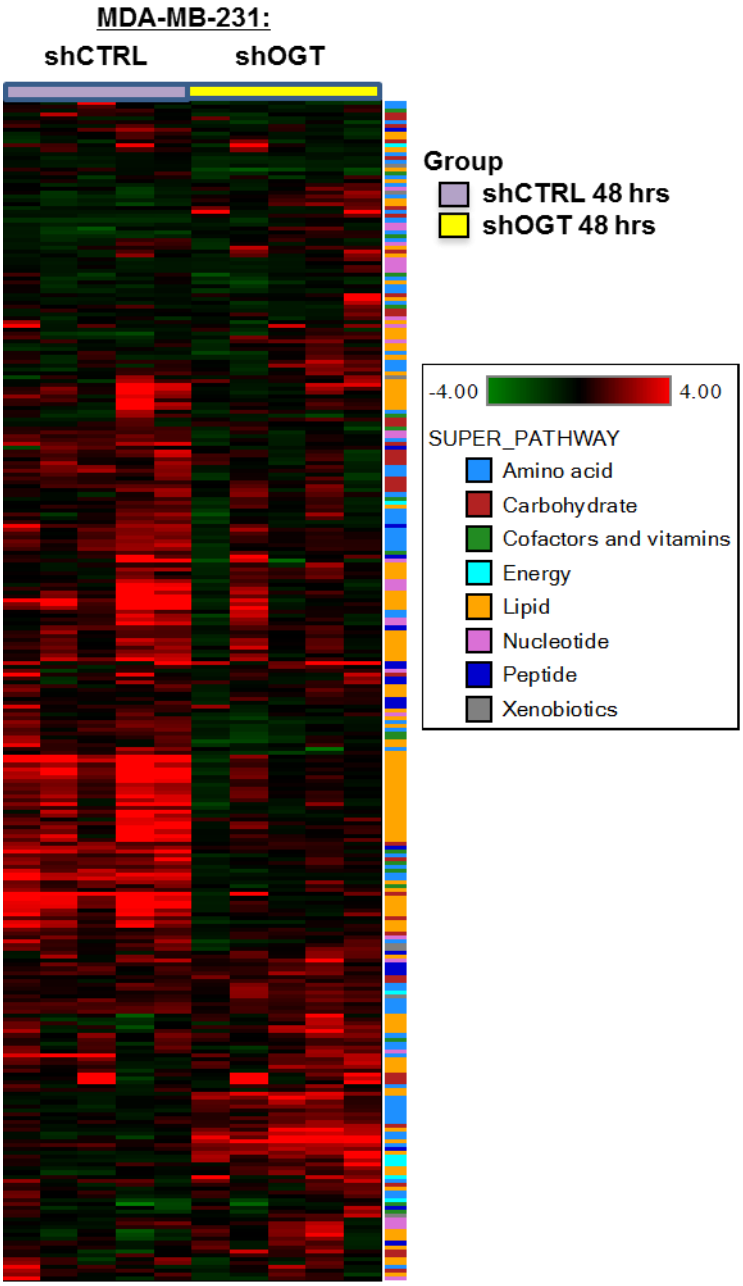

Figure 33: Significant changes occur in metabolites from all superpathways listed in MDA-MB-231 cells upon OGT suppression. Heat map displaying decreased values (green) and increased (red) metabolites in MDA-MB-231 cells comparing control (purple) to cells where OGT has been suppressed via RNAi for 48 hours (yellow).

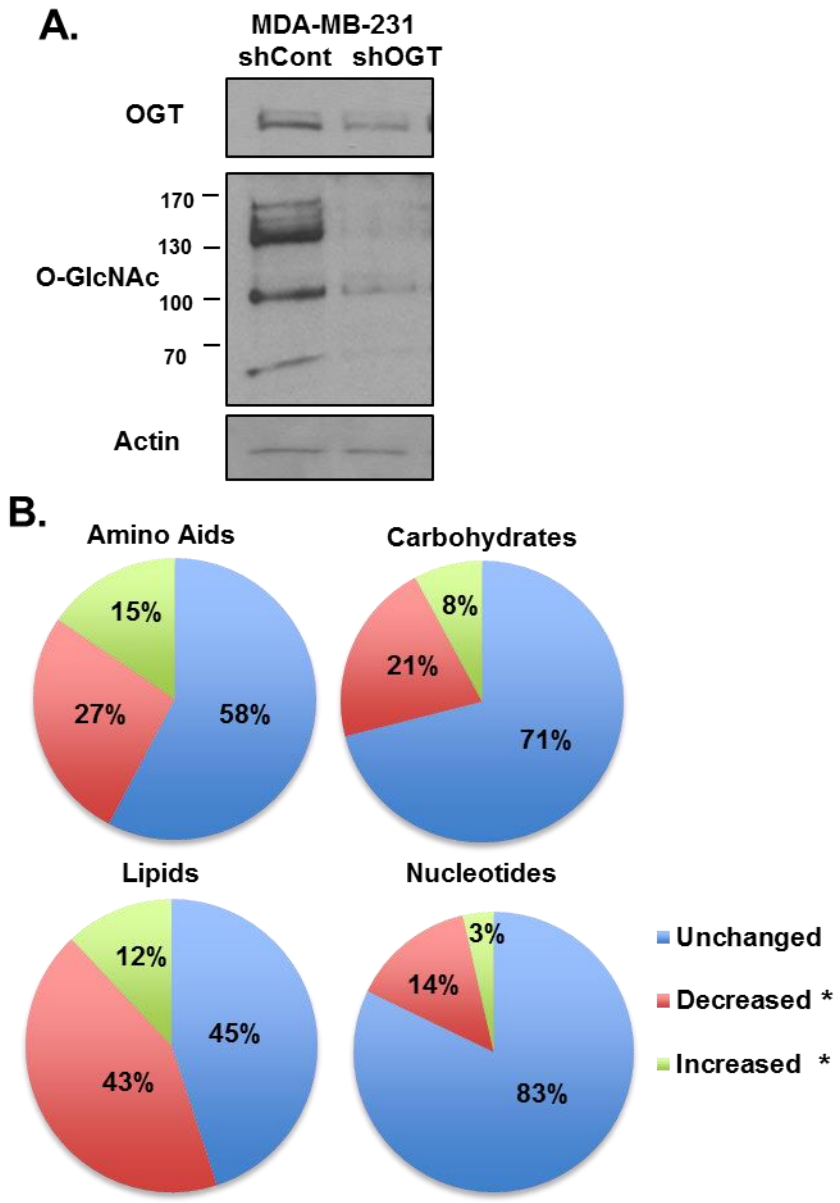

Figure 34: Significant changes occur in metabolites from all metabolite categories shown in MDA-MB-231 cells upon OGT suppression. (A) MDA-MB-231 cells expressing control and shOGT plasmids were analyzed via western blot using the indicated antibodies. (B) Pie charts displaying significant changes found in metabolites categorized as amino acids, carbohydrates, lipids and nucleotides when comparing MDA-MB-231 control and shOGT cells analyzed via LC-MS. Unchanged metabolites (blue), decreased metabolites (red) and increased metabolites (green). Mean +/- SE *$p<0.05$.

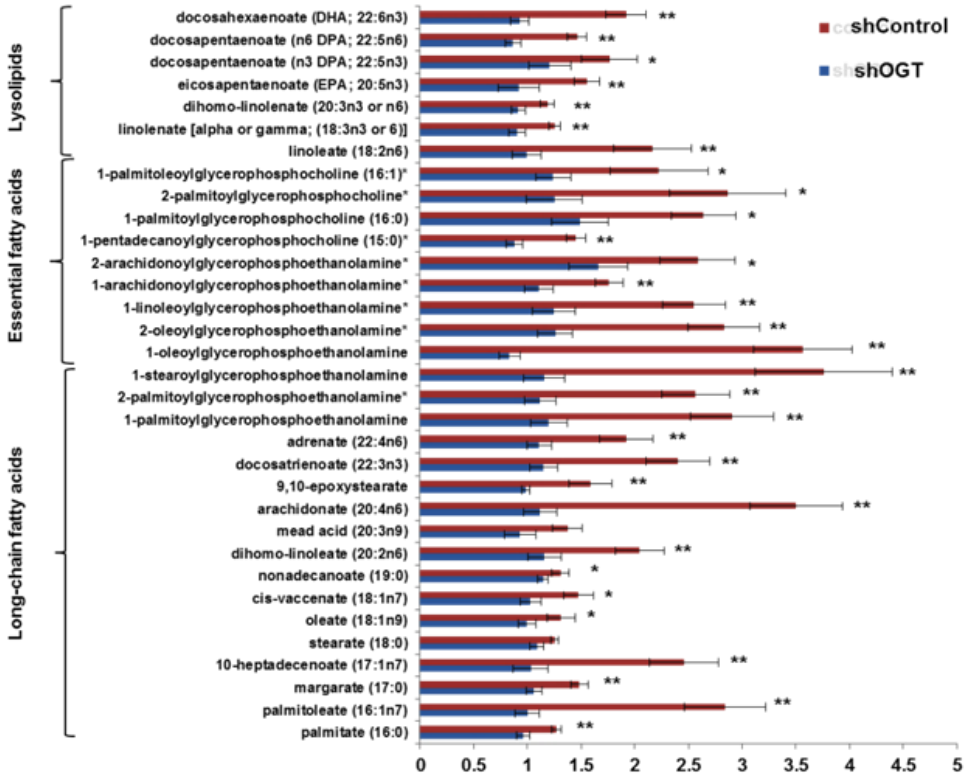

Figure 35: Significant decreases occur in many lipid metabolites in MDA-MB-231 cells upon OGT inhibition MDA-MB-231 cells expressing control and shOGT plasmids were analyzed via LC-MS. Mean +/- SE *p<0.05, ** p< 0.005.

Sub Pathway	Biochemical Name	Platform	shOGT 48h/shCTRL 48h	p-value
Carnitine metabolism	carnitine	LC/MS pos	1.43	0.002
	3-dehydrocarnitine*	LC/MS pos	1.21	0.0112
	palmitoylcarnitine	LC/MS pos	1.63	0.023
	stearoylcarnitine	LC/MS pos	1.56	0.0285
	oleoylcarnitine	LC/MS pos	1.82	0.0522
Essential Fatty Acids	linoleate (18:2n6)	LC/MS neg	0.41	0.0002
	linolenate [alpha or gamma; (18:3n3 or 6)]	LC/MS neg	0.44	8.50E-05
	dihomo-linolenate (20:3n3 or n6)	LC/MS neg	0.31	0.0002
	eicosapentaenoate (EPA; 20:5n3)	LC/MS neg	0.23	1.44E-05
	docosapentaenoate (n3 DPA; 22:5n3)	LC/MS neg	0.44	0.0007
	docosapentaenoate (n6 DPA; 22:5n6)	LC/MS neg	0.49	0.001
	docosahexaenoate (DHA; 22:6n3)	LC/MS neg	0.63	0.0042

Figure 36: Changes in essential fatty acid and carnitine metabolites in MDA-MB-231 48 hours after OGT inhibition Carnitine and essential fatty acid metabolite changes comparing MDA-MB-231-control and MDA-MB-231-shOGT as analyzed via LC-MS or GC-MS. Significant decreases (dark green) and increases (dark red) $p<0.05$ and nearly significant decreases (light green) and decreases (pink) $p>0.05$.

Sub Pathway	Biochemical Name	Platform	shOGT 48h/shCTRL 48h	p-value
Long Chain Fatty Acid	palmitate (16:0)	LC/MS neg	0.75	0.0017
	palmitoleate (16:1n7)	LC/MS neg	0.35	1.51E-05
	margarate (17:0)	LC/MS neg	0.71	0.0023
	10-heptadecenoate (17:1n7)	LC/MS neg	0.42	0.0002
	stearate (18:0)	LC/MS neg	0.87	0.0455
	oleate (18:1n9)	GC/MS	0.76	0.0152
	cis-vaccenate (18:1n7)	GC/MS	0.7	0.0038
	nonadecanoate (19:0)	LC/MS neg	0.88	0.0652
	10-nonadecenoate (19:1n9)	LC/MS neg	0.65	0.0097
	dihomo-linoleate (20:2n6)	LC/MS neg	0.57	0.0021
	mead acid (20:3n9)	LC/MS neg	0.68	0.0287
	arachidonate (20:4n6)	LC/MS neg	0.32	0.0005
	docosatrienoate (22:3n3)	LC/MS neg	0.48	0.0007
	adrenate (22:4n6)	LC/MS neg	0.58	0.005
Fatty Acid, Oxidized	9,10-epoxystearate	LC/MS neg	0.62	0.0211
Fatty Acid, Monohysroxyl	2-hydroxystearate	LC/MS neg	0.62	0.0739
Fatty Acid, dicarboxylate	2-hydroxyglutarate	GC/MS	2.74	9.60E-10
Fatty Acid/ BCAA metabolism	propionylcarnitine	LC/MS pos	1.8	6.28E-08
	butyrylcarnitine	LC/MS pos	1.19	0.082
Lysolipids	1-palmitoylglycerophosphoethanolamine	LC/MS neg	0.64	0.0223
	2-palmitoylglycerophosphoethanolamine*	LC/MS pos	0.61	0.0004
	1-oleoylglycerophosphoethanolamine	LC/MS neg	0.44	0.0023
	2-oleoylglycerophosphoethanolamine*	LC/MS neg	0.56	0.0223
	1-linoleoylglycerophosphoethanolamine*	LC/MS neg	0.46	0.0091
	1-arachidonoylglycerophosphoethanolamine*	LC/MS neg	0.72	0.0029
	2-arachidonoylglycerophosphoethanolamine*	LC/MS pos	0.77	0.0017
	2-docosapentaenoylglycerophosphoethanolamine*	LC/MS pos	1.6	0.0017
	1-stearoylglycerophosphoglycerol	LC/MS neg	2.06	4.04E-06
	2-stearoylglycerophosphoglycerol*	LC/MS neg	2.33	4.12E-08
	1-pentadecanoylglycerophosphocholine (15:0)*	LC/MS pos	0.59	0.0009
	1-palmitoylglycerophosphocholine (16:0)	LC/MS pos	0.68	0.0419
	2-palmitoylglycerophosphocholine*	LC/MS pos	0.59	9.94E-05
	1-palmitoleoylglycerophosphocholine (16:1)*	LC/MS pos	0.49	2.84E-05
	2-palmitoleoylglycerophosphocholine*	LC/MS pos	1.24	0.007
	1-oleoylglycerophosphocholine (18:1)	LC/MS pos	0.56	0.0118
	1-linoleoylglycerophosphocholine (18:2n6)	LC/MS pos	0.66	0.0431
	2-arachidonoylglycerophosphocholine*	LC/MS pos	0.79	0.0378
	1-docosapentaenoylglycerophosphocholine (22:5n3)*	LC/MS pos	0.71	0.0444
	2-docosahexaenoylglycerophosphocholine*	LC/MS pos	1.28	0.0343
	1-stearoylglycerophosphoinositol	LC/MS neg	0.55	0.0001
	1-arachidonoylglycerophosphoinositol*	LC/MS neg	0.5	0.0132
	2-arachidonoylglycerophosphoinositol*	LC/MS neg	0.52	0.0089
	2-oleoylglycerophosphoinositol*	LC/MS neg	0.37	0.0347
	1-oleoylglycerophosphoserine	LC/MS neg	0.43	0.0049
	2-oleoylglycerophosphoserine*	LC/MS neg	0.6	0.0104
	1-palmitoylplasmenylethanolamine*	LC/MS neg	0.49	0.0106
	1-stearoylplasmenylethanolamine*	LC/MS neg	0.57	0.0381
	2-eicosapentaenoylglycerophosphoethanolamine*	LC/MS pos	0.71	3.29E-05
	1-oleoylplasmenylethanolamine*	LC/MS neg	0.29	0.0007
Sphinolipids	sphinganine	LC/MS pos	1.45	0.0002
	sphingosine	LC/MS pos	1.4	0.0015
Sterol/steroid	7-beta-hydroxycholesterol	GC/MS	0.67	0.0559

Figure 37: Changes in fatty acid metabolites in MDA-MB-231 48 hours after OGT inhibition MDA-MB-231 cells expressing control and shOGT plasmids were analyzed via LC-MS or GC-MS. Mean values for measured metabolite from MDA-MB-231-shOGT normalized to MDA-MB-231-control. Significant decreases (dark green) and increases (dark red) $p<0.05$ and nearly significant decreases (light green) and decreases (pink) $p>0.05$.

Sub Pathway	Biochemical Name	Platform	shOGT 48h/shCTRL 48h	p-value
Glcyine,serine and threonine metabolism	glycine	GC/MS	0.73	0.0047
	N-acetylserine	LC/MS pos	0.78	0.0012
	N-acetylthreonine	LC/MS neg	0.45	1.69E-10
Alanine and aspartate metabolism	aspartate	GC/MS	0.36	6.43E-07
	alanine	GC/MS	0.87	0.0589
	N-acetylalanine	LC/MS neg	0.77	0.0013
	N-acetylaspartate (NAA)	LC/MS pos	1.98	2.46E-10
glutamate metabolism	glutamate	LC/MS pos	1.13	0.0663
	glutamine	LC/MS pos	0.8	0.0079
	N-acetyl-aspartyl-glutamate (NAAG)	LC/MS pos	1.57	6.43E-05
histidine metabolism	histidine	LC/MS neg	0.66	0.0009
lysine metabolism	pipecolate	LC/MS pos	0.59	3.98E-06
phenylalanine and tyrosine metabolism	phenylalanine	LC/MS pos	0.88	0.0952
	p-cresol sulfate	LC/MS neg	0.82	0.0209
	tyrosine	LC/MS pos	0.82	0.0127
	phenylacetylglycine	LC/MS neg	1.74	0.0008
tryptophan metabolism	kynurenine	LC/MS pos	0.64	0.006
	tryptophan	LC/MS pos	0.81	0.002
	C-glycosyltryptophan*	LC/MS pos	0.72	0.0003
valine, leucine and isoleucine metabolism	3-methyl-2-oxovalerate	LC/MS neg	2.62	0.0021
	isoleucine	LC/MS pos	0.8	0.0033
	leucine	LC/MS pos	0.82	0.0182
	4-methyl-2-oxopentanoate	LC/MS neg	2.93	0.0007
	isobutyrylcarnitine	LC/MS pos	1.62	0.001
	2-methylbutyrylcarnitine (C5)	LC/MS pos	1.13	0.0609
	isovalerylcarnitine	LC/MS pos	2.21	1.42E-06
	tiglyl carnitine	LC/MS pos	0.22	1.84E-13
cysteine, methionine, metabolism	cysteine	GC/MS	0.36	0.0559
	N-formylmethionine	LC/MS neg	0.83	0.0135
	methionine	LC/MS pos	0.85	0.0993
creatine metabolism	creatine	LC/MS pos	1.74	1.19E-05
polyamine metabolism	5-methylthioadenosine (MTA)	LC/MS pos	1.19	0.0015
	putrescine	GC/MS	1.51	0.0001
	spermidine	LC/MS pos	1.32	0.0641
glutathione metabolism	5-oxoproline	LC/MS neg	0.8	0.0914
	cysteine-glutathione disulfide	LC/MS pos	0.37	0.0056
	ophthalmate	LC/MS pos	1.53	4.18E-05

Figure 38: Changes in metabolites in MDA-MB-231 48 hours after OGT inhibition
MDA-MB-231 cells expressing control and shOGT plasmids were analyzed via LC-MS or GC-MS. Mean values for measured metabolite from MDA-MB-231-shOGT normalized to MDA-MB-231-control. Significant decreases (dark green) and increases (dark red) $p<0.05$ and nearly significant decreases (light green) and decreases (pink) $p>0.05$.

Sub Pathway	Biochemical Name	Platform	shOGT 48h/shCTRL 48h	p-value
dipeptide	pro-hydroxy-pro	LC/MS pos	0.53	0.0013
gamma glutamyl	gamma-glutamylglutamine	LC/MS pos	0.53	2.65E-05
	gamma-glutamyltyrosine	LC/MS pos	0.82	0.0561
	gamma-glutamylthreonine*	LC/MS pos	1.59	0.0002
fructose, mannose, AAAA	fructose	GC/MS	2.15	0.0932
	lactose	GC/MS	1.35	0.0102
	mannitol	GC/MS	0.58	0.0008
	sorbitol	GC/MS	0.65	0.0001
pyruvate metabolism	lactate	GC/MS	0.89	0.0842
krebs cycle	citrate	GC/MS	3.55	0.0014
	cis-aconitate	LC/MS neg	2.46	0.0024
	alpha-ketoglutarate	GC/MS	4.42	0.2085
	malate	GC/MS	1.3	0.0032
nicotinate and nicotinamide metabolism	nicotinamide adenine dinucleotide (NAD+)	LC/MS pos	0.7	0.0004
	nicotinate adenine dinucleotide (NAAD+)	LC/MS neg	0.72	0.0121
	1-methylnicotinamide	LC/MS pos	0.7	1.48E-05
Nuclotide sugars, pentose metabolsim	arabitol	GC/MS	0.72	0.0015
	sedoheptulose-7-phosphate	GC/MS	0.45	0.0019
	gluconate	GC/MS	0.24	8.53E-05
	ribulose	GC/MS	0.55	0.0268
	UDP-glucuronate	LC/MS neg	0.86	0.0163
	xylulose	GC/MS	0.61	0.0701
pyridoxal	pyridoxal	LC/MS pos	0.7	0.048
riboflavin metabolism	flavin adenine dinucleotide (FAD)	LC/MS neg	0.85	0.0048
	riboflavin (Vitamin B2)	LC/MS pos	1.01	0.8198
	flavin mononucleotide (FMN)	LC/MS neg	0.55	1.84E-06
thiamine metabolism	thiamin (Vitamin B1)	LC/MS pos	0.74	0.008
	thiamin diphosphate	LC/MS neg	0.95	0.4314
viamin b6 metabolism	pyridoxine (Vitamin B6)	LC/MS pos	0.8	0.0114
purine metabolism	inosine	LC/MS neg	0.82	0.0547
	guanine	LC/MS pos	0.54	0.0765
	guanosine	LC/MS pos	0.69	0.0469
pyrimidine metabolism	uracil	GC/MS	0.46	0.0271
	5,6-dihydrouracil	GC/MS	0.59	0.0033
	cytidine 5'-monophosphate (5'-CMP)	LC/MS pos	1.16	0.027
	cytidine-3'-monophosphate (3'-CMP)	LC/MS pos	0.75	0.0025
	orotate	GC/MS	0.7	0.0814

Figure 39: Changes in metabolites in MDA-MB-231 48 hours after OGT inhibition MDA-MB-231 cells expressing control and shOGT plasmids were analyzed via LC-MS or GC-MS. Mean values for measured metabolite from MDA-MB-231-shOGT normalized to MDA-MB-231-control. Significant decreases (dark green) and increases (dark red) $p<0.05$ and nearly significant decreases (light green) and decreases (pink) $p>0.05$.

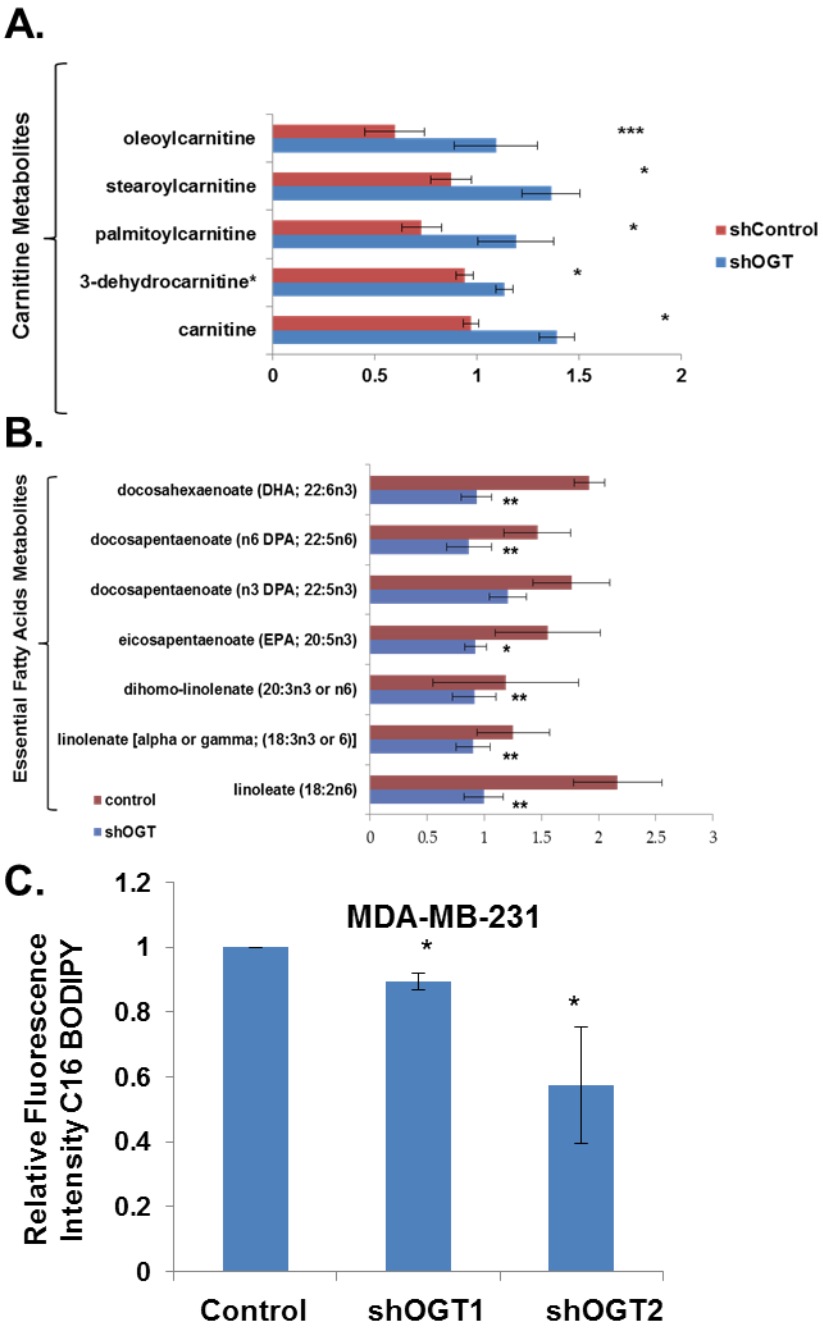

Figure 40: Significant changes occur in essential and carnitine lipid metabolites in MDA-MB-231 cells upon OGT inhibition(A) MDA-MB-231 cells expressing control and shOGT plasmids were analyzed via LC-MS. Significant increases in carnitine metabolites between control (red) and shOGT (blue) MDA-MB-231 cells. (B) Essential fatty acids measured via LC-MS in MDA-MB-231 control (red) and shOGT (blue) cells. (C) Uptake of C16 –fluorescent lipid mimetic in MDA-MB-231 control, shOGT1 and shOGT2 cells as measured via FACS. Mean +/- SE *p<0.05, ** p< 0.01, ***p<0.005.

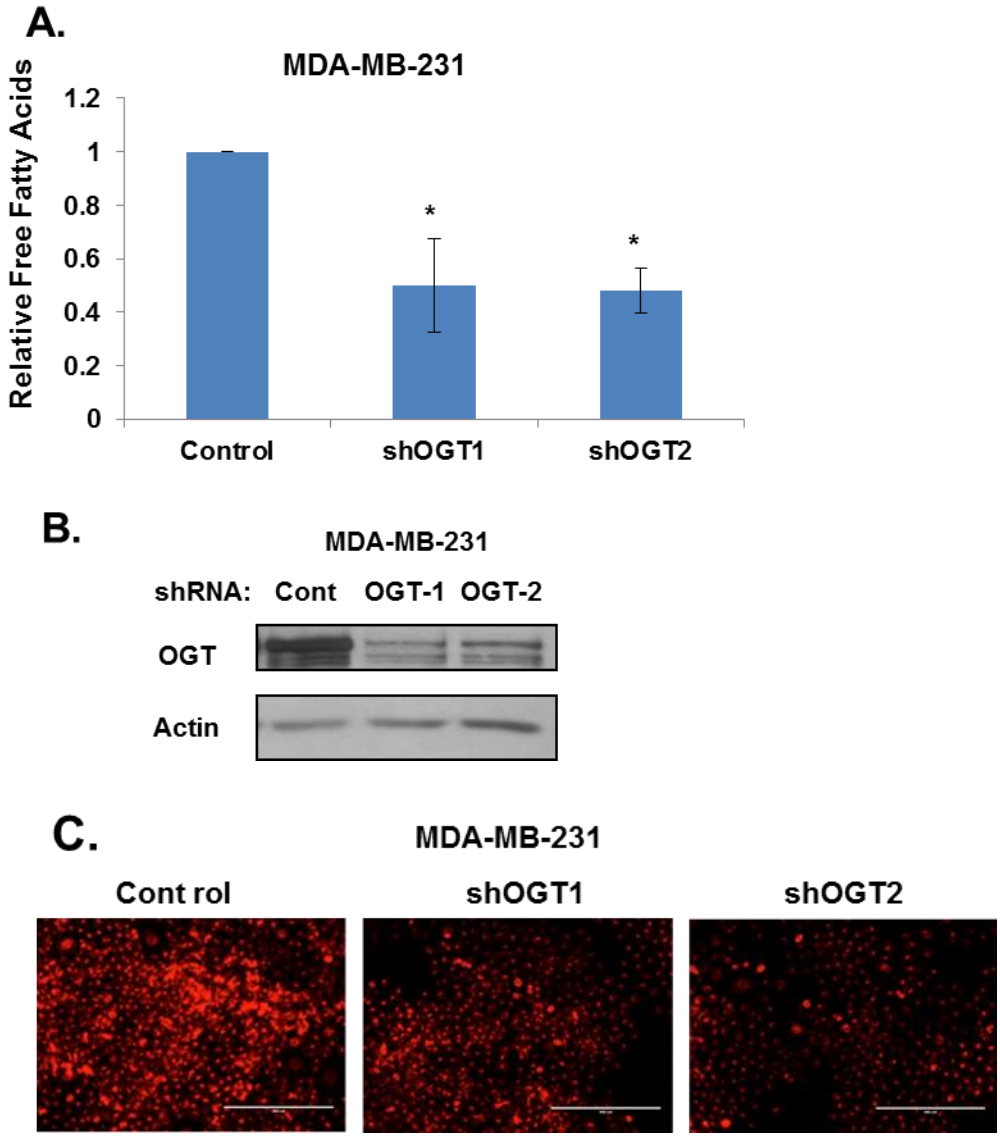

Figure 41: OGT inhibition decreases free fatty acids and lipid droplets in MDA-MB-231 cells (A) Free fatty acids were isolated and measured from MDA-MB-231 cells expressing control, shOGT-1 and shOGT-2 plasmids. (B) Western blot analysis of MDA-MB-231 control, shOGT-1 and shOGT-2 cells analyzed with the indicated antibodies. (C) Representative images of fluorescent imaging of nile red stained MDA-MB-231 control, shOGT-1 and shOGT-2 cells.

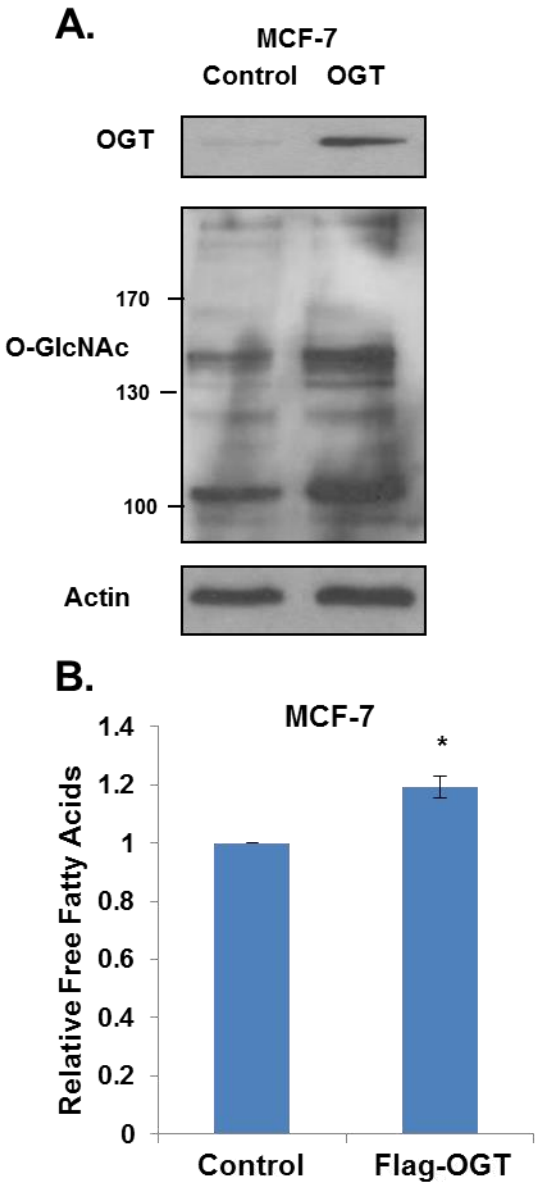

Figure 42: OGT overexpression in MCF7 cells results in increased relative free fatty acids (A) Cell lysates from MCF7 cells stably overexpressing control or Flag-OGT were collected for western blot analysis with the indicated antibodies. (B) Measurement of relative free fatty acids in MCF7 stably overexpressing control or Flag-OGT. Mean ± SE. *$p<0.05$

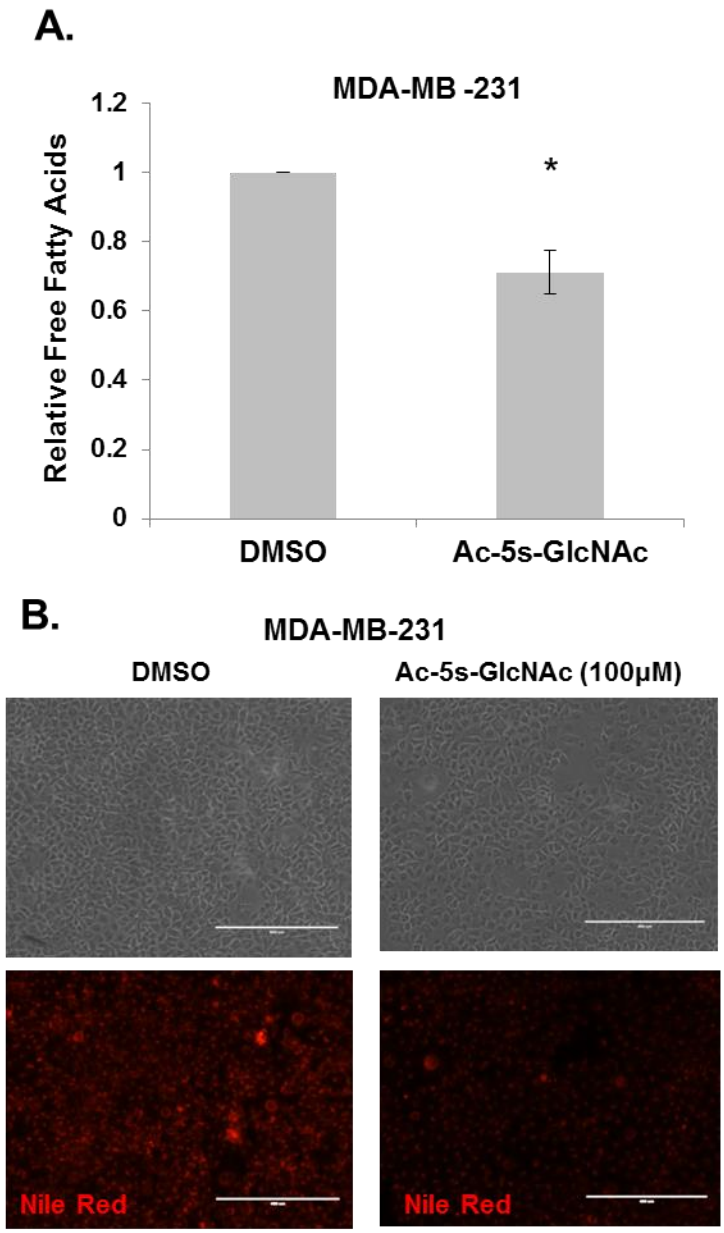

Figure 43: Pharmacological inhibition of OGT decreases free fatty acids and lipid droplets in MDA-MB-231 cells (A) Free fatty acids were isolated and measured from MDA-MB-231 cells treated with vehicle control (DMSO) or Ac-5sGlcNAc (100uM) for 24 hours. (B) Representative bright field and immunofluorescence images of nile red stained MDA-MB-231 treated with control DMSO or Ac-5sGlcNAc for 24 hours. Mean $\pm$ SE; * p-value< 0.05.

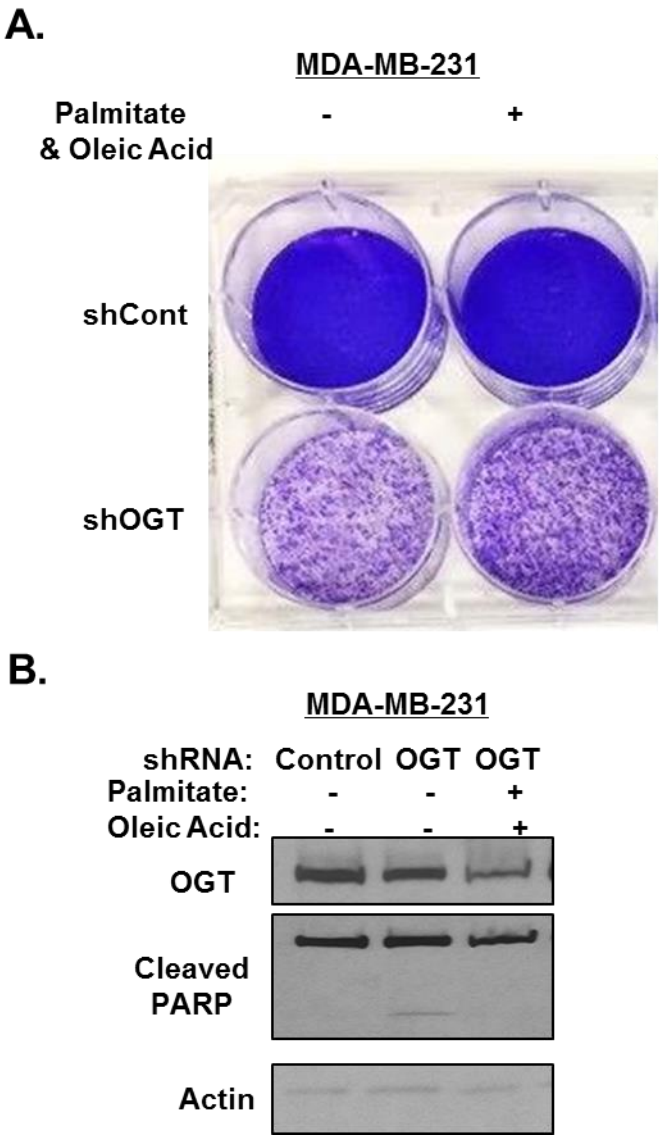

Figure 44: Addition of exogenous lipids partly restores growth in conditions of OGT suppression in MDA-MB-231 cells (A) Crystal Violet stained 2D MDA-MB-231 cells containing control or stable OGT suppression for 6 days treated with control PBS/BSA solution or 100um Sodium Palmitate and 40um Oleic acid in PBS/BSA. (B) Western blot analysis of MDA-MB-231 cells representing the conditions in (A) analyzed with the indicated antibodies.

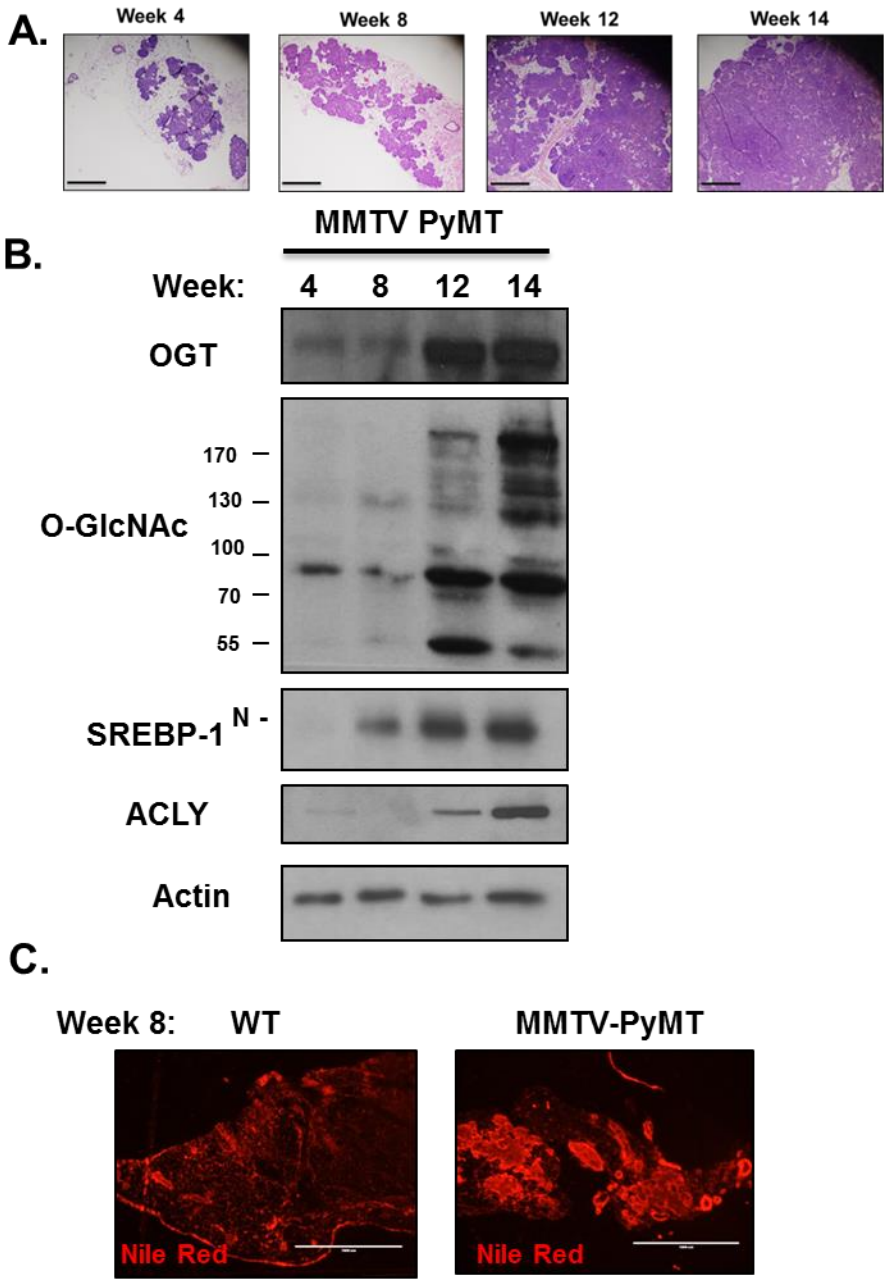

Figure 45: OGT and SREBP-1 protein expression correlate with tumor progression *in vivo*. (A) H&E staining of mammary fat pads collected from MMTV-PyMT mice at weeks 4, 8, 12 and 14. (B) Cell lysates was collected from mammary fat pad tissue collected from MMTV-PyMT mice at 4, 8, 12 and 14 weeks of age for immunoblot analysis with the indicated antibodies. (C) Representative images of nile red stained mammary fat pad tissue collected from WT and MMTV-PyMT mice at 8 weeks of age.

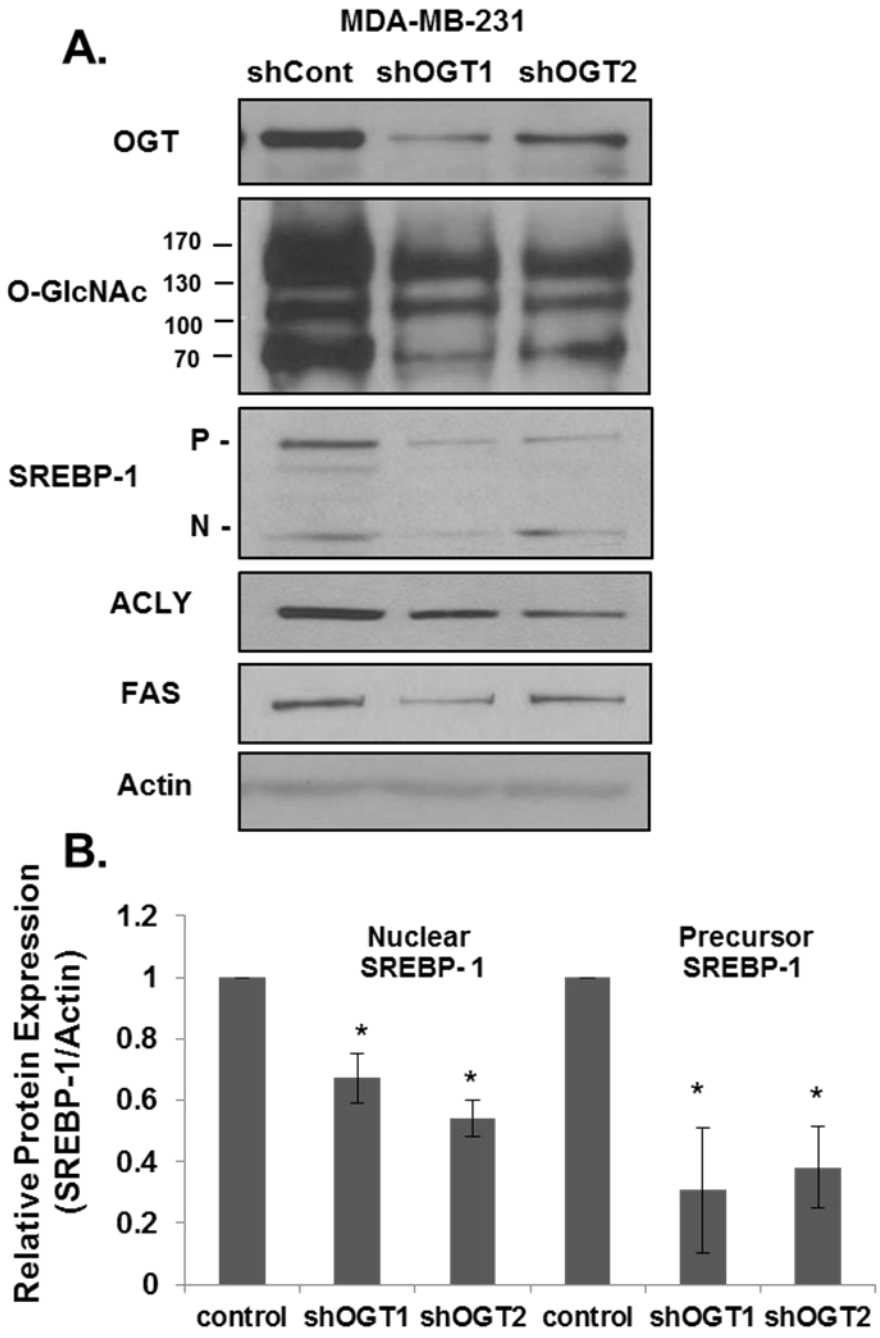

Figure 46: OGT inhibition results in decreased SREBP-1 protein in MDA-MB-231 cells (A) Cell lysates from MDA-MB-231 cells expressing control, OGT-1 or OGT-2 shRNA were collected for immunoblot analysis with the indicated antibodies (top). SREBP-1 nuclear (N) and precursor (P) are indicated on the left. (B) SREBP-1 protein expression was quantified and normalized to actin (below). Mean +/- SE *p<0.01. Statistical analysis performed for separate SREBP-1 forms examined comparing shOGT1 and shOGT2 samples to control.

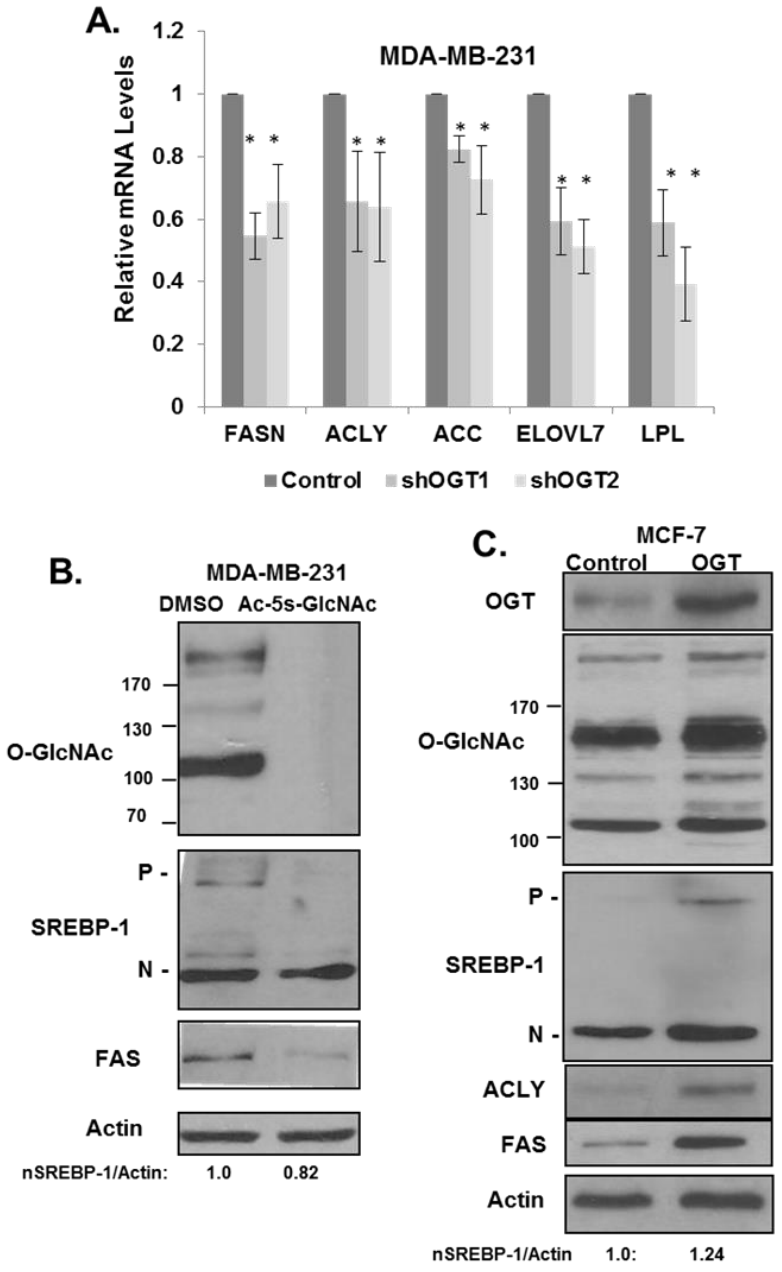

Figure 47: OGT regulates SREBP-1 expression in breast cancer cells (A) Measurement of relative mRNA expression of SREBP-1 target genes from control or stable OGT shRNA expressing MDA-MB-231 cells using qRT-PCR. (B) Western blot of MDA-MB-231 cells treated for 48 hours with control (DMSO) or 100 mM Ac-5s-GlcNAc analyzed with the indicated antibodies. (C) Western blot analysis of MCF7 cells stably overexpressing control or Flag-OGT analyzed with the indicated antibodies. Mean ± SE. *$p<0.05$ **$p< 0.01$. Statistical analysis performed for separate genes examined comparing shOGT1 and shOGT2 samples to control.

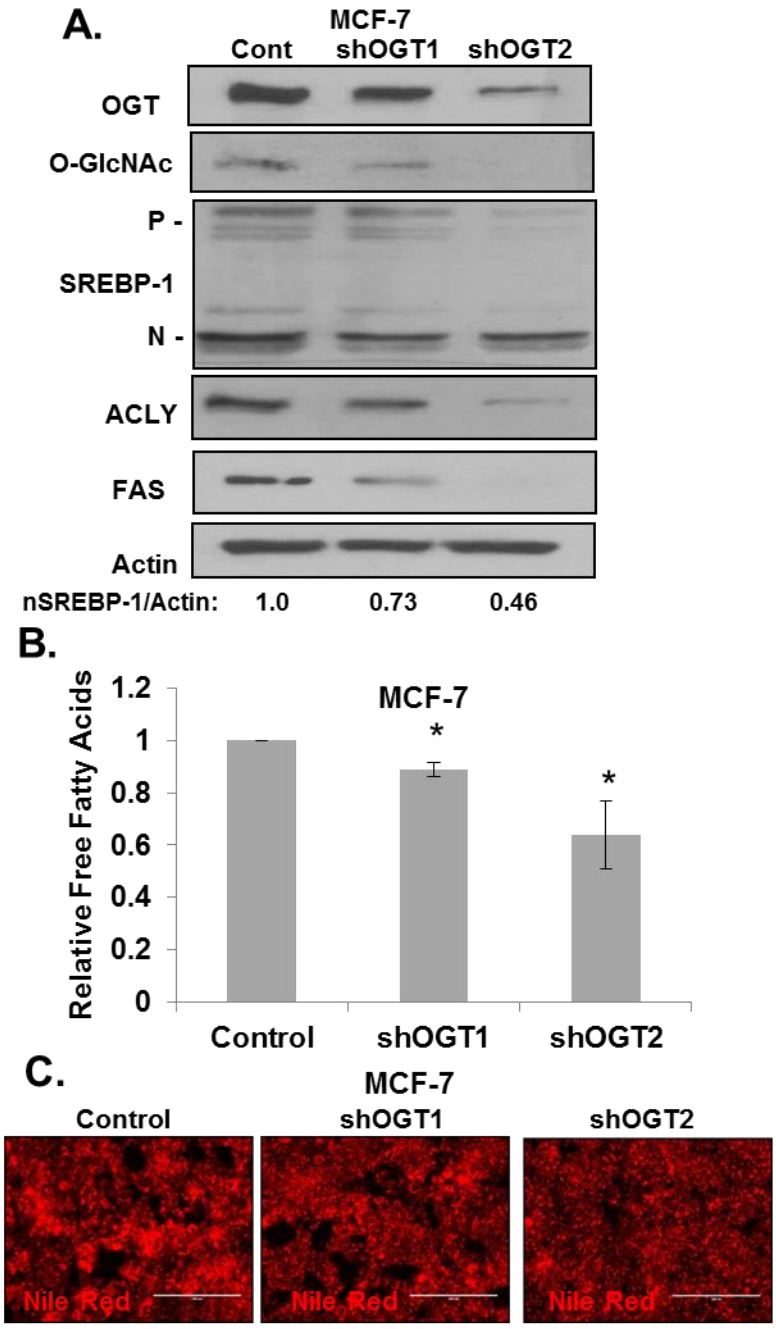

Figure 48: OGT inhibition decreases SRBEP-1, free fatty acids and lipid droplets in MCF7 cells (A) Western blot analysis of MCF7 control, shOGT-1 and shOGT-2 cells analyzed with the indicated antibodies. (B) Free fatty acids were isolated and measured from MCF7 cells expressing control, shOGT-1 or shOGT-2. (C) Representative images of fluorescent imaging of nile red stained MCF7 control, shOGT-1 and shOGT-2 cells. Mean ± SE. *$p<0.05$.

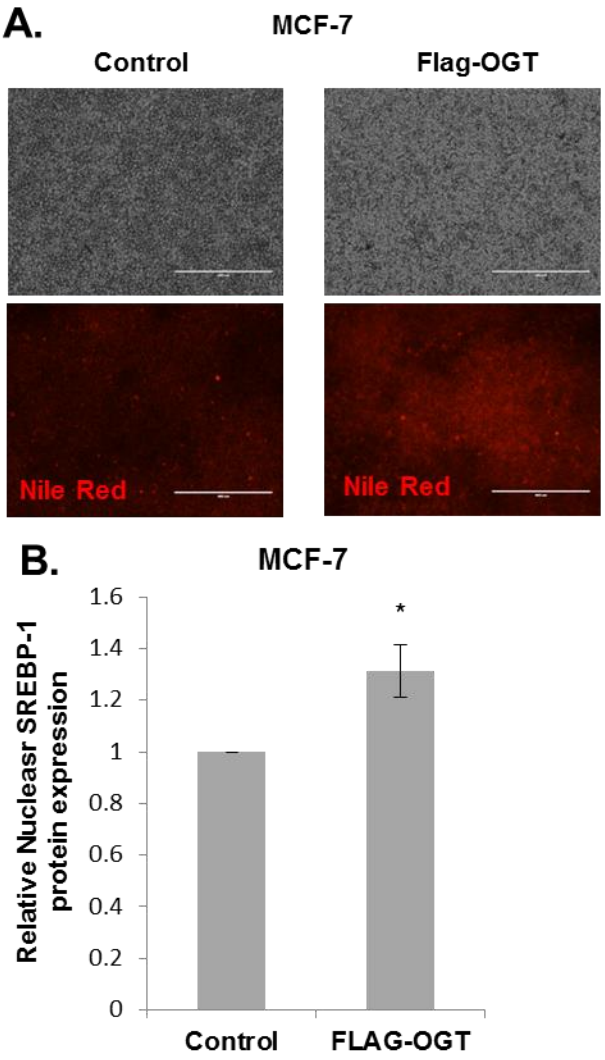

Figure 49: OGT overexpression increases lipid droplet content and increases nuclear SREBP-1 expression (A) Representative images of bright field and nile red stained MCF7 cells containing control or Flag-OGT plasmid. (B) Quantification of relative SREBP-1 protein expression from immunoblot analysis of MCF7 cells containing control or Flag-OGT plasmid. Mean $\pm$ SE; * p-value< 0.05.

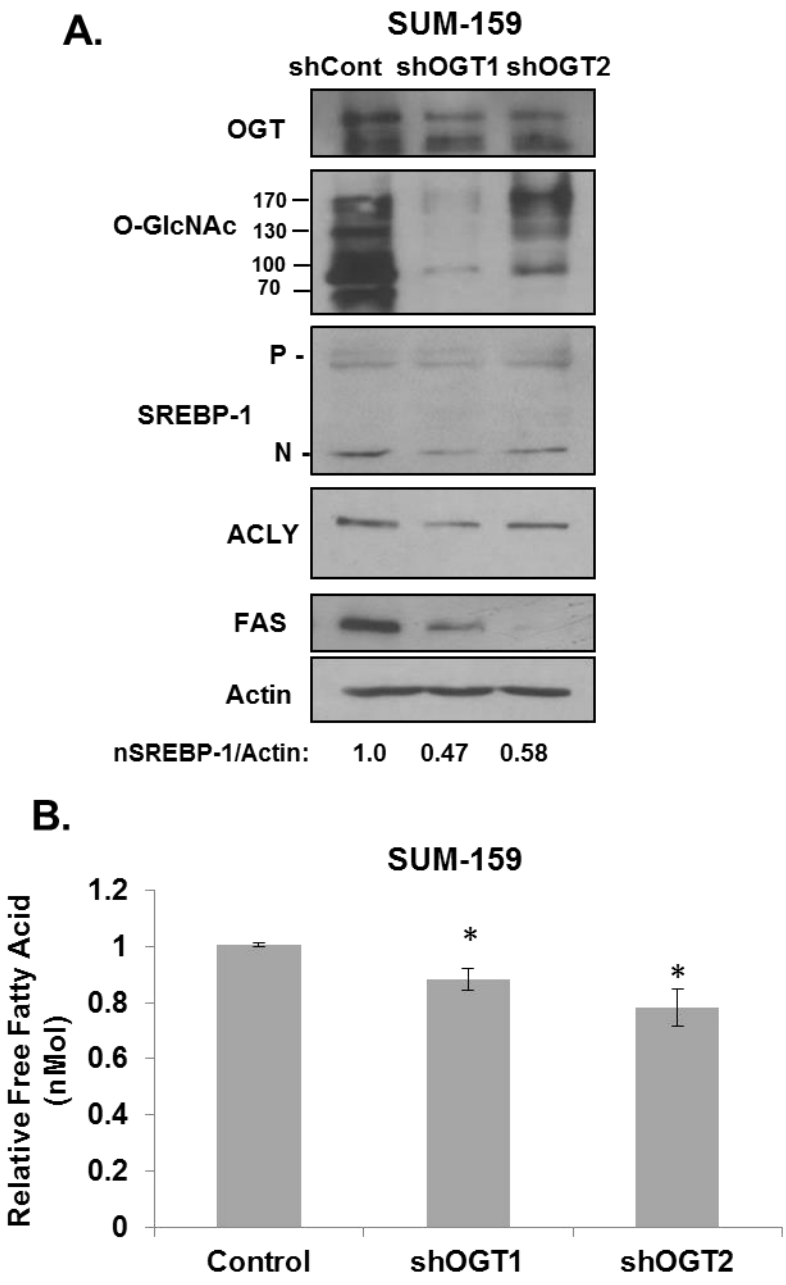

Figure 50: OGT inhibition decreases SREBP-1 and free fatty acids in SUM-159 cells (A) Western blot analysis of SUM-159 control, shOGT-1 and shOGT-2 cells analyzed with the indicated antibodies. (B) Free fatty acids were isolated and measured from SUM-159 cells expressing control, shOGT-1 or shOGT-2. Mean ± SE. *$p<0.05$.

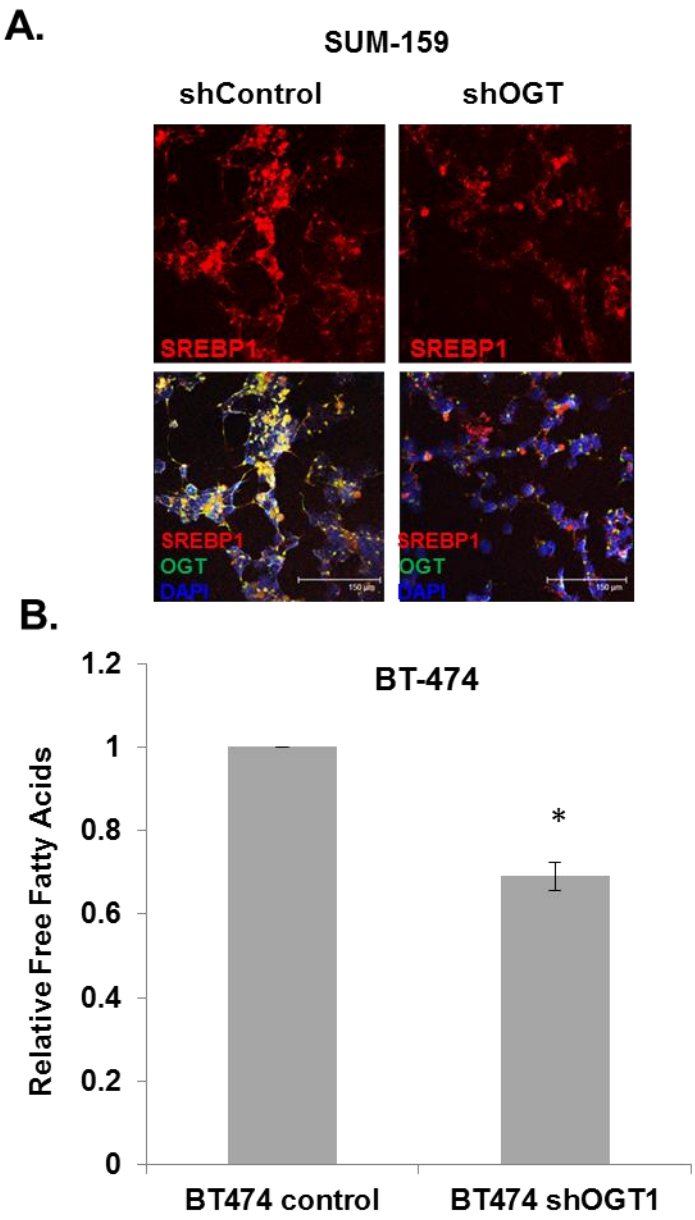

Figure 51: OGT inhibition decreases SREBP-1 in SUM-159 cells and free fatty acids in BT-474 cells (A) Representative images of immunofluorescence in 3-D culture of SUM-159 control and shOGT-1 cells analyzed with the indicated antibodies and stains. (B) Free fatty acids were isolated and measured from BT-474 cells expressing control and shOGT-1. Mean $\pm$ SE; * p-value< 0.01.

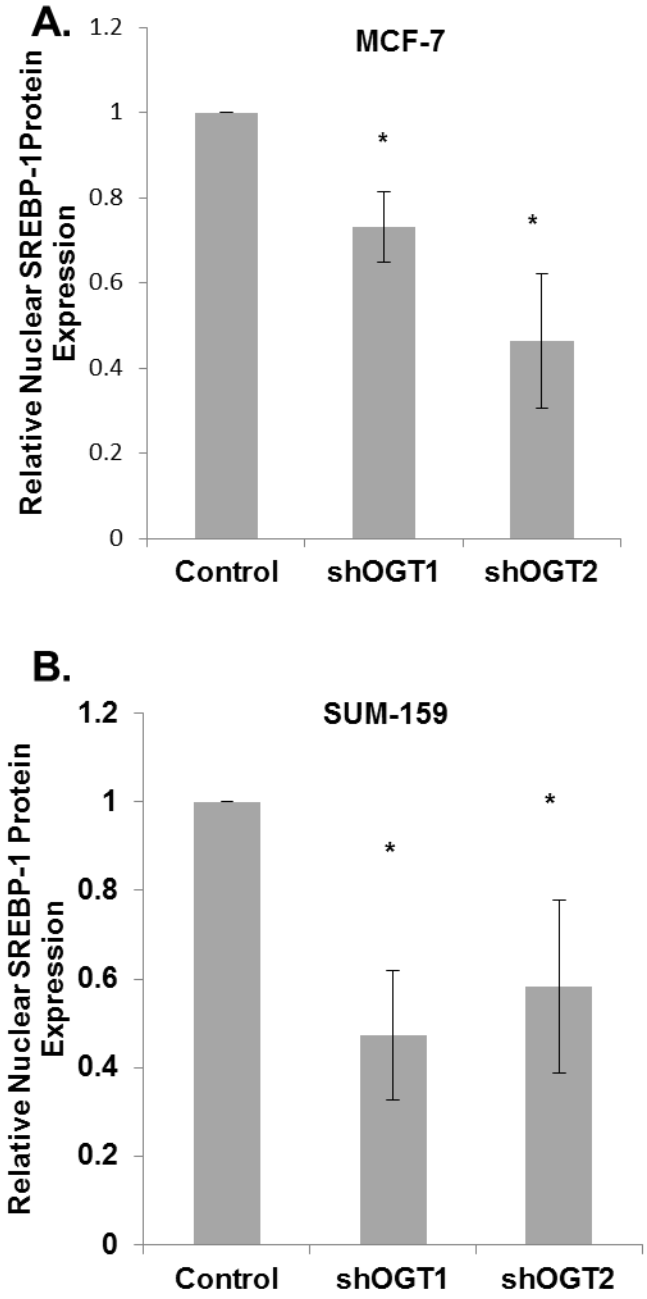

Figure 52: OGT inhibition decreases SREBP-1 expression in MCF7 and SUM-159 cells (A-B) Quantification of western blot analysis of MCF7 (A) and SUM-159 (B) expressing control, OGT#1 and OGT#2 shRNA. Mean $\pm$ SE; * p-value< 0.05.

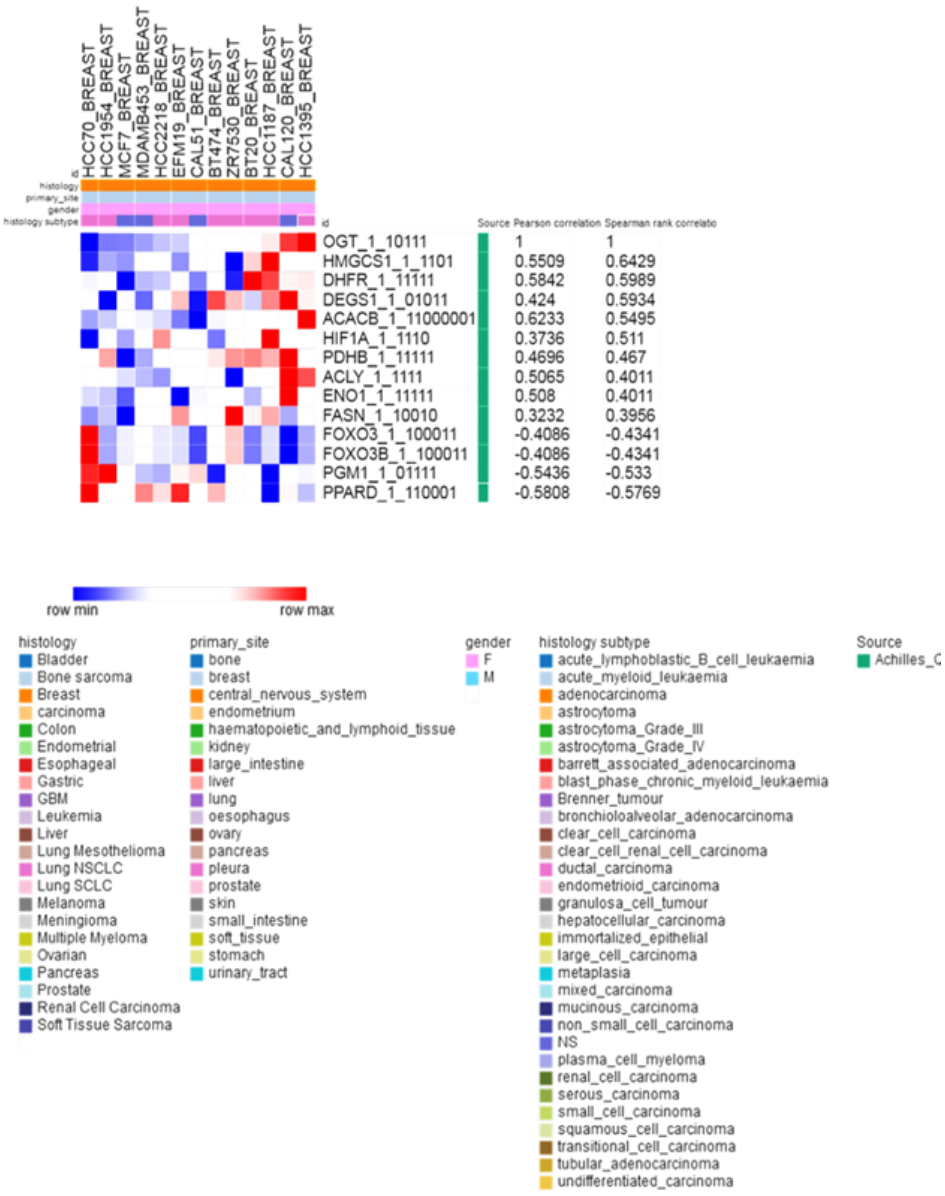

Figure 53: Essentiality Scores (gene dependency) for OGT correlate with lipogenic genes Essentiality scores for breast cancer cell lines presented as a heat map displaying OGT essentiality and Pearson correlation and Spearman rank correlations for lipogenic and various other genes. *Data provided by M. Ivan.*

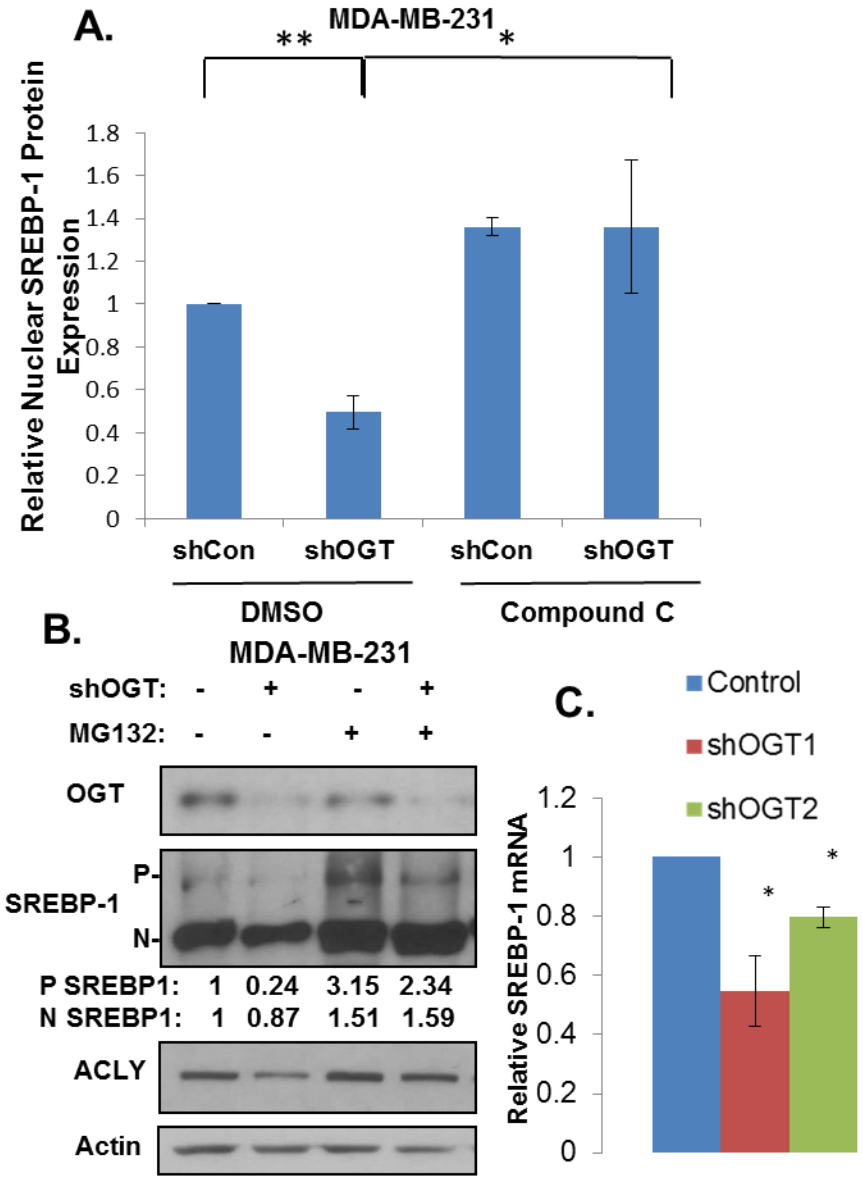

Figure 54: AMPK activity is required for OGT regulation of SREBP-1 (A) Quantification of MDA-MB-231 control and OGT shRNA expressing cells treated with vehicle control (DMSO) or 10uM Compound C for 24 hours. (B) Western blot analysis of MDA-MB-231 cells expressing control or OGT shRNA treated with control vehicle (DMSO) or 10uM MG132 for 24 hours analyzed with the indicated antibodies. (C) Relative SREBP-1 mRNA expression as measured by qRT-PCR from MDA-MB-231 cells expressing control, OGT#1, and OGT#2 shRNA. Mean $\pm$ SE; * p-value< 0.05, ** p-value< 0.01.

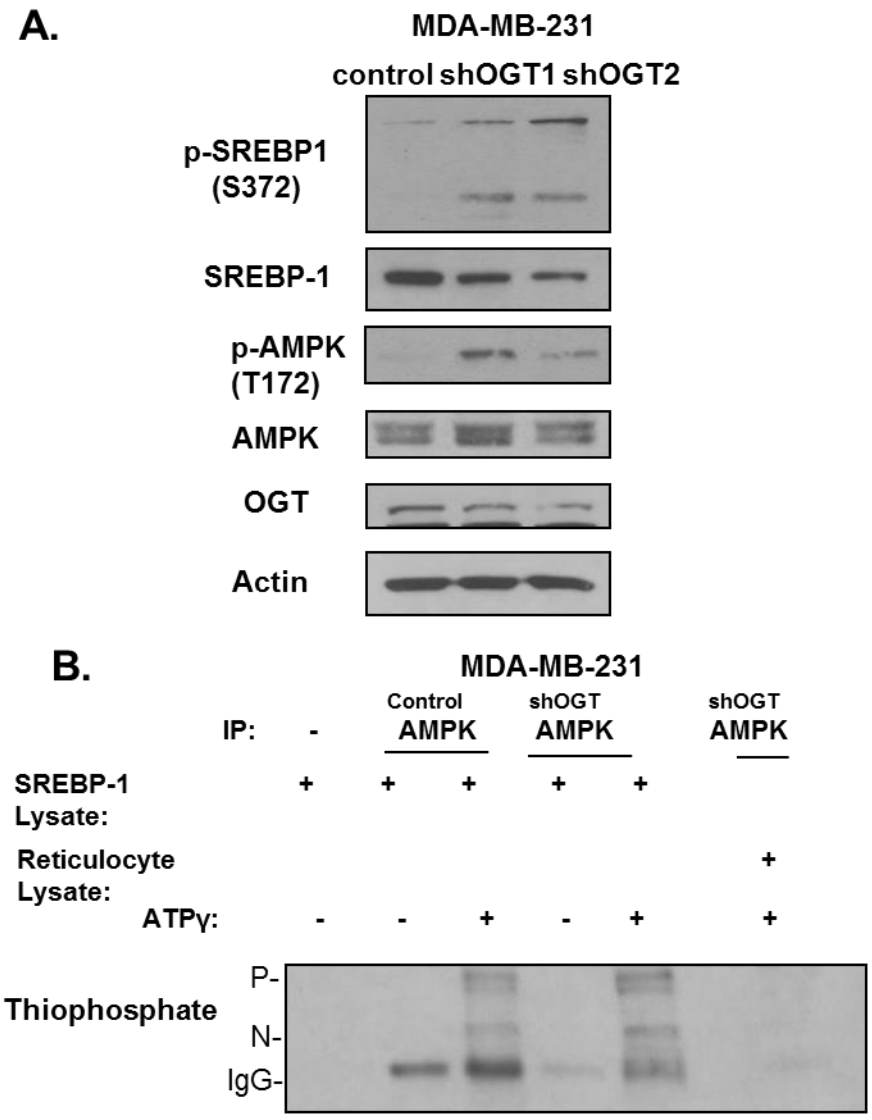

Figure 55: OGT inhibition in MDA-MB-231 cells result in AMPK activation and phosphorylation of SREBP-1 (A) Cell lysates from MDA-MB-231 cells expressing control, OGT-1 or OGT-2 shRNA were analyzed via western blot with the indicated antibodies. (B) Western blot analysis of *in vitro* kinase assay using SREBP-1 protein from reticulocyte lysate, ATPγ, and AMPK was immunoprecipitated from control or shOGT MDA-MB-231 cells. SREBP-1 nuclear and precursor are indicated by N and P markings, IgG heavy chain from immunoprecipitation is marked by IgG.

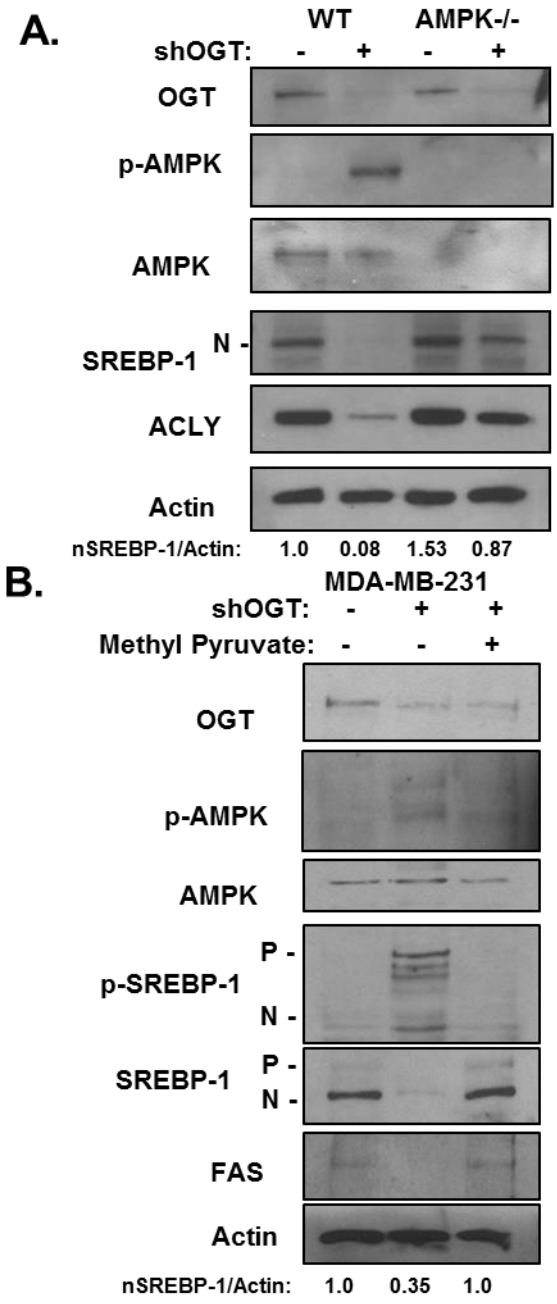

Figure 56: OGT inhibition in MDA-MB-231 cells result in AMPK is required for OGT regulation of SREBP-1 and can be blocked through reversing AMPK activation in breast cancer cells (A) WT and AMPK -/- MEFs expressing control and OGT shRNA were analyzed via western blot with the indicated antibodies. (B) Western blot analysis of MDA-MB-231 control cells and shOGT cells treated with vehicle control or 10uM methyl pyruvate using the indicated antibodies.

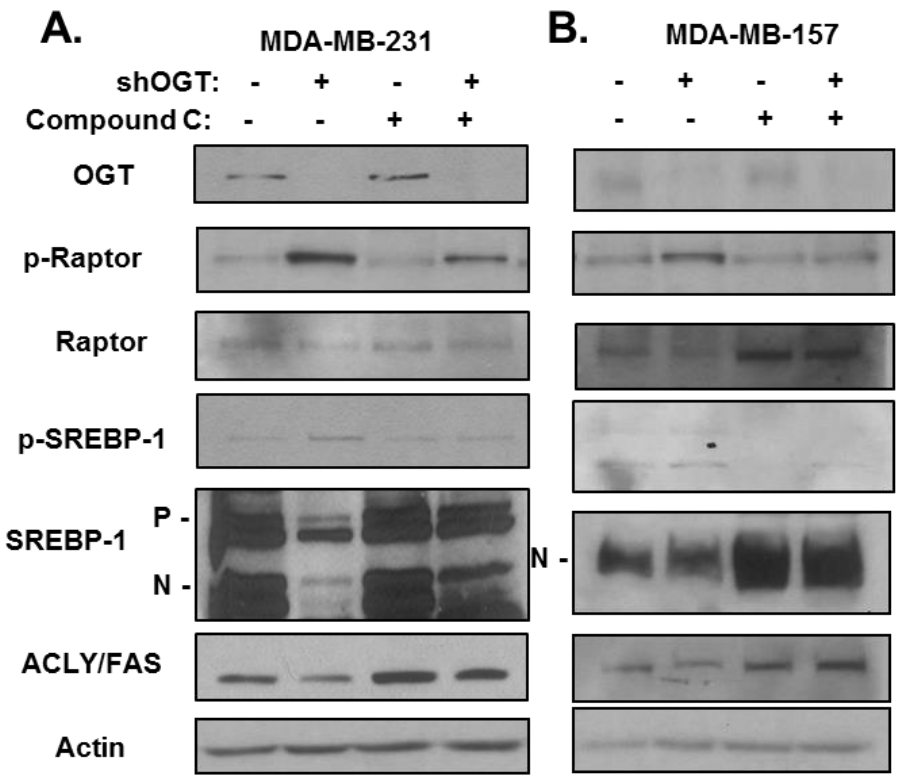

Figure 57: AMPK activity is required for OGT regulation of SREBP-1 (A) MDA-MB-231 cells expressing control and OGT shRNA treated with control vehicle (DMSO) or 10uM Compound C for 24 hours were analyzed via western blot with the indicated antibodies. (B) Western blot analysis of MDA-MB-157 cells expressing control or OGT shRNA treated with control vehicle (DMSO) or 10uM Compound C for 24 hours analyzed with the indicated antibodies.

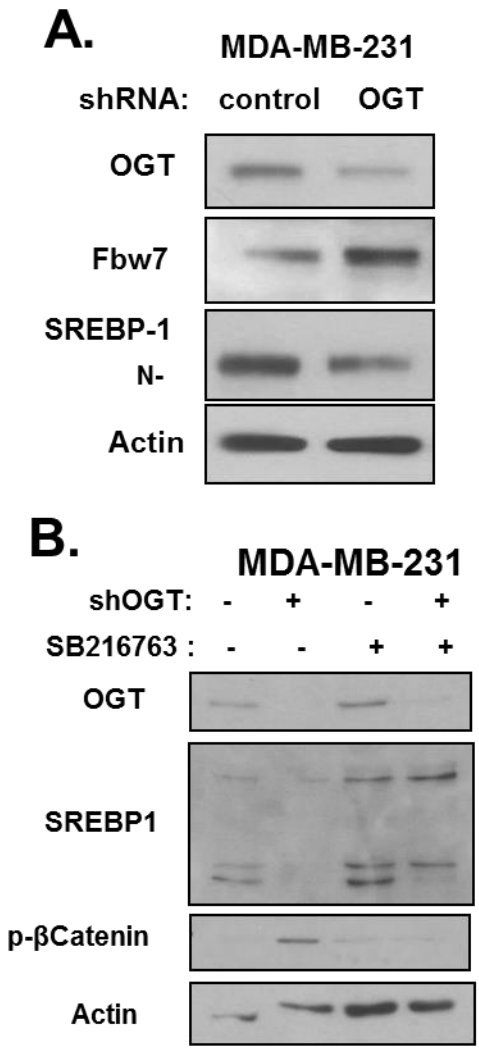

Figure 58: FBW7 is elevated by OGT suppression and OGT regulation of SREBP-1 partly requires GSK3β (A) MDA-MB-231 control and OGT shRNA expressing cell lysates were analyzed by western blot using the indicated antibodies. (B) Western blot analysis of MDA-MB-231 cells expressing control or OGT shRNA treated with control vehicle (DMSO) or 10uM SB216762 for 24 hours analyzed with the indicated antibodies.

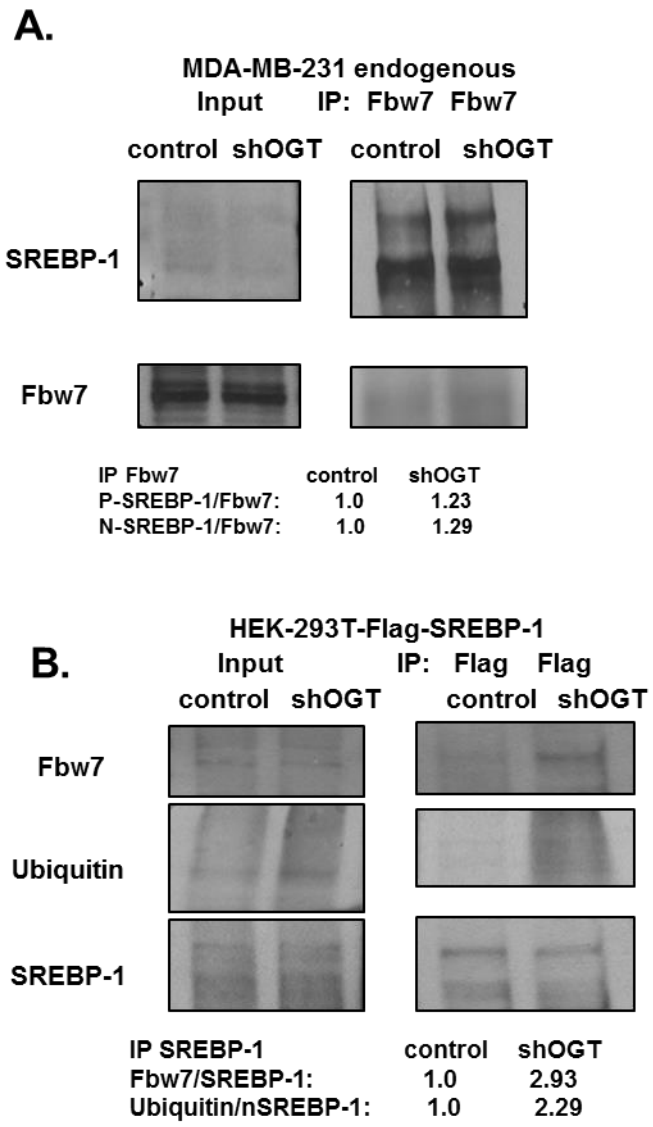

Figure 59: FBW7- SREBP-1 interaction is increased when OGT is suppressed (A) Immunoprecipitation of Fbw7 from MDA-MB-231 control and OGT shRNA expressing cell lysates were analyzed by western blot using the indicated antibodies. (B) Western blot analysis of immunoprecipitation of FLAG-SREBP-1 from HEK-293T cells expressing control or OGT shRNA transfected with FLAG-SREBP-1 were analyzed with the indicated antibodies.

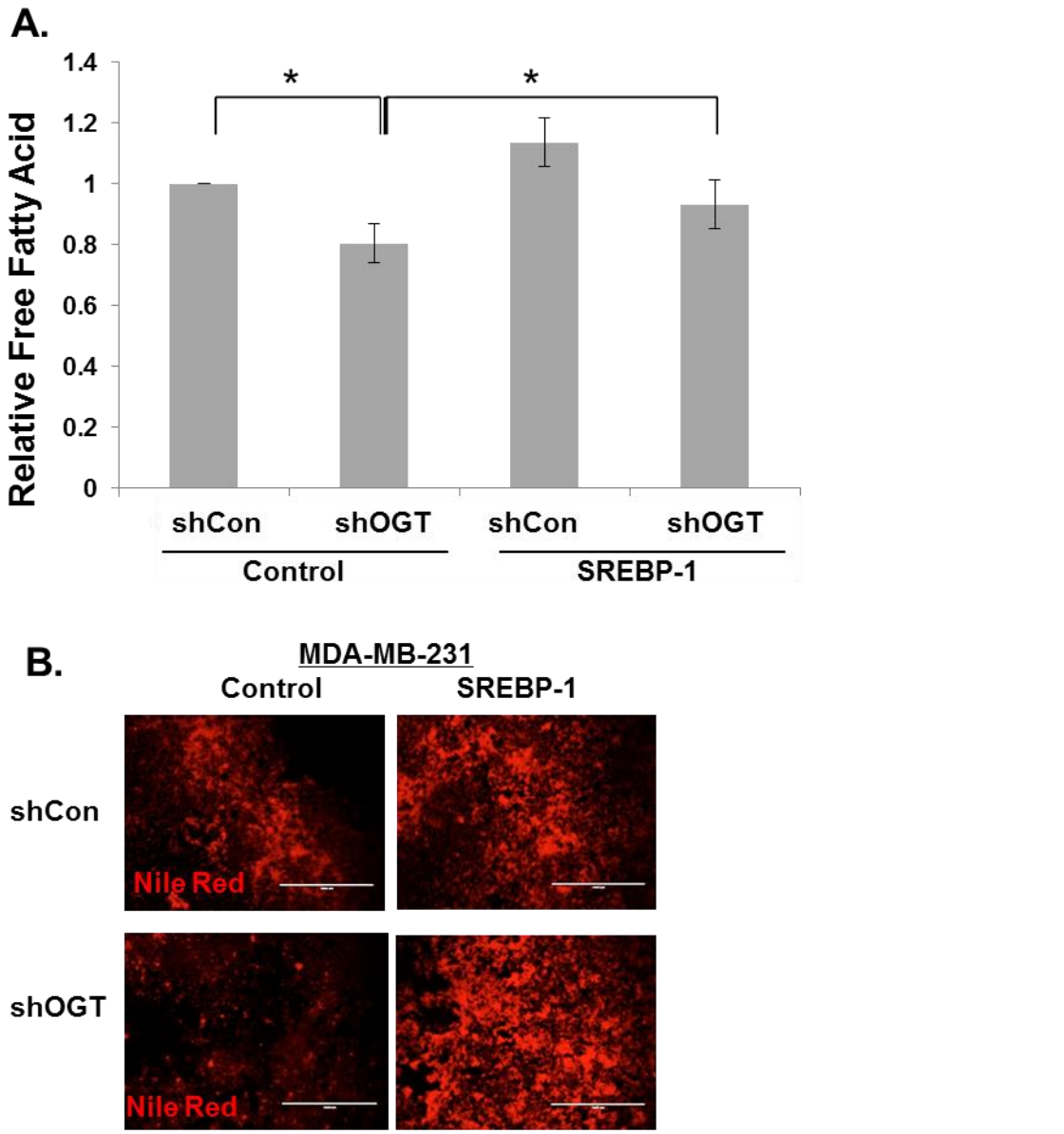

Figure 60: SREBP-1 restoration rescues free fatty acids and lipid droplets (A) Relative free fatty acids were quantified after isolation from MDA-MB-231-control or MDA-MB-231-SREBP-1 control and OGT shRNA expressing cells.(B) Representative fluorescent images of nile red stained cells corresponding to the conditions in (A). Mean $\pm$ SE; * p-value< 0.05.

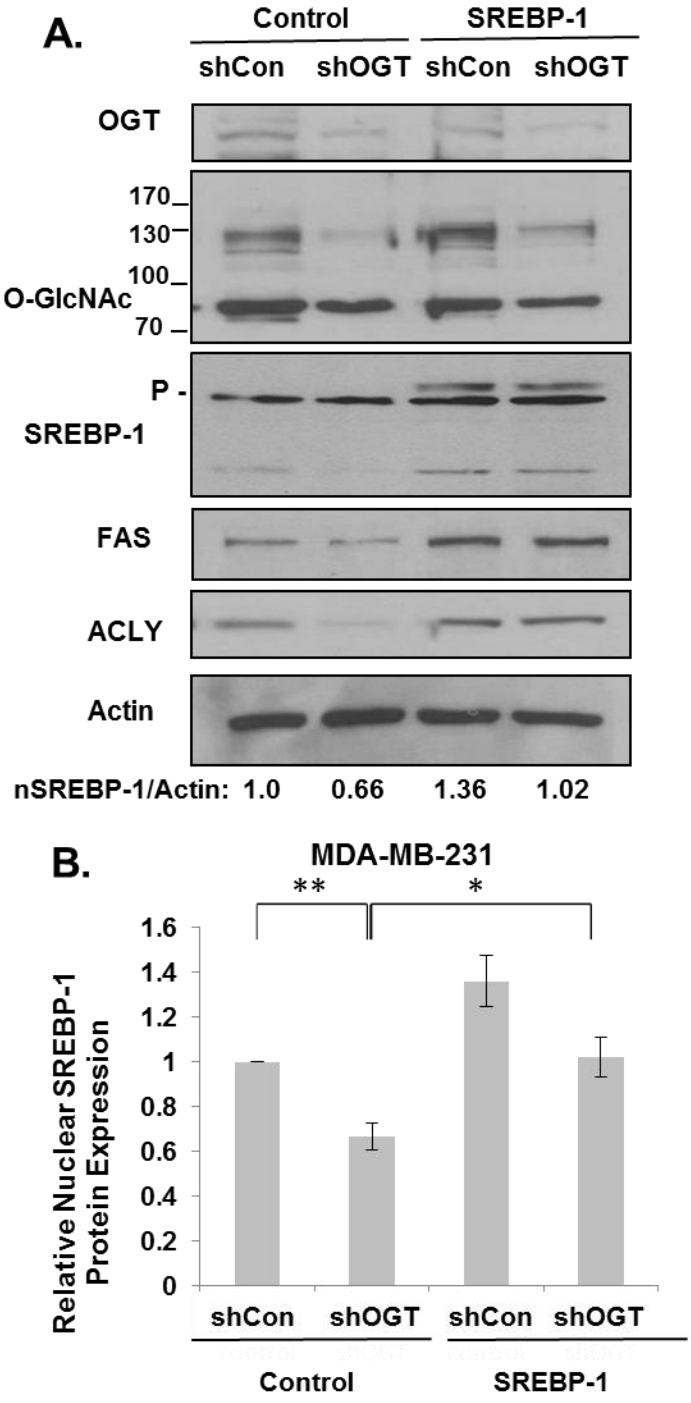

Figure 61: SREBP-1 restoration rescues expression of FAS and ACLY (A) MDA-MB-231-control or MDA-MB-231-SREBP-1 control and OGT shRNA expressing cell lysates were analyzed by western blot using the indicated antibodies. (B) Quantification of western blot analysis of conditions shown in (A). Mean $\pm$ SE; * p-value< 0.005. **p-value< 0.001.

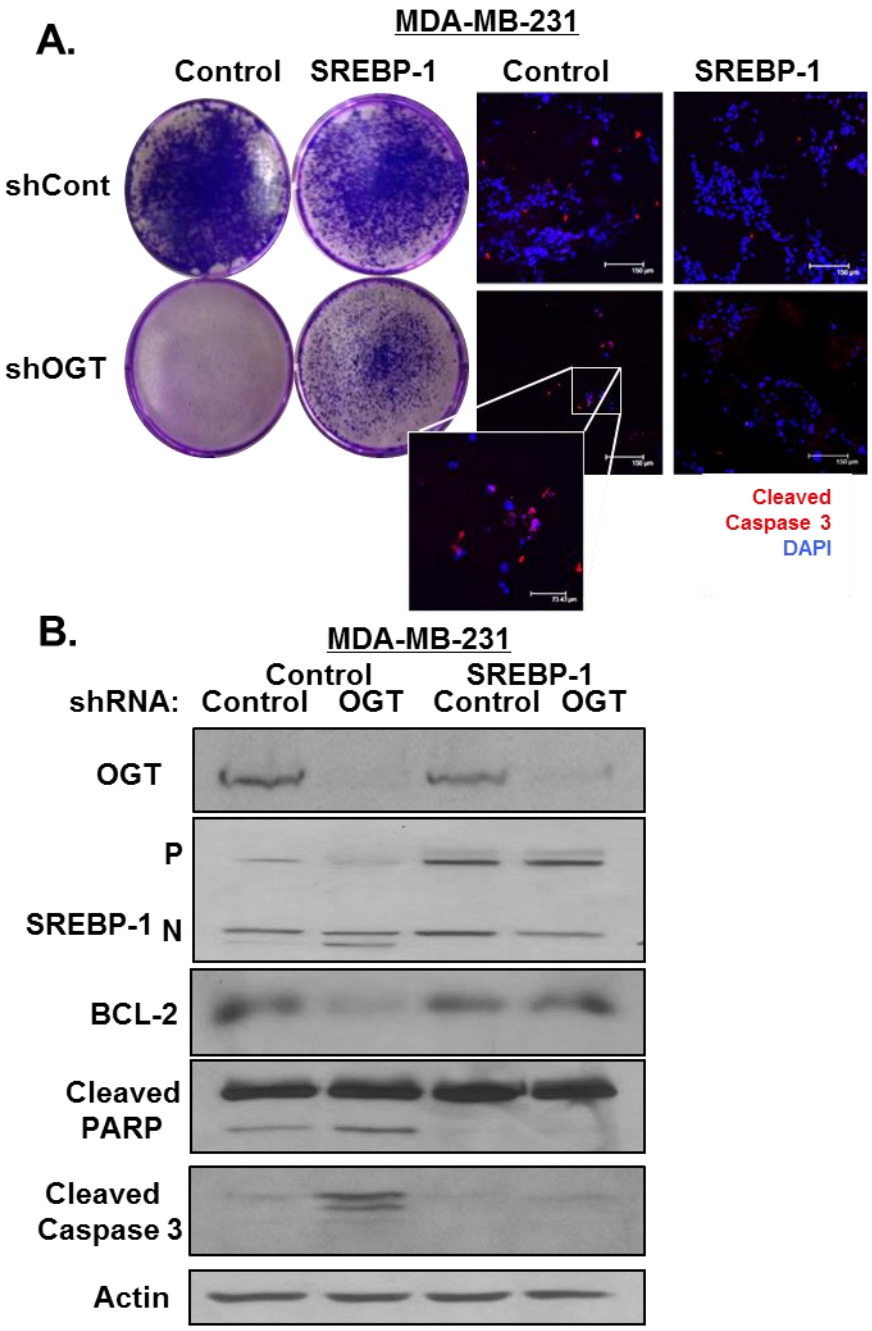

Figure 62: Cell death induced by OGT suppression is partly rescued after SREBP-1 restoration (A) Representative images of 2D crystal violet stained and fluorescent images of 3D cultured MDA-MB-231-control and MDA-MB-231-SREBP-1 expressing control and OGT shRNA. (B) MDA-MB-231-control or MDA-MB-231-SREBP-1 control and OGT shRNA expressing cell lysates were analyzed with the indicated antibodies by western blot.

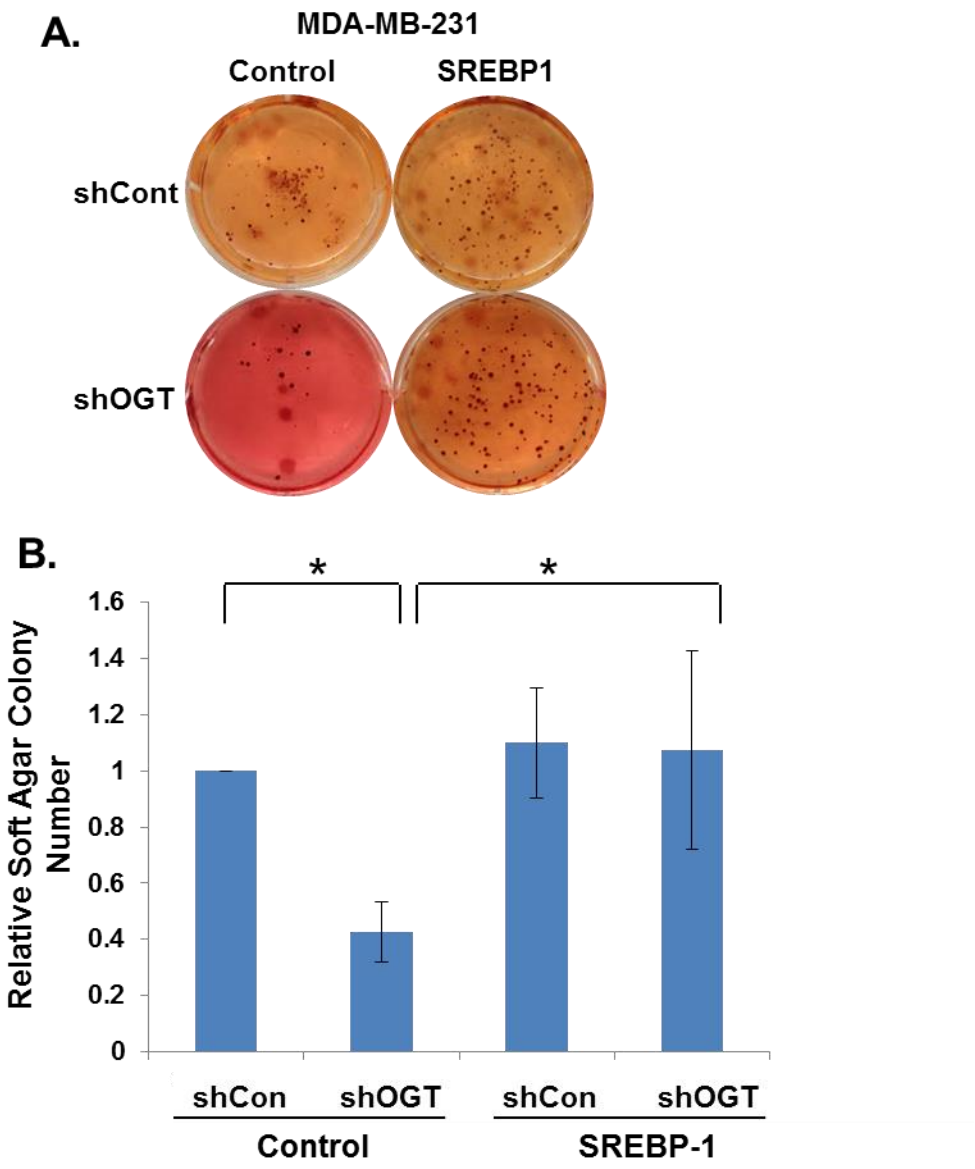

Figure 63: Soft agar colony assay defects caused by OGT suppression is partly rescued after SREBP-1 restoration (A) Representative images of soft agar colony forming assays of MDA-MB-231-control and MDA-MB-231-SREBP-1 expressing control and OGT shRNA cells cultured for 21 days after fixation and INT staining. (B) Quantification of soft agar colonies of MDA-MB-231-control or MDA-MB-231-SREBP-1 control and OGT shRNA expressing cell. Mean $\pm$ SE; * p-value< 0.05.

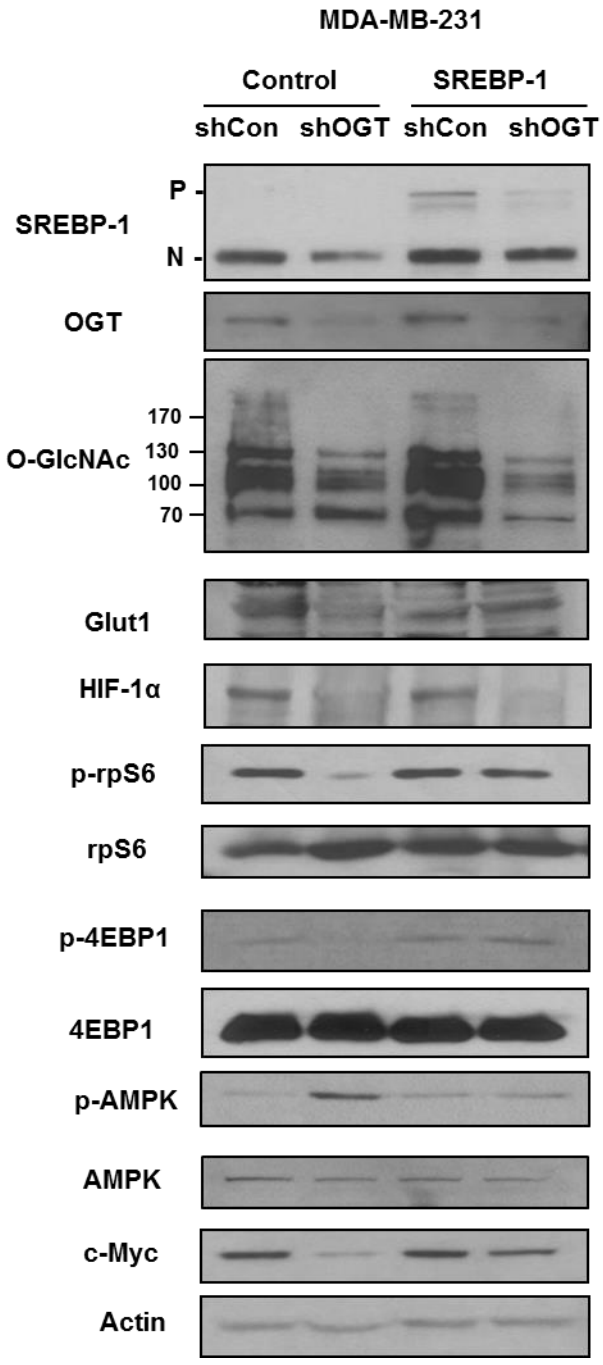

Figure 64: SREBP-1 restoration prevents decreases in mTOR signaling that occur in response to OGT suppression Western blot analysis of cell lysates from MDA-MB-231-control and MDA-MB-231-SREBP-1 expressing control and OGT shRNA cells using the indicated antibodies.

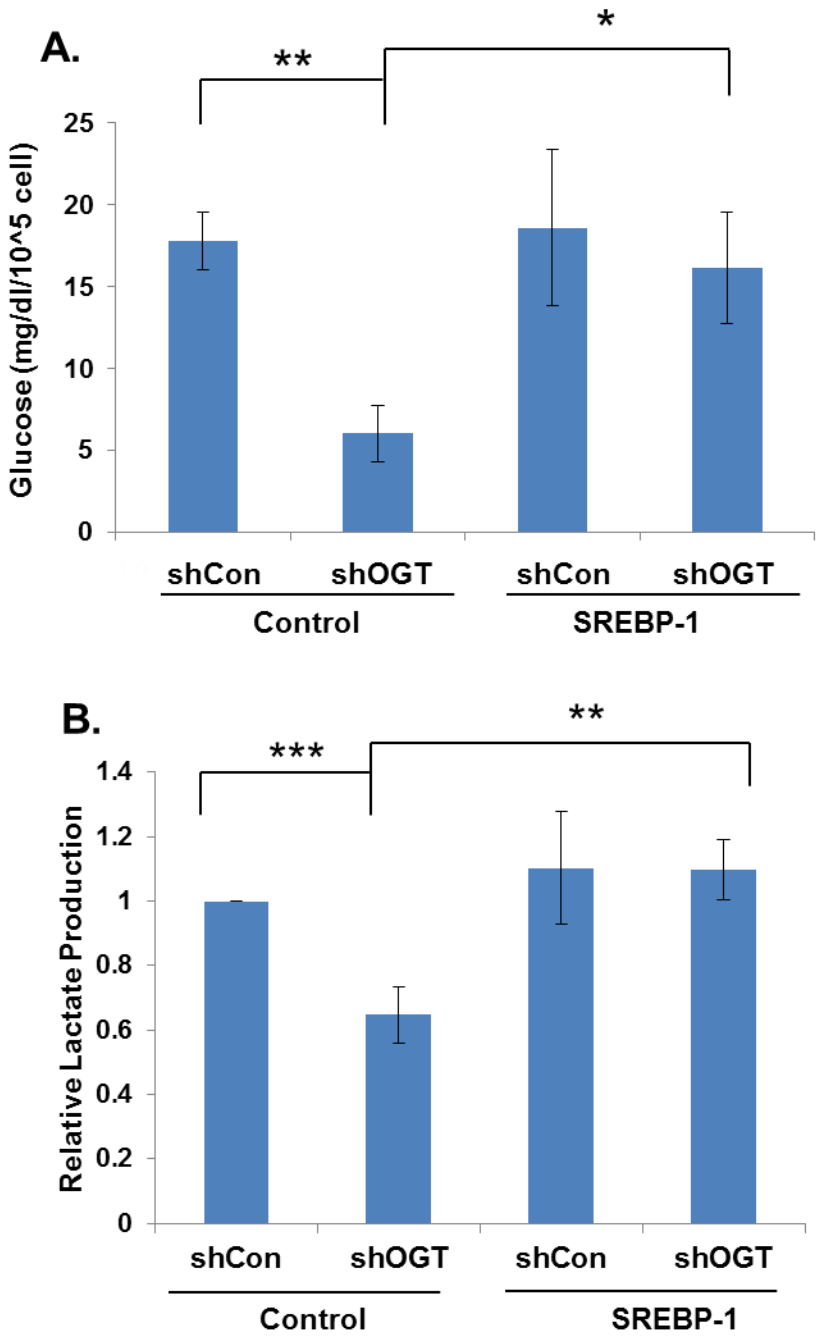

Figure 65: OGT-suppression induced decreases in glycolysis are prevented when SREBP-1 expression is restored (A) Glucose consumption calculated from glucose measurements from media from cultured MDA-MB-231-control and MDA-MB-231-SREBP-1 expressing control and OGT shRNA cells for 48 hours. (B) Relative lactate was measured after 48 hours from media of cultured MDA-MB-231-control and MDA-MB-231-SREBP-1 cells expressing control and OGT shRNA. Mean $\pm$ SE; * p-value< 0.05, ** p-value< 0.01, *** p-value< 0.001

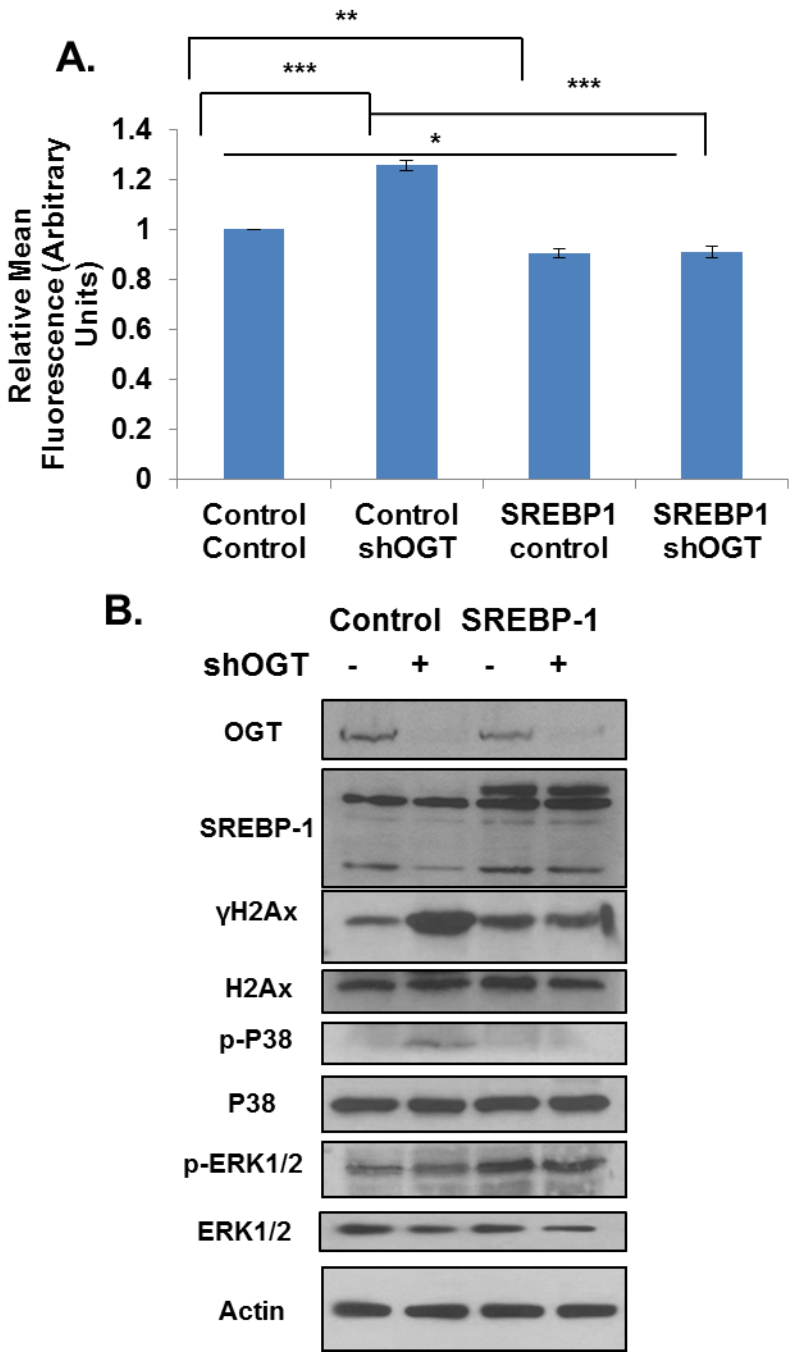

Figure 66: OGT-suppression induced ROS increases, DNA damage and cell stress pathway activation is prevented by overexpressing SREBP-1 expression (A) Relative intracellular ROS as measured by DCF-DA staining of MDA-MB-231 cells expressing control or SREBP-1 plasmids as well as control or OGT shRNA. (B) Western blot analysis of cell lysates from MDA-MB-231-control and MDA-MB-231-SREBP-1 expressing control and OGT shRNA cells using the indicated antibodies. Mean $\pm$ SE; * p-value< 0.01, ** p-value< 0.05,***p-value< 0.001.

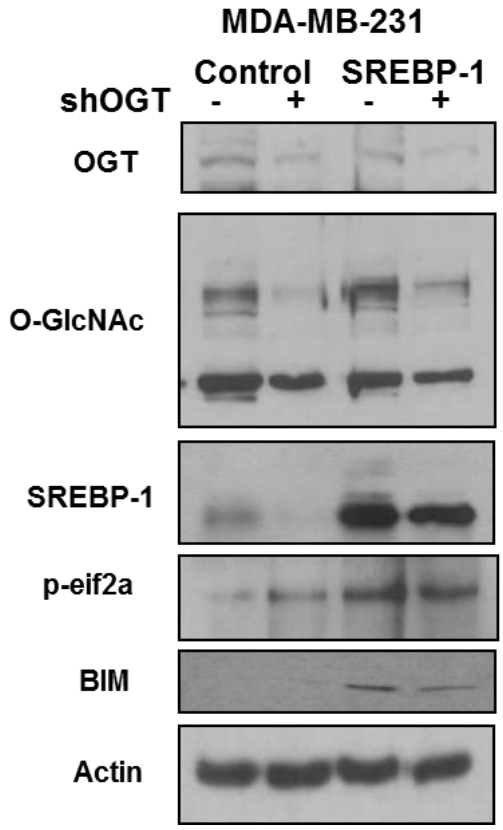

Figure 67: OGT-suppression induced ER stress in not prevented by restoring SREBP-1 expression Western blot analysis of cell lysates from MDA-MB-231-control and MDA-MB-231-SREBP-1 expressing control and OGT shRNA cells using the indicated antibodies.

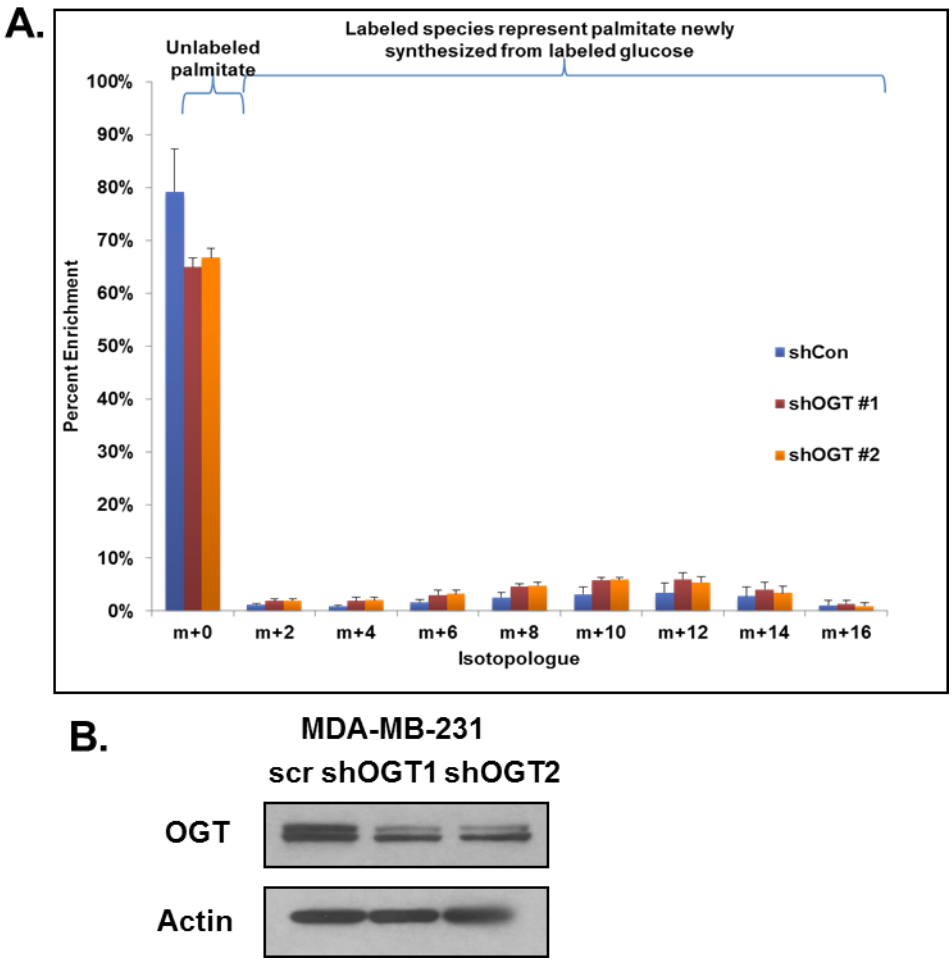

Figure 68: FAME Analysis shows glucose can be used to synthesize palmitate even when OGT is suppressed (A) Fatty Acid Methyl Ester (FAME) Analysis GC-MS measurement of unlabelled (m+0) and labelled palmitate isolated from MDA-MB-231 cells expressing control, OGT#1 and OGT#2 shRNA. (B) Western blot corresponding to cells used in (A). *Data provided by J. Lee and K. Wellen.*

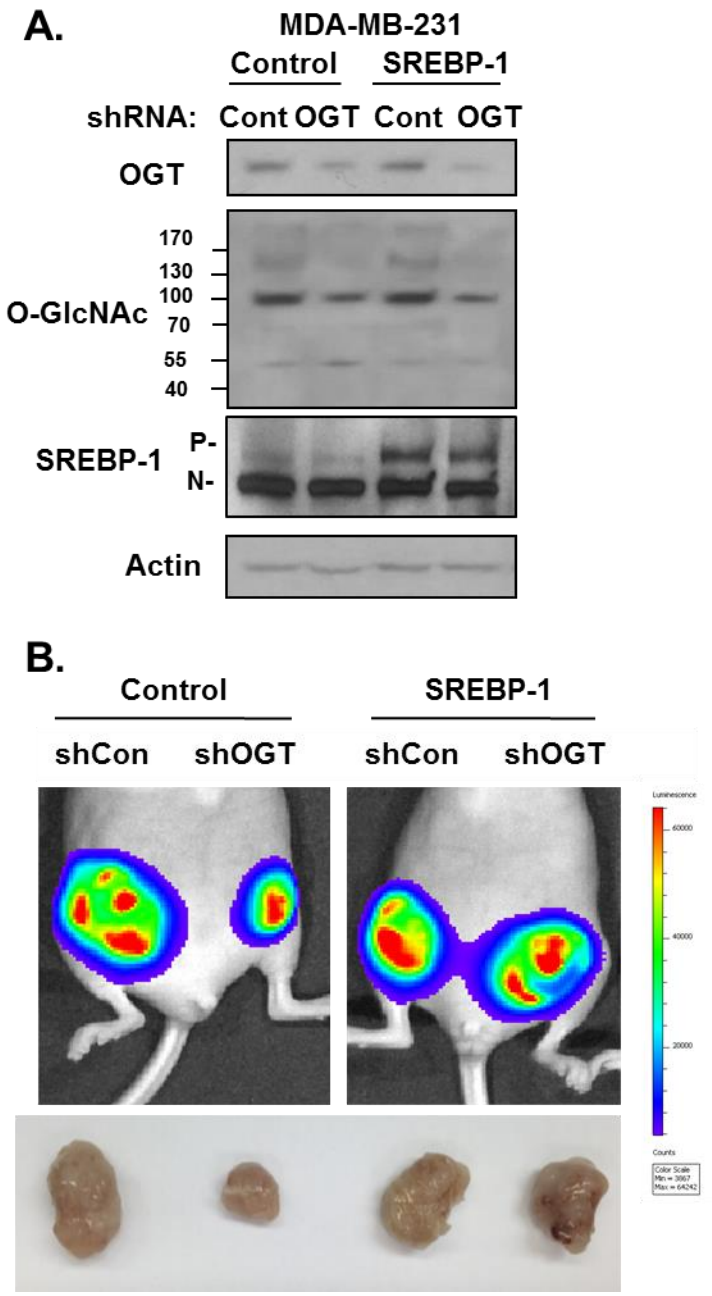

Figure 69: Decreased *in vivo* tumor growth in response to OGT inhibition is prevented when SREBP-1 expression is restored (A) Western blot analysis of cell lysates from MDA-MB-231-control and MDA-MB-231-SREBP-1 expressing control and OGT shRNA cells using the indicated antibodies. (B) Representative images of IVIS bioluminescent imaging as well as tumors removed from Nu/Nu mice injected with cells corresponding to the conditions in (A).

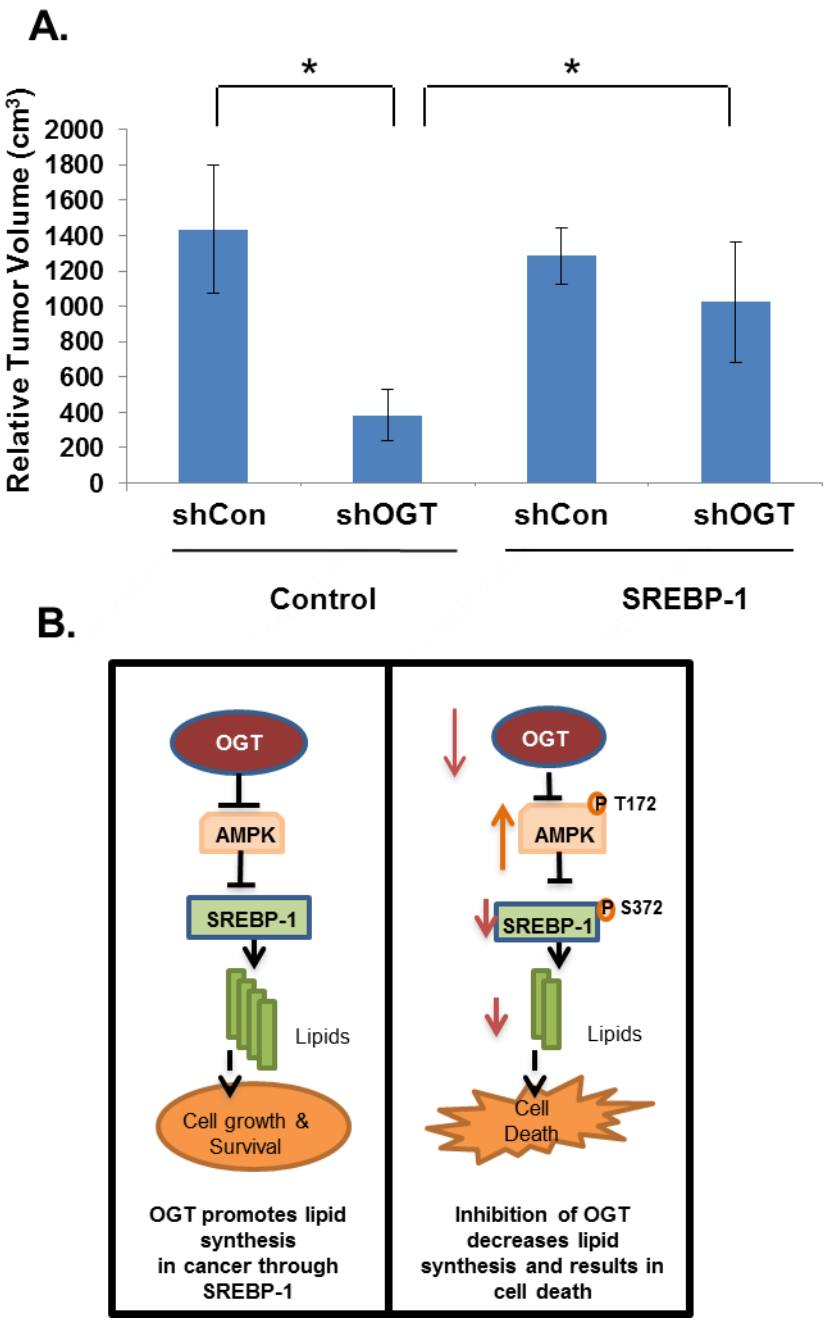

Figure 70: Decreased *in vivo* tumor growth in response to OGT inhibition is prevented when SREBP-1 expression is restored and model of OGT regulation of SREBP-1 (A) Quantification of tumor volume at endpoint using caliper measurements from Nu/Nu orthotopic xenograft mice. (B) Model of OGT regulation of SREBP-1 via AMPK and SREBP-1 contribution to cancer cell viability. Mean ± SE; * p-value< 0.05.

4.4 Discussion

Cancer cells generate fatty acids via *de novo* synthesis to support rapid tumor growth and survival [176]. In this study, we demonstrate that O-GlcNAcylation, elevated in nearly all cancers [52], acts as a key nutrient sensor to control SREBP expression and lipid metabolism in cancer cells. We show that O-GlcNAcylation, via metabolic control of AMPK signaling, regulates SREBP-1 phosphorylation and stability and its transcriptional targets ACLY and FAS to regulate lipid metabolism and cancer cell growth and survival (Figure 70B). Our study uncovers the critical function of O-GlcNAcylation in controlling lipid metabolism in tumor cells linking OGT regulation of metabolism to AMPK signaling and SREBP regulation. Thus, elevated O-GlcNAcylation not only maintains aerobic glycolysis in cancer cells [21], but also maintains lipid metabolism via regulation of SREBP independent of OGT regulation of HIF-1□.

O-GlcNAcylation has been shown to regulate key transcription factors that directly bind to promoters of a number of metabolic enzymes including c-Myc [177], HIF-1□ [21] and now SREBP1. These transcription factors allow for coordinate up- and down-regulation of entire metabolic processes associated with the Warburg effect in cancer cells [178]. c-Myc has been shown to be directly O-GlcNAcylated on threonine 58 [179] and increase its protein stability. Consistent with these studies, reducing OGT and O-GlcNAcylation reduces protein levels of c-Myc. Surprisingly, overexpression of SREBP-1 restored c-Myc protein levels in OGT depleted cells suggesting that SREBP-1 regulation of c-Myc overrides it regulation by O-GlcNAcylation. This, along with reversing GLUT1 expression, may explain why overexpression of SREBP-1 partly restores glucose and lactate levels in OGT-depleted cells. Importantly, SREBP-1

restoration of metabolic defects and mTOR signaling was independent of regulation of HIF-1□. Recent studies suggest that SREBP-2 can regulate stem cell-like properties in prostate cancer cells in part via transcriptional activation of c-Myc [159]. It has also been shown that SREBP-1 directly interacts with c-Myc to enhance its transcriptional program regulating pluripotency in the context of somatic cells. It is therefore plausible that SREBP-1 may regulate c-Myc in other conditions by direct binding or through other mechanisms and that SREBP-1 may have broader functions beyond lipid synthesis regulation in cancer cells [180].

As noted in the review by Guo et al. [181], regulation of SREBP-1 in cancer appears more complex than regulation in non-transformed tissue. With respect to GSK3β and FBW7- dependent degradation of SREBP-1, [173, 174] it would be interesting to explore how manipulation of OGT affects this mechanism of regulation of SREBP-1 in breast cancer, as both GSK3β and its regulator AKT are found to be O-GlcNAc modified in different cell types [182, 183]. It is also still unclear if AMPK regulation is through increasing SREBP-1 degradation and if these mechanisms are linked. In both non-transformed and cancer tissue SCAP appears to play an important role in SREBP-1 regulation. It was recently demonstrated that N-glycosylation of SCAP (in response to increasing glucose) regulated the interaction between SCAP and Insig-1 and therefore SREBP-1 activation in tumor cells [184]. Our studies suggest that in breast cancer cells and MEFs, nutrient sensor O-GlcNAcylation can regulate SREBP-1 protein levels and its transcriptional targets via regulation of AMPK.

Although the requirement of lipogenesis has been well chronicled in a variety of cancer tissues, inhibition of this process as a means of therapy has proved challenging.

Much focus has been concentrated on factors upstream of SREBP-1 such as EGFR, mTOR and P13K [181] however FAS and ACLY inhibitors do exist. Genetic inhibition of lipogenesis downstream of SREBP-1 favors the use of inhibitors against enzymes such as FAS and ACLY for the treatment of cancer. Compounds targeting FAS such as cerulenin, C75 and orlistat demonstrated effective inhibition of cancer cell growth/survival but resulted in unintended consequences of decreased food intake and body weight in animal studies which ultimately halted their prospects as potential cancer therapeutics [112]. More recently, the FAS inhibitor TVB-2640, which carries a more favorable tolerability [185], entered phase I clinical trials for solid malignant tumors [176]. We propose that OGT inhibition may be a way to provide anti-tumor effects, via reduction of lipogenic enzymes.

As OGT and O-GlcNAc play a role in other pathologies, such as atherosclerosis and diabetes, the regulation of SREBP-1 may be important in these contexts as well. Work by Li et. Al demonstrated that AMPK regulates SREBP-1 in diet-induced insulin resistant mice and activation of AMPK to inhibit SREBP-1 protects these animals from hepatic steatosis, hyperlipidemia, and accelerated atherosclerosis in these conditions [158]. AMPKα and γ are both known to be directly O-GlcNAcylated [186] and OGT is known to be phosphorylated by AMPK implying intensive cross-talk between nutrient sensitive regulatory mechanisms of cellular behavior. AMPK activation by OGT in breast cancer may be in response to changes in metabolism such as glucose uptake, rather than direct O-GlcNAcylation changes as our data shows that restoring nutrients that support bioenergetics, in the context of OGT suppression, reverses this activation. Interestingly, direct O-GlcNAc modification was previously found to occur on and regulate

Carbohydrate-responsive Element Binding Protein (ChREBP) and Liver X Receptor (LXR), both important transcriptional regulators of lipid metabolism in the liver [170, 187]. The O-GlcNAcylation status of these factors in cancer and their relation to lipid synthesis have yet to be explored but are of interest since in hepatocytes these factors reinforce lipogenic signaling through SREBP-1 and each other [188].

Together this work links OGT and O-GlcNAcylation to direct regulation of lipid metabolism, a process critical for cancer cell growth and survival. The detrimental consequences to cancer cell health imparted through inhibition of lipogenesis via genetic or pharmacological means have been demonstrated *in vitro*, however clinical efforts have not met initial hopes [189]. Targeting OGT in cancer may serve as a therapeutic alternative to directly targeting enzymes such as FAS or ACLY in not only breast cancer but in other cancers as well.

CHAPTER 5: OGT REGULATES LIPID LEVELS AND LIPOGENIC GENES IN LACTATION

5.1 Introduction

5.1.1 Introduction to and development of the mammary gland

The mammary gland is an incredibly complex secretory organ due to its composition consisting of multiple cell types, its role as the distinguishing factor defining mammals, and its development into adulthood which differs from other organs [190]. The mammary gland functions to provide nourishment to newborns as it develops not only *in utero*, and puberty, but also undergoes immense developmental and physiological changes in adulthood during pregnancy to achieve nutrient production in response to altered

hormonal cues. Regulation of mammary gland development in puberty and adulthood differs from that in embryogenesis in that *in utero* signals that dictate developmental changes originate from the mesenchyme [191]. In puberty and adulthood, hormonal regulation causes differentiation to generate alveoli (structures capable of secreting milk during lactation). When the demand for milk subsides, the process of involution commences during which time remodeling occurs to the mammary gland returning it to a state similar to physiology prior to pregnancy [191]. Careful and deliberate coordination of many signals is required for proper changes within the mammary gland.

Development of the mammary gland has been well described and begins *in utero* with the generation of rudimentary ductal structures that subsequently become bulbs of epithelial cells developing from placodes which are ectoderm structures [190]. Both elongation from the terminal end bud and ductal branching occur after birth, mainly during and after puberty [192]. The terminal end bud is a structure at the tip of growing ducts and drives ductal growth through proliferation. Tree-like ductal arrangement occurs as secondary ductal branches fill more than half of the stroma [191]. The remaining space can be filled by continuous secondary and tertiary ductal growth and alveolar buds that occur during pregnancy. During pregnancy, the mammary epithelium, comprised of both basal and luminal cells, expand into the fat pad from the nipple. The fat pad contains not only adipocytes but also endothelial cells and immune cells [191]. The small population of stem cells, capable of differentiating to different cell types in the mammary gland, exists as basal myoepithelial lineage-restricted cells [193]. Basal myoepithelial cells also generate the outer layer of the gland which contracts to release milk. Both ducts and alveolar structures, which secrete milk, are generated by luminal epithelial cells (Figure

71A) [191]. It is important to note that proliferation and apoptosis of epithelial cells occurs in the mammary gland during each estrus cycle but the sequence of events that occurs during pregnancy is much more rapid, dramatic and sustained [190, 191]. As the epithelilal compartment spreads, existing adipose is diluted [194]. The luminal epithelial cells generate and release milk proteins into the alveoli where milk is pushed through the ducts towards the nipple by contraction [190]. In mid-pregnancy, massive proliferation generates more and larger epithelial cells and secretory activation is initiated. Complete lobuloaveoular differentiation (generating a circular lumen surrounded by a single layer of polarized alveolar epithelial cells encased by myoepithelial cells) is denoted by the formation of lipid droplets and particular gene expression changes. Milk and proteins enter the lumen in preparation of secretion as the female and offspring near parturition [195].

5.1.2 Signaling that regulates mammary gland development

Signaling mechanisms originating both locally (from regions such as the surrounding ECM) as well as from other organs (such as the ovary) dictate the changes that mark progression through stages of pregnancy and lactation [194, 196]. Early in pregnancy, both progesterone and prolactin (PRL) initiate remarkable proliferation. Wnt4 and Nf-KB are thought to mediate the effects of PRL, in concert with JAK2/Stat5 which are activated directly by PRL receptor [196]. ErbB4 signaling receptor (EGFR family member) cooperatively actives Stat5 [195, 197]. All of these signaling alterations act to drive proliferation, establish polarity, coordinate cell-cell interactions and regulate the production of proteins during alveolar morphogenesis. Expression of glucose and nutrient transporters is imperative for the procurement of building blocks that contribute

to the production of main milk components including lactose, protein and lipids. Glucose transporter GLUT1, sodium/glucose transporter Slc5a1, amino acid transporters Slc7a5 and Slc1a4, and the fatty acid transporter Slc27a3 are all upregulated at the transcript level between 1.25 and 2.9 fold at the onset of lactation [194].

It has been noted that tissue remodeling and morphological and signaling mechanisms that occur during mammary gland development are also pertinent in cancer biology as many of these same pathway changes are mimicked as they become deregulated and dysfunctional in disease [192]. One such biological process that is deregulated in cancer and active in mammary development (specifically lactation) is lipid synthesis.

5.1.3 Lipids and lipogenic genes in lactation

As stated previously, most normal tissue do not need *de novo* lipogenesis or expression of lipogenic enzymes because their requirement for fatty acids is met by utilization of those circulating in the blood stream derived from the diet. One exception to this is the lactating mammary gland which *does* activate lipid synthetic genes and produce lipids. During pregnancy, it has been determined that adipocytes contained in the fat pad decrease their lipid content which implies that they serve as a reserve to donate to lipid content in milk [190], however it has also been found that *de novo* lipogenesis increases to generate lipids, which along with proteins, provides nutrients to offspring, with fat percentage of milk ~30% [194]. In this context, lipids contribute high-energy metabolites necessary for lipid membranes, ATP generation and the synthesis of myelin needed for proper brain development [194]. *SREBF1* transcript increases in early lactation as compared to

expression in late pregnancy and SREBP1c -/- mice have lactation defects demonstrating the importance of lipid synthesis in lactation [194].

Expression of lipogenic genes was found to significantly increase from late pregnancy to early lactation. Rudolph et. Al compared mammary glands from pregnant mice at day P17 (late pregnancy) and L2 (early lactation) examining expression of a large panel of metabolic genes. They noted an increase in many glycolytic genes such as; glucose transporters, glucose-6-phosphate dehydrogenase 2, pyruvate kinase (muscle) (PKM2), lactate dehydrogenase (LDHA), This correlated with a decrease in several TCA genes, changes which parallel those associated with cancer cells metabolism compared to normal (termed the Warburg effect which was outlined in Chapter 1) [194]. They also found that in early lactation, alpha-lactalalbumin (a gene regulated by the Stat5 transcription factor) was upregulated nearly 15 fold [194, 198]. The changes in glycolytic genes could provide substrates for use in the synthesis of fatty acids. They noted that genes required for *de novo* fatty acid synthesis and triglyceride synthesis were also upregulated significantly in early lactation compared to late pregnancy. This included *ACLY*, *FASN*, *ELOVL1*, Malic enzyme (*Mod1*), Stearyl-CoA desaturase 1/2 (*Scd1* and *Scd2*, and Long-chain Acyl CoA synthetase 1 (*Acsl1*). While OGT has roles in development, its contribution to mammary development and processes associated with pregnancy had yet to be examined (with the exception of placental studies mentioned in Chapter 1).

5.2 Results

5.2.1 O-GlcNAcylation regulates lipogenesis in lactation *in vivo*

We examined the role of OGT in the regulation of *de novo* lipogenesis in a non-cancerous *in vivo* tissue system. The lactating (murine) mammary gland is one of the most active lipid synthesizing organs known as it produces an estimated 32 grams of triacylglycerides (TAG) over a 20 day lactation period, a mass similar to murine body weight [192, 194]. While multiple regulatory layers exist and several substrates are used to synthesize TAG, a crucial source is *de novo* synthesized lipids [194]. In support of the role of lipogenic genes in the production of lipids in milk, it has been demonstrated that SREBP-1 and many of its transcriptional targets are upregulated at secretory activation [194]. To determine if OGT regulates SREBP-1 or *de novo* lipogenesis in lactation, we manipulated OGT expression in B6.129-Ogttm1Gwh/J *OGT floxed Cre* mice at various stages of lactation. The first experimental design (Figure 71B) was the deletion of *ogt* at weaning. Female B6.129-Ogttm1Gwh/J *OGT floxed Cre* mice were bred to generate offspring and we established that the female B6.129-Ogttm1Gwh/J *OGT floxed Cre* was capable of feeding pups after their birth. We allowed the female mice to nurse their litters until weaning at which point they were injected for three days once daily with adenoviral-GFP (Ad-GFP) as control or adenoviral-Cre recombinase (Ad-Cre) to delete *ogt* in the inguinal fat pad. We assessed the delivery of adenovirus to the mammary fat pad using the Ad-GFP fat pad after collection and determined that we achieved delivery to approximately 60% of the tissue [199]. It was evident from western blotting that OGT expression was still detectable in Ad-Cre sample however it was sufficiently decreased. Immunohistochemical (IHC) analysis of mammary fat pads also revealed a dramatic decrease in OGT expression in the Ad-Cre sample compared to Ad-GFP control (Figure

74A, 76A, 77A). Histological staining confirmed that mammary glands of the pregnant females contained many more milk secreting cells compared to control virgin B6.129-Ogttm1Gwh/J *OGT floxed Cre* mice. There were substantial morphological changes present when *ogt* was deleted as determined by H&E staining (Figure 74A). When examining lipogenesis, both lipid droplet content as well as SREBP-1 and FAS expression were decreased as a result of *ogt* deletion (Figure 74A).

We also examined B6.129-Ogttm1Gwh/J *OGT floxed Cre* female non-lactating mammary tissue by injecting control (Ad-GFP) and Ad-Cre to knockout *ogt* and then collected mammary fat pads for examination of expression of lipogenic enzymes. We found that even in normal non-lactating tissue *ogt* deletion resulted in decreased expression of SREBP-1 and FAS (Figure 72A, 73A). However, there were negligible effects on lipid droplet content when *ogt* was deleted indicating that the expression of these enzymes may not affect lipid levels in non-lactating tissue (Figure 73B). Since expression of lipogenic enzymes is reported to be minimal as lipid synthesis is not an active process under these conditions [141] changes in levels of protein that are present may not result in biological consequences and may therefore have little meaning.

We examined the role of OGT on factors in lactation by deleting *ogt* at the beginning of lactation. Post-parturition, adenoviral Cre or adenoviral GFP was injected into the fat pads of the B6.129-Ogttm1Gwh/J *OGT floxed Cre* females daily for three days starting on the day of litter birth. After which point, offspring were allowed to feed *ad lib* for 21 days then weaned, at which point female B6.129-Ogttm1Gwh/J *OGT floxed Cre* mouse mammary fat pads were harvested (Figure 75). We confirmed knockout by western blot and IHC (Figure 76A, 77A) and observed that deletion of *ogt* in the mammary fat pad

decreased lipid droplets as measured by nile red staining (Figure 76A) and the amount of milk secreting cells (Figure 76A). Pups were weighted at various points throughout lactation as weight has previously been used as a proxy for nutrient content delivered, specifically lipid content [200]. Pups suckled from *ogt* knockout mice had significantly reduced average litter weight compared to control (Ad-GFP) fed pups (Figure 78A). Compared litters contained the same number of offspring. Consistent with decreased lipid droplets, we also noted a decrease in SREBP-1 and FAS protein expression upon *ogt* deletion as measured by western blot analysis and IHC (Figures 76A, 77A), confirming the requirement of OGT in lipogenenic enzyme expression associated with lactation. Changes in IHC H&E staining shown upon *ogt* deletion are similar to those seen upon *Src* deletion which could mean that *ogt* deletion accelerates involution. Accelerated involution phenotypes during lactation observed when *Src* was deleted was hypothesized to be a result of decreased secretory activation [201]. Not only did we observe decreases in expression of lipogenic genes when *ogt* was deleted in early lactation, but many signaling regulators required for proper lactogenesis and maintenance of lactation were also decreased. When compared to control dams (Ad-GFP), OGT null (Ad-Cre) expressed less total ErbB2, ErbB3, and ErbB4 (all EGFR family members) (Figure77A). Casein protein expression was dramatically decreased when *ogt* was deleted in the lactating mammary gland, which in concert with decreased lipid droplets, could contribute to reduced caloric content and therefore pup weight (Figure77A).

5.3 Figures and Figure Legends

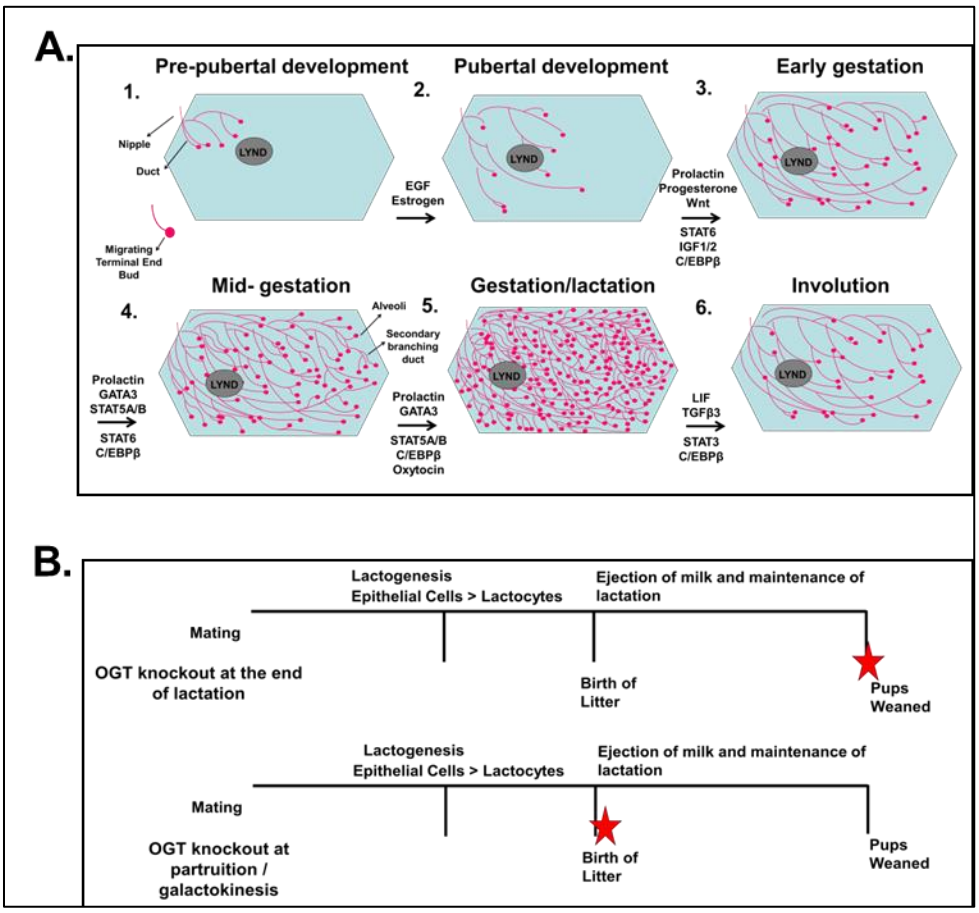

Figure 71: Mammary fat pad development and experimental design of OGT deletion in mammary fat pads (A) Mammary fad pad development through pregnancy consists of six stages. Outgrowth of ducts begins at the nipple and continues into secondary branching structures capped by terminal end buds. Many signaling factors influence and regulate the proper biological changes required for lactation. When lactation is complete involution and apoptosis of structures occurs. LYND indicated lymph node. (B) Schematic of experimental procedures of deletion of *ogt* at different time points indicated by red stars. These included time points at weaning (end of lactation), and parturition (birth of litter).

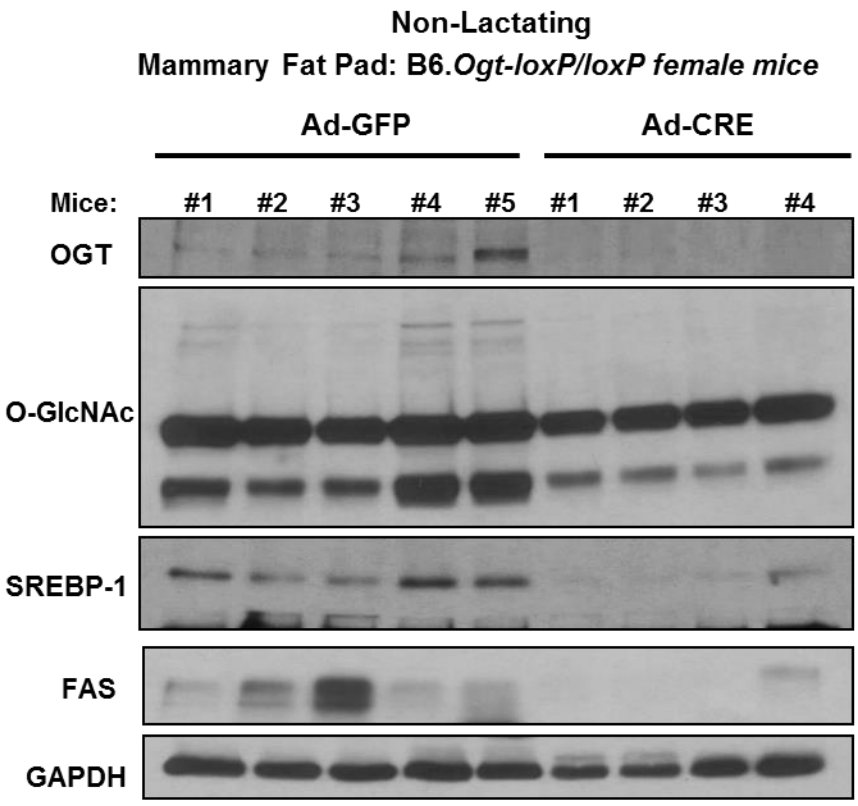

Figure 72: Deletion of OGT in non-lactating B6.*Ogt-loxP/loxP female mice* mammary fat pads decreases expression of SREBP-1 and FAS Western blot analysis of lysate extracted from mammary fat pads of B6.*Ogt-loxP/loxP female mice* injected with adenoviral-GFP or adenoviral-Cre recombinase using the indicated antibodies.

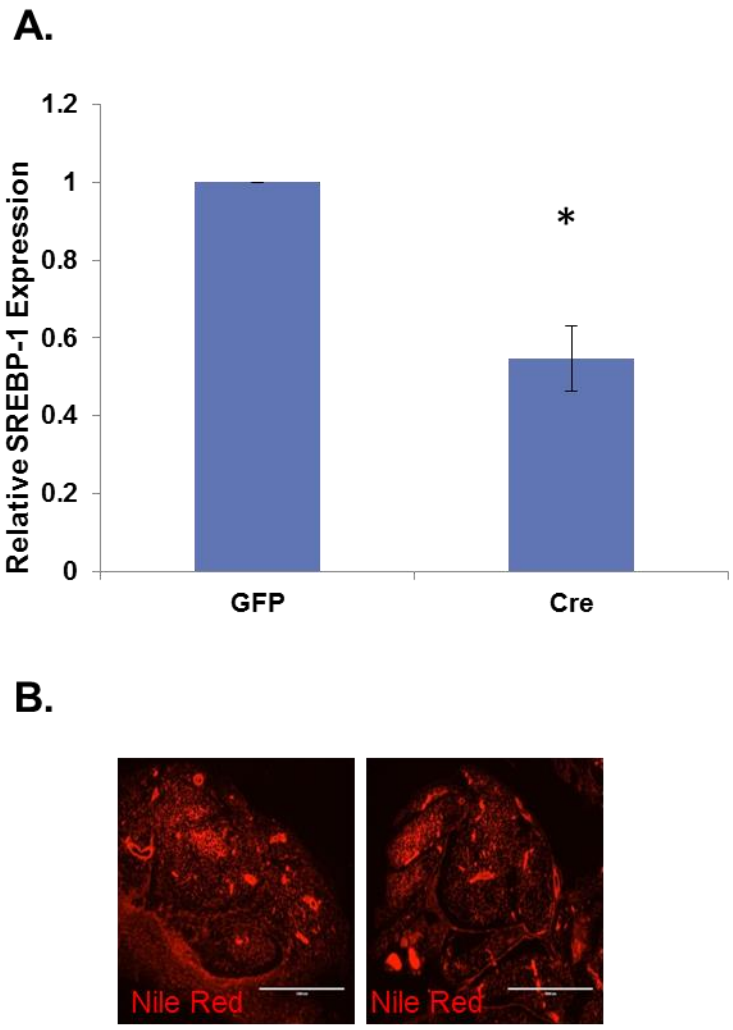

Figure 73: Deletion of OGT in non-lactating B6.*Ogt-loxP/loxP female mice* mammary fat pads decreases expression of SREBP-1 (A) Quantification of SREBP-1 from western blot analysis of lysate extracted from mammary fat pads of B6.*Ogt-loxP/loxP female mice* injected with adenoviral-GFP or adenoviral-Cre recombinase using the indicated antibodies. (B) Nile red staining of fat pads removed from Ad-GFP and Ad-Cre injected B6.*Ogt-loxP/loxP* female mouse mammary fat pads. Mean $\pm$ SE; * p-value< 0.001.

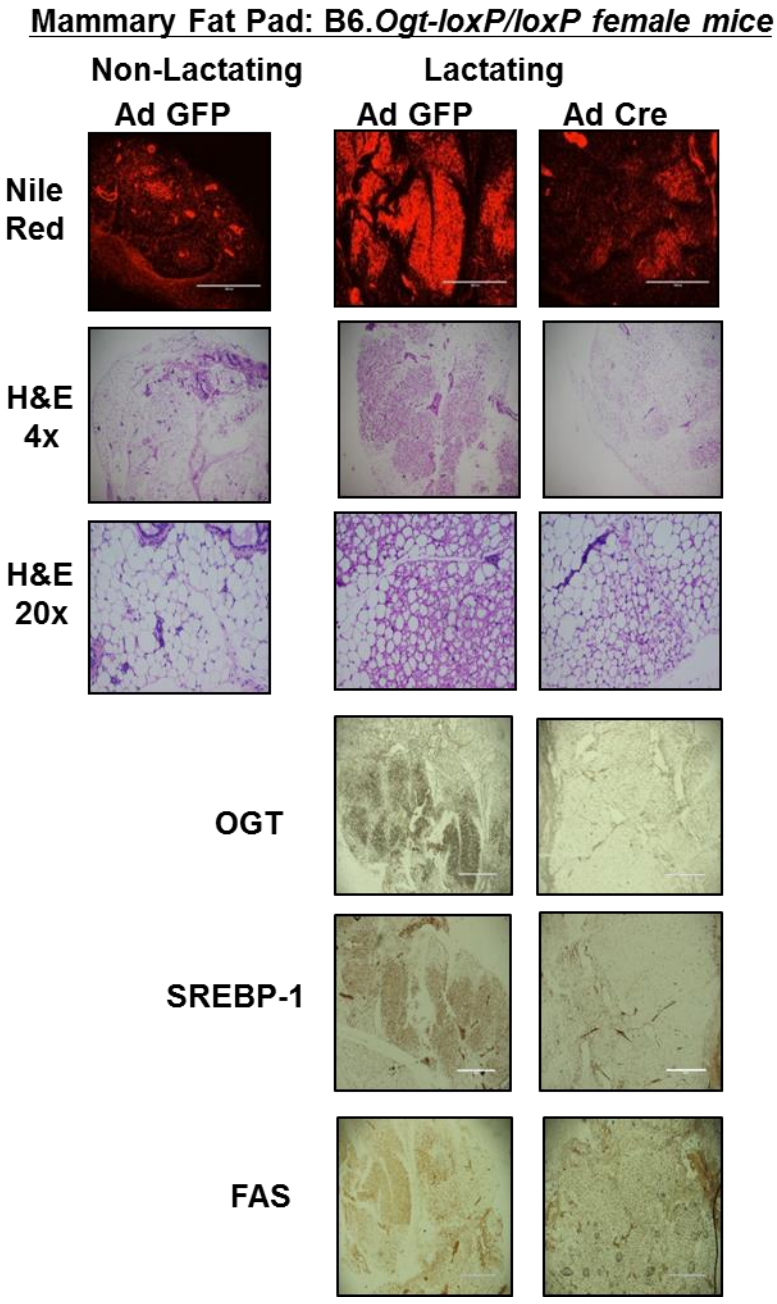

Figure 74: Deletion of OGT in Lactating B6.*Ogt-loxP/loxP female mice* mammary fat pads decreases lipid droplets and expression of SREBP-1 and FAS Immunohistochemistry staining of mammary fat tissue from lactating and non-lactating B6.*Ogt-loxP/loxP* female mice injected with Ad-GFP or Ad-Cre at weaning (21 days after parturition for lactating mice).

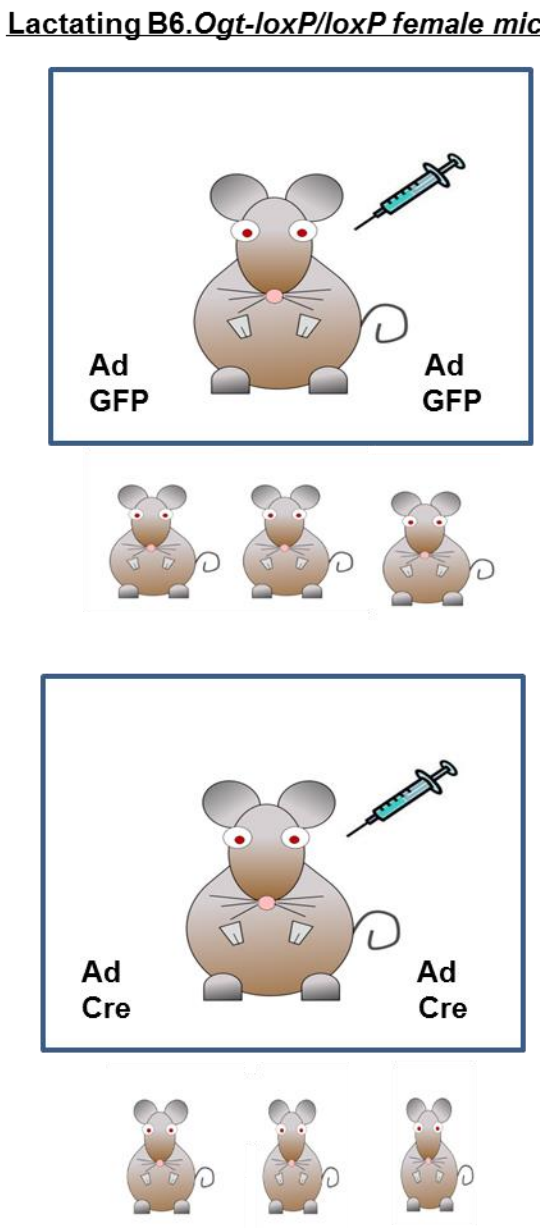

Figure 75: Schematic for experimental assessment of pup weight as proxy of nutritional delivery in Ad-GFP (control) and Ad-Cre (OGT k/o) mammary fat pads injected at parturition B6.*Ogt-loxP/loxP female mice* were injected with Ad-GFP or Ad-Cre at parturition (pup birth) for three days. Weight of litters were recorded until weening (~3 weeks after birth). Mammary fat pads were collected from adult females at weaning and IHC was performed.

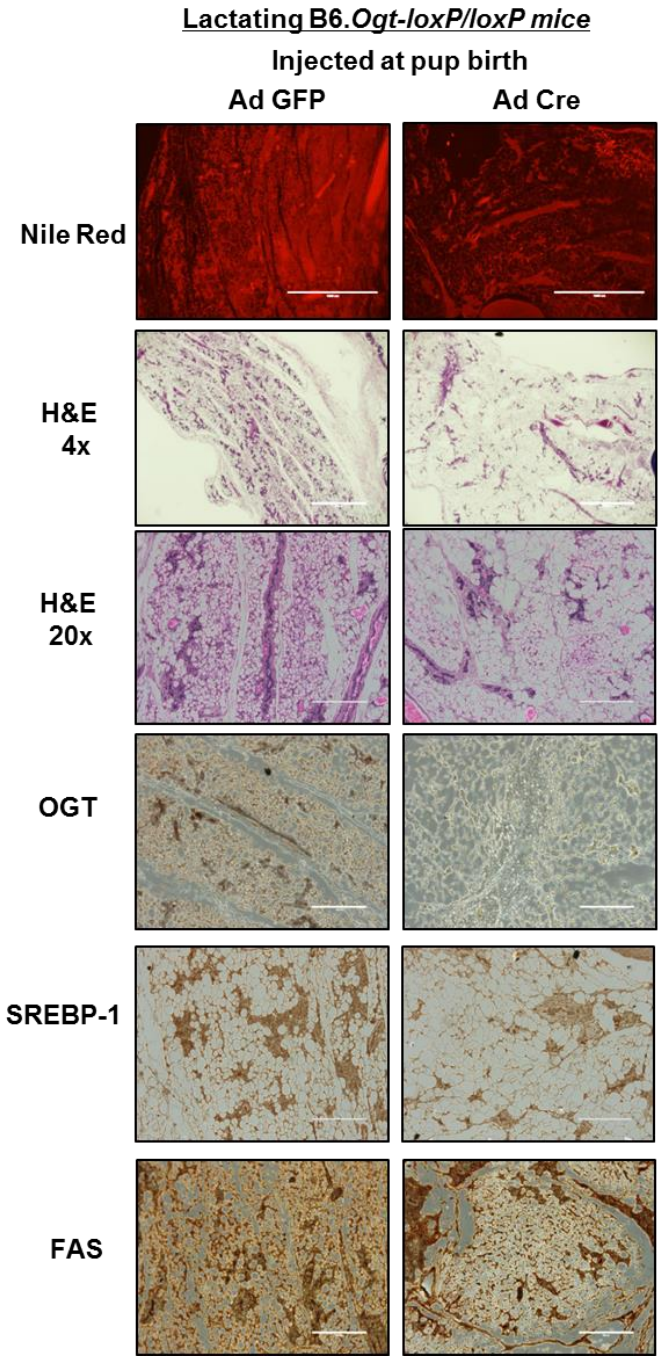

Figure 76: Deletion of OGT in lactating B6.*Ogt-loxP/loxP* female mice mammary fat pads decreases lipid droplets, lactocytes and expression of SREBP-1 and FAS Immunohistochemistry staining of mammary fat tissue from lactating and non-lactating B6.*Ogt-loxP/loxP female mice* injected with Ad-GFP or Ad-Cre parturition and collected at weaning.

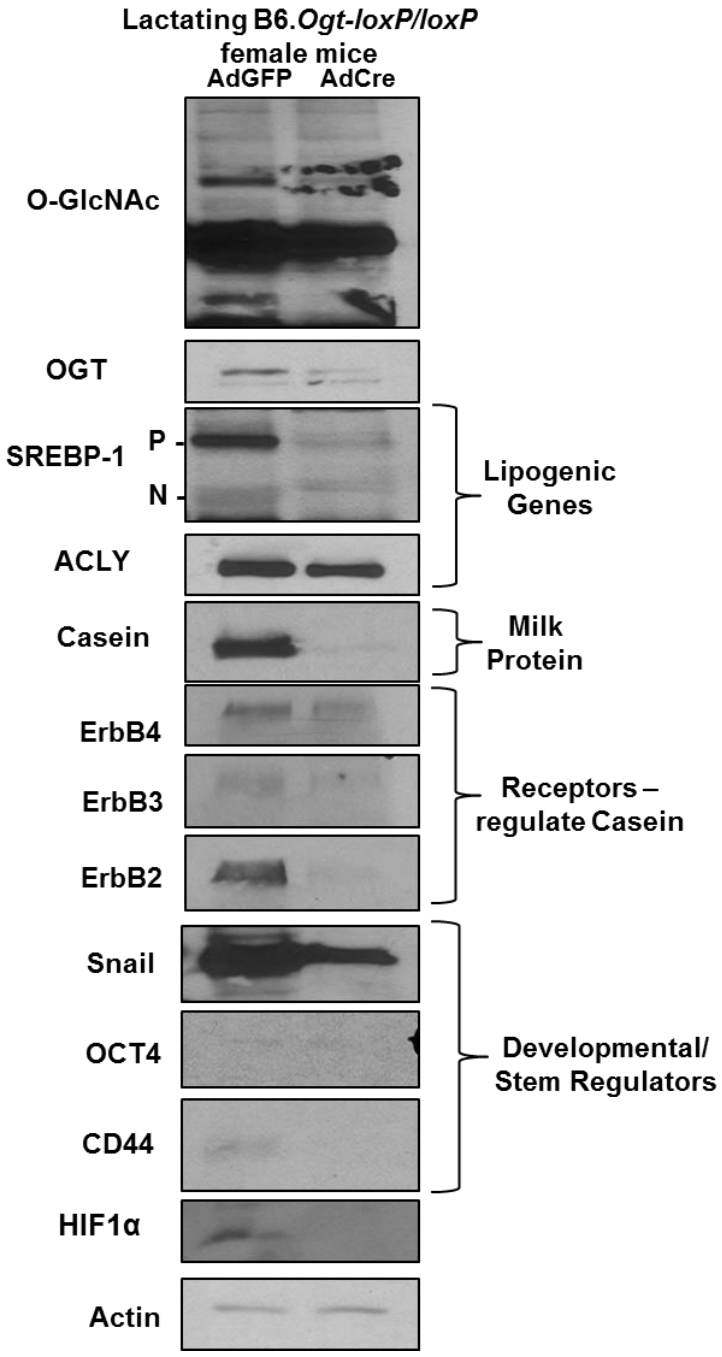

Figure 77: Deletion of OGT in lactating B6.*Ogt-loxP/loxP female mice* mammary fat pads decreases expression of lipogenic genes, receptors, milk protein casein and developmental genes. Western blot analysis of lysate extracted from mammary fat pads of B6.*Ogt-loxP/loxP* female mice injected with adenoviral-GFP or adenoviral-Cre recombinase at parturition using the indicated antibodies.

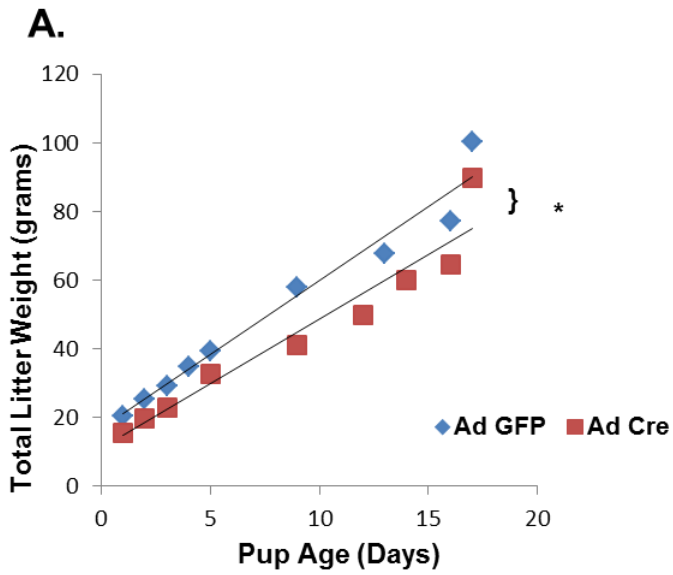

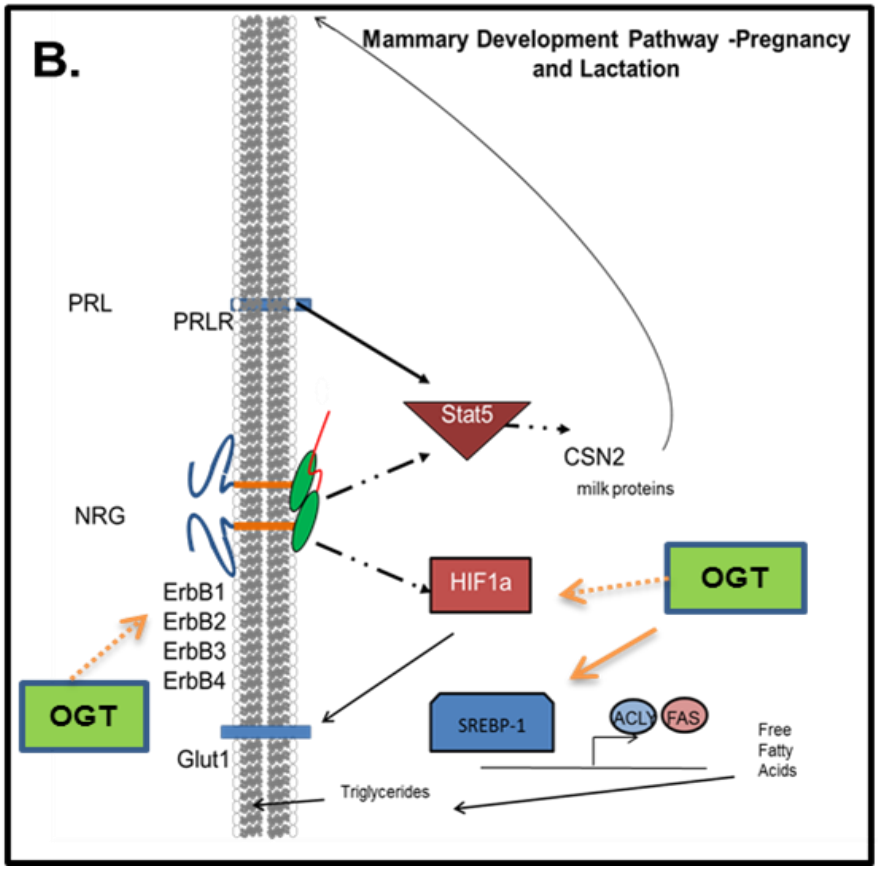

Figure 78: Deletion of OGT in lactating B6.*Ogt-loxP/loxP female mice* mammary fat pads decreases pup litter weight. (A) Total weight of litters (each containing 9 pups) fed from Ad-GFP control injected or Ad-Cre injected dams for 21 days. One-Way ANCOVA comparison *p<0.05 (B) Model by which OGT could regulate expression of key factors required in lactogenesis.

5.4 Discussion

It is clear from this data that OGT is playing an important role in proper expression of several factors needed for the production of nutrients during lactation. This is evident by OGT-suppression induced decreases in expression of signaling receptors such as the EGFR family members examined, β Casein which serves as milk protein and lipogenic enzymes such as ACLY and FAS and their upstream regulator SREBP-1 transcription factor (Figure 77A). This conclusion can also be drawn due to the decreased pup weight in litters containing the same number of pups when fed from dams where *ogt* has been deleted compared to control (Figure 78A). It is unclear if the decrease in pup weight is due to decreased production of lipids which contributes to milk calories. It is very likely a consequence of a variety of changes that occur in response to *ogt* deletion including decreased expression of factors required for lipogenesis as well as the decreased production of milk protein (Casein). Casein is regulated through factors in the EGFR family (shown here to decrease upon *ogt* deletion in lactation) as well as other factors that we have not examined including STAT5 (Figure 78B). It is also possible that the decrease in HIF1α upon *ogt* deletion may lead to decreased uptake of glucose required for lipogenesis through the glucose transporter GLUT1. It is of interest to determine if lipids in milk are decreased by the changes we observe in SREBP-1, FAS and ACLY, as here we have only demonstrated that within the mammary fat pad itself, rather than in milk, there is a decrease in lipid droplets (contain triglycerides made from FFA). We have also observed morphological changes by H&E stain that appear similar to the accelerated involution during lactation observed in Src -/- lactating dams [201]. In that manuscript, it was concluded that this enhanced involution phenotype resulted from a

failure of secretory activation. In the case of *ogt* deletion, further experimental aims are required to distinguish between blocked differentiation or another possibility which is the induction of cell death.

CHAPTER 6: METHODS

Metabolite Analysis

MDA-MB-231 cells were cultured and stably infected with control or OGT shRNA for 48 hours as described above. Cells were counted, and approximately 107 cells per sample were spun down at 300g for 3 min in a polystyrene tube. Cells were washed twice with PBS and then snap-frozen on dry ice and stored at −80 °C until analysis by Metabolon (Durham, NC). The untargeted metabolic profiling platform employed for this analysis combined three independent platforms: ultrahigh performance liquid chromatography/tandem mass spectrometry (UHLC/MS/MS^2) optimized for basic species, UHLC/MS/MS^2 optimized for acidic species, and gas chromatography/mass spectrometry (GC/MS). Cells were homogenized in a minimum volume of water and 100µL withdrawn for subsequent analyses. Using an automated liquid handler (Hamilton LabStar, Salt Lake City, UT), protein was precipitated from the homogenized cells with methanol that contained four standards to report on extraction efficiency. The resulting supernatant was split into equal aliquots for analysis on the three platforms as described previously [202, 203]. Aliquots, dried under nitrogen and vacuum-desiccated, were subsequently either reconstituted in 50µL 0.1% formic acid in water (acidic conditions) or in 50µL 6.5mM ammonium bicarbonate in water, pH 8 (basic conditions) for the two UHLC/MS/MS^2 analyses or derivatized to a final volume of 50µL for GC/MS analysis using equal parts bistrimethyl-silyl-trifluoroacetamide and solvent mixture

acetonitrile:dichloromethane:cyclohexane (5:4:1) with 5% triethylamine at 60°C for one hour. In addition, three types of controls were analyzed in concert with the experimental samples: samples generated from pooled experimental samples served as technical replicates throughout the data set, extracted water samples served as process blanks, and a cocktail of standards spiked into every analyzed sample allowed instrument performance monitoring. For UHLC/MS/MS^2 analysis, aliquots were separated using a Waters Acquity UPLC (Waters, Millford, MA) and analyzed using an LTQ mass spectrometer (Thermo Fisher Scientific, Inc., Waltham, MA) that consisted of an electrospray ionization (ESI) source and linear ion-trap (LIT) mass analyzer. The MS instrument scanned 99-1000 *m/z* and alternated between MS and MS^2 scans using dynamic exclusion with approximately 6 scans per second. Derivatized samples for GC/MS were separated on a 5% phenyldimethyl silicone column with helium as the carrier gas and a temperature ramp from 60°C to 340°C and then analyzed on a Thermo-Finnigan Trace DSQ MS (Thermo Fisher Scientific, Inc.) operated at unit mass resolving power with electron impact ionization and a 50-750 atomic mass unit scan range. Metabolites were identified by automated comparison of the ion features in the experimental samples to a reference library of chemical standard entries that included retention time, molecular weight (*m/z*), preferred adducts, and in-source fragments as well as associated MS spectra and curated by visual inspection for quality control using software previously described [204]. Experimental samples and controls were randomized across a one-day platform run. Any missing values were assumed to be below the limits of detection and for statistical analyses and data display purposes, these values were imputed with the compound minimum (minimum value imputation) after

normalization to total protein for each sample. Statistical analysis of log-transformed data was performed using Array Studio software (Omicsoft, Inc) and R (http://cran.r-project.org/). Welch's t-tests were performed to compare data between experimental groups. Multiple comparisons were accounted for by estimating the false discovery rate (FDR) using q-values.

Tissue Culture

MCF-10A, SKBR-3, BT474, MDA-MB-231 and MCF-7 cells were purchased from ATCC and cultured following instructions. MDA-MB-231 cells stably overexpressing plko.FLAG-SREBP1 (Addgene- plasmid 32017 from Dr. D Sabatini) and MCF7-FLAG--OGT cells were generated through production of lentivirus. Control-scrambled CCTAAGGTTAAGTCGCCCTCGCTCTAGCGA GGGCGACTTAACCTT (Addgene, Cambridge, MA, USA), c-Myc#1 CCGGCAGGAACTATGACCTCGACTACTCGAGTAGTCGAGGTCATAGTTCCTG TTTTTG, c-Myc#2 CCGGCAGGAACTATGACCTCGACTACTCGAGTAGTCGAGGTCATAGTTCCTG TTTTTG, HSP90 #1 CCGGGAAGGATGGTGACAAGAAGAACTCGAGTTCTTCTTGTCACCA

TCCTTCTTTTTG, HSP90#2 CCGGTATGGCATGACAACTACTTTACTCGAGTAA

AGTAGTTGTCATGCCATATTTTG (Sigma Aldrich, St. Louis, MO, USA).

OGT knockdown was achieved using two different lentiviral constructs. OGT shRNA constructs were acquired from Sigma and the sequences used for OGT-1: GCCCTAAGTTTGAGTCCAAATCTCGAGATTTGGACTCAAACTTAGGGC and for

OGT-2:

GCTGAGCAGTATTCCGAGAAACTCGAGTTTCTCGGAATACTGCTCAGC.

Control shRNA was acquired through Addgene (plasmid 1864), from D. Sabatini (Whitehead Institute for Biomedical Research, MIT) and the sequence used was: CCTAAGGTTAAGTCGCCCTCGCTCGAGCGAGGGCGACTTAACCTTAGG.

pLKO-Puro vectors carrying control (scramble sequence) shRNA, c-MYC shRNA (c-MYC#1 and c-MYC#2 shRNA sequences), HSP90 shRNA (HSP90#1 and HSP90#2 shRNA sequences) and OGT shRNA sequences (OGT-1 or OGT-2) shRNA were packaged into VSVG-pseudotyped lentiviruses, through co-transfection of HEK-293T packaging cells with 10 μg of vector DNA and appropriate packaging vectors. Viral production was carried out as previously described [59]. SUM-159 cells were a generous gift of T. Seagroves. WT and AMPKα1/α2 KO MEFs were kindly provided by B Viollet (INSERM) and cultured as previously described [157].Wild type and TSC2-/- MEFS were a gift from Aristotelis Astreinidis, Drexel University College of Medicine. CommaD cells were a gift from Senthil Muthuswamy, University of Toronto. MCF-10A-ErbB2 (NeuT) [59], MCF-10A-AKT (Myr-AKT1) [205] and MCF-10A-MEK2 (MEK2-DD) [205] cells have been previously described. The pWZL-Blast-c-MYC plasmid (kindly provided by Michael Amatangelo, Drexel University) was used to make MCF-10A cells stably overexpressing c-MYC (MCF-10A-c-MYC). Cells were infected with retrovirus and selected as previously described [59].

Establishing MMTV-Myc cells

MMTV-c-Myc transgenic females were procured from the Mouse Models of Human Cancer Consortium (MMHCC; stock O1XG2) under protocols approved by the

University of Tennessee Health Science Center. Mammary epithelial tumor cell (MTEC) lines were generated from late stage carcinomas, grown in DMEM/F12 + 2% FBS and then routinely passaged in culture using a 3:1 ratio of dispaseII/tryspin as previously described [206]. This cell line was established by Dr. Tiffany Seagroves with technical support from Raisa Krutilina and Luciana P. Schwab.

Western blotting

Western blotting procedures were carried out as previously described [59]. Briefly, Cells were collected in RIPA lysis buffer (150mM NaCl, 1% NP40, 0.5% DOC, 50mM Tris-HCl at pH 8, 0.1% SDS, 10% glycerol, 5mM EDTA, 20mM NaF and 1mM Na_3VO_4, 1 µg/ml each of pepstatin, leupeptin, and aprotinin, 200 µg/ml phenyl-methylsulfonyl-fluoride). Lysates were cleared by centrifugation at 14,000 x g for 20 minutes at 4 ^oC and analyzed by SDS-PAGE and autoradiography. Antibodies were purchased from the following companies; Anti-SREBP1 (Novus Biologicals, Abcam), Anti-OGT (Sigma, Santa Cruz), Anti-O-GlcNAc (Santa Cruz, Sigma), Anti-FAS (Cell Signaling), Anti-ACLY (abcam), Anti-phospho-SREBP1 (S372) (Cell Signaling), Anti-phospho-AMPK (T172) (Cell Signaling), Anti-AMPK (Cell Signaling), Anti-FLAG (Sigma), Anti-Cleaved Caspase 3 (Cell Signaling), Anti-Actin (Santa Cruz), Anti- Cleaved PARP (Cell Signaling), Anti-Bcl2 (Santa Cruz), Anti-Glut1 (Abcam), Anti-Hif1α (Novus Biologicals), Anti-ACC (Cell Signaling) Anti-phospho-Raptor (S792) (Cell Signaling), Anti-Raptor (Cell Signaling), Anti-c-MYC (Novus Biologicals), Anti-S6 Ribosomal protein (Cell Signaling), Anti-phospho-S6 Ribosomal Protein (S240/244) (Cell Signaling), Anti-4EBP1 (Cell Signaling), Anti-phsopho-4EBP1 (T70) (Cell Signaling), Anti-c-MYC (Santa Cruz), Anti-ERK2 (D-2) (Santa Cruz), Anti-Cyclin D1 (Santa Cruz),

Anti-phospho-Akt (Ser473) (Cell Signaling), Anti-phospho-Akt (T308) (Cell Signaling), Anti- P70 S6 Kinase (Cell Signaling), Anti-Tuberin/TSC2 (Cell Signaling), Anti-AKT (Cell Signaling), Anti-phospho-P70-S6 Kinase (T389) (Cell Signaling), Anti-phospho-4EBP1 (T70) (Cell Signaling), Anti-4EBP1 (53H17) (Cell Signaling), Anti-BIM (Cell Signaling), Anti-CHOP (L63F7) (Cell Signaling), Anti-phospho-eIF2α (Cell Signaling), Anti-eIF2α (Cell Signaling), Anti-phospho-ERK (T185/Y187) (Invitrogen Corporation), Anti-O-GlcNAc (CTD110.6) (Sigma), Anti-HSP90 alpha (Enzo Life Sciences), Anti-MGEA5 (OGA) (Proteintech Group) Anti-γH2A.X (S139) (Abcam), Anti-H2A.X (Cell Signaling), Anti-P38 (Cell Signaling), Anti-phospho-P38 (T180/Y182) (Cell Signaling). Densitometry was performed using Image J Software (National Institutes of Health, Bethesda, MA).

Immunoprecipitation

MDA-MB-231 cells expressing control or OGT shRNA or HEK-293T cells transfected with human-SREBP-1c were lysed and extracted with radioimmune precipitation assay buffer (RIPA) (150 mM NaCl, 1% NP40, 0.5% DOC, 50 mM TrisHCL at pH 8, 0.1% SDS, 10% glycerol, 5 mM EDTA, 20 mM NaF, and 1 mM Na3VO4) supplemented with 1 μg/ml each of pepstatin, leupeptin, aprotinin, and 200 μg/ml PMSF. Protein G Sepharose beads were pre-cleared Lysates were incubated with indicated antibodies overnight at 4 degrees C. Samples were then subjected to immunoprecipitation using protein G Sepharose beads followed by 3x washes in 1x phosphate buffered saline + 0.1% Tween 20. Immunoprecipitated proteins were suspended in 5x protein buffer and boiled for 5 minutes at 100 degrees C then centrifuged prior to western blot analysis using the indicated antibodies.

Free Fatty Acid Quantification

Free Fatty Acids were isolated and quantified using the Fatty Acid Kit from Biovision as per the manufacturers' instructions. Briefly, cells were counted and equal numbers from each sample were used for quantification. Lipids were isolated using a choloform/1% Triton X solution and needle lysing. Cells were centrifuged and the lipid containing layer was dried. Lipids were resuspended and acyl-CoA derivatives were generated using a kit provided enzyme. Colormetric detection of lipids was performed in a Synergy HT plate reader (BIO-TEK Instruments Inc.) at 570 nm. Spectrometric numbers were plotted against a standard and data was normalized to control and presented graphically.

Nile Red Staining of Cells and Tissue

Cells were fixed using 4% Formalin and washed in 1xPBS prior to staining. Stock solution of 0.5mg/ml was made in acetone and diluted to 5ug/ml in PBS for use. Working solution was gently added to cells and incubated for 30 minutes away from light. Cells were then washed three times in 1x PBS and visualized and photographed on EVOS FL (Life technologies) using Texas Red filter.

Inhibitors and treatments

Cell were seeded at 5 x 10^6 were treated for 16 hours with either; 0.1% DMSO (Sigma, St. Louis, MO, USA), LY294002 30 µM (Promega WI, USA), Rapamycin 50 nM (Enzo Biochem NY, USA) or U0126 30 µM (Promega WI, USA). OGT inhibitor Ac-5SGlcNAc has been previously described [76] and HSP90 inhibitor 17-AAG (Selleck Biochem, Houston, TX, USA) was used at indicated concentrations. Lactacystin (Calibiochem, Billerica, MA,USA) was used at 10 µM in combination with indicated

treatments. SB216763 (Sigma, St. Louis, MO, USA) was used at a concentration of 10μM for 6 hours. Cells were treated with 10μM Compound C (Calbiochem), 10μM methyl pyruvate, or 10μM MG132 for 24 hours. Ac-5s-GlcNAc was added to plated cells at a concentration of 100μM (unless indicated at other concentration) for either 24 or 48 hours as indicated. Exogenous lipids consisted of 1%BSA/PBS100μM sodium palmitate and 40μM oleic acid and were added to media on plated cells for 48 hours.

***in vitro* kinase assay**

In-vitro kinase assay SREBP-1 protein was generated using TNT-T7 Quick Coupled Transcription/Translation System (Promega) and the human-FLAG-SREBP-1c plasmid, following manufacturers' instructions, was incubated with 20 μl of Protein-G Agarose beads after immunoprecipitation of AMPKα from MDA-MB-231 control or MDA-MB-231 shOGT cell lysates in kinase buffer (50 mM HEPES [pH 7.5], 0.65 mM MgCl2, 0.65 mM MnCl2, 12.5 mM NaCl) with 500 μM ATPγS. Kinase reactions were then incubated at 30°C for 30 minutes. When appropriate, PNBM (dissolved in DMSO) was added at 2.5 mM, and reactions were incubated at room temperature for one hour followed by the addition of 4X protein sample buffer and reactions were boiled for five minutes. Western bloat analysis was used to analyze reactions using the indicated antibodies.

mRNA expression

RNA was isolated from cells using Qiagen RNEasy products and protocols (Qiagen, Valencia, CA, USA). Taqman gene expression assay primer probes for primer probes for OGT (Hs00914634_g1), c-MYC (Hs00905030_m1), HSP90AA1 (Hs00743767_sH), SREBF-1 (Hs1088691-m1), ACLY (Hs00982738-m1), FASN (Hs0105622-m1),

ACACA (Hs01046047-m1), ELOVL7 (Hs00405151-m1), LPL (Hs00173425-m1) and Cyclophilin A (PPIA) (Hs99999904_m1) were purchased from Applied Biosystems (Foster City, CA, USA). qRT-PCR was performed as previously described [207] using Brilliant II qRT-PCR Master Mix 2 Kit (Stratagene) using Applied Biosystems 7500 machine according to the manufacturer's protocols. Expression levels were analyzed using Data Assist v2.0 (Life Technologies, Grand Island, NY, USA).

Animal experiments

Athymic nude Nu/Nu 5-6 week old female mice (Charles River, Wilmington, MA, USA) were anesthetized with 4% isoflurane and inoculated with 1.5 x 10^6 MDA-MB-231 cells stably expressing luciferase and either pBabe-Control or plko-SREBP-1c as well as either Control or OGT shRNA. Cells were injected in 100 µl of 1x PBS containing 20% matrigel (Invitrogen) using a 271/2-gauge needle into the fourth inguinal mammary fat pad. For bioluminescence imaging, mice were injected intraperitoneally with 200 µl of D-luciferin solution (9 mg/ml; Caliper Life Sciences, Hopkinton, MA). Imaging was completed using IVIS 200 imaging system 3 hours after the mammary fat pad injection to detect the distribution of breast cancer cells as well as weekly to monitor tumor growth and results were analyzed using Living Image software (Caliper Life Sciences). Tumors were measured weekly using digital calipers (Fowler Co., Inc., Newton, MA, USA) along and perpendicular to the longest dimension. Tumor volumes were calculated as V=(length)x(width)2 x0.52. At endpoint tumors were excised. All protocols involving the use of animals were approved by the Institutional Animal Care and Use Committee (IACUC) at Drexel University College of Medicine. MMTV-PyMT mice mammary fat pads/tumors were isolated at indicated ages and were lysed or fixed for IHC. Histology

was performed as previously described [60]. B6.129-Ogttm1Gwh/J females used for fat pad injections have been previously described [18] and were obtained as a kind gift from S Jones (University of Louisville). Mice were injected directly into the mammary fat pad with Ad5-CMV-GFP or Ad5-CMV-Cre (2.7 × 107 PFU, from the Baylor College of Medicine). B6.129-Ogttm1Gwh/J females were a kind gift of S Jones (University of Louisville) and were previously described [18] Mice were injected directly into the mammary fat pad with Ad5-CMV-GFP or Ad5-CMV-Cre (2.7 × 107 PFU, from the BaylorCollege of Medicine) post parturition daily for three days. Animals groups were not blinded. Histology was performed as previously described [60].

PYMT Lysate and Tissue

Tissue was collected from mammary fat pads of MMTV-PyMT female mice at 4, 8, 12 and 14 weeks of age. Tissue was processed for whole cell lysate as described previously [76, 207] and was used in western blotting procedures as described above.

Lactate Assay

Lactate production was measured with the Lactate Assay Kit II (BioVision, Milpitas, CA), by assaying conditioned media, according to the manufacturer's protocol.

DCF-DA Assay

. Total cellular ROS was assessed using 2,7-dichlorodihydrofluorescein diacetate (DCFH-DA) (Sigma). MDA-MB-231-control and MDA-MB-231-SREBP-1 cells expressing control or OGT shRNA plasmids were seeded at a density of 100,000 cells per well in a 6 well plate and following 48 hours of growth, cells were trypsinized, washed with phosphate buffered saline, and re-suspended in PBS containing 10μM DCFH-DA.

Following a 30-min incubation, cells were collected by centrifugation, re-suspended in 1x PBS, and analyzed by flow cytometry using a Guava Easy-Cyte Mini flow cytometer. Mean fluorescence was normalized to final cell count also determined by FACS analysis.

Soft Agar Colony forming Assay

Media containing 1% agarose was coated and solidified in a 6 well plate. 10,000 cells per condition were mixed with 0.3% agarose and plated on top of bottom agarose layer. After growth in standard incubator conditions (20% O_2, 5% CO_2, 95%, 37 degree C) for 21 days, cells were fixed and stained p-Iodonitrotetrazolium (INT)- violet and colonies were counted.

BODIPY upake

4,4-Difluoro-5,7-Dimethyl-4-Bora-3a,4a-Diaza-s-Indacene-3-Hexadecanoic Acid (BODIPY FL-C16) was purchased from Invitrogen. Briefly, cells were trypsinized with 0.05% Trypsin and quenched with 1% Fatty Acid Free Albumin/PBS. Cells were then counted and washed in warm PBS and incubated with BODIPY FL-C16/1% BSA/PBS solution at room temperature for 20 minutes. Cells were then washed in cold PBS three times, resuspended in 1ml PBS and FACS (using a Guava Easy-Cyte Mini flow cytometer) was used to quantify mean Green Log fluorescence, gating for viable cells. Fluorescence was then averaged and presented as relative mean normalized to control cells +/- SE.

FAME Assay

Cells were infected with control lentivirus or lentivirus targeting OGT. After 48 hours of selection, cells were incubated for 24 hours in media containing 10mM 13C Glucose/Glucose Free DMEM. Equal numbers of cells were then collected from each sample, lipids extracted using a standard chloroform/methanol procedure previously described [208]. The chloroform fraction was dried under nitrogen and redissolved in methanol/toluene. Derivitization occured after addition of acethylchloride (14mM) and butylated hydroxtoluene (0.45mM) and heating at 100 degrees C for one hour. Post cooling, 0.56 M aqueous sodium carbonate was missed with the solution which was prepared for injection into Agilent 5975C GC-MS system equipped with a single quadrupole mass detector by centrifugation and transfer to appropriate glassware... A polar DB-5 column was used for chromatography and data was focused on measurements of palmitate. Mass spectrometry data was normalized to an internal control and to control samples and represented as a relative value. Data was analyzed using MSD ChemStation software from Agilent Isocor, written for the Python programming environment to account for natural 13C abundance. Analyses were performed by Joyce Lee and Dr. Kathryn Wellen.

Crystal Violet Staining

MCF10A or MMTV-Myc cells were plated at a density of 200,000 cells per well in a 6 well plate. After 24 hours they were treated with the indicated concentrations of Ac-5s-GclNAc or vehicle control (DMSO) for 48 hours. Cells were then stained with 0.5% Crystal violet (Hexamethylpararosaniline chloride**) (**Sigma). MDA-MB-231 cells were made to express the indicated plasmids (either infected with lentivirus- control or OGT shRNA or retrovirus – control or SREBP-1, then selected) and plated at a density of

20,000 cells per well in a 6-well plate, grown for 8 days then crystal violet stained as indicated. Quantification of staining was performed by suspending dried stained wells with 1ml of 1% sodium deoxycholate and read at 590nm in a spectrometer.

Immunofluorescent Staining and 3D culture

MDA-MB-231-control or MDA-MB-231-SREBP-1 cells expressing control or OGT shRNA, in respective media containing 2% Matrigel, were plated at a density of 5,000 cells per well in an 8-well chamber slide (BD Biosciences) coated with ~50 µl of Matrigel. Cells were fixed using 4% formalin and Immunofluorescence of 3D structures was performed using antibodies to cleaved caspase-3, SREBP-1 or OGT then stained with 4′,6-diamidino-2-phenylindole and fluorescent secondary antibodies coupled with Alexa-Fluor dyes (Molecular Probes, Carlsbad, CA, USA). Confocal analysis was performed by using the Leica DM6000B Confocal Microscope (Leica). Images were generated containing scale bars using the Leica Imaging Software (Wetzlar, Germany) and converted to Tiff format.

Immunohistochemistry (IHC)

Tissues were fixed and paraffin embedded. Slides were first deparaffinized using 2x 10 minutes xylene, then a series of ethanol consisting of 3x 5minutes each; 100%, 90%, 70% and ddH20. Antigen retrieval consisted of heating slides in 1x citrate buffer pH 6.0 for 30 minutes in a pressure cooker/steamer then cooled f or 30 minutes. After 3x 3 minute washes in 1x PBS, internal peroxidase quench was achieved using 3% Hydrogen Peroxide/tap water followed by 3x 1x PBS washes. Tissue was then blocked in 5% horse serum/1x PBS for 90 minutes at room temperature. Primary antibody was made in

blocking serum and incubated on tissue overnight at 4 degrees in humidified chambers. Prior to secondary antibody addition, using VECTASTAIN Universal Elite ABC HRP Kit (Vector Laboratories) tissues were washed 3x in 1x PBS. This was wash was performed post-secondary antibody as well. The ABC kit was then used following manufacturers' instructions and subsequently DAB Peroxidase (HRP) Substrate Kit (Vector Laboratories). Slides were then washed in tap water and dehydrated following reverse deparaffinization protocol, mounted and visualized by microscopy.

Statistical Analysis

All results shown are results of at least three independent experiments and shown as averages and presented as mean ± s.e. P-values were calculated using a Student's two-tailed test (* represents at least P-value 0.05, where indicated *p-value $\leq$ 0.05 or **p-value $\leq$ 0.01 or as marked in figure legend). Appropriate sample size was chosen to achieve significance using this analysis. Statistical analysis of growth rate of mice was performed using ANCOVA. *p-value < 0.05.

Glucose Uptake

Cells were plated at a density of 100,000 cells/well in a 6 well plate. After 48 hours, media was collected and cells were counted using the Guava Easy Cyte Plus system and CytoSoft (version 5.3) (Millipore Corporation). Control media and each sample were measured on an Accu-chek Active (Roche) Glucose consumption was calculated by subtracting sample measurement from control and normalizing to cell number.

Mammary Fat Pad

Virgin or pregnant females were injected in the all mammary fat pads (virgin- inguinal fat pad) with Adenoviral Cre Recombinase or Adenoviral GFP daily for three days post-wean or post-parturition as indicated in figure legends or text. Offspring fed *ad* lib for 21 days. Mammary fat pads were then collected and protein was extracted for western blot analysis or for immunohistochemistry staining after paraffin imbedding. Pup weight was recorded over time and compared between litters fed from OGT WT and OGT -/- female mothers.

Essentiality determination using Project Achilles

The Project Achilles database consists of shRNA depletion scores from a pooled hairpin library tested on a large collection of cancer cell lines. Briefly, an essentiality score is available for a given gene in a specific cell line if multiple targeting hairpins exhibit similar enrichment or depletion patterns in vitro. Details regarding score calculation have been previously reported [209, 210]. As this approach maximizes the selection of the "on target" shRNAs, the score provides a quantitative measure of gene importance for cell viability and/or proliferation. For identifying genes with similar essentiality value to OGT in the specific context of breast cancer cell lines, we used the openly available Morpheus platform (Broad/MIT). The approximately 5,700 genes present were ranked versus OGT using the "nearest neighbor" analysis. Analyses were performed by Dr. Mircea Ivan.

CHAPTER 7: DISCUSSION AND FUTURE DIRECTIONS

7.1 Discussion

7.1.1Significance of OGT/O-GlcNAcylation

As indicated by each new mechanism of signaling revealed, the regulation of cellular responses and behavior aimed at cell survival and sustenance form incredibly complex networks, often influencing broad cellular processes. Layers of regulation of protein expression exist not only at the level of production, through transcription and translation, but also in maintenance and function of protein via mechanisms which control activity (if the protein is an enzyme) and stability / degradation. The pivotal role that post-translational modifications play in controlling proteins and therefore signaling and cellular behavior has become evident with most efforts aimed at understanding common PTMs like phosphorylation. The appreciation of a seemingly unnoticed glycosylation has grown as techniques to examine and quantify less abundant modifications have become available.

As mentioned above, a role for OGT in the etiology or maintenance of various diseases has appeared over the last two decades through the efforts of many groups [10]. Our lab has characterized the elevation of OGT in breast and prostate cancer and uncovered that the presence of OGT in breast cancer is required for cell viability, invasion and metastasis [21, 59]. We have also detailed the promotion of angiogenesis, invasion and metastasis in prostate cancer by OGT [60]. In this thesis we focused on how OGT protein is elevated in breast cancer in an attempt to understand why this finding is so universal across breast cancer subtypes and has also been observed in many other cancer types. We also aimed to determine if OGT was responsible for promoting other metabolic phenotypes of cancer extending beyond glycolysis which we recently linked to OGT and O-GlcNAcylation in breast cancer [21]. Our findings reveal that OGT expression required signaling through PI3K/AKT/mTOR. Downstream of mTOR, c-Myc was found

to be both required and sufficient to promote OGT elevation and an increase in global O-GlcNAcylation. The chaperone HSP90 interacts with OGT and acts to stabilize OGT protein only in the presence of c-Myc and we hypothesize that this forms a positive feed-forward loop due to the fact that O-GlcNAcylation on c-Myc functions to block its degradation [177]. Non-transformed mammary epithelial cell line MCF10A did not offer any response to OGT inhibition. However, breast cancer cells containing elevated c-Myc levels (MTEC-MYC) were susceptible to OGT pharmacological inhibition and induced apoptosis upon treatment in Ac-5sGlcNAc. With respect to the other goal of this thesis, we found that decreasing OGT results in a downregulation of many lipid metabolites. We pursued the idea that OGT could promote lipid synthesis in breast cancer cells and determined that OGT is required for SREBP-1 nuclear and precursor protein expression as well as the expression of many of its transcriptional targets. OGT enhances expression of the lipid synthesis promoting transcription factor SREBP-1 by suppressing AMPK activation. OGT inhibition activates AMPK which then directly phosphorylates SREBP-1 and acts to decrease its expression. OGT suppression also increases the interaction between SREBP-1 and its E3 ligase FBXW7, potentially through GSK3β, a stipulation that needs to be investigated further. We had previously shown that OGT inhibition results in breast cancer cell death and attributed some of that effect to a role of OGT in cancer, the promotion of glycolysis through HIF1α [21]. Here, we show that decreases in SREBP-1 also contributes to apoptosis induced in response to OGT suppression. Restoring SREBP-1 protein expression to basal levels after OGT depletion significantly rescued cancer cell viability *in vitro* and tumor growth *in vivo*. Due to the similarity in lipid synthesis in breast cancer and in lactation in the breast, we also examined OGT in

this context. *ogt* deletion *in vivo* in B6.*Ogt-loxP/loxP* female mice results in decreased expression of lipogenic genes and decreased lipid droplet content in lactating mammary glands. Deletion of *ogt*, both at the time of weaning (late lactation) and at parturition (beginning of lactation), results in decreased expression of SREBP-1 and FAS as measured by IHC and/or western blot analysis. We also saw changes in signaling factors related to lactogenesis, milk production and β Casein protein production when *ogt* was deleted at parturition. The changes in pup litter weight of those fed from dams where *ogt* was deleted compared to control fed pups indicated that pups received less nutrients/calories contributing to their mass, either in the form of lipids or protein. This could result from decreases in signaling that is required during activation of lactation such as upstream RTKS or more directly through SREBP-1. Beyond lipid regulatory processes, OGT affected expression of the milk protein β Casein. The mechanism by which this occurs requires further investigation as OGT could be acting on STAT5 signaling which is known to regulate Casein. It is also important to more solidly determine if the changes seen are due to a block in lactogenesis.

The ultimate goal of identifying elevated expression in cancer is to recognize novel biomarkers and therapeutic targets. We feel from the above work and the body of literature surrounding OGT and O-GlcNAcylation in cancer that the importance of this post-translation modification and this enzyme can be appreciated. Demonstrations of the requirement of OGT for cancer cell survival show potential utility in targeting this enzyme.

7.1.2Targeting OGT

Various studies demonstrate a therapeutic window may exist to specifically target OGT and O-GlcNAcylation in cancer cells [76, 177, 211]. A number of novel chemicals have been developed to target OGT and reduce O-GlcNAcylation in mammalian cells. Namely, small molecule OGT inhibitors [212] and UDP-GlcNAc salvage pathway analogs [213]. In the past 10 years, Walker and colleagues [212, 214] have developed a number of OGT inhibitors aimed at providing insights to the biological and structural function of the enzyme in mammalian cells. Namely, the commercially available small molecule inhibitor ST045849, has been recently shown to stimulate cell death in prostate cancer cells when used in combination with alanine amidotransferase inhibitors [211].

Vocadlo and colleagues [212], have identified a biosynthetic thiosugar, Ac-5SGlcNAc, that can be salvaged in cells yielding a nucleotide sugar analog that acts to inhibit OGT. Interestingly, these OGT inhibitors have been shown to reduce breast and prostate cancer phenotypes including cell growth and invasion, and increase metabolic stress and apoptosis via reducing expression of potent oncogenes such as FOXM1, c-MYC and HIF-1αβ [59, 60, 76, 177, 207]. In this thesis we also show that Ac-5sGlcNAc treatment results in decreased expression of SREBP-1 and lipogenic enzymes. More recently, the PI3K inhibitor, GDC-0941 demonstrated synergy with OGT inhibition to sensitize ovarian cancer cells and induce apoptosis *in vitro* [215]. The chemosensitizing effects of PI3K pathway inhibition with metabolic defects observed when targeting OGT may provide a promising combinatorial strategy.

Little data exists to predict potential toxicity of targeting OGT using pharmacological inhibitors as a therapeutic strategy to combat cancer growth. Our lab and others have demonstrated through xenograft studies that RNAi inhibition of OGT results in decreased

tumor growth *in vivo*, however systemic administration of an O-GlcNAcylation inhibitor and its potential toxicities to various tissues has yet to be explored. We can postulate that systemic inhibition of OGT with a specific inhibitor may result in adverse events in normal cells with high OGT expression such as the insulin secreting cells of the pancreas. Alejandro and colleagues [20] demonstrated that β-cell specific *ogt* genetic deletion at embryonic day 13.5 results in mice having β-cell failure and diabetes. OGT deficient β-cells displayed loss of mass and function, in part, due to elevated ER stress induced-apoptosis, much like what was seen in breast cancer cells upon OGT inhibition [76]. However, *ogt* ablation in mature β-cells in 12 week old mice, had no effect on β-cell mass and mice did not develop diabetes. This study highlights that adult tissues may not be as sensitive to O-GlcNAcylation inhibition when compared to developing tissues in mammals as well as the importance of understanding the various and complex roles of OGT in adult tissue.

Other potential toxicities may exist in tissues of the brain, as O-GlcNAc is found to be abundant within the brain and decreased O-GlcNAcylation correlates with Alzheimer's phenotypes, potentially through direct modification of tau which is decreased in AD patient brain tissue [46]. The review by Yuzwa et. al. highlights recent work in which pharmacological means to increase levels of O-GlcNAc in the brain results in protective effects in mouse models of AD [46]. Inhibitory effects on neuronal excitability were seen when *ogt* was genetically deleted in AgRP neurons [216]. The ablation of *ogt* in this cell type protected the animals from diet-induced obesity and diabetes showing the complex dynamics of O-GlcNAc in the brain. With this in mind, any negative impact of inhibition of OGT in this tissue could be strategically avoided

through the development of pharmacological OGT inhibitors that are incapable of crossing the blood brain barrier. With significant efforts, OGT may prove to serve as a therapeutic target in breast and several other cancer types and will hopefully confirm and validate the substantial anti-tumor effects we and other see when OGT is targeted genetically.

7.2 Future Directions

From the data presented here we hypothesize that OGT inhibition may synergize with HSP90 inhibitors as well as targeted therapies to lipogenesis. As mentioned previously more than a dozen HSP90 inhibitors are currently at least beginning clinical trials. HSP90 acts to inhibit the degradation of a variety of cancer associated proteins and OGT/O-GlcNAcylation promotes expression of many important oncogenes [52, 217]. We feel that the broad reaching effects of each inhibitor alone could, in combination, lead to a highly anti-tumor effect. There are multiple inhibitors available that serve to inhibit lipogenic enzymes at different points in the pathway. Although the requirement of lipogenesis has been well chronicled in a variety of cancer tissues, inhibition of this process as a means of therapy has proved challenging. Much focus has been concentrated on factors upstream of SREBP-1 such as EGFR, mTOR and P13K [181] however FAS and ACLY inhibitors do exist. Genetic inhibition of lipogenesis downstream of SREBP-1 favors the use of inhibitors against enzymes such as FAS and ACLY for the treatment of cancer. Compounds targeting FAS such as such as cerulenin, C75 and orlistat demonstrated effective inhibition of cancer cell growth/survival but resulted in unintended consequences of decreased food intake and body weight in animal studies which ultimately halted their prospects as potential cancer therapeutics [112]. ACLY

inhibitors (hydroxycitrate, SB-201076, SB-204990 and Compound 9 aka BMS-303414) have demonstrated more potential as therapeutic agents against obesity and dyslipidemia as *in vivo* animal studies showed drastic decreases in plasma triglycerides, cholesterol and in some cases glucose along with weight loss or prevention of weight gain in high-fat fed animals [218]. We propose that OGT inhibition may serve as an alternative strategy of targeting lipogenesis. Also, combination therapy may provide synergistic effects thereby potentially decreasing negative consequences of the above inhibitors, such as dramatic weight loss, while still enacting the same anti-tumor results seen with genetic inhibition studies. Although insufficiently studied here, our metabolic data points to an increase in the process of β-oxidation as measured by levels of carnitine metabolites when OGT was suppressed in breast cancer cells. Within the realm of lipid metabolism, it would be interesting to pursue the idea that OGT inhibition upregulates this process before eventually activating apoptosis. It makes sense that the decrease in glucose uptake and activation of AMPK induced by OGT inhibition would trigger catabolic pathways in an attempt to generate energy and promote survival. This could be tested through the addition of radiolabeled fatty acids (palmitate or oleate) to MDA-MB-231-control and MDA-MB-231-shOGT cells and conversion to labelled CO_2 can be quantified via scintillation counting as a measure of fatty acid oxidation. This could also be addressed through use of the Seahorse Bioscience technology which allows for measurement of fatty acid oxidation as a readout of oxygen consumption rate and can distinguish between use of exogenous and endogenous sources. If we confirm that survival post OGT inhibition is prolonged through activation of β-oxidation, an alternative anti-tumor strategy could be to target β-oxidation in conjunction with OGT. Another major area of

lipid metabolism that remains uncharted in relation to OGT and O-GlcNAcylation is cholesterol. As presented here, OGT regulates SREBP-1 via AMPK. AMPK also regulates SREBP-2 which plays a major role in transcriptionally controlling cholesterol synthesis. It is possible that OGT may also affect this transcription factor which is processed through the same means as SREBP-1 in terms of maturation.

Due to the change in enzymes regulating production of acetyl-CoA (data in this thesis and unpublished data), it is reasonable to hypothesize that acetylation is linked to OGT and O-GlcNAcylation. We have shown here that ACLY (citrate to acetyl-CoA) is positively regulated by OGT and have also found that ACSS2 (acetate to acetyl-CoA) is regulated similarly (data not shown) in breast cancer cells. Not only do we believe that OGT promotes production of acetyl-CoA in breast cancer, we have recently demonstrated that OGT negatively regulates the tumor suppressor deacetylase SIRT1 [199]. The consequence of suppression of SIRT1 by expression of OGT in breast cancer was found to be the promotion of FOXM1 and invasion, however this data combined with our knowledge of acetyl-CoA producing enzymes implies much broader implications in gene expression especially if other sirtuins are found to respond to OGT modulation. Since acetyl-CoA contributes to the production of UDP-GlcNAc and is therefore needed for O-GlcNAc modification, the network between these factors becomes more complex.

OGT may play an important role in cellular aging. It has long been understood that steady declines in cellular function results in onset and progression of various diseases and likelihood of the development of disease dramatically increases with age. Caloric restriction (CR) is the only recognized intervention that is known to extend both mean and maximal lifespan [219]. CR also delays onset of age-related diseases such as

diabetes, neurodegenerative disease and cancer. CR is defined as reduction in caloric intake without malnutrition (generally encompassing an intake of 20-40% less calories than a normal diet) [220]. Many cellular changes occur in CR cells that may contribute to life-span extension and anti-cancer properties. These include decreases in growth factors, anabolic hormones, inflammatory cytokines, oxidative stress and enhanced autophagy [221]. A more specific molecular definition of CR mimetics was recently described that includes: interventions that elicit a) the induction of autophagy, b) favoring deacetylation of proteins within the cell through decreasing cytosolic acetyl-CoA and/or induction of expression or activity of deacetylases which catalyze removal of acetyl groups from a range of proteins [222]. Since OGT inhibition causes both decreases in enzymes that promote acetyl-CoA production and increases in at least one sirtuin, we believe that OGT inhibition could mimic caloric restriction. It would be very interesting to determne if other characteristics of CR mimetics are associated with OGT and O-GlcNAc such as autophagy, especially because of the known links between OGT and AMPK and autophagy's relationship with AMPK [156]. Overall there are many unexplored connections between OGT and cellular and organismal biology that can be pursued. Despite the remaining unknowns, advancements in our ability to detect the O-GlcNAc modification as well as a persistent interest in metabolic disorders and a renewed interest in classifying cancer as such have brought light to the importance of this small sugar post-translational modification. OGT and O-GlcNAcylation may serve clinically useful as either a biomarker or as a therapeutic avenue in several diseases in the near future.

REFERENCES:

1. Marshall, S., V. Bacote, and R.R. Traxinger, *Discovery of a metabolic pathway mediating glucose-induced desensitization of the glucose transport system. Role of hexosamine biosynthesis in the induction of insulin resistance.* J Biol Chem, 1991. **266**(8): p. 4706-12.
2. McClain, D.A., *Hexosamines as mediators of nutrient sensing and regulation in diabetes.* Journal of diabetes and its complications, 2002. **16**(1): p. 72-80.
3. Hanover, J.A., M.W. Krause, and D.C. Love, *Bittersweet memories: linking metabolism to epigenetics through O-GlcNAcylation.* Nature reviews. Molecular cell biology, 2012. **13**(5): p. 312-21.
4. Hart, G.W., M.P. Housley, and C. Slawson, *Cycling of O-linked beta-N-acetylglucosamine on nucleocytoplasmic proteins.* Nature, 2007. **446**(7139): p. 1017-22.
5. Varki, A., et al., *"The O-GlcNAc Modification"*, in *Essentials of Glycobiology*. 1999, Cold Spring Harbor Laboratory Press: Cold Spring Harbor, NY.
6. Levine, Z.G. and S. Walker, *The Biochemistry of O-GlcNAc Transferase: Which Functions Make It Essential in Mammalian Cells?* Annu Rev Biochem, 2016. **85**: p. 631-57.
7. Hardiville, S. and G.W. Hart, *Nutrient regulation of signaling, transcription, and cell physiology by O-GlcNAcylation.* Cell Metab, 2014. **20**(2): p. 208-13.
8. Hart, G.W., et al., *Cross talk between O-GlcNAcylation and phosphorylation: roles in signaling, transcription, and chronic disease.* Annual review of biochemistry, 2011. **80**: p. 825-58.
9. Comer, F.I. and G.W. Hart, *O-GlcNAc and the control of gene expression.* Biochimica et biophysica acta, 1999. **1473**(1): p. 161-71.
10. Bond, M.R. and J.A. Hanover, *O-GlcNAc Cycling: A Link Between Metabolism and Chronic Disease.* Annual review of nutrition, 2013. **33**: p. 205-29.
11. Lubas, W.A., et al., *O-Linked GlcNAc transferase is a conserved nucleocytoplasmic protein containing tetratricopeptide repeats.* J Biol Chem, 1997. **272**(14): p. 9316-24.
12. Jinek, M., et al., *The superhelical TPR-repeat domain of O-linked GlcNAc transferase exhibits structural similarities to importin alpha.* Nat Struct Mol Biol, 2004. **11**(10): p. 1001-7.
13. Yang, X., et al., *Phosphoinositide signalling links O-GlcNAc transferase to insulin resistance.* Nature, 2008. **451**(7181): p. 964-9.
14. Iyer, S.P. and G.W. Hart, *Roles of the tetratricopeptide repeat domain in O-GlcNAc transferase targeting and protein substrate specificity.* J Biol Chem, 2003. **278**(27): p. 24608-16.
15. Pathak, S., et al., *The active site of O-GlcNAc transferase imposes constraints on substrate sequence.* Nat Struct Mol Biol, 2015. **22**(9): p. 744-50.
16. Capotosti, F., et al., *O-GlcNAc transferase catalyzes site-specific proteolysis of HCF-1.* Cell, 2011. **144**(3): p. 376-88.
17. Daou, S., et al., *Crosstalk between O-GlcNAcylation and proteolytic cleavage regulates the host cell factor-1 maturation pathway.* Proc Natl Acad Sci U S A, 2011. **108**(7): p. 2747-52.

18. O'Donnell, N., et al., *Ogt-dependent X-chromosome-linked protein glycosylation is a requisite modification in somatic cell function and embryo viability.* Mol. Cell. Biol., 2004. **24**: p. 1680-1690.
19. Wells, L., *Mutations in O-GlcNAc Transferase Linked to X-linked Intellectual Disability.* The Federation of American Societies for Experimental Biology Journal, 2016 **1**(1 Supplement 98.5).
20. Alejandro, E.U., et al., *Disruption of O-linked N-Acetylglucosamine Signaling Induces ER Stress and beta Cell Failure.* Cell Rep, 2015. **13**(11): p. 2527-38.
21. Ferrer, C.M., et al., *Nutrient sensor O-GlcNAcylation regulates cancer metabolism and survival stress signaling via regulation of HIF-1 pathway.* Molecular Cell, 2014. **(In Press)**.
22. Howerton, C.L. and T.L. Bale, *Targeted placental deletion of OGT recapitulates the prenatal stress phenotype including hypothalamic mitochondrial dysfunction.* Proc Natl Acad Sci U S A, 2014. **111**(26): p. 9639-44.
23. Swamy, M., et al., *Glucose and glutamine fuel protein O-GlcNAcylation to control T cell self-renewal and malignancy.* Nat Immunol, 2016. **17**(6): p. 712-20.
24. Wells, L., et al., *Dynamic O-glycosylation of nuclear and cytosolic proteins: further characterization of the nucleocytoplasmic beta-N-acetylglucosaminidase, O-GlcNAcase.* J Biol Chem, 2002. **277**(3): p. 1755-61.
25. Alonso, J., M. Schimpl, and D.M. van Aalten, *O-GlcNAcase: promiscuous hexosaminidase or key regulator of O-GlcNAc signaling?* J Biol Chem, 2014. **289**(50): p. 34433-9.
26. Toleman, C., et al., *Characterization of the histone acetyltransferase (HAT) domain of a bifunctional protein with activable O-GlcNAcase and HAT activities.* J Biol Chem, 2004. **279**(51): p. 53665-73.
27. Rao, F.V., et al., *Structure of a bacterial putative acetyltransferase defines the fold of the human O-GlcNAcase C-terminal domain.* Open Biol, 2013. **3**(10): p. 130021.
28. Keembiyehetty, C., et al., *Conditional knock-out reveals a requirement for O-linked N-Acetylglucosaminase (O-GlcNAcase) in metabolic homeostasis.* J Biol Chem, 2015. **290**(11): p. 7097-113.
29. Zhu, Y., et al., *O-GlcNAc occurs cotranslationally to stabilize nascent polypeptide chains.* Nat Chem Biol, 2015. **11**(5): p. 319-25.
30. Fujiki, R., et al., *GlcNAcylation of histone H2B facilitates its monoubiquitination.* Nature, 2011. **480**(7378): p. 557-60.
31. Bauer, C., et al., *Phosphorylation of TET proteins is regulated via O-GlcNAcylation by the O-linked N-acetylglucosamine transferase (OGT).* J Biol Chem, 2015. **290**(8): p. 4801-12.
32. Chu, C.S., et al., *O-GlcNAcylation regulates EZH2 protein stability and function.* Proc Natl Acad Sci U S A, 2014. **111**(4): p. 1355-60.
33. Li, M.D., et al., *O-GlcNAc signaling entrains the circadian clock by inhibiting BMAL1/CLOCK ubiquitination.* Cell Metab, 2013. **17**(2): p. 303-10.
34. Yang, X., F. Zhang, and J.E. Kudlow, *Recruitment of O-GlcNAc transferase to promoters by corepressor mSin3A: coupling protein O-GlcNAcylation to transcriptional repression.* Cell, 2002. **110**(1): p. 69-80.

35. Shen, D.L., et al., *Insights into O-linked N-acetylglucosamine ([0-9]O-GlcNAc) processing and dynamics through kinetic analysis of O-GlcNAc transferase and O-GlcNAcase activity on protein substrates.* J Biol Chem, 2012. **287**(19): p. 15395-408.
36. Zhang, X., et al., *MAPK/ERK signaling pathway-induced hyper-O-GlcNAcylation enhances cancer malignancy.* Mol Cell Biochem, 2015. **410**(1-2): p. 101-10.
37. Muthusamy, S., et al., *E2F1 Transcription Factor Regulates O-linked N-acetylglucosamine (O-GlcNAc) Transferase and O-GlcNAcase Expression.* J Biol Chem, 2015. **290**(52): p. 31013-24.
38. Krzeslak, A., et al., *Gene expression of O-GlcNAc cycling enzymes in human breast cancers.* Clin Exp Med, 2012. **12**(1): p. 61-5.
39. Whelan, S.A., M.D. Lane, and G.W. Hart, *Regulation of the O-linked beta-N-acetylglucosamine transferase by insulin signaling.* J Biol Chem, 2008. **283**(31): p. 21411-7.
40. Zhang, F., C.M. Snead, and J.D. Catravas, *Hsp90 regulates O-linked beta-N-acetylglucosamine transferase: a novel mechanism of modulation of protein O-linked beta-N-acetylglucosamine modification in endothelial cells.* American journal of physiology. Cell physiology, 2012. **302**(12): p. C1786-96.
41. Liu, Y., et al., *Decreased glucose transporters correlate to abnormal hyperphosphorylation of tau in Alzheimer disease.* FEBS Lett, 2008. **582**(2): p. 359-64.
42. Arnold, C.S., et al., *The microtubule-associated protein tau is extensively modified with O-linked N-acetylglucosamine.* J Biol Chem, 1996. **271**(46): p. 28741-4.
43. Liu, F., et al., *O-GlcNAcylation regulates phosphorylation of tau: a mechanism involved in Alzheimer's disease.* Proc Natl Acad Sci U S A, 2004. **101**(29): p. 10804-9.
44. Li, X., et al., *Concurrent alterations of O-GlcNAcylation and phosphorylation of tau in mouse brains during fasting.* Eur J Neurosci, 2006. **23**(8): p. 2078-86.
45. Dong, D.L., et al., *Glycosylation of mammalian neurofilaments. Localization of multiple O-linked N-acetylglucosamine moieties on neurofilament polypeptides L and M.* J Biol Chem, 1993. **268**(22): p. 16679-87.
46. Yuzwa, S.A. and D.J. Vocadlo, *O-GlcNAc and neurodegeneration: biochemical mechanisms and potential roles in Alzheimer's disease and beyond.* Chem Soc Rev, 2014. **43**(19): p. 6839-58.
47. Slawson, C., R.J. Copeland, and G.W. Hart, *O-GlcNAc signaling: a metabolic link between diabetes and cancer?* Trends Biochem Sci, 2010. **35**(10): p. 547-55.
48. Ball, L.E., M.N. Berkaw, and M.G. Buse, *Identification of the major site of O-linked beta-N-acetylglucosamine modification in the C terminus of insulin receptor substrate-1.* Mol Cell Proteomics, 2006. **5**(2): p. 313-23.
49. Copeland, R.J., G. Han, and G.W. Hart, *O-GlcNAcomics--Revealing roles of O-GlcNAcylation in disease mechanisms and development of potential diagnostics.* Proteomics Clin Appl, 2013. **7**(9-10): p. 597-606.
50. Vander Heiden, M.G., L.C. Cantley, and C.B. Thompson, *Understanding the Warburg effect: the metabolic requirements of cell proliferation.* Science, 2009. **324**(5930): p. 1029-33.

51. Wellen, K.E. and C.B. Thompson, *Cellular metabolic stress: considering how cells respond to nutrient excess.* Mol Cell, 2010. **40**(2): p. 323-32.
52. Ferrer, C.M., V.L. Sodi, and M.J. Reginato, *O-GlcNAcylation in Cancer Biology: Linking Metabolism and Signaling.* J Mol Biol, 2016. **428**(16): p. 3282-94.
53. Chou, T.Y., C.V. Dang, and G.W. Hart, *Glycosylation of the c-Myc transactivation domain.* Proc Natl Acad Sci U S A, 1995. **92**(10): p. 4417-21.
54. Kawauchi, K., et al., *Loss of p53 enhances catalytic activity of IKKbeta through O-linked beta-N-acetyl glucosamine modification.* Proc Natl Acad Sci U S A, 2009. **106**(9): p. 3431-6.
55. McClain, D.A., et al., *Altered glycan-dependent signaling induces insulin resistance and hyperleptinemia.* Proc Natl Acad Sci U S A, 2002. **99**(16): p. 10695-9.
56. Yang, W.H., et al., *Modification of p53 with O-linked N-acetylglucosamine regulates p53 activity and stability.* Nat Cell Biol, 2006. **8**(10): p. 1074-83.
57. Ozcan, S., S.S. Andrali, and J.E. Cantrell, *Modulation of transcription factor function by O-GlcNAc modification.* Biochim Biophys Acta, 2010. **1799**(5-6): p. 353-64.
58. Wang, Z., *Extensive crosstalk between O-GlcNAcylation and phosphorylation regulates cytokinesis.* Sci. Signal., 2010. **3**: p. ra2.
59. Caldwell, S.A., et al., *Nutrient sensor O-GlcNAc transferase regulates breast cancer tumorigenesis through targeting of the oncogenic transcription factor FoxM1.* Oncogene, 2010. **29**(19): p. 2831-42.
60. Lynch, T.P., et al., *Critical role of O-Linked beta-N-acetylglucosamine transferase in prostate cancer invasion, angiogenesis, and metastasis.* J Biol Chem, 2012. **287**(14): p. 11070-81.
61. Ma, Z. and K. Vosseller, *O-GlcNAc in cancer biology.* Amino Acids, 2013. **45**(4): p. 719-33.
62. Griffiths, B., et al., *Sterol regulatory element binding protein-dependent regulation of lipid synthesis supports cell survival and tumor growth.* Cancer Metab, 2013. **1**(1): p. 3.
63. Shaw, P., et al., *Regulation of specific DNA binding by p53: evidence for a role for O-glycosylation and charged residues at the carboxy-terminus.* Oncogene, 1996. **12**(4): p. 921-30.
64. Medina, L., K. Grove, and R.S. Haltiwanger, *SV40 large T antigen is modified with O-linked N-acetylglucosamine but not with other forms of glycosylation.* Glycobiology, 1998. **8**(4): p. 383-91.
65. Chou, T.Y. and G.W. Hart, *O-linked N-acetylglucosamine and cancer: messages from the glycosylation of c-Myc.* Advances in experimental medicine and biology, 2001. **491**: p. 413-8.
66. Hanover, J.A., *Glycan-dependent signaling: O-linked N-acetylglucosamine.* FASEB journal : official publication of the Federation of American Societies for Experimental Biology, 2001. **15**(11): p. 1865-76.
67. Yang, W.H., et al., *NFkappaB activation is associated with its O-GlcNAcylation state under hyperglycemic conditions.* Proceedings of the National Academy of Sciences of the United States of America, 2008. **105**(45): p. 17345-50.

68. Gu, Y., et al., *GlcNAcylation plays an essential role in breast cancer metastasis.* Cancer Res, 2010. **70**(15): p. 6344-51.
69. Champattanachai, V., et al., *Proteomic analysis and abrogated expression of O-GlcNAcylated proteins associated with primary breast cancer.* Proteomics, 2013. **13**(14): p. 2088-99.
70. Itkonen, H.M., et al., *O-GlcNAc transferase integrates metabolic pathways to regulate the stability of c-MYC in human prostate cancer.* Cancer Res, 2013.
71. Yi, W., et al., *Phosphofructokinase 1 glycosylation regulates cell growth and metabolism.* Science, 2012. **337**(6097): p. 975-80.
72. Mi, W., et al., *O-GlcNAcylation is a novel regulator of lung and colon cancer malignancy.* Biochim Biophys Acta, 2011. **1812**(4): p. 514-9.
73. Zhu, Q., et al., *O-GlcNAcylation plays a role in tumor recurrence of hepatocellular carcinoma following liver transplantation.* Medical oncology, 2012. **29**(2): p. 985-93.
74. Rozanski, W., et al., *Prediction of bladder cancer based on urinary content of MGEA5 and OGT mRNA level.* Clinical laboratory, 2012. **58**(5-6): p. 579-83.
75. Shi, Y., et al., *Aberrant O-GlcNAcylation characterizes chronic lymphocytic leukemia.* Leukemia, 2010. **24**(9): p. 1588-98.
76. Ferrer, C.M., et al., *O-GlcNAcylation regulates cancer metabolism and survival stress signaling via regulation of the HIF-1 pathway.* Mol Cell, 2014. **54**(5): p. 820-31.
77. Krzeslak, A., et al., *Gene expression of O-GlcNAc cycling enzymes in human breast cancers.* Clinical and experimental medicine, 2012. **12**(1): p. 61-5.
78. Yehezkel, G., et al., *O-linked beta-N-acetylglucosaminylation (O-GlcNAcylation) in primary and metastatic colorectal cancer clones and effect of N-acetyl-beta-D-glucosaminidase silencing on cell phenotype and transcriptome.* J Biol Chem, 2012. **287**(34): p. 28755-69.
79. Beishline, K. and J. Azizkhan-Clifford, *Sp1 and the 'hallmarks of cancer'.* FEBS J, 2015. **282**(2): p. 224-58.
80. Du, X.L., et al., *Hyperglycemia-induced mitochondrial superoxide overproduction activates the hexosamine pathway and induces plasminogen activator inhibitor-1 expression by increasing Sp1 glycosylation.* Proc Natl Acad Sci U S A, 2000. **97**(22): p. 12222-6.
81. Donovan, K., et al., *O-GlcNAc modification of transcription factor Sp1 mediates hyperglycemia-induced VEGF-A upregulation in retinal cells.* Invest Ophthalmol Vis Sci, 2014. **55**(12): p. 7862-73.
82. Dauphinee, S.M., M. Ma, and C.K. Too, *Role of O-linked beta-N-acetylglucosamine modification in the subcellular distribution of alpha4 phosphoprotein and Sp1 in rat lymphoma cells.* J Cell Biochem, 2005. **96**(3): p. 579-88.
83. Prat, A., et al., *Clinical implications of the intrinsic molecular subtypes of breast cancer.* Breast, 2015. **24 Suppl 2**: p. S26-35.
84. Byler, S., et al., *Genetic and epigenetic aspects of breast cancer progression and therapy.* Anticancer Res, 2014. **34**(3): p. 1071-7.
85. Cancer Genome Atlas, N., *Comprehensive molecular portraits of human breast tumours.* Nature, 2012. **490**(7418): p. 61-70.

86. Hanahan, D. and R.A. Weinberg, *Hallmarks of cancer: the next generation.* Cell, 2011. **144**(5): p. 646-74.
87. Singletary, S.E., *Rating the risk factors for breast cancer.* Ann Surg, 2003. **237**(4): p. 474-82.
88. Polyak, K., *Breast cancer: origins and evolution.* J Clin Invest, 2007. **117**(11): p. 3155-63.
89. McCormick, F., *Signalling networks that cause cancer.* Trends Cell Biol, 1999. **9**(12): p. M53-6.
90. Santa-Maria, C.A. and W.J. Gradishar, *Changing Treatment Paradigms in Metastatic Breast Cancer: Lessons Learned.* JAMA Oncol, 2015. **1**(4): p. 528-34; quiz 549.
91. Andre, F. and C.C. Zielinski, *Optimal strategies for the treatment of metastatic triple-negative breast cancer with currently approved agents.* Ann Oncol, 2012. **23 Suppl 6**: p. vi46-51.
92. Longley, D.B. and P.G. Johnston, *Molecular mechanisms of drug resistance.* J Pathol, 2005. **205**(2): p. 275-92.
93. Brewster, A.M., et al., *Residual risk of breast cancer recurrence 5 years after adjuvant therapy.* J Natl Cancer Inst, 2008. **100**(16): p. 1179-83.
94. Karakashev, S.V. and M.J. Reginato, *Hypoxia/HIF1alpha induces lapatinib resistance in ERBB2-positive breast cancer cells via regulation of DUSP2.* Oncotarget, 2015. **6**(4): p. 1967-80.
95. Bose, R., et al., *Activating HER2 mutations in HER2 gene amplification negative breast cancer.* Cancer Discov, 2013. **3**(2): p. 224-37.
96. Niikura, N., et al., *Loss of human epidermal growth factor receptor 2 (HER2) expression in metastatic sites of HER2-overexpressing primary breast tumors.* J Clin Oncol, 2012. **30**(6): p. 593-9.
97. Hurvitz, S.A., et al., *A phase 2 study of everolimus combined with trastuzumab and paclitaxel in patients with HER2-overexpressing advanced breast cancer that progressed during prior trastuzumab and taxane therapy.* Breast Cancer Res Treat, 2013. **141**(3): p. 437-46.
98. Boroughs, L.K. and R.J. DeBerardinis, *Metabolic pathways promoting cancer cell survival and growth.* Nat Cell Biol, 2015. **17**(4): p. 351-9.
99. Kaelin, W.G., Jr., *Cancer and altered metabolism: potential importance of hypoxia-inducible factor and 2-oxoglutarate-dependent dioxygenases.* Cold Spring Harb Symp Quant Biol, 2011. **76**: p. 335-45.
100. Warburg, O., *On the origin of cancer cells.* Science, 1956. **123**(3191): p. 309-14.
101. DeBerardinis, R.J., et al., *The biology of cancer: metabolic reprogramming fuels cell growth and proliferation.* Cell Metab, 2008. **7**(1): p. 11-20.
102. Shaw, R.J. and L.C. Cantley, *Ras, PI(3)K and mTOR signalling controls tumour cell growth.* Nature, 2006. **441**(7092): p. 424-30.
103. Jones, R.G. and C.B. Thompson, *Tumor suppressors and cell metabolism: a recipe for cancer growth.* Genes Dev, 2009. **23**(5): p. 537-48.
104. Dang, C.V. and G.L. Semenza, *Oncogenic alterations of metabolism.* Trends Biochem Sci, 1999. **24**(2): p. 68-72.
105. Zoncu, R., A. Efeyan, and D.M. Sabatini, *mTOR: from growth signal integration to cancer, diabetes and ageing.* Nat Rev Mol Cell Biol, 2011. **12**(1): p. 21-35.

106. Zoncu, R., A. Efeyan, and D.M. Sabatini, *mTOR: from growth signal integration to cancer, diabetes and ageing.* Nature reviews. Molecular cell biology, 2011. **12**(1): p. 21-35.
107. Horiuchi, D., B. Anderton, and A. Goga, *Taking on challenging targets: making MYC druggable.* Am Soc Clin Oncol Educ Book, 2014: p. e497-502.
108. Dang, C.V., *MYC, metabolism, cell growth, and tumorigenesis.* Cold Spring Harbor perspectives in medicine, 2013. **3**(8).
109. DeBerardinis, R.J., et al., *Beyond aerobic glycolysis: transformed cells can engage in glutamine metabolism that exceeds the requirement for protein and nucleotide synthesis.* Proc Natl Acad Sci U S A, 2007. **104**(49): p. 19345-50.
110. Dang, C.V., A. Le, and P. Gao, *MYC-induced cancer cell energy metabolism and therapeutic opportunities.* Clinical cancer research : an official journal of the American Association for Cancer Research, 2009. **15**(21): p. 6479-83.
111. Hynes, N.E. and T. Stoelzle, *Key signalling nodes in mammary gland development and cancer: Myc.* Breast cancer research : BCR, 2009. **11**(5): p. 210.
112. Flavin, R., et al., *Fatty acid synthase as a potential therapeutic target in cancer.* Future Oncol, 2010. **6**(4): p. 551-62.
113. Menendez, J.A. and R. Lupu, *Fatty acid synthase and the lipogenic phenotype in cancer pathogenesis.* Nat Rev Cancer, 2007. **7**(10): p. 763-77.
114. Harris, A.L., *Hypoxia--a key regulatory factor in tumour growth.* Nat Rev Cancer, 2002. **2**(1): p. 38-47.
115. Semenza, G.L., *Defining the role of hypoxia-inducible factor 1 in cancer biology and therapeutics.* Oncogene, 2010. **29**(5): p. 625-34.
116. Generali, D., et al., *Hypoxia-inducible factor-1alpha expression predicts a poor response to primary chemoendocrine therapy and disease-free survival in primary human breast cancer.* Clin Cancer Res, 2006. **12**(15): p. 4562-8.
117. Palm, W., et al., *The Utilization of Extracellular Proteins as Nutrients Is Suppressed by mTORC1.* Cell, 2015. **162**(2): p. 259-70.
118. Ying, H., et al., *Oncogenic Kras maintains pancreatic tumors through regulation of anabolic glucose metabolism.* Cell, 2012. **149**(3): p. 656-70.
119. Shackelford, D.B. and R.J. Shaw, *The LKB1-AMPK pathway: metabolism and growth control in tumour suppression.* Nat Rev Cancer, 2009. **9**(8): p. 563-75.
120. Sengupta, S., T.R. Peterson, and D.M. Sabatini, *Regulation of the mTOR complex 1 pathway by nutrients, growth factors, and stress.* Mol Cell, 2010. **40**(2): p. 310-22.
121. Wellen, K.E., et al., *The hexosamine biosynthetic pathway couples growth factor-induced glutamine uptake to glucose metabolism.* Genes Dev, 2010. **24**(24): p. 2784-99.
122. Gwinn, D.M., et al., *AMPK phosphorylation of raptor mediates a metabolic checkpoint.* Mol Cell, 2008. **30**(2): p. 214-26.
123. Hardie, D.G., *AMPK: a target for drugs and natural products with effects on both diabetes and cancer.* Diabetes, 2013. **62**(7): p. 2164-72.
124. Neve, R.M., et al., *A collection of breast cancer cell lines for the study of functionally distinct cancer subtypes.* Cancer Cell, 2006. **10**(6): p. 515-27.
125. Luo, J., B.D. Manning, and L.C. Cantley, *Targeting the PI3K-Akt pathway in human cancer: rationale and promise.* Cancer Cell, 2003. **4**(4): p. 257-62.

126. Reginato, M.J., et al., *Bim regulation of lumen formation in cultured mammary epithelial acini is targeted by oncogenes.* Molecular and cellular biology, 2005. **25**(11): p. 4591-601.
127. Schmidt, E.V., et al., *Growth controls connect: interactions between c-myc and the tuberous sclerosis complex-mTOR pathway.* Cell Cycle, 2009. **8**(9): p. 1344-51.
128. Teng, S.C., et al., *Direct activation of HSP90A transcription by c-Myc contributes to c-Myc-induced transformation.* The Journal of biological chemistry, 2004. **279**(15): p. 14649-55.
129. Schulte, T.W. and L.M. Neckers, *The benzoquinone ansamycin 17-allylamino-17-demethoxygeldanamycin binds to HSP90 and shares important biologic activities with geldanamycin.* Cancer chemotherapy and pharmacology, 1998. **42**(4): p. 273-9.
130. Solit, D.B., H.I. Scher, and N. Rosen, *Hsp90 as a therapeutic target in prostate cancer.* Seminars in oncology, 2003. **30**(5): p. 709-16.
131. Stewart, T.A., P.K. Pattengale, and P. Leder, *Spontaneous mammary adenocarcinomas in transgenic mice that carry and express MTV/myc fusion genes.* Cell, 1984. **38**(3): p. 627-37.
132. Morrish, F., et al., *c-Myc activates multiple metabolic networks to generate substrates for cell-cycle entry.* Oncogene, 2009. **28**(27): p. 2485-91.
133. Dang, C.V., *Rethinking the Warburg effect with Myc micromanaging glutamine metabolism.* Cancer research, 2010. **70**(3): p. 859-62.
134. Sawai, A., et al., *Inhibition of Hsp90 down-regulates mutant epidermal growth factor receptor (EGFR) expression and sensitizes EGFR mutant tumors to paclitaxel.* Cancer Res, 2008. **68**(2): p. 589-96.
135. Chou, T.Y., G.W. Hart, and C.V. Dang, *c-Myc is glycosylated at threonine 58, a known phosphorylation site and a mutational hot spot in lymphomas.* The Journal of biological chemistry, 1995. **270**(32): p. 18961-5.
136. Overath, T., et al., *Mapping of O-GlcNAc sites of 20 S proteasome subunits and Hsp90 by a novel biotin-cystamine tag.* Mol Cell Proteomics, 2012. **11**(8): p. 467-77.
137. Huang, M.J., et al., *A small-molecule c-Myc inhibitor, 10058-F4, induces cell-cycle arrest, apoptosis, and myeloid differentiation of human acute myeloid leukemia.* Exp Hematol, 2006. **34**(11): p. 1480-9.
138. Wang, H., et al., *Disruption of Myc-Max heterodimerization with improved cell-penetrating analogs of the small molecule 10074-G5.* Oncotarget, 2013. **4**(6): p. 936-47.
139. Sidera, K. and E. Patsavoudi, *HSP90 inhibitors: current development and potential in cancer therapy.* Recent Pat Anticancer Drug Discov, 2014. **9**(1): p. 1-20.
140. Horton, J.D., J.L. Goldstein, and M.S. Brown, *SREBPs: transcriptional mediators of lipid homeostasis.* Cold Spring Harb Symp Quant Biol, 2002. **67**: p. 491-8.
141. Swinnen, J.V., K. Brusselmans, and G. Verhoeven, *Increased lipogenesis in cancer cells: new players, novel targets.* Curr Opin Clin Nutr Metab Care, 2006. **9**(4): p. 358-65.

142. Santos, C.R. and A. Schulze, *Lipid metabolism in cancer.* FEBS J, 2012. **279**(15): p. 2610-23.
143. Walker, A.K., et al., *A conserved SREBP-1/phosphatidylcholine feedback circuit regulates lipogenesis in metazoans.* Cell, 2011. **147**(4): p. 840-52.
144. Beckner, M.E., et al., *Identification of ATP citrate lyase as a positive regulator of glycolytic function in glioblastomas.* Int J Cancer, 2010. **126**(10): p. 2282-95.
145. Porstmann, T., et al., *A new player in the orchestra of cell growth: SREBP activity is regulated by mTORC1 and contributes to the regulation of cell and organ size.* Biochem Soc Trans, 2009. **37**(Pt 1): p. 278-83.
146. Li, W., et al., *Repression of endometrial tumor growth by targeting SREBP1 and lipogenesis.* Cell Cycle, 2012. **11**(12): p. 2348-58.
147. Tania, M., M.A. Khan, and Y. Song, *Association of lipid metabolism with ovarian cancer.* Curr Oncol, 2010. **17**(5): p. 6-11.
148. Yahagi, N., et al., *Co-ordinate activation of lipogenic enzymes in hepatocellular carcinoma.* Eur J Cancer, 2005. **41**(9): p. 1316-22.
149. Szutowicz, A., J. Kwiatkowski, and S. Angielski, *Lipogenetic and glycolytic enzyme activities in carcinoma and nonmalignant diseases of the human breast.* Br J Cancer, 1979. **39**(6): p. 681-7.
150. Hatzivassiliou, G., et al., *ATP citrate lyase inhibition can suppress tumor cell growth.* Cancer Cell, 2005. **8**(4): p. 311-21.
151. Migita, T., et al., *ATP citrate lyase: activation and therapeutic implications in non-small cell lung cancer.* Cancer Res, 2008. **68**(20): p. 8547-54.
152. Zaidi, N., et al., *ATP citrate lyase knockdown induces growth arrest and apoptosis through different cell- and environment-dependent mechanisms.* Mol Cancer Ther, 2012. **11**(9): p. 1925-35.
153. Wellen, K.E., et al., *ATP-citrate lyase links cellular metabolism to histone acetylation.* Science, 2009. **324**(5930): p. 1076-80.
154. Thupari, J.N., M.L. Pinn, and F.P. Kuhajda, *Fatty acid synthase inhibition in human breast cancer cells leads to malonyl-CoA-induced inhibition of fatty acid oxidation and cytotoxicity.* Biochem Biophys Res Commun, 2001. **285**(2): p. 217-23.
155. Luo, Z., M. Zang, and W. Guo, *AMPK as a metabolic tumor suppressor: control of metabolism and cell growth.* Future Oncol, 2010. **6**(3): p. 457-70.
156. Kim, J., et al., *AMPK and mTOR regulate autophagy through direct phosphorylation of Ulk1.* Nat Cell Biol, 2011. **13**(2): p. 132-41.
157. Laderoute, K.R., et al., *5'-AMP-activated protein kinase (AMPK) is induced by low-oxygen and glucose deprivation conditions found in solid-tumor microenvironments.* Mol Cell Biol, 2006. **26**(14): p. 5336-47.
158. Li, Y., et al., *AMPK phosphorylates and inhibits SREBP activity to attenuate hepatic steatosis and atherosclerosis in diet-induced insulin-resistant mice.* Cell Metab, 2011. **13**(4): p. 376-88.
159. Li, X., et al., *SREBP-2 promotes stem cell-like properties and metastasis by transcriptional activation of c-Myc in prostate cancer.* Oncotarget, 2016. **7**(11): p. 12869-84.
160. Ma, Y. and L.M. Hendershot, *The unfolding tale of the unfolded protein response.* Cell, 2001. **107**(7): p. 827-30.

161. Palorini, R., et al., *Glucose starvation induces cell death in K-ras-transformed cells by interfering with the hexosamine biosynthesis pathway and activating the unfolded protein response.* Cell Death Dis, 2013. **4**: p. e732.
162. Kurtoglu, M., et al., *Under normoxia, 2-deoxy-D-glucose elicits cell death in select tumor types not by inhibition of glycolysis but by interfering with N-linked glycosylation.* Mol Cancer Ther, 2007. **6**(11): p. 3049-58.
163. Shore, G.C., F.R. Papa, and S.A. Oakes, *Signaling cell death from the endoplasmic reticulum stress response.* Curr Opin Cell Biol, 2011. **23**(2): p. 143-9.
164. Nakano, A., et al., *Glycolysis inhibition inactivates ABC transporters to restore drug sensitivity in malignant cells.* PLoS One, 2011. **6**(11): p. e27222.
165. Pelicano, H., et al., *Glycolysis inhibition for anticancer treatment.* Oncogene, 2006. **25**(34): p. 4633-46.
166. Chu, K.Y., et al., *ATP-citrate lyase reduction mediates palmitate-induced apoptosis in pancreatic beta cells.* J Biol Chem, 2010. **285**(42): p. 32606-15.
167. Li, X., et al., *Fatostatin Displays High Antitumor Activity in Prostate Cancer by Blocking SREBP-Regulated Metabolic Pathways and Androgen Receptor Signaling.* Mol Cancer Ther, 2014.
168. Kamisuki, S., et al., *A small molecule that blocks fat synthesis by inhibiting the activation of SREBP.* Chem Biol, 2009. **16**(8): p. 882-92.
169. Freed-Pastor, W.A., et al., *Mutant p53 disrupts mammary tissue architecture via the mevalonate pathway.* Cell, 2012. **148**(1-2): p. 244-58.
170. Guinez, C., et al., *O-GlcNAcylation increases ChREBP protein content and transcriptional activity in the liver.* Diabetes, 2011. **60**(5): p. 1399-413.
171. Greenspan, P., E.P. Mayer, and S.D. Fowler, *Nile red: a selective fluorescent stain for intracellular lipid droplets.* J Cell Biol, 1985. **100**(3): p. 965-73.
172. Guy, C.T., R.D. Cardiff, and W.J. Muller, *Induction of mammary tumors by expression of polyomavirus middle T oncogene: a transgenic mouse model for metastatic disease.* Mol Cell Biol, 1992. **12**(3): p. 954-61.
173. Sundqvist, A., et al., *Control of lipid metabolism by phosphorylation-dependent degradation of the SREBP family of transcription factors by SCF(Fbw7).* Cell Metab, 2005. **1**(6): p. 379-91.
174. Bengoechea-Alonso, M.T. and J. Ericsson, *A phosphorylation cascade controls the degradation of active SREBP1.* J Biol Chem, 2009. **284**(9): p. 5885-95.
175. Amemiya-Kudo, M., et al., *Transcriptional activities of nuclear SREBP-1a, -1c, and -2 to different target promoters of lipogenic and cholesterogenic genes.* J Lipid Res, 2002. **43**(8): p. 1220-35.
176. Rohrig, F. and A. Schulze, *The multifaceted roles of fatty acid synthesis in cancer.* Nat Rev Cancer, 2016.
177. Itkonen, H.M., et al., *O-GlcNAc transferase integrates metabolic pathways to regulate the stability of c-MYC in human prostate cancer cells.* Cancer Res, 2013. **73**(16): p. 5277-87.
178. Shaw, R.J. and L.C. Cantley, *Decoding key nodes in the metabolism of cancer cells: sugar & spice and all things nice.* F1000 Biol Rep, 2012. **4**: p. 2.

179. Chou, T.Y., G.W. Hart, and C.V. Dang, *c-Myc is glycosylated at threonine 58, a known phosphorylation site and a mutational hot spot in lymphomas.* J. Biol. Chem., 1995. **270**: p. 18961-18965.
180. Wu, Y., et al., *Srebp-1 Interacts with c-Myc to Enhance Somatic Cell Reprogramming.* Stem Cells, 2016. **34**(1): p. 83-92.
181. Guo, D., et al., *Targeting SREBP-1-driven lipid metabolism to treat cancer.* Curr Pharm Des, 2014. **20**(15): p. 2619-26.
182. Shi, J., et al., *O-GlcNAcylation regulates ischemia-induced neuronal apoptosis through AKT signaling.* Sci Rep, 2015. **5**: p. 14500.
183. Lubas, W.A. and J.A. Hanover, *Functional expression of O-linked GlcNAc transferase. Domain structure and substrate specificity.* J Biol Chem, 2000. **275**(15): p. 10983-8.
184. Cheng, C., et al., *Glucose-Mediated N-glycosylation of SCAP Is Essential for SREBP-1 Activation and Tumor Growth.* Cancer Cell, 2015. **28**(5): p. 569-81.
185. Buckley, D., Heuer, T., O'Farrell, M., McCulloch, B. & and G. Kemble, *Translational studies of a first-in-class FASN Inhibitor, TVB-2640, linking preclinical studies to clinical laboratory observations in solid tumor patients.* . Molecular Cancer Research, 2016. **14** ((Suppl. 1)): p. Abstr. A75
186. Bullen, J.W., et al., *Cross-talk between two essential nutrient-sensitive enzymes: O-GlcNAc transferase (OGT) and AMP-activated protein kinase (AMPK).* J Biol Chem, 2014. **289**(15): p. 10592-606.
187. Anthonisen, E.H., et al., *Nuclear receptor liver X receptor is O-GlcNAc-modified in response to glucose.* J Biol Chem, 2010. **285**(3): p. 1607-15.
188. Baldini, S.F. and T. Lefebvre, *O-GlcNAcylation and the Metabolic Shift in High-Proliferating Cells: All the Evidence Suggests that Sugars Dictate the Flux of Lipid Biogenesis in Tumor Processes.* Front Oncol, 2016. **6**: p. 6.
189. Sadowski, M.C., et al., *The fatty acid synthase inhibitor triclosan: repurposing an anti-microbial agent for targeting prostate cancer.* Oncotarget, 2014. **5**(19): p. 9362-81.
190. Inman, J.L., et al., *Mammary gland development: cell fate specification, stem cells and the microenvironment.* Development, 2015. **142**(6): p. 1028-42.
191. Macias, H. and L. Hinck, *Mammary gland development.* Wiley Interdiscip Rev Dev Biol, 2012. **1**(4): p. 533-57.
192. Anderson, S.M., et al., *Key stages in mammary gland development. Secretory activation in the mammary gland: it's not just about milk protein synthesis!* Breast Cancer Res, 2007. **9**(1): p. 204.
193. Prater, M.D., et al., *Mammary stem cells have myoepithelial cell properties.* Nat Cell Biol, 2014. **16**(10): p. 942-50, 1-7.
194. Rudolph, M.C., et al., *Metabolic regulation in the lactating mammary gland: a lipid synthesizing machine.* Physiol Genomics, 2007. **28**(3): p. 323-36.
195. Oakes S., H.H.O.C., *Key stages in mammary gland development - The alveolar switch: coordinating the proliferative cues and cell fate decisions that drive the formation of lobuloalveoli from ductal epithelium.* Breast Cancer Res, 2006. **8**(207).
196. Oakes, S.R., et al., *Prolactin regulation of mammary gland development.* J Mammary Gland Biol Neoplasia, 2008. **13**(1): p. 13-28.

197. Naylor, M.J., et al., *Transcriptional changes underlying the secretory activation phase of mammary gland development.* Mol Endocrinol, 2005. **19**(7): p. 1868-83.
198. Soulier, S., et al., *Introduction of a proximal Stat5 site in the murine alpha-lactalbumin promoter induces prolactin dependency in vitro and improves expression frequency in vivo.* Transgenic Res, 1999. **8**(1): p. 23-31.
199. Ferrer, C.M., et al., *O-GlcNAcylation regulates breast cancer metastasis via SIRT1 modulation of FoxM1 pathway.* Oncogene, 2016. **under review**.
200. Bobrovnikova-Marjon, E., et al., *PERK-dependent regulation of lipogenesis during mouse mammary gland development and adipocyte differentiation.* Proc Natl Acad Sci U S A, 2008. **105**(42): p. 16314-9.
201. Watkin, H., et al., *Lactation failure in Src knockout mice is due to impaired secretory activation.* BMC Dev Biol, 2008. **8**: p. 6.
202. Reitman, Z.J., et al., *Profiling the effects of isocitrate dehydrogenase 1 and 2 mutations on the cellular metabolome.* Proc Natl Acad Sci U S A, 2011. **108**(8): p. 3270-5.
203. Evans, A.M., et al., *Integrated, nontargeted ultrahigh performance liquid chromatography/electrospray ionization tandem mass spectrometry platform for the identification and relative quantification of the small-molecule complement of biological systems.* Analytical chemistry, 2009. **81**(16): p. 6656-67.
204. Dehaven, C.D., et al., *Organization of GC/MS and LC/MS metabolomics data into chemical libraries.* Journal of cheminformatics, 2010. **2**(1): p. 9.
205. Reginato, M.J., et al., *Integrins and EGFR coordinately regulate the pro-apoptotic protein Bim to prevent anoikis.* Nature cell biology, 2003. **5**(8): p. 733-40.
206. Schwab, L.P., et al., *Hypoxia-inducible factor 1alpha promotes primary tumor growth and tumor-initiating cell activity in breast cancer.* Breast cancer research : BCR, 2012. **14**(1): p. R6.
207. Sodi, V.L., et al., *mTOR/MYC Axis Regulates O-GlcNAc Transferase Expression and O-GlcNAcylation in Breast Cancer.* Mol Cancer Res, 2015. **13**(5): p. 923-33.
208. Bligh, E.G. and W.J. Dyer, *A rapid method of total lipid extraction and purification.* Can J Biochem Physiol, 1959. **37**(8): p. 911-7.
209. Chen Y, M.J., Chen X, Doman T, Gong X, Zhang Y, Hamm N, Ma X, Higgs R, Bhagwat S, Buchanan S, Peng S, Staschke K, Yadav V, Yue Y, Kouros-Mehr H, *Identification of Druggable Cancer Driver Genes Amplified across TCGA Datasets.* PLOS One, 2014. **9**(5).
210. Cheung, H.W., et al., *Systematic investigation of genetic vulnerabilities across cancer cell lines reveals lineage-specific dependencies in ovarian cancer.* Proc Natl Acad Sci U S A, 2011. **108**(30): p. 12372-7.
211. Itkonen, H.M., et al., *Inhibition of O-GlcNAc transferase activity reprograms prostate cancer cell metabolism.* Oncotarget, 2016.
212. Ortiz-Meoz, R.F., et al., *A small molecule that inhibits OGT activity in cells.* ACS Chem Biol, 2015. **10**(6): p. 1392-7.
213. Gloster, T.M., et al., *Hijacking a biosynthetic pathway yields a glycosyltransferase inhibitor within cells.* Nat Chem Biol, 2011. **7**(3): p. 174-81.
214. Gross, B.J., B.C. Kraybill, and S. Walker, *Discovery of O-GlcNAc transferase inhibitors.* J Am Chem Soc, 2005. **127**(42): p. 14588-9.

215. Kwei, K.A., J.B. Baker, and R.J. Pelham, *Modulators of sensitivity and resistance to inhibition of PI3K identified in a pharmacogenomic screen of the NCI-60 human tumor cell line collection.* PLoS One, 2012. **7**(9): p. e46518.
216. Ruan, H.B., et al., *O-GlcNAc transferase enables AgRP neurons to suppress browning of white fat.* Cell, 2014. **159**(2): p. 306-17.
217. Miyata, Y., H. Nakamoto, and L. Neckers, *The therapeutic target Hsp90 and cancer hallmarks.* Curr Pharm Des, 2013. **19**(3): p. 347-65.
218. Ma, Z., C.H. Chu, and D. Cheng, *A novel direct homogeneous assay for ATP citrate lyase.* J Lipid Res, 2009. **50**(10): p. 2131-5.
219. Hursting, S.D., et al., *Calorie restriction, aging, and cancer prevention: mechanisms of action and applicability to humans.* Annu Rev Med, 2003. **54**: p. 131-52.
220. Muhammad, M., Magaji, R., Mohammed, A., Isa, A., Magaji, M., *Effect of Resveratrol as Caloric Restriction Mimetic and Environmental Enrichment on Neurobehavioural Responses in Young Healthy Mice.* Advances in Neuroscience, 2014. **2014**(Article ID 545170): p. 7.
221. Longo, V.D. and L. Fontana, *Calorie restriction and cancer prevention: metabolic and molecular mechanisms.* Trends Pharmacol Sci, 2010. **31**(2): p. 89-98.
222. Madeo, F., et al., *Caloric restriction mimetics: towards a molecular definition.* Nat Rev Drug Discov, 2014. **13**(10): p. 727-40.